UNIVERSIDAD NACIONAL AUTÓNOMA DE MÉXICO

PROGRAMA DE DOCTORADO EN CIENCIAS BIOMÉDICAS

FACULTAD DE MEDICINA

CONTROL DE LA PIRUVATO.FERREDOXINA ÓXIDO REDUCTASA SOBRE EL FLUJO GLUCOLÍTICO EN *Entamoeba histolytica*

TESIS

QUE PARA OPTAR EL GRADO DE DOCTORA EN CIENCIAS (BIOMÉDICAS)

PRESENTA

Q.A. ERIKA PINEDA RAMÍREZ

TUTORA:

DRA. EMMA CECILIA SAAVEDRA LIRA

PROGRAMA DE DOCTORADO EN CIENCIAS BIOMÉDICAS

INTEGRANTES DEL COMITÉ TUTOR

DR. ARMANDO GÓMEZ PUYOU (INSTITUTO DE FISIOLOGÍA CELULAR)

DR. RAFAEL MORENO SÁNCHEZ (INSTITUTO DE FISIOLOGÍA CELULAR)

México, D. F. 2014

El jurado del examen de Examen Doctoral estuvo integrado por:

PRESIDENTE: Dra. Selva Rivas Arancibia
Facultad de Medicina, UNAM

SECRETARIA: Dra. Emma Cecilia Saavedra Lira
Depto. Bioquímica, INC Ignacio Chávez

VOCAL: Dr. Adolfo García Sáinz
Instituto de Fisiología Celular, UNAM

VOCAL: Dra. Patricia Talamás Rohana
CINVESTAV, Unidad Zacatenco

VOCAL: Dr. Juan Pablo Pardo Vázquez
Facultad de Medicina, UNAM

El proyecto se realizó en el departamento de Bioquímica del Instituto Nacional de Cardiología Ignacio Chávez.

La presente tesis estuvo bajo la tutoría de la Dra. Emma Cecilia Saavedra Lira.

Durante mis estudios de posgrado conté con una beca por parte de CONACyT para la realización de este proyecto.

A mis flacos:
porque no hay un solo día en que no piense en ustedes.

A Mary, Javier, Rosalba, Lauro, Paco, César e Ira:
por todo su apoyo y cariño. Son mi motivación y mi ejemplo a seguir.

Agradecimientos:

A la Dra. Emma Saavedra, por toda su confianza y paciencia. Gracias por ayudarme a crecer y enseñarme a ser una persona más fuerte.

Al Dr. Rafael Moreno, por sus enseñanzas y por alentarme a llegar más lejos.

A Rus, por toooooda la ayuda, por tu amistad y por los buenos momentos. Eres una gran amiga, ¡te quiero mucho amibi!

A Ricardo, porque gracias a ti estoy en Cardio, por apoyarme y escucharme siempre, porque eres lo que yo quiero llegar a ser. Te admiro y te quiero mucho.

A Viri, gracias por la amistad y por apoyarme para crecer juntas.

A Zabdi por tu amistad, por aconsejarme y por los buenos momentos; a Cita y Esteph por confiar en mí, por su paciencia y por enseñarme a enseñar. A Ake por el apoyo y cariño, a Paco por escucharme y siempre alentarme a seguir adelante, a Aldo y a Toño por su amistad, apoyo y risas.

A Álvaro, Juan Carlos. José Salud y Belem por sus consejos y apoyo.

Al resto del departamento de bioquímica, por sus sugerencias y por ayudarme a crecer.

A mi familia, por estar siempre a mi lado. Sin ustedes no habría logrado llegar hasta aquí. Son mi más grande tesoro y mi fortaleza. ¡Los amo!

ÍNDICE

RESUMEN 7
ABSTRACT 11
ABREVIATURAS: 15
CAPÍTULO 1. INTRODUCCIÓN 16
1.1. Epidemiología de la amibiasis 16
1.2. Ciclo biológico de E. histolytica 19
1.3. Metabolismo energético en E. histolytica 21
Capítulo del libro: Glucose metabolism and its controlling mechanisms in *Entamoeba histolytica* 24
1.4. Breve descripción de la piruvato:ferredoxina oxidoreductasa 63
1.4.1 Antecedentes de la PFOR de E. histolytica 64
1.5. Introducción al Análisis de Control Metabólico 66
1.5.1 Estrategias experimentales para determinar los coeficientes de control de las enzimas de una vía metabólica 68
1.6. Distribución de control de la glucólisis amibiana 71
CAPÍTULO 2. PLANTEAMIENTO DEL PROBLEMA, HIPÓTESIS Y OBJETIVOS 73
2.1 Planteamiento del problema 73
2.2. Hipótesis 74
2.3. Objetivo general 74
2.4. Objetivos particulares 74
CAPÍTULO 3. CARACTERIZACIÓN CINÉTICA DE LA PFOR, MECANISMO DE INHIBICIÓN POR O_2 *in vitro* Y SU RELEVANCIA *in vivo* 75
3.1. Caracterización cinética de la EhPFOR en extractos celulares en condiciones controladas de oxígeno 77
3.2. Mecanismos de inhibición de la PFOR por oxígeno 79
3.3. Evaluación de la cinética de inactivación de la PFOR in vivo y su impacto en el flujo glucolítico 83
3.4. Artículo: Pyruvate:ferredoxin oxidoreductase and bifunctional aldehyde-alcohol dehydrogenase are essential for energy metabolism under oxidative stress in Entamoeba histolytica. 86
3.5. Datos que no se mostraron en el artículo 87
3.5.1 Reactivación de la EhPFOR 101

3.5.2 Efecto de las EROs sobre la actividad de la EhPFOR 102
3.5.3 Caracterización cinética de la ADHE recombinante 103
3.6. Discusión General de los resultados de sección parte del estudio..... 106
3.7 Conclusión 109
CAPÍTULO 4. DETERMINACIÓN DEL COEFICIENTE DE CONTROL DE LA PFOR Y LA ADHE SOBRE EL FLUJO GLUCOLÍTICO EN CONDICIONES AERÓBICAS..... 110
4.1 Estrategia experimental general..... 111
4.2. Resultados..... 113
4.2.1 Estrategia de inhibición de la actividad enzimática..... 113
4.2.2 Determinación de los coeficientes de control del flujo glucolítico..... 115
4.3. Discusión..... 118
4.5. Conclusión: 120
4.6. Artículo: The bifunctional aldehyde-alcohol dehydrogenase controls etanol and acetate production in Entamoeba histolytica under aerobic conditions 122
CAPÍTULO 5. DETERMINACIÓN DE LA DISTRIBUCIÓN DE CONTROL DE LA GLUCÓLISIS EN CÉLULAS INTACTAS DE *E. histolytica* A TRAVÉS DEL ANÁLISIS DE ELASTICIDADES 129
5.1. Introducción al análisis de elasticidades..... 130
5.2. Diseño experimental..... 133
5.3. Resultados..... 135
5.3.1 Requisitos para la aplicación del análisis de elasticidades..... 135
5.3.2 Determinación de los coeficientes de elasticidad..... 138
5.3.3 Determinación de los CaEiJ..... 140
5.4. Discusión del análisis de elasticidades de la glucólisis en E. histolytica 144
Capítulo 6. DISCUSIÓN y CONCLUSIONES GENERALES Y PERSPECTIVAS 146
6.1. Discusión general de la tesis 146
6.2. Conclusiones generales..... 149
6.3. Perspectivas 149
7. BIBLIOGRAFÍA..... 151
8. ANEXO 154

RESUMEN

En el metabolismo energético de *Entamoeba histolytica* la glucólisis es la única vía para obtener ATP y en sus últimas reacciones la conversión de piruvato a acetil-coenzima A la lleva a cabo la piruvato:ferredoxina oxido reductasa (PFOR). Esta enzima contiene tres centros Fe-S los cuales son altamente sensibles a las especies reactivas de oxígeno (EROs). Al respecto, antecedentes de nuestro grupo de trabajo demostraron que al incubar trofozoítos de amibas en condiciones suprafisiológicas de oxígeno, a la par de que hay una inhibición drástica de la PFOR, se acumulan los intermediarios glucolíticos G6P, F6P y piruvato, y disminuye la producción de etOH. Estos antecedentes llevaron a proponer la hipótesis de que debido a la fuerte inhibición por oxígeno de la PFOR, esta enzima puede ser un punto de control de la glucólisis amibiana cuando este parásito microaerofílico se expone a condiciones aeróbicas tales como las que se encuentran en el hígado, su órgano blanco en el hospedero en los casos de absceso hepático amibiano.

Debido a la poca información bioquímica de la PFOR amibiana, primero se realizó la caracterización cinética y el estudio de los mecanismos de inhibición de su actividad por especies reactivas de oxígeno (EROs), cuyos resultados se describen en el capítulo 3 de esta tesis. La caracterización cinética de la enzima se llevó a cabo en condiciones de pH y temperatura cercanas a las fisiológicas utilizando la enzima presente en extractos clarificados del parásito. Los valores de afinidad (*Km*) por sus sustratos fueron muy similares a las concentraciones de los mismos en los parásitos, esto sugiere que la enzima no se encuentra limitada por sus sustratos *in vivo* Se ensayaron los oxoácidos α-cetoglutarato y α-cetibutirato como sustratos alternativos pero la afinidad de la enzima por estos fue 3 veces menor que por piruvato. Esto sugirió que los oxoácidos provenientes de la degradación de aminoácidos no pueden entrar a la glucólisis a nivel de la PFOR y ser una fuente de ATP al convertirse en acetato por la AcCoAS.

Se analizaron los mecanismos de inactivación por EROs de la PFOR tanto de la enzima presente en extractos como en células completas. La enzima presente en la fracción solubilizada de parásitos se inactivó al 90% al incubarla por 30 min en condiciones saturantes de oxígeno; esta inactivación es reversible al adicionar Fe^{2+} en condiciones reductoras, y se torna irreversible cuando la incubación excede dicho intervalo. Los ligandos acetil-CoA y CoA protegieron de la inactivación por O_2 mientras que el piruvato aceleró la inactivación. Las enzimas antioxidantes superóxido dismutasa y catalasa también protegieron de la inactivación, lo que indicó que las EROs estaban involucradas en el mecanismo de inactivación siendo el superóxido la especie que inhibe preferentemente a la enzima.

Por otro lado, al analizar el efecto del reto con oxígeno en trofozoítos amibianos se observó que a la par de la inhibición de la PFOR también se inhibía al 67% la actividad de aldehído deshidrogenasa de la enzima bifuncional aldehído-alcohol deshidrogenasa (ADHE) mientras que las demás enzimas glucolíticas no se afectaron. El efecto de O_2 sobre la actividad de la ADHE no se había reportado antes en la literatura. Después del reto con oxígeno, las amibas se incubaron en normoxia para evaluar el efecto de la inhibición en los flujos metabólicos. La inhibición de la PFOR y ADHE trajo como consecuencia la disminución en la producción de etanol y un ligero incremento en el flujo hacia acetato; sin embargo, después de una hora, los parásitos fueron capaces de recuperar las actividades de ambas enzimas y restablecer el flujo hacia etanol a niveles normales.

Los resultados de esta primera parte del trabajo experimental indicaron que la inhibición del metabolismo energético de las amibas expuestas a una condición de estrés oxidante se debe a la inhibición no solamente de la PFOR, sino también de la ADHE, por lo tanto, además de la determinación del grado de control que tiene la PFOR sobre la glucólisis amibiana en condiciones de aerobiosis, que era el objetivo principal de la tesis, también se estableció como prioritario determinar el grado de control de la ADHE. Los resultados de los hallazgos de este análisis se describen en el capítulo 4 de esta tesis y se resumen en las siguientes líneas.

El grado de control que ejerce una enzima sobre el flujo de la vía metabólica a la que pertenece se puede determinar aplicando los fundamentos del Análisis del Control Metabólico (MCA). Dicho grado de control del flujo de una enzima es un valor numérico que se denomina coeficiente de control de flujo, C_{aEi}^{J}, donde J es flujo y aEi es la actividad de la enzima, transportador, bloque de enzimas o reacciones químicas *Ei* de la vía metabólica. Se determinaron los C_{aEi}^{J} de la PFOR y ADHE por titulación con inhibidores utilizando difeniliodonio y disulfiram y se establecieron las condiciones experimentales en las cuales estos compuestos inhiben de manera específica a estas enzimas sin afectar el resto de las enzimas de la vía metabólica. En paralelo a la inhibición de la actividad de estas enzimas se determinaron los flujos a etanol y acetato y de las gráficas de flujo *versus* actividad enzimática se determinaron los C_{aEi}^{J}. Como resultado se obtuvo que en condiciones de aerobiosis, la PFOR posee un C_{aEi}^{J} para el flujo de etanol del 7% mientras que, de manera sobresaliente la ADHE tuvo un coeficiente de control del 33%. Estos resultados indican que de las dos enzimas susceptibles de ser inhibidas en condiciones aeróbicas, la ADHE controla más que la PFOR el flujo de la glucólisis en el parásito. La razón de este mayor control es que la ADHE presente en los trofozoítos representa solamente el 10% de la actividad que tiene la PFOR, por lo que aunque la ADHE se inhibe en menor porcentaje en condiciones aeróbicas, la poca actividad remanente limita el flujo metabólico.

Para avanzar en el conocimiento de la estructura de control del metabolismo de la glucosa en *E. histolytica* no es suficiente con determinar el grado de control de algunas enzimas de la vía. La PFOR y ADHE controlan en conjunto el 40% del flujo total de la vía, por lo tanto el 60% restante debe de residir en las reacciones de la vía que no fueron evaluadas. Por lo tanto, se realizó el análisis de elasticidades como otra aproximación experimental del MCA para determinar la distribución de control de la vía completa. Estos estudios se describen en el capítulo 5 de esta tesis.

Una ventaja del análisis de elasticidades es que permite identificar las reacciones de una vía que tienen mayor control del flujo utilizando células enteras y se basa en determinar cómo cambian las velocidades de las reacciones de la vía cuando se cambian las concentraciones de los intermediarios. Para tal efecto se hicieron variar en

los trofozoítos las concentraciones de los intermediarios G6P, F6P y pyr para hacer variar las velocidades (*i.e.,* los flujos) de los bloques de enzimas que producen y consumen cada uno de estos metabolitos. De las gráficas de flujo de la vía *versus* concentración de intermediario se determinaron los coeficientes de elasticidad y a través de los teoremas de la sumatoria, conectividad y de la ramificación del MCA se determinaron los C^{J}_{aEi} de los bloques principales que constituyen la glucólisis amibiana. Los resultados indican que el bloque de enzimas del transportador de glucosa, la hexocinasa y la degradación del glucógeno controlan el 72-80% el flujo de la vía, seguido por el bloque consumidor de piruvato (PFOR y ADHE) con un 31% del control; esta distribución de control concuerda con el control que ejercen la PFOR y ADHE obtenidos por titulación con inhibidores. Por otro lado el bloque de ocho enzimas y sus ramificaciones desde la fosfofructocinasa dependiente de pirofosfato (PPi-PFK) hasta la piruvato fosfato dicinasa (PPDK) controla 20-28% mientras que la síntesis de glucógeno controla del -13 a -22% el flujo de la vía.

Estos resultados indican que en condiciones aeróbicas agudas, el flujo de la glucólisis recae principalmente en las etapas iniciales de la vía. A pesar de que las enzimas PFOR y ADHE son muy sensibles al estrés oxidante, en condiciones de aerobiosis experimental la ADHE puede participar con el 30% del control de flujo de la vía. Así mismo, la distribución de control de la glucólisis de *E. histolytica* indica que si se desea inhibir a la glucólisis de este parásito como una estrategia alternativa a la actual, sería más adecuado inhibir a alguna(s) de las enzimas del bloque con mayor control de flujo, o alternativamente, inhibir a la ADHE la cual tiene un coeficiente de control alto. Por otro lado, las enzimas dependientes de pirofosfato PPi-PFK y PPDK que alguna vez se propusieron como blancos terapéuticos por ser peculiaridades del parásito controlan poco el flujo de la vía, por lo que se requerirían una inhibición farmacológica completa para afectar el metabolismo energético del parásito.

ABSTRACT

In the energy metabolism of *Entamoeba histolytica*, glycolysis is the only pathway to obtain ATP and in its last reactions the conversion of pyruvate to acetyl-coenzyme A is carried out by pyruvate:ferredoxin oxidoreductase (PFOR). This enzyme contains three Fe-S clusters which are highly sensitive to reactive oxygen species (ROS). On this regard, previous findings from our research group demonstrated that amebal trophozoites incubated under supraphysiologycal oxygen conditions, in addition to a drastic PFOR inhibition, there is accumulation of the glycolytic metabolites G6P, F6P and pyruvate, and a decrease in etOH production. These results led us to hypothesize that due to the high PFOR oxygen inhibition, the enzyme may be a limiting reaction for amebic glycolysis when this microaerophilic parasite is exposed to aerobic conditions such as those found in the liver, one of its target organ in the host in cases of amebic liver abscess.

Due to the limited biochemical information of amoebic PFOR, first its kinetic characterization was performed and further the mechanisms of inhibition of its activity by reactive oxygen species (ROS) were analyzed; these results are described in chapter 3 of this thesis. The kinetic characterization of the enzyme was carried out using the enzyme present in amebal clarified extracts and under conditions of pH and temperature that resemble the physiological ones. The affinity values (*Km*) for its substrates were very similar to the concentrations of those metabolites in the parasites, this suggests that the enzyme is not limited by its substrates *in vivo*. The oxoacids α -ketobutyrate and α –ketoglutarate were tested as alternative substrates but the affinity for these metabolites was lower than that for pyruvate. This suggested that oxoacids derived from amino acid degradation cannot supply glycolysis at the level of PFOR and be a source of ATP when they are converted to acetate by the AcCoAS as was previously proposed.

The mechanisms of PFOR inactivation by ROS were analyzed in live cells and clarified cell extracts. The enzyme present in the solubilized fraction of parasites was inactivated at 90% by incubating the cell sample for 30 min at saturating oxygen conditions, this inactivation was reversible upon Fe^{2+}addition under reducing conditions; it becomes irreversible when incubation exceeds that time interval. Its ligands acetyl-CoA and CoA protected from inactivation by O_2 while pyruvate accelerated inactivation. The antioxidant enzymes superoxide dismutase and catalase also protected from inactivation, indicating that ROS were involved in the mechanism of inactivation, being superoxide the ROS type that preferentially inhibits the enzyme.

Moreover, the effect of the oxygen challenge on amebal trophozoites was analyzed. It was determined that together with PFOR inhibition, the aldehyde dehydrogenase activity of the bifunctional aldehyde-alcohol dehydrogenase (ADHE) was also inhibited in 67% while other glycolytic enzymes were not affected. The effect of O_2 on the activity of ADHE has not been reported before in the literature. After the oxygen challenge, the amoebas were incubated under normoxia to evaluate the effect on metabolic fluxes. PFOR and ADHE inhibition resulted in decreased ethanol production and a slight increase in the acetate flux; however, after an hour in normoxia, the parasites restored the enzyme activities as well the ethanol flux to normal levels.

The results of this part of the experimental work indicated that the energy metabolism inhibition of amoebas exposed to oxidative stress condition is due not only to PFOR inhibition but also to ADHE impairment. Therefore, in addition to determining the PFOR degree of control over amoebic glycolysis under aerobic conditions, which was the main objective of the thesis, we also established as a priority to determine the degree of control of ADHE. The results of the findings of these analyses are described in chapter 4 of this thesis and summarized in the following lines.

The control exerted by an enzyme over the flux of its metabolic pathway can be determined by applying the fundamentals of Metabolic Control Analysis (MCA). The degree of control of an enzyme over the pathway flux is a numerical value called flux control coefficient,C_{aEi}^{J}, where J is flux and aEi is the activity (a) of an enzyme, transporter, group of pathway enzymes or chemical reactions *Ei* . The C_{aEi}^{J} of ADHE and

PFOR were determined by titration with inhibitors using disulfiram and diphenyliodonium, respectively. Experimental conditions were established in which the compounds specifically inhibited these enzymes without affecting other pathway enzymes. In parallel to inhibition of the enzyme activity the fluxes to ethanol and acetate were determined, and from the dependency of fluxes versus enzyme activity the C_{aEi}^{J} were determined. Under aerobic conditions and over ethanol flux, PFOR displayed a C_{aEi}^{J} of 7% whereas outstandingly the ADHE had a control coefficient of 33%. These results indicated that of the two enzymes susceptible of being inhibited under aerobic conditions, ADHE exerted higher control than PFOR over the glycolytic flux in the parasite. The reason for the higher ADHE control is that in amoebal trophozoites, this enzyme represents only 10 % the activity PFOR; therefore, although ADHE is inhibited to a lesser extent than PFOR under aerobic conditions, its low remaining activity limited the glycolytic flux.

To advance in the knowledge of the control structure of the complete glucose catabolism in *E. histolytica* it is not enough to determine the degree of control of some pathway enzymes. Together, PFOR and ADHE control 40% of the total flux of the pathway; therefore, the remaining 60 % must reside in the other pathway reactions that were not inhibited. Therefore, elasticity analysis was performed which is another MCA experimental approach to determine the control distribution of complete pathways. These studies are described in Chapter 5 of this thesis

The advantage of elasticity analysis is that allows identification of the reactions that have higher flux control using the whole live cells. It is based on the determination of how the rate of an enzyme or group enzymes changes to variation in the concentrations of their pathway intermediaries. To that end, the concentrations of G6P, F6P and pyr were varied in the trophozoites to change the rate of the group of reactions that produce and consume these metabolites. From the plots of flux *versus* intermediary concentration, the elasticity coefficients were determined and by applying the summation, connectivity and branch theorems of the MCA, the C_{aEi}^{J} of major groups of glycolytic enzymes/reactions were determined. The results indicated that the group of enzymes constituted by the glucose transport, hexokinase and glycogen degradation

control by 72-80 % the pathway flux, followed by the pyruvate consumer block (PFOR and ADHE) with 31% of the control. The latter value is in agreement with the control of PFOR and ADHE obtained by titration with inhibitors. Furthermore, the group of eight enzymes and their ramifications from the pyrophosphate dependent phosphofructokinase (PPi-PFK) to pyruvate phosphate dikinase (PPDK) controls 20-28 %, whereas the glycogen synthesis exerted -13 to -22 % control of the pathway flux.

The results of this thesis indicated that under acute aerobic conditions, glycolytic flux is mainly controlled by the initial pathway reactions. Although PFOR and ADHE are highly susceptible to oxidative stress, in the aerobic experimental conditions, ADHE had 30% of the pathway flux control.

The control distribution of glycolysis in *E. histolytica* indicates that to inhibit the parasitic pathway as an alternative to the existing therapeutic strategy, it would be more suitable to inhibit one or at least two of the enzymes that have the higher control of flux. Furthermore, the pyrophosphate -dependent enzymes PPi - PFK and PPDK, which have been proposed as therapeutic targets had low flux control coefficient, Therefore, it would be required a complete pharmacological inhibition of these enzymes to affect the parasite energy metabolism.

ABREVIATURAS:

AcCoAS: acetil-CoA sintetasa

Acetil-CoA: acetil-coenzyma A;

ADHE: alcohol-aldehído deshidrogenasa bifuncional;

Cat: catalasa

DPI: cloruro de difenil iodonio

DSF: disulfiram

EROs: especies reactivas de oxígeno

EtOH: etanol

F6P: fructosa-6-fosfato

G6P: glucose-6-fosfato

HK: hexocinasa

HXT: transportador de glucosa

PFOR: piruvato:ferredoxina oxidoreductasa

PGAM: 3- fosfoglicerato mutasa

PPDK, piruvato fosfato dicinasa

Pyr: piruvato

SOD: superóxido dismutasa

CAPÍTULO 1. INTRODUCCIÓN

1.1. Epidemiología de la amibiasis

La amibiasis es una enfermedad muy común en países en vías de desarrollo, entre los que se encuentra Malasia y Bangladesh. A mediados de los años 80s se reportó hasta 100,000 muertes anuales (Walsh, 1986), mientras que la Organización Mundial de la Salud estableció que esta enfermedad era la cuarta causa de muertes por parásitos a nivel mundial [WHO 2004]. *E. histolytica* genera manifestaciones clínicas solo en el 10-20% de las personas infectadas; en el resto cursan con la infección de manera asintomática, por lo que en la mayoría de los casos estos pacientes no reciben tratamiento y se vuelven transmisores de la enfermedad (Mackey-Lawrence y Petri Jr, 2011).

Durante mucho tiempo las estadísticas de infección por *E. histolytica* aportaron valores muy elevados de esta enfermedad, los cuales pudieron haberse sobreestimado debido a que no se contaban con las estrategias experimentales para diferenciar a *E. histolytica* (la especie más infectiva y virulenta) de *E. dispar* o *E. moshkovskii,* debido a que son morfológicamente indistinguibles al microscopio (McAuliffe *et al*, 2013). Sin embargo, en las últimas décadas se han desarrollado estrategias de detección inmunológicas (reacción antígeno-anticuerpo) y moleculares (detección de isoformas enzimáticas y uso de sondas de DNA), para establecer la presencia de diversas especies amibianas en las muestras clínicas, por lo que las pruebas de detección se hicieron más específicas (Ximénez *et al,* 2011). En México se reportó una seroprevalencia del 9.7% en la población general (Ximénez, 2006). La amibiasis es una de las principales causas de consulta médica a nivel nacional, con 1 millón de casos anuales. La parasitosis afecta más a las personas que viven en condiciones sanitarias precarias de nuestro país, sobre todo en la población infantil de 0 a 4 años (Figura1.1) (Cuadernos FUNSALUD 2008).

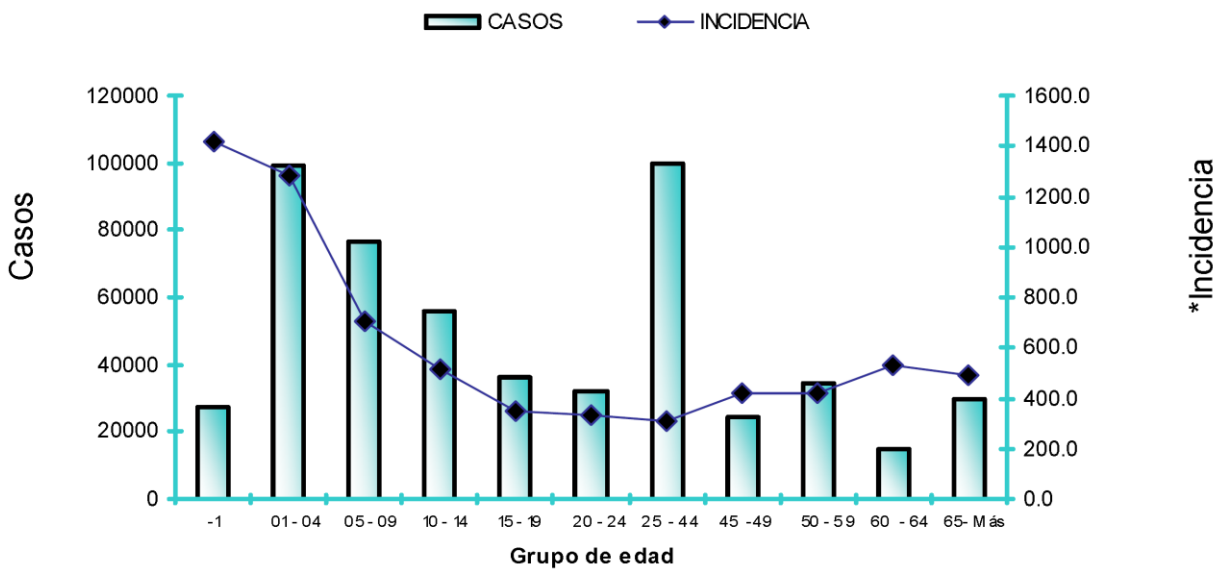

Fig. 1.1. Incidencia de amibiasis por intervalo de edad en la República Mexicana en 2008. Incidencia por cada 100,000 habitantes. Fuente: SUIVE/DGAE/Secretaría de Salud

Las estadísticas reportadas en 2010 por la Secretaria de Salud establecieron que la amibiasis intestinal era la novena causa de morbilidad en el territorio nacional, por encima de la diabetes mellitus tipo II (Tabla 1.1).

Tabla 1.1 Principales causas de morbilidad en nuestro país en 2010- Fuente CENAVECE (www.dgepi.salud.gob.mx/anuario/)

1.- Infecciones respiratorias agudas
2.- Infecciones intestinales por otros organismos y las mal definidas
3.- Infección de vías urinarias
4.- Otitis media aguda
5.- Amibiasis intestinal
6.- Conjuntivitis
7.- Otras helmintiasis
8.- Candidiasis urogenital
9.- Varicela
10.- Neumonía y Bronconeumonía

Esta infección tiene la mayor incidencia en los estados del sur del país, siendo los más afectados Guerrero y Oaxaca, seguidos por Chiapas, Yucatán, Tabasco y Campeche (Figura 1.2). Estos datos están relacionados con las condiciones socioeconómicas de los estados más afectados, siendo aquellos donde hay más pobreza los que presentan el mayor número de casos.

Figura 1.2. Distribución de la amibiasis intestinal en México durante el 2010. Fuente CENAVECE 2010.

1.2. Ciclo biológico de E. histolytica

El ciclo biológico de *E. histolytica* comprende dos estadios: el quiste y el trofozoíto (Fig. 1.3). Los humanos son el principal hospedero y la principal fuente de transmisión (Mackey-Lawrence y Petri Jr 2011).

La forma móvil del parásito es el trofozoíto, la cual es el estadio vegetativo que coloniza el lumen del intestino grueso para multiplicarse; este puede invadir la mucosa intestinal generando así la amibiasis intestinal. En algunos casos, la infección puede complicarse cuando la amiba invade otros tejidos a través de su diseminación sanguínea por la vena porta, generando lesiones extra intestinales como el absceso hepático, el pulmonar y en mucho menor medida el cerebral. (Zermeño *et al*, 2013).

Se ha propuesto que cuando los trofozoítos se encuentran en condiciones de estrés por nutrientes durante su paso por el colón transversal y descendente, se inicia el proceso de enquistamiento (Caballero-Salcedo et al, 1994)Ali et al, 2004). El quiste

es el estadio de resistencia y transmisión amibiano. Los quistes se excretan en las heces de los enfermos y si las condiciones de higiene no son las adecuadas, estas contaminan el agua y los alimentos, cerrando así el ciclo biológico del parásito (Fig. 1.3). También se ha reportado la transmisión sexual oral-anal, sobre todo entre la población homosexual.

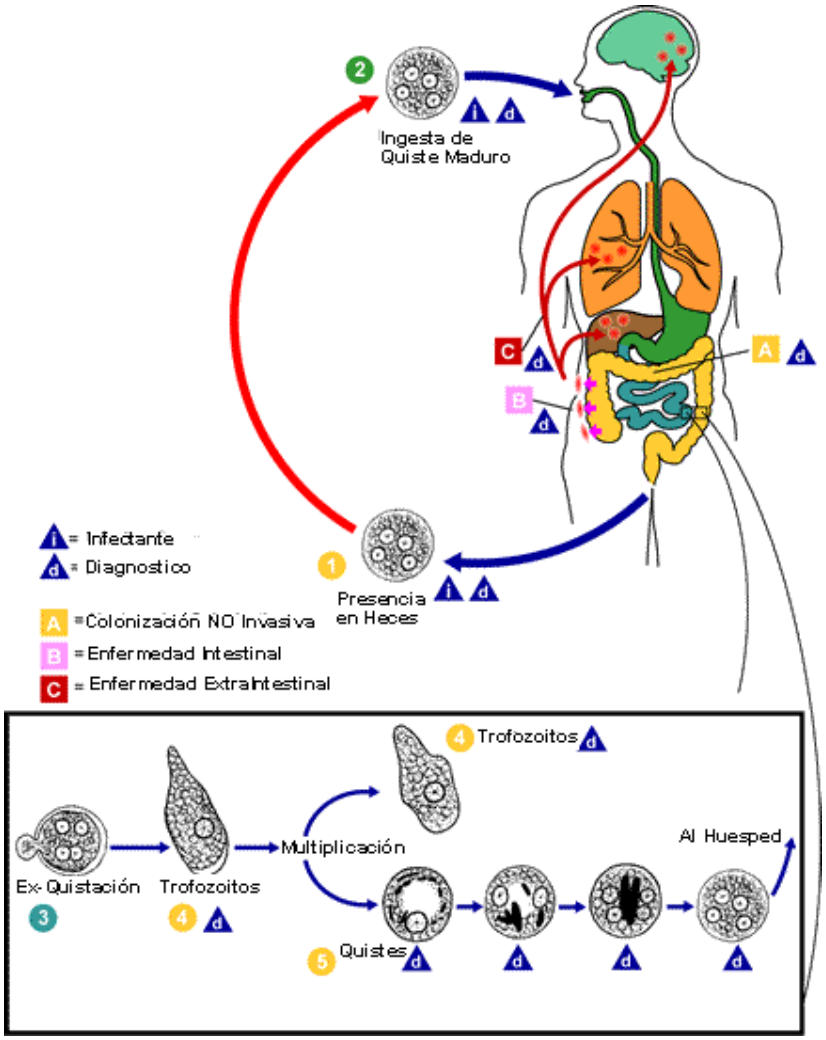

Figura 1.3. Ciclo biológico de *Entamoeba histolytica*. Tomado de http://amebiasis-semanaculturallasallana.blogspot.mx/2013/11/ciclo-evolutivo-de-la-entamoeba.html

1.3. Metabolismo energético en E. histolytica

Entamoeba histolytica tiene como principal vía de obtención de energía en forma de ATP a la glucólisis, debido a que no lleva a cabo ciclo de Krebs ni fosforilación oxidativa (Reeves, 1984; Saavedra et al, 2005). Esta vía (Fig. 1.4) presenta diferencias importantes con la glucólisis que ocurre en células humanas. Tiene dos enzimas dependientes de pirofosfato, la fosfofructocinasa (PPi-PFK) (Reeves *et al* 1976; Deng *et al* 1998) y la piruvato fosfato dicinasa (PPDK) (Reeves 1968; Saavedra-Lira *et al* 1998), las cuales catalizan reacciones reversibles en condiciones fisiológicas y no están sujetas a regulación alostérica como ocurre con sus contrapartes en mamíferos, la ATP-fosfofructocinasa (ATP-PFK) y la piruvato cinasa (PYK), las cuales son importantes puntos de control en la glucólisis de células humanas. Aunque se han detectado actividades de ATP-PFK y PYK en *E. histolytica*, sus actividades son un orden de magnitud menores comparadas con sus contrapartes dependientes de PPi y probablemente no contribuyen significativamente al flujo glucolítico (Saavedra *et al*, 2004; Saavedra et al, 2007). Otras diferencias importantes son: 1) la HK amibiana se inhibe fuertemente por AMP (Reeves *et al* 1967; Saavedra *et al*, 2005), mientras que el inhibidor de la HK de mamíferos es la glucosa-6-fosfato (G6P); 2) en la primera reacción de fosforilación a nivel de sustrato, la fosfoglicerato cinasa amibiana sintetiza preferentemente GTP en lugar de ATP y 3) la amiba tiene una 3-fosfoglicerato mutasa independiente de 2,3 difosfoglicerato, típica de bacterias.

Otras particularidades se encuentran en la transformación del piruvato. En mamíferos el complejo de la piruvato deshidrogenasa descarboxila y oxida al piruvato para producir acetil-coenzima A (acetil-CoA), CO_2 y NADH; esta enzima cataliza una reacción irreversible y tiene una regulación alostérica por diversos metabolitos que influye en los flujos de glucólisis y gluconeogénesis. En contraste, en amibas, el piruvato es descarboxilado y oxidado de manera reversible por la piruvato:ferredoxina oxidoreductasa (PFOR) para formar acetil-CoA, CO_2 y ferredoxina reducida (Reeves *et al* 1977). Hasta la fecha no se han encontrado moduladores alostéricos de la PFOR. Posteriormente, en condiciones anaeróbicas o de microaerobiosis, la acetil-CoA puede ser transformada a etanol por la acción de una alcohol deshidrogenasa bifuncional

(ADHE), la cual tiene actividades de acetaldehído y alcohol deshidrogenasa. Alternativamente, en condiciones aeróbicas, una fracción del acetil-CoA (10%) se transforma en acetato por una acetato tiocinasa (AcCoAS).

Como parte de una de las actividades del doctorado escribí una revisión del metabolismo de la glucosa en amiba y sus posibles mecanismos de control, la cual sirvió como una primera versión para una revisión más extensa en inglés que será un capítulo del libro “Amebiasis: Biology and Pathogenesis”, editado por A. Bhattacharya y T. Nozaki, el cual será publicado en el 2014 por la editorial Springer Japón. Cabe mencionar que la última revisión publicada acerca del metabolismo de *E. histolytica* se publicó hace treinta años por Richard Reeves (Reeves 1984), cuya investigación originó mucho del conocimiento que se tiene acerca del metabolismo de este parásito.

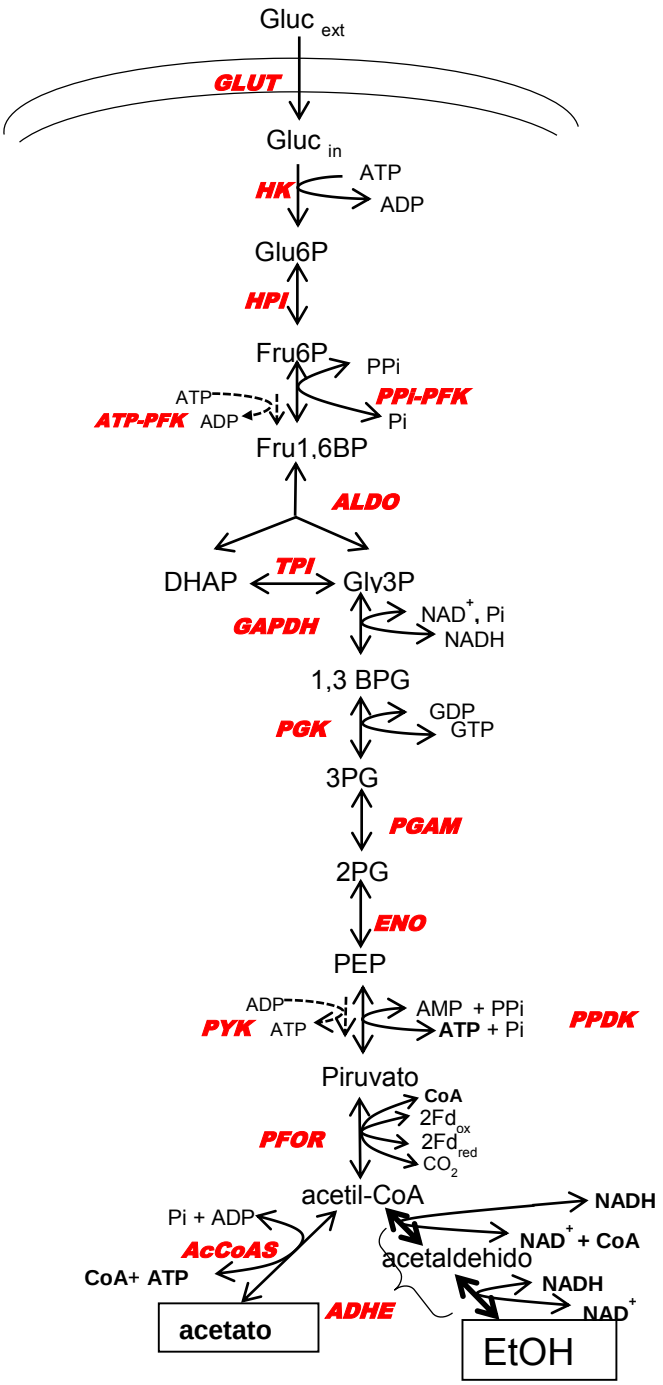

Fig. 1.4. Glucólisis en *E. histolytica*

GLUT,Transportador de glucosa; HK, hexocinasa; PPi-PFK, fosfrofructocinasa dependiente de pirofosfato; ATP-PFK, fosfofructocinasa dependiente de ATP; ALDO, aldolasa; TPI, triosafosfato isomerasa; GAPDH, gliceraldehído-3-fosfato deshidrogenasa; PGK, 3-fosfoglicerato cinasa; PGAM, 3-fosfoglicerato mutasa; ENO, enolasa; PPDK, piruvato fosfato dicinasa; PYK, piruvato cinasa; PFOR, piruvato:ferredoxina oxidoreductasa; ADHE, alcohol deshidrogenasa bifuncional; AcCoAS, acetato tiocinasa; Glu_{ext} , glucosa externa; Glu_{in}, glucosa interna; G6P, glucosa-6-fosfato; F6P, fructosa-6-fosfato; F1,6BP, fructosa-1,6-bifosfato; G3P, gliceraldehído-3-fosfato; DHAP, dihidroxiacetona fosfato; 1,3BPG, 1,3-bifosfoglicerato; 3PG, 3-fosfoglicerato; 2PG, 2-fosfoglicerato; PEP, fosfoenolpiruvato, acetil-CoA, acetil-coenzima A; PPi, pirofosfato; Pi, fosfato inorgánico; EtOH, etanol

Capítulo del libro: Glucose metabolism and its controlling mechanisms in *Entamoeba histolytica*

Erika Pineda, Rusely Encalada, Citlali Vázquez, Zabdi González, Rafael Moreno-Sánchez and Emma Saavedra

Glucose metabolism and its controlling mechanisms in *Entamoeba histolytica*

Erika Pineda, Rusely Encalada, Citlali Vázquez, Zabdi González, Rafael Moreno-Sánchez and Emma Saavedra [#]

Departamento de Bioquímica, Instituto Nacional de Cardiología Ignacio Chávez. México D.F., 14080, México.

[#]Corresponding author
Emma Saavedra, Ph.D.
Departamento de Bioquímica. Instituto Nacional de Cardiología Ignacio Chávez.
Juan Badiano No. 1 Col. Sección XVI, Tlalpan, México D.F. 14080, México
Tel. (5255) 5573-2911 ext. 1298.
e-mail: emma_saavedra2002@yahoo.com

Abstract

Entamoeba histolytica lacks the genes encoding the enzymes of the Krebs cycle and oxidative phosphorylation; therefore, glycolysis is the main pathway for ATP supply and for providing carbon skeleton precursors for the synthesis of macromolecules. External glucose is metabolized through a fermentative glycolysis producing mainly ethanol and, to a lower extent, acetate as end-products. The pathway in the parasite deviates in several aspects from the typical glycolysis present in mammals and yeasts. For instance, (i) the use of pyrophosphate as high-energy phosphate donor in several reactions; (ii) the feasibility of thermodynamic reversibility of all pathway reactions under physiological conditions; and (iii) the presence of fermentative enzymes similar to those of anaerobic bacteria. These and other enzyme peculiarities impose different mechanisms of control of the glycolytic fermentative flux in the parasite compared to the highly allosterically regulated glycolysis in other eukaryotic cells. In this chapter, we summarize the previous and current knowledge of the carbohydrate metabolism in *E. histolytica* and analyze its underlying controlling mechanisms by applying the fundamentals of Metabolic Control Analysis.

Keywords

Glycolysis, chitin synthesis, glycogen metabolism, Metabolic Control Analysis, flux control coefficient, controlling step, drug target

1. Introduction

Entamoeba histolytica and other members of the same genus live in microaerophilic environments of <5% O_2 atmospheric in *in vitro* culture (Band and Cirrito 1979, Gillin and Diamond 1981), which is approximately <30 μM dissolved O_2. Such O_2 concentration is close to that found in the human colon (0.1- 4.4%) (Taylor et al. 1981, Ladas et al. 2007). Therefore, *E. histolytica* is adapted to catabolize external glucose through fermentative glycolysis since it does have neither mitochondria nor the enzymes of the oxidative phosphorylation typical of aerobic cells.

The glycolytic enzymes and the anaerobic and microaerophilic route of glucose degradation in *E. histolytica* (Fig. 1) were mostly characterized in the late 60´s-early 80´s by Richard E. Reeves, who depicted the intermediary metabolism in the parasite (Reeves 1984). Most recently, a comprehensive compendium of the carbohydrate metabolism genes annotated in the *E. histolytica* genome was published (Clark et al. 2007). The recombinant amebal glycolytic enzymes have been recently kinetically characterized under near-physiological conditions (Saavedra et al. 2005) and relevant kinetic parameters are summarized in Table 1.

An integral analysis of the controlling mechanisms of the metabolic pathway has been performed by our group through metabolic modeling of the entire pathway and by theoretically and experimentally applying the fundamentals of Metabolic Control Analysis (Saavedra et al. 2005, Saavedra et al. 2007, Moreno-Sánchez et al. 2008a). This approach allows the quantitative determination of the degree of control that each enzyme/transporter has on the pathway flux and allows to understand the molecular basis of the controlling and regulatory mechanisms of metabolic pathways (reviewed in Moreno-Sánchez et al. 2008b).

2. Biochemical properties of the *E. histolytica* glycolytic enzymes

Glucose is taken up from the extracellular environment by a low activity and low affinity glucose transport (GLUT) mechanism (Serrano and Reeves 1974); up to date, its molecular identity has not been associated to any gene (Clark et al. 2007) (Table 1). Amebal GLUT activity is not inhibited by compounds that affect mammalian GLUTs such as colchicine and phloretin (Serrano and Reeves 1974), which suggests a highly divergent molecular nature from typical GLUT transporters. However, similar to mammalian GLUTs, amebal GLUT is also potently inhibited by cytochalasin B (*Ki* of 3 μM; Rusely Encalada and Emma Saavedra, unpublished results). In his pioneering studies, Reeves proposed that as the amebal glucose transport and pathway flux exhibited similar rates, GLUT could represent a rate limiting step of the glycolytic flux (Serrano and Reeves 1975).

Once internalized, glucose is immediately phosphorylated since no free intracellular glucose has been detected (Serrano and Reeves 1975). This reaction is catalyzed by hexokinase (HK; EC 2.7.1.1) which consumes one mole of ATP to produce glucose-6-phosphate (Glu6P) and ADP (Fig 1). In the *E. histolytica* genome there are two genes coding for isoforms HKI and HKII which have 89% identity at the amino acid sequence level (Ortner et al. 1995, Clark et al. 2007). The differences in the isoelectric points of the HK isoforms caused by these changes have been used to distinguish *E. histolytica* from *E. dispar* (Sargeaunt 1987, Ortner et al. 1997a). As most HKs, the amebal enzymes function as dimers and catalyze a reaction far from equilibrium (Keq ~ 844) which precludes its reversibility under physiological conditions. Kinetically, both *E. histolytica* HK isoforms have similar high affinities for glucose (Reeves et al. 1967,

Kroschewski et al. 2000, Saavedra et al. 2005) (Table 1), but they differ in their affinity for ATP, which is higher in the HKI isoform (Kroschewski et al. 2000). None of them use fructose or galactose as substrates, although they can use mannose but with low affinity ($Km_{mannose}$ HKI= 1 mM; HKII >2 mM) (Kroschewski et al. 2000). In addition, PPi is a potent, non-essential mixed-type activator of HKI (Table 1) (Moreno-Sánchez et al. 2008a). Remarkably, Glu6P does not inhibit amebal HKs as occurs for the mammalian enzymes in which serves as a regulatory mechanism (Wilson 2003); instead, amebal HKs are potently and competitively inhibited by AMP and ADP against ATP with *Ki* of 24-36 and 120-235 μM, respectively (Reeves et al. 1967, Kroschewski et al. 2000, Saavedra et al. 2005); these *Ki* values are well within the physiological concentrations found in trophozoites (1.6 mM AMP, 3.3 mM ADP, 5 mM ATP) (Saavedra et al. 2007). Therefore, the ratios of the adenine nucleotide pools (i.e., ATP/ADP and ATP/AMP) may serve as regulatory mechanisms of this reaction.

Glu6P is isomerized to fructose-6-phosphate (Fru6P) by hexose phosphate isomerase (HPI; EC 5.3.1.9) (Fig. 1). The *E. histolytica* genome contains two genes encoding HPIs which differ in the insertion/deletion of seven amino acids (Clark et al. 2007) and its isoforms have been used to distinguish different isolates from *E. histolytica* or *E. dispar* (Sargeaunt 1987, Razmjou et al. 2006). The enzyme is functional as dimer (Saavedra et al. 2005) and catalyzes a reaction near its thermodynamic equilibrium (Keq ~ 0.3) under physiological conditions, which may preclude a relevant controlling role on the glycolytic flux (Saavedra et al. 2007). However, it has been recently demonstrated that the amebal enzyme can be potently inhibited by erythrose-4-phosphate (Ery4P), an intermediary of the non-oxidative branch of pentose phosphate pathway (PPP), with a *Ki*

value of 5.9 μM (Marín-Hernández et al. 2011). Therefore, the PPP branch flux may indirectly exert control on the first reactions of the glycolytic flux.

The next step of glycolysis is phosphorylation of Fru6P to fructose-1,6-bisphosphate (Fru1,6BP). In most cells, this reaction is catalyzed by an allosterically modulated, tetrameric ATP-dependent phosphofructokinase (ATP-PFK; EC 2.7.1.11) (Moreno-Sánchez R et al. 2012), which catalyzes an irreversible reaction under physiological conditions due to thermodynamic constraints (Keq ~2300). In contrast, in *E. histolytica*, 90% of PFK activity is accounted by a pyrophosphate-dependent phosphofructokinase (PPi-PFK; EC 2.7.1.90), which catalyzes a fully reversible reaction (Keq ~ 3.2) under physiological conditions (Reeves et al. 1974, Reeves et al. 1976, Saavedra et al. 2005, Saavedra et al. 2007). In the amebal genome there is only one gene for PPi-PFK coding for a protein of 60 kDa (Clark et al. 2007). This enzyme has been kinetically characterized (Reeves et al. 1974, Reeves, Serrano and South 1976, Bruchhaus et al. 1996, Deng et al. 1998, Saavedra et al. 2005). It functions as dimer showing moderate affinity for PPi and Fru6P at physiological pH (Saavedra et al. 2005) (Table 1). The physiological concentrations of Fru6P (1.1 mM) and PPi (0.45 mM) (Saavedra et al. 2007) represent only 1-2 times the *Km* values (Table 1), although to circumvent this limitation, the cells express relatively high PPi-PFK content/activity (Saavedra et al. 2007). It is tempting to speculate that the use of PPi instead of ATP at the level of PFK prevents the negative effect of the turbo design of glycolysis, in which at high glucose concentration, the first ATP consuming reactions of glycolysis may exhaust the ATP before being re-synthesized in the late stages of the pathway (Teusink et al. 1998).

Interestingly, the specificity for PPi of amebal PPi-PFK can be changed to ATP by introducing the single mutation Asn105Gly; this change in the PPi-PFK gene might have phylogenetic implications (Chi and Kemp 2000). Besides Fru6P, the enzyme can use sedoheptulose-7-phosphate (sedoheptul-7P) to produce sedoheptulose 1,7 bisphosphate (sedoheptul 1,7BP) (Reeves et al. 1976); hence, the complete non-oxidative branch of PPP can be catalyzed by the combined action of PPi-PFK, transketolase (TK) and aldolase (Susskind et al. 1982) (Fig. 1).

In addition, the *E. histolytica* genome also contains three genes encoding ATP-dependent PFKs of 48 kDa (Clark et al. 2007) which have only 17% identity with the PPi-PFK sequence (Chi et al. 2001). The ATP-PFK is an allosterically modulated enzyme with low affinity for Fru6P (Km_{Fru6P} = 3.6 mM). Considering that (i) the physiological Fru6P concentration of 1.1 mM (Saavedra et al. 2007) is less than its *Km* value and (ii) within the cell, there is one-order of magnitude lower ATP-PFK activity than PPi-PFK activity (Saavedra et al. 2007), it seems that the contribution of ATP-PFK to the glycolytic flux in *E. hystolytica* is negligible. Therefore, the physiological function of this enzyme remains to be elucidated.

Fru1,6BP is cleaved to glyceraldehyde-3-phosphate (Gly3P) and dihydroxyacetone phosphate (DHAP) (Fig. 1) by a type II metal-dependent Fru1,6BP aldolase (ALDO; EC 4.1.2.13) which diverges from type I metal-independent aldolases present in plants and animals (Sánchez et al. 2002, Saavedra et al. 2005). Two genes are present in the amebal genome differing in an insertion of 28 amino acids (Clark et al. 2007). The *E. histolytica* enzyme is a tetramer that shows high affinity for Fru1,6BP (Table 1) (Kalra et al. 1969, Saavedra et al. 2005) and can be saturated in *in vivo* conditions (Fru1,6BP concentration of 0.43 mM) (Saavedra et al. 2005, Saavedra et al.

2007). The enzyme prefers Co^{2+} as an essential cofactor but other divalent metals can also be used (Kalra et al. 1969, Saavedra et al. 2005). PPi is a competitive inhibitor of the enzyme (Moreno-Sánchez et al. 2008a) (Table 1). As mentioned above, ALDO may participate in the non oxidative branch of the PPP, by cleaving sedoheptul-1,7BP to DHAP and Ery4P (Susskind et al. 1982). Hence, Fru6P, DHAP and Gly3P are precursors of the non-oxidative PPP to produce ribose-5-P (R5P) for the synthesis of nucleotides (Fig. 1).

Inter-conversion of DHAP to Gly3P is catalyzed by triosephosphate isomerase (TPI; E.C. 5.3.1.1). Only one gene is found in the amebal genome (Clark et al. 2007, Landa et al. 1997) and the enzyme has been crystallized (Rodríguez-Romero et al. 2002). In most cells, the enzyme is the most catalytically efficient of the glycolytic enzymes despite its low affinity for substrates (Table 1) (Saavedra et al. 2005) and it catalyzes a reaction close to equilibrium (Keq ~ 0.05); therefore its control over the glycolytic flux is negligible (Saavedra et al. 2007).

Next, Gly3P is phosphorylated and oxidized to 1,3 bisphosphoglycerate (1,3BPG) by glyceraldehyde-3-phosphate dehydrogenase (GAPDH; E.C.1.2.1.12) transferring two electrons to NAD^+. In the *E. histolytica* genome there are 5 annotated GAPDH genes (Clark et al. 2007). The enzyme is a tetramer that shows high affinity for its ligands and specificity for NAD^+ (Saavedra et al. 2005) (Table 1). Recently it was reported that the amebal enzyme is ADP-ribosylated and excreted to the extracellular milieu (Álvarez et al. 2007). This post translational modification suggests that other functions besides its metabolic role might be operating in amebas; indeed, GAPDH is a typical example of a moonlighting enzyme, *i.e.* enzymes that have other physiological functions besides its main and essential metabolic role (Collingridge et al. 2010). In this last regard, it has

been described that GAPDH is involved in gene regulation, cell signaling, and DNA integrity (Sirover 2011).

The first substrate level phosphorylation reaction of glycolysis is catalyzed by 3-phosphoglycerate kinase (PGK; E.C. 2.7.2.3). There is only one gene coding for the amebal dimeric enzyme (Clark et al. 2007). In general, PGKs of most cells transfer the phosphate from position 1 of 1,3 BPG to ADP producing 3-phosphoglycerae (3PG) and ATP. However, the amebal PGK has two orders of magnitude higher preference for guanine nucleotides (Reeves and South 1974, Saavedra et al. 2005, Encalada et al. 2009), although by means of a nucleotide transphosphorylase, ATP can be readily synthesized from GTP. By site directed mutagenesis analysis we demonstrated that tyrosine 239 and glutamic acid 309 are involved in the higher affinity for guanine nucleotides (Encalada et al. 2009).

3-phosphoglycerate mutase (PGAM; E.C. 5.4.2.1) isomerizes 3PG to 2-phosphoglycerate (2PG). Five genes are annotated in the amebal genome as PGAMs (Clark et al. 2007), from which two correspond to bacterial-like 2,3 bisphosphoglycerate (2,3BPG)- independent PGAMs which are not related to the 2,3BPG-dependent PGAMs present in mammalian cells. Accordingly, the recombinant amebal enzyme does not require the cofactor for activity (Saavedra et al. 2005). The enzyme is a monomer which has low affinity for 3PG (Saavedra et al. 2005), and it is present in low content/activity in the cell (Saavedra et al. 2007) (Table 1); these data suggested that the enzyme represents a constraint in the pathway flux which was further demonstrated by metabolic modeling (Saavedra et al. 2007, Moreno-Sánchez et al. 2008a). The enzyme is competitively inhibited by PPi (Table 1) (Moreno-Sánchez et al. 2008a) and it is also inhibited in amebas incubated with reactive oxygen species (Husain et al. 2012).

Enolase (ENO; E.C.4.2.1.11) converts 2PG into phosphoenolpyruvate (PEP). There is only one gene in the amebal genome coding for this enzyme (Clark et al. 2007). The amebal enzyme is a tetramer and shows high affinity for its ligands (Saavedra et al. 2005), whereas 3PG and PPi are weak competitive inhibitors (Table 1) (Moreno-Sánchez et al. 2008a). Recently it was demonstrated that amebal ENO may translocate to the nucleus where inhibits cytosine-5-methyltransferase 2 (Dnmt2) that participates in DNA and tRNA methylation (Tovy et al. 2010). Moreover, ENO protein from *Entamoeba invadens*, *E. histolytica* and *Naegleria fowleri* has also been found in vesicle and cyst walls (Segovia-Gamboa et al. 2011). Thus, the ENO non-glycolytic functions described for other cells (Collingridge et al. 2010) can be also extended to the amebal protein.

In most cells, PEP is dephosphorylated to pyruvate (Pyr) producing ATP in the second reaction of glycolytic substrate-level phosphorylation catalyzed by pyruvate kinase (PYK; E.C. 2.7.1.40). Thermodinamically, this reaction is irreversible under physiological conditions (Keq ~ 3.2×10^5). In contrast, amebas have the PPi-dependent enzyme pyruvate phosphate dikinase (PPDK; E.C. 2.7.9.1) which catalyze a reversible reaction at physiological pHs (Keq ~ 0.005) and is also present in anaerobic bacteria, other protists as trypanosomatids and plants. The tetrameric enzyme transfers high-energy phosphate groups from PEP and PPi to AMP to produce ATP, Pi and Pyr (Reeves 1968, Saavedra-Lira et al. 1998, Saavedra et al. 2005,). The enzyme kinetic parameters have been determined (Saavedra-Lira et al 1998, Saavedra et al. 2005). Despite being the slowest enzyme in its pure form, this inconvenient is circumvented by its high content/activity in the cell and its high affinity for substrates (Table 1).

In addition, the amebal genome contains three open reading frames for putative PYK genes (Clark et al. 2007) and the kinetic characterization of a PYK activity in

cytosolic parasite extracts was reported by our group (Saavedra et al. 2004). The amebal PYK activity represents only 10% of the PPDK activity within the cell (Table 1) (Saavedra et al. 2007); and shows non-essential activation by Fru1,6BP like many other PYKs (Saavedra et al. 2004). However, the recombinant or native enzyme has not been purified and studied neither its physiological function elucidated.

2.1. Alternative routes of PEP to Pyr transformation

Alternatively to PPDK (and to a minor extent PYK), amebas can transform PEP to Pyr by three sequential reactions (Fig. 1). First, a PEP carboxytransphosphorylase (PEPCT; E.C. 4.1.1.38) (Reeves 1970) catalyzes carboxylation of PEP to oxaloacetate (OAA) using Pi as co-substrate instead of GDP as the typical PEP carboxykinase (E.C. 4.1.1.32). Hence, the amebal enzyme produces PPi, thus representing another source of PPi for glycolytic enzymes, whereas in bacteria, PEPCT serves for anaplerotic supply of OAA. Further, OAA is reduced to malate by a NADH-dependent malate dehydrogenase (MDH; E.C.1.1.1.37) and malate is in turn decarboxylated and oxidized by a $NADP^+$-dependent and decarboxylating malate dehydrogenase (malic enzyme; ME; E.C. 1.1.1.40) to produce Pyr (Reeves 1970). The resulting effect of this PEP-Pyr loop is transhydrogenation of NADH to NADPH making available NAD^+ for glycolysis, and PPi and dicarboxylic acids for anaplerotic purposes. Unfortunately, the gene encoding a PEPCT has not been identified (Clark et al. 2007) and to date, no kinetic information has been reported for these enzymes. ME has been used to distinguish *E.histolytica/E. dispar* from other amebas (Sargeaunt 1987).

3. Pyruvate metabolism

3.1 Pyruvate decarboxylation and oxidation

Pyruvate is at a crossroad of glucose catabolism (Fig. 1). *E. histolytica* lacks pyruvate dehydrogenase and pyruvate decarboxylase; hence, decaboxylation and oxidation of Pyr to acetyl-coenzyme A (acetyl-CoA) and CO_2 is catalyzed by pyruvate:ferredoxin oxidoreductase (PFOR; E.C. 1.2.7.1) which transfers two electrons to two ferredoxin (Fd) molecules (Reeves et al. 1977, Lo and Reeves 1978,). Two genes for PFOR and seven for Fd are annotated in the amebal genome (Clark et al. 2007). Reduced Fd (Fd_{red}) is involved in metronidazole activation, the current drug used to treat amebiasis. It has been demonstrated that PFOR down-regulation appears not to be a mechanism for resistance against this drug; instead, superoxide dismutase and peroxiredoxin over-expression and Fd down-regulation were observed in metronidazole resistant strains (Wassmann et al. 1999). The kinetic properties of the amebal PFOR have been determined (Reeves et al. 1977, Lo and Reeves 1978, Pineda et al. 2010). PFOR is the third most abundant enzyme activity from the amebal fermentative pathway, only preceded by PGK and TPI (Pineda et al. 2010) (Table 1). At physiological pH, the enzyme has low affinity for Pyr and high for coenzyme A (CoA); high acetyl-CoA concentration is a potent inhibitor (Pineda et al. 2010). The enzyme can use other 2-oxoacids such as oxaloacetate and α–ketobutyrate but with extremely low affinities (*Km* >10 mM) and cannot use α-ketoglutarate (Pineda et al. 2010). Consequently, these carbon-skeletons derived from amino acid degradation appear not to be physiologically used by PFOR for acetyl-CoA formation as previously suggested (Clark et al 2007). Therefore, other 2-oxoacid oxidoreductases are very likely involved in amino acid utilization as fuels.

PFOR contains three iron-sulfur clusters which are highly sensitive to oxidation and inactivation by ROS (Imlay 2006). In agreement, the amebal PFOR is inhibited at low micromolar concentrations of O_2 and H_2O_2 (Table 1) (Pineda et al. 2010, Ramos-Martínez et al. 2009). Our group reported that *E. histolytica* subjected to an acute supra-physiological O_2 concentration (0.63 mM) promoted accumulation of Glu6P, Fru6P and Pyr and diminished EtOH and ATP contents. These changes were the result of strong inhibition of PFOR and the NADH-dependent bifunctional aldehyde-alcohol dehydrogenase (ADHE; E.C. 1.2.1.10 1.1.1.1) (Pineda et al. 2010, Ramos-Martínez et al. 2009). Interestingly, virulent *E. histolytica* was able to rapidly restore PFOR activity after the insult whereas non-virulent amebas were not, suggesting a more robust antioxidant protection in the former (Ramos-Martínez 2009).

3.2 Ethanol formation

Acetyl-CoA produced by PFOR is further transformed to EtOH which is the main product of glucose catabolism in amebas. In *E. histolytica*, EtOH fluxes under aerobic conditions are 15-39 nmoles EtOH/min x mg cell protein, values which are one order of magnitude higher than those for acetate formation of 2.8-3.6 nmoles acetate/min x mg cell protein determined under the same condition (Saavedra et al. 2007, Pineda et al. 2010, Pineda et al. 2013). Under anaerobic conditions (N_2 atmosphere) axenic amebas does not produce acetate (Reeves et al. 1977). Hence, contrary to the common belief, *E. histolytica* mainly produce EtOH under both anaerobic and aerobic conditions.

Ethanol production from acetyl-CoA is catalyzed by ADHE (Lo and Reeves 1978). This enzyme is similar to the bifunctional enzyme present in bacteria, in which the N-terminal domain contains the aldehyde dehydrogenase activity whereas the C-terminal

domain has the alcohol dehydrogenase activity containing an Fe^{2+} binding site (Espinosa et al. 2001). The enzyme transforms acetyl-CoA to EtOH through a thiohemiacetal intermediary bound to the enzyme which is further reduced to EtOH (Fig. 1). Two NADH molecules are oxidized *per* EtOH produced in the overall ADHE reaction; since one NADH *per* pyruvate formed is synthesized by GAPDH in glycolysis, then, the extra NADH molecule required to synthesize EtOH can be provided by Fd_{red} produced in the PFOR reaction. Fd_{red} can be oxidized by a ferredoxin:NAD^+ oxidoreductase ($Fd:NAD^+$ OR) producing NADH and regenerating oxidized Fd (Fd_{ox}) (Lo and Reeves 1978, Bringaud et al. 2010) (Fig. 1).

Recombinant ADHE has been kinetically characterized (Lo and Reeves 1978, Espinosa et al. 2001, Bruchhaus and Tannich 1994, Yong et al. 1996). The enzyme has almost two-three orders of magnitude higher affinity for acetyl-CoA and acetaldehyde than for EtOH (Table 1). This suggests that ADHE *in vivo* mostly functions in the direction of EtOH production. The enzyme is also highly sensitive to inhibition by oxidative stress (Pineda et al. 2010).

Interestingly, ADHE can form helical rod-like ultra-structures called spirosomes which serve for its stabilization (Avila et al. 2002). Moreover, this enzyme seems to be associated with Fe^{2+} transport from the extracellular milieu (Reyes-López et al. 2011), which suggests additional functional roles for this enzyme.

At least other 17 genes coding for alcohol dehydrogenases and one for aldehyde dehydrogenase have been annotated in the *E. histolytica* genome (Clark et al. 2007). Two NADPH-dependent alcohol dehydrogenases (ADH1 and ADH3), and one $NADP^+$-dependent aldehyde dehydrogenase have been kinetically characterized (see Clark et al. 2007 for a review). These enzymes can use free medium-chain and aromatic

aldehydes but not acetyl-CoA as substrates. Therefore, they seem not to be involved in fermentative glycolysis and their physiological functions have not been elucidated. Then, ADHE is the main enzyme involved in EtOH formation in amebas.

3.3 Acetate metabolism

Under aerobic conditions, part of the acetyl-CoA can be alternatively transformed to acetate (Fig. 1) by an ADP-forming acetyl-CoA synthetase (AcCoAS; E.C. 6.2.1.13) named after the reverse reaction and also known as acetate thiokinase (Reeves et al. 1977). In amebas it catalyzes hydrolysis of the high-energy thioester bond of acetyl-CoA to synthesize ATP from ADP and Pi (Reeves et al. 1977). In contrast to the most common acetate thiokinases which use AMP and PPi as substrates, the amebal, giardial and some anaerobic bacterial enzymes use ADP and Pi (Reeves et al. 1977, Field et al 2000). Recently we reported the properties of the enzyme in the *E. histolytica* cytosolic fractions (Pineda et al. 2010); the enzyme has lower affinity for acetyl-CoA compared to ADHE (Table 1), hence, the latter represent an important competitor of AcCoAS for the metabolite (Fig. 1).

There is controversy on the functional role of acetate formation in amebas. It was early described by Richard Reeves that amebas subjected to aerobic conditions can produce 75% acetate and 25% EtOH whereas under anaerobic conditions this ratio was reversed and EtOH production was favored (Reeves et al. 1977). As ATP is synthesized during production of acetate, it has been thought that amebas are able to support aerobic conditions because they have an extra provision of ATP. However, we have consistently found that after a challenge of hyperoxia (0.63 mM O_2) or under mild aerobic conditions (air-equilibrated saline buffer, 0.18 mM O_2), trophozoites can produce

a maximum of just 20% acetate from glucose catabolism (Pineda et al. 2010, Pineda et al. 2013). After the supra-physiological O_2 challenge, *E. histolytica* trophozoites show decreased ADHE activity and decreased EtOH formation, whereas AcCoAS activity remains unaltered and acetate formation slightly increases (Pineda et al. 2010). ADHE inhibition induced by ROS, can bring about a build-up of acetyl-CoA which can stimulate the flux through AcCoAS resulting in increased acetate production. However, under conditions where ADHE is 50% inhibited by disulfiram, the low flux through the acetate branch is not sufficient to maintain the steady ATP concentration in the cell (Pineda et al. 2013). These results indicate that contribution of AcCoAS to the ATP supply seems negligible. Hence, we have hypothesized that under prolonged aerobic conditions, an increased acetate flux may transiently drain the acetyl-CoA accumulation caused by ADHE inhibition regenerating CoA (Fig. 1). It may be also possible that build-up of acetyl-CoA could serve for the synthesis of other biomolecules. All these hypotheses remain to be tested.

Amebas also have a PPi-dependent acetate kinase (AcK) which synthesize PPi and acetate starting from acetyl-phosphate (acetyl-P) and Pi (Reeves and Guthrie 1975) (Fig. 1). It has been demonstrated that the enzyme can only catalyze the reaction in the direction of acetate formation (Reeves and Guthrie 1975, Fowler et al. 2012). In contrast, in other microorganisms that use acetate as carbon fuel, AcK catalyzes acetyl-P production using acetate as substrate and ATP as high-energy P-donor; acetyl-P is further transformed to acetyl-CoA by a phosphotransacetylase, an enzyme which is absent in amebas. The native (Reeves and Guthrie 1975) and recombinant (Fowler et al. 2012; Citlali Vázquez and Emma Saavedra, unpublished results) amebal AcKs have been characterized. The enzyme reported by Fowler et al. showed lower affinities for

acetyl-P (0.5 mM) and Pi (48.9 mM) compared to those determined for the native (Reeves and Guthrie 1975) and our recombinant enzyme (0.02-0.07 and 2.2-2.6 mM, respectively). This discrepancy may be due to the low sensitivity of the enzymatic assay used by them. In *E. histolytica*, Pi concentration is near 5.4 mM (Saavedra et al. 2007) whereas acetyl-P has not been detected (Citlali Vázquez and Emma Saavedra, unpublished results). It is unknown whether other acyl-phosphates can be used by the amebal enzyme. Further studies are required to determine the physiological role of this AcK in *E. histolytica.*

4. Main glycolytic branches

4.1 Glycogen metabolism

Glu6P is another glycolytic metabolite localized at an important cross-road. Amebas lack the genes coding for the enzymes of the PPP oxidative branch: glucose-6-phosphate dehydrogenase, 6-phosphogluconolactonase and 6-phosphogluconate dehydrogenase (Reeves 1984, Clark et al. 2007). Hence, Glu6P can continue through its fermentative route and serve as precursor for glycogen synthesis, or is a glycogen degradation product (Fig. 1). Glu6P is inter-converted to glucose-1P (Glu1P) by the action of phosphoglucomutase (PGM) (Takeuchi et al. 1977a). This enzyme together with HK has been used as the gold standards to distinguish *E. histolytica* from *E. dispar* (Sargeaunt 1987, Ortner et al. 1997b). Glycogen is abundant in the parasite accounting for up to 3 M of stored glucose equivalents (Saavedra et al. 2007); therefore, glycogen synthesis is highly active in amebas grown on high external glucose concentrations. Glycogen synthesis (Fig. 1) is performed by the sequential action of UDP-glucose pyrophosphorylase (UDP-Gluc PPiase) and glycogen synthase (GS) (Takeuchi et al.

1977a, Reeves 1984,). Then, glycogen synthesis may be an important source of PPi (Reeves 1984, Saavedra et al. 2007)] (Fig. 1). On the other hand, glycogen degradation is catalyzed by the action of glycogen phosphorylase (GP) (Takeuchi et al. 1977b, Reeves 1984). No information is available on the mechanisms that regulate the synthesis and degradation of glycogen.

4.2 Chitin synthesis

It has been recently demonstrated in *E. invadens* that glycogen degradation mainly provides the carbon-skeletons for chitin synthesis (Samanta and Ghosh 2012, Jeelani et al. 2012). Glu6P from glycogen degradation, or from external glucose, isomerizes to Fru6P by HPI (Fig. 1). Fru6P is the glycolytic precursor for chitin synthesis. This metabolite is in turn isomerized and aminated by glucosamine-6-phosphate isomerase (GN6PI) to produce glucosamine-6-phosphate (GlcN6P), the first intermediate of chitin synthesis (Fig. 1). Increase in the level of this metabolite during encystation of *E. invadens* (Samanta and Ghosh 2012, Jeelani et al. 2012), and in *E. histolytica* subjected to oxidative stress (Hussain et al. 2012) has been observed. It has been recently demonstrated that *E. histolytica* can form cyst-type structures induced by ROS which stimulate chitin synthesis (Aguilar-Díaz et al. 2010).

4.3. Amino acid synthesis

Glycolytic triose-phosphates are precursors for amino acid synthesis: 3PG for serine, glycine and cysteine (Nozaki et al. 2005) and Pyr for alanine (Fig. 1). Genes encoding the enzymes in the respective routes have been identified in the *E. histolytica* genome (Clark et al. 2007). Ser and Cys synthesis are relevant for amebas since they

lack glutathione (Fahey et al. 1984), the main antioxidant molecule in most cells; therefore Cys replaces GSH as the antioxidant metabolite in amebas. In comparison, other amino acid synthesis pathways are not present or reduced, because these metabolites can be abundant in the extracellular medium by the action of a great variety of amebal proteases. On this regard, amebas are able to actively take up and consume a wide range of amino acids (Zuo and Coombs 1995).

5. Controlling mechanisms of amebal fermentative glycolysis

The amebal HK, PPi-PFK and PPDK markedly diverge in their enzymatic properties from those of the tightly-regulated mammalian HK, ATP-PFK and PYK which are, together with GLUT, the main controlling and regulatory steps of glycolysis in these last cells (reviewed in Moreno-Sánchez et al. 2008b). Moreover, with the exception of HK, in amebas all the reactions from HPI to ADHE are thermodynamically reversible under physiological conditions (Fig. 1). Thus, it seems that neither allosteric regulatory mechanisms nor thermodynamic constraints can be applied to identify and determine what controls the fermentative glycolysis in *E. histolytica*. Therefore, it becomes apparent that only an integral analysis of all the parameters and variables of the pathway, *i.e.* enzyme/transporter kinetic properties and levels of enzyme/transporter expression, metabolite concentrations and metabolic fluxes in the cell, and using the fundamentals of Metabolic Control Analysis (MCA) (Fell 1997, Moreno-Sánchez et al. 2008b) for analysis, it is possible to identify/determine the control structure and understand the underlying controlling mechanisms of the pathway in this parasite.

5.1 Metabolic Control Analysis

Metabolic Control Analysis (MCA) is a Systems Biology approach that analyzes metabolic networks with the goal of elucidating their underlying mechanism of control and regulation (Fell 1997, Moreno-Sánchez et al. 2008b, Westerhoff 2011). On this regard, MCA makes a clear distinction between control and regulation of metabolism. *"Control"* indicates the extent to which the flux or the concentration of an intermediary of a metabolic pathway is altered when the activity of one step (or group of steps) is changed. These values are quantitatively represented by the *flux*- and *concentration-control coefficients*, respectively. *"Regulation"* refers to how the flux of a pathway or a metabolite level is modified when the rate of an individual step is changed by cellular factors other than their substrates/products (*e.g.* enzyme activity modulators such as hormones and ions), and is quantitatively represented by the *response coefficient* (Fell 1997). Regulation is more related to the homeostatic control of metabolic pathways.

MCA studies have demonstrated that, contrary to the common concept of rate-limiting step used in biochemistry textbooks and scientific literature outside metabolic regulation, the control of a pathway is distributed in different degrees among all the pathway components, with two or three steps displaying the highest control (reviewed in Fell 1997, Moreno-Sánchez et al. 2008b). Thus, using MCA it is possible to determine the control distribution of a pathway flux in any cell model.

The flux control coefficient is symbolized as C^{J}_{ai}, in which J is the pathway flux and a is the activity of an enzyme/transporter i in the cell. To determine the C^{J}_{ai}, the enzyme/transporter within the cell has to be gradually titrated above and below the wild type level (the reference point) and the pathway flux has to be in parallel assessed. From plots of normalized pathway flux *versus* enzyme activity, the C^{J}_{ai} is calculated from the slope of the tangent of the fitting of the closest points to the WT level (Fig. 2A).

Performing this experiment for each pathway enzyme, the whole set of C^J_{ai} can be calculated and hence the pathway control distribution. The sum of all C^J_{ai} in the pathway have to be add up 1 (Summation theorem of MCA). In concordance, an enzyme with a C^J_{ai} equals to 1 (enzyme E1 in Fig. 2A) means that it is the one and only controlling step of the pathway flux, *i.e.* it is a true rate-limiting step. In contrast, an enzyme with a C^J_{ai} approaching zero (enzyme E2 in Fig. 2A) means that it has negligible control on the pathway flux.

Experiments similar to those described in Fig. 2A to determine the control distribution of a metabolic pathway, which seems simple at first glance, has demanded the design of several different experimental strategies to change the enzyme rate in the cells of only one enzyme at a time, without affecting the rest of the pathway enzymes/transporters. MCA has been successfully applied to several pathways such as oxidative phosphorylation in normal and tumor cells and glycolysis in several biological models (reviewed in Moreno-Sánchez et al. 2008b).

5.2 Kinetic modeling of metabolic pathways

Bioinformatics tools have been incorporated to MCA studies to construct kinetic models of several pathways to determine their control distribution (for a kinetic model database see the JWS Online Cellular Systems Modeling at http://jjj.biochem.sun.ac.za/index.html and Hübner et al. 2011). This approach is now called bottom-up systems biology to distinguish it from the top-bottom systems biology strategies that are fueled of data obtained from high-throughput transcriptomic, proteomic and metabolomic analyses (Westerhoff 2011). Only a few kinetic models of glycolysis in pathologic cells have been reported, in particular for tumor cells (Marín-

Hernández et al. 2011) and human parasites *Trypanosoma brucei* (Bakker et al. 1999) and *E. histolytica* by our research group (Saavedra et al. 2007, Moreno-Sánchez et al. 2008a). The reason of this scarcity of studies derives from the fact that metabolic modeling requires for an elevated amount of experimental data for their construction and validation (Hübner et al. 2011).

The aim of kinetic modeling is to build a computational representation that may reproduce the physiological behavior of a metabolic/signaling pathway using the knowledge of the kinetic properties of the individual enzymes and transporters (Snoep 2005). A validated model should predict with the highest possible accuracy the pathway´s behavior in the cell regarding flux rates, metabolite concentrations and control structure, and unveil not-so-apparent properties (Snoep 2005). Kinetic models that apply MCA also help to identify the kinetic mechanisms of why an enzyme controls or does not control a pathway flux or a metabolite concentration.

5.3 Kinetic modeling of amebal glucose fermentation

To construct the kinetic model of amebal glycolysis (Saavedra et al. 2007) it was necessary to determine the kinetic properties of all the pathway enzymes from HK to PPDK determined under the same experimental conditions and close to the physiological pH, temperature and ionic composition values as described in (Saavedra et al. 2005). Such dataset included the affinity for substrates, products, activators and inhibitors for each pathway reaction. Moreover, it was also necessary to determine the enzyme maximal activities (*Vmax*) in the forward and reverse direction of each reaction, metabolite concentrations and pathway fluxes within amebal trophozoites, employing the same strain and under identical incubation conditions. Using the enzyme kinetic data,

appropriate rate equations for each reaction and concentrations of some precursors that supply the pathway such as glucose, ATP, Pi and NAD^+, were assembled in the software Gepasi (later renamed CoPaSi from Complex Pathway Simulator, both of which allow MCA (Hoops et al. 2006)) used as bioinformatics platform. After several rounds of refinement, in which *in vivo* experimentation was required, a kinetic model emerged that could predict the metabolite concentrations and pathway fluxes to values acceptably close to those determined *in vivo* in amebas incubated in the presence of 10 mM glucose (Saavedra et al. 2007). The agreement between modeling and experimentation allowed validation of the kinetic model as a tool to analyze the pathway control distribution.

The model predicted that the highest flux-control steps corresponded to HK, PGAM, glycogen synthesis and PPi synthesis, showing C^J_{ai} *values* of 0.73, 0.65, -0.32 and -0.28, respectively (Table 1); the latter two reactions with negative signs mean that they represent branches that drain metabolites from the main pathway (Saavedra et al. 2007). The main reason of the high HK control is that it is one of the less abundant glycolytic activities/contents in the cell (Table 1); the contribution of AMP and ADP competitive inhibition to the HK controlling role was lower because of the high ATP concentration present in amebas. However, it is possible that these metabolites may have homeostatic control on the metabolic pathway. PGAM also exhibited significant flux-control because it showed low activity/content in the cell (Table 1). These main controlling roles of HK and PGAM were further validated by *in vitro* pathway reconstitution of the two pathway sections and kinetic modeling (Moreno-Sánchez et al. 2008a). This last study allowed identification of new interactions of metabolites different

to substrates and products for several of the enzymes; for example the inhibitory effect of PPi over ALDO, PGAM and ENO and its activation effect over HK.

Some limitations of the amebal kinetic model (Saavedra et al. 2007) were that it did not explicitly include kinetics of glucose transport neither those of the fermentative enzymes PFOR, ADHE, and AcCoAS because, at that time, few or no kinetic parameters were available for these enzymes. For GLUT, the values reported by Reeves (Serrano and Reeves 1974, Serrano and Reeves 1975) were recalculated and used in the model which however were unable to reproduce the metabolite concentrations and fluxes found in the cells (Saavedra et al 2007). This was an important inconvenience because it has been demonstrated by kinetic modeling that glucose transport has significant control on glycolysis of several biological models (reviewed in Moreno-Sánchez et al. 2008b).

5.4 Flux control distribution of amebal glucose fermentation in intact cells

The C^{J}_{ai} of PFOR and ADHE have been recently determined in live amebal trophozoites by inhibitor titration, another MCA strategy, using diphenyleniodonium and disulfiram as specific inhibitors, respectively. The analysis was performed in amebas subjected to aerobic conditions because PFOR and ADHE are susceptible to inhibition by oxidative stress (Ramos-Martínez et al. 2009, Pineda et al. 2010, Pineda et al. 2013). The results showed that PFOR has low control on the fluxes to EtOH and acetate ($C^{JEtOH/\ Jacetate}_{PFOR} < 0.09$), whereas ADHE emerged as the main controlling step of both fluxes ($C^{JEtOH}_{ADHE} = 0.33$ and $C^{Jacetate}_{ADHE} = -0.19$). The analysis also indicated negligible AcCoAS control on both fluxes (Pineda et al. 2013).

Another MCA strategy called elasticity analysis (Moreno-Sánchez et al. 2008b) can be used to determine the flux control exerted by groups of enzymes/transporters of a given pathway in intact cells. This strategy involves determination of the sensitivity (elasticity coefficient) of a group of enzymes to change its rate when a pathway metabolite (M) changes its concentration; M can be any measurable pathway intermediary in the cell. To determine the elasticity coefficients, variations in the steady-state concentration of M are attained, for instance, by gradually increasing the pathway precursor supply and by inhibiting the last pathway reactions. In each experimental setting, the M concentration and pathway flux are in parallel determined in the cells to calculate the elasticity coefficients of the producer and consumer group of enzymes connected through M. From the elasticity coefficients, the C^{J}_{ai} is calculated through the connectivity theorem of MCA (for a review see Moreno-Sánchez et al. 2008b). Following this strategy and moving along the intermediaries Glu6P, Fru6P and Pyr, it was determined that the group constituted by GLUT, HK and glycogen degradation controls ~0.75 the glycolytic flux, whereas the group formed by PFOR, ADHE and AcCoAs controls 0.15-0.23. (Erika Pineda and Emma Saavedra, manuscript in preparation). These results are in agreement with those obtained by both kinetic modeling and inhibitor titration and highlight the relevance of the first segment of the glycolytic pathway, along with ADHE, in controlling the glucose catabolism in the parasite.

6. MCA and drug targeting

Metabolic Control Analysis can be used to identify and validate drug targets in metabolic pathways by identifying the most controlling steps as additional criteria to the

essentiality determined by genetic methods (Hornberg et al. 2007, Saavedra et al. 2007, Moreno-Sánchez et al. 2008b, Hübner et al 2011, Moreno-Sánchez et al. 2010, Olin-Sandoval et al. 2012). The plot shown in Fig. 2A helps us to understand why the majority of gene-silencing experiments identify as essential their targets. Decreasing by more than 80-90% the activity/content of both, controlling and non-controlling steps in a metabolic or signaling pathway, results in a significant decrease in the pathway flux or function. Therefore, a convenient drug-target should be an enzyme/protein which needs to be just slightly inhibited to significantly decrease the pathway flux (enzyme E1 in Fig. 2A), *i.e.* appropriate drug targets should be the components that mainly control the pathway function.

Based on the marked kinetic/genetic differences, the PPi-dependent enzymes have long been proposed as targets for drug-development to tackle the energy metabolism pathway of amebas. The results described on the control distribution of *E. histolytica* fermentative glycolysis using different MCA strategies established that PPi-PFK and PPDK did not exert significant control on the pathway flux and metabolite concentrations. By using kinetic modeling, it was predicted the degree of enzyme inhibition required to decrease the amebal glycolytic flux (Fig. 2B) (Saavedra et al. 2007) and/or the ATP concentration (data not shown). As expected from its low control (Table 1), PPi-PFK and PPDK have to be inhibited by 70% and 92%, respectively, to decrease the pathway flux by 50%. In contrast, a similar pathway flux inhibition can be attained by inhibiting HK and PGAM by only 24% and 55 %, respectively (Fig. 2B) (Saavedra et al.2007). Therefore, after determining the essentiality of an enzyme/protein by genetic methods, kinetic modeling and MCA can help to prioritize drug targets by identifying the main controlling steps in metabolic pathways of parasitic and pathological cells

(Hornberg et al. 2007, Saavedra et al. 2007, Moreno-Sánchez et al. 2008b, Moreno-Sánchez et al. 2010, Marín-Hernández et al. 2011, Olin-Sandoval et al. 2012). On this regard, inhibitors against amebal HK have been identified (Saucedo-Mendiola et al. 2013).

7. CONCLUSIONS

The divergent kinetic properties of the amebal glycolytic-fermentative enzymes compared to their human counterparts did not allow envisioning the controlling and regulatory mechanisms of this pathway in the parasite. By applying MCA-designed experiments and *in silico* metabolic modeling, the main controlling steps in amebal glycolysis were identified. HK, glycogen metabolism (and very probably glucose transport) are important controlling reactions of the first pathway section whereas PGAM and ADHE control the latest stages. By Increasing the knowledge of the kinetic parameters of the enzymes from the most important glycolytic branches together with metabolomic studies will advance our understanding of the dynamic of control and regulation of the intermediary metabolism in *E. histolytica*.

Acknowledgments

Research in the authors´ laboratory received financial support from CONACyT-México (grants No. 83084 and 178638 to E.S.).

References

- Aguilar-Díaz H, Díaz-Gallardo M, Laclette JP, Carrero JC (2010) *In vitro* induction of *Entamoeba histolytica* cyst-like structures from trophozoites. PLoS Negl Trop *Dis* **4**, e607.
- Alvarez AH, Martinez-Cadena G, Silva ME, Saavedra E & Avila EE (2007) *Entamoeba histolytica*: ADP-ribosylation of secreted glyceraldehyde-3-phosphate dehydrogenase. Exp Parasitol 117: 349-356.

- Avila EE, Martínez-Alcaraz ER, Barbosa-Sabanero G, Rivera-Baron EI, Arias-Negrete S, Zazueta-Sandoval R (2002) Subcellular localization of the NAD+-dependent alcohol dehydrogenase in *Entamoeba histolytica* trophozoites. J Parasitol 88(2):217-22.

- Bakker BM, Michels PA, Opperdoes FR, Westerhoff HV (1999) What controls glycolysis in bloodstream form Trypanosoma brucei?J Biol Chem 274: 14551-9.

- Band RN and Cirrito H (1979) Growth response of axenic *Entamoeba histolytica* to hydrogen, carbon dioxide, and oxygen. J Protozool 26: 282-6.

- Bringaud F, Ebikeme C, Boshart M (2010) Acetate and succinate production in amoebae, helminths, diplomonads, trichomonads and trypanosomatids: common and diverse metabolic strategies used by parasitic lower eukaryotes. Parasitology 137: 1315-31.

- Bruchhaus I, Tannich E (1994) Purification and molecular characterization of the NAD^+-dependent acetaldehyde/alcohol dehydrogenase from *Entamoeba histolytica*. Biochem J 303: 743-748.

- Bruchhaus I, Jacobs T, Denart M, Tannich E (1996) Pyrophosphate-dependent phosphofructokinase of *Entamoeba histolytica*: molecular cloning, recombinant expression and inhibition by pyrophosphate analogues. Biochem J 316: 57-63.

- Chi A, Kemp RG (2000) The primordial high energy compound: ATP or inorganic pyrophosphate? J Biol Chem 275: 35677-35679.

- Chi AS, Deng Z, Albach RA & Kemp RG (2001) The two phosphofructokinase gene products of *Entamoeba histolytica*. J Biol Chem 276: 19974-19981.

- Clark CG, Alsmark UC, Tazreiter M, Saito-Nakano Y, Ali V, Marion S, Weber C, Mukherjee C, Bruchhaus I, Tannich E, Leippe M, Sicheritz-Ponten T, Foster PG, Samuelson J, Noël CJ, Hirt RP, Embley TM, Gilchrist CA, Mann BJ, Singh U, Ackers JP, Bhattacharya S, Bhattacharya A, Lohia A, Guillén N, Duchêne M, Nozaki T, Hall N. (2007) Structure and content of the *Entamoeba histolytica* genome. Adv Parasitol 65: 51-190.

- Collingridge PW, Brown RW, Ginger ML (2010) Moonlighting enzymes in parasitic protozoa. Parasitology 137: 1467-75.

- Deng Z, Huang M, Singh K, Albach RA, Latshaw SP, Chang KP, Kemp RG (1998) Cloning and expression of the gene for the active PPi-dependent phosphofructokinase of *Entamoeba histolytica*. Biochem J 329: 659-664.

- Encalada R, Rojo-Dominguez A, Rodriguez-Zavala JS, Pardo JP, Quezada H, Moreno-Sanchez R & Saavedra E (2009) Molecular basis of the unusual catalytic preference for GDP/GTP in *Entamoeba histolytica* 3-phosphoglycerate kinase. FEBS J 276: 2037-2047.

- Espinosa A, Yan L, Zhang Z, Foster L, Clark D, Li E, Stanley SL Jr. (2001) The bifunctional *Entamoeba histolytica* alcohol dehydrogenase 2 (EhADH2) protein is necesary for amebic growth and survival and requires an intact C-terminal domain for both alcohol dehydrogenase and acetaldehyde dehydrogenase activity. J Biol Chem 276: 20136-20143.

- Fahey RC, Newton GL, Arrick B, Overdank-Bogart T, Aley SB (1984) *Entamoeba histolytica*: a eukaryote without glutathione metabolism. Science 224(4644):70-2.

- Fell D (1997) Understanding the control of metabolism. Portland Press, London.

- Field J, Rosenthal B, Samuelson J (2000) Early lateral transfer of genes encoding malic enzyme, acetyl-CoA synthetase and alcohol dehydrogenases from anaerobic prokaryotes to *Entamoeba histolytica.* Mol Microbiol 38: 446-455.

- Fowler ML, Ingram-Smith C, Smith KS (2012) Novel pyrophosphate-forming acetate kinase from the protist *Entamoeba histolytica*. Eukaryot Cell 11: 1249-1256.

- Gillin FD, Diamond LS (1981) *Entamoeba histolytica* and *Giardia lamblia*: effects of cysteine and oxygen tension on trophozoite attachment to glass and survival in culture media. Exp Parasitol 52(1):9-17.

- Hoops S, Sahle S, Gauges R, Lee C, Pahle J, Simus N, Singhal M, Xu L, Mendes P & Kummer U (2006) COPASI--a COmplex PAthway SImulator. Bioinformatics 22: 3067-3074.

- Hornberg JJ, Bruggeman FJ, Bakker BM, Westerhoff HV (2007) Metabolic control analysis to identify optimal drug targets. Prog Drug Res 64: 172-189.

- Hübner K, Sahle S, Kummer U (2011) Applications and trends in systems biology in biochemistry. FEBS J 278: 2767-857.

- Husain A, Sato D, Jeelani G, Soga T, Nozaki T (2012) Dramatic increase in glycerol biosynthesis upon oxidative stress in the anaerobic protozoan parasite *Entamoeba histolytica.* PLoS Negl Trop Dis 6: e1831.

- Imlay JA (2006) Iron-sulphur clusters and the problem with oxygen. Mol Microbiol 59: 1073-1082.

- Jeelani G, Sato D, Husain A, Escueta-de Cadiz A, Sugimoto M, Soga T, Suematsu M, Nozaki T (2012) Metabolic profiling of the protozoan parasite *Entamoeba invadens* revealed activation of unpredicted pathway during encystation. PLoS One 7: e37740.

- Kalra IS, Dutta G, Mohan-Rao VK (1969) *Entamoeba histolytica*: Effect of metal ions, metal binders, therapeutics, antibiotics, and inhibitors on aldolase activity. Exp Parasitol 24: 26-31.

- Kroschewski H, Ortner S, Steipe B, Scheiner O, Wiedermann G, Duchêne M (2000) Differences in substrate specificity and kinetic properties of the recombinant hexokinases HXK 1 and HXK 2 from *Entamoeba histolytica*. Mol Biochem Parasitol 105: 71-80.

- Ladas SD, Karamanolis G and Ben-Soussan E (2007) Colonic gas explosion during therapeutic colonoscopy with electrocautery. World J Gastroenterol 13: 5295-8.

- Landa A, Rojo-Domínguez A, Jiménez L, Fernández-Velasco DA (1997) Sequencing, expression and properties of triosephosphate isomerase from *Entamoeba histolytica*. Eur J Biochem 247: 348-355.

- Lo HS, Reeves RE (1978) Pyruvate-to-ethanol pathway in *Entamoeba histolytica*. Biochem J 171: 225-230.

- Marín-Hernández A, Gallardo-Pérez JC, Rodríguez-Enríquez S, Encalada R, Moreno-Sánchez R, Saavedra E (2011) Modeling cancer glycolysis. Biochim Biophys Acta 1807,:755-67.

- Moreno-Sanchez R, Encalada R, Marin-Hernandez A & Saavedra E (2008a) Experimental validation of metabolic pathway modeling. FEBS J 275: 3454-3469.

- Moreno-Sánchez R, Saavedra E, Rodríguez-Enríquez S, Olín-Sandoval V (2008b) Metabolic control analysis:a tool for designing strategies to manipulate metabolic pathways. J Biomed Biotechnol 2008:597913.

- Moreno-Sánchez R, Saavedra E, Rodríguez-Enríquez S, Gallardo-Pérez JC, Quezada H, Westerhoff HV (2010) Metabolic control analysis indicates a change of strategy in the treatment of cancer. Mitochondrion 10: 626-639.

- Moreno-Sánchez R, Marín-Hernández A, Gallardo-Pérez JC, Quezada H, Encalada R, Rodríguez-Enríquez S, Saavedra E (2012) Phosphofructokinase type 1 kinetics, isoform expression, and gene polymorphisms in cancer cells. J Cell Biochem 113(5):1692-703

- Nozaki T, Ali V, Tokoro M (2005) Sulfur-containing amino acid metabolism in parasitic protozoa. Adv Parasitol 60**:**1-99.

- Olin-Sandoval V, González-Chávez Z, Berzunza-Cruz M, Martínez I, Jasso-Chávez R, Becker I, Espinoza B, Moreno-Sánchez R, Saavedra E (2012) Drug target validation of the trypanothione pathway enzymes through metabolic modelling. FEBS J 279:1811-33.

- Ortner S, Plaimauer B, Binder M, Scheiner O, Wiedermann G, Duchêne M (1995) Molecular analysis of two hexokinase isoenzymes from *Entamoeba histolytica*. Mol Biochem Parasitol 73(1-2):189-98

- Ortner S, Clark CG, Binder M, Scheiner O, Wiedermann G, Duchêne M (1997a) Molecular biology of hexokinases isoenzyme pattern that distinguishes pathogenic *Entamoeba histolytica* from nonpathogenic *Entamoeba dispar*. Mol Biochem Parasitol 86: 85-94

- Ortner S, Binder M, Scheiner O, Wiedermann G, Duchêne M (1997b) Molecular and biochemical characterization of phosphoglucomutases from *Entamoeba histolytica* and *Entamoeba dispar*. Mol Biochem Parasitol 90(1):121-9.

- Pineda E, Encalada R, Rodriguez-Zavala JS, Olivos-Garcia A, Moreno-Sanchez R & Saavedra E (2010) Pyruvate:ferredoxin oxidoreductase and bifunctional aldehyde-alcohol dehydrogenase are essential for energy metabolism under oxidative stress in *Entamoeba histolytica*. FEBS J 277: 3382-3395.

- Pineda E, Encalada R, Olivos-García A, Néquiz M, Moreno-Sánchez R, Saavedra E (2013) The bifunctional aldehyde-alcohol dehydrogenase controls ethanol and acetate production in *Entamoeba histolytica* under aerobic conditions. FEBS Lett. 587: 178-184.

- Ramos-Martinez E, Olivos-Garcia A, Saavedra E, Nequiz M, Sanchez EC, Tello E, El-Hafidi M, Saralegui A, Pineda E, Delgado J, et al. (2009) Entamoeba histolytica: oxygen resistance and virulence. Int J Parasitol 39: 693-702.

- Razmjou E, Haghighi A, Rezaian M, Kobayashi S, Nozaki T (2006) Genetic diversity of glucose phosphate isomerase from *Entamoeba histolytica.* Parasitol Int 55: 307-311.

- Reeves RE (1968) A new enzyme with the glycolytic function of pyruvate kinase. J Biol Chem 263: 3202-3204.
-
- Reeves RE (1970) Phosphopyruvate carboxylase from *Entamoeba histolytica*. Biochim Biophys Acta 220: 346-349.
-
- Reeves RE (1984) Metabolism of *Entamoeba histolytica* Schaudinn,1903. Adv Parasitol 23: 105-142.
-
- Reeves RE, Guthrie JD (1975) Acetate kinase (pyrophosphate). A fourth pyrophosphate-dependent kinase from *Entamoeba histolytica*. Biochem Biophys Res Commun 66: 1389-95
-

- Reeves RE, South D (1974) Phosphoglycerate kinase (GTP). An enzyme from *Entamoeba histolytica* selective for guanine nucleotides. Biochim Biophys Res Comm 58: 1053-1057.
-
Reeves RE, Montalvo F, Sillero A (1967) Glucokinase from *Entamoeba histolytica* and related organism. Biochemistry 6: 1752-1760.

- Reeves RE, South DJ, Blytt HJ, Warren LG (1974) Pyrophosphate:D-fructose 6-phosphate 1-phosphotransferase. A new enzyme with the glycolytic function of 6-phosphofructokinase. J Biol Chem 249: 7737-7741.

- Reeves RE, Serrano R, South DJ (1976) 6-phosphofructokinase (pyrophosphate). Properties of the enzyme from *Entamoeba histolytica* and its reaction mechanism. J Biol Chem 251: 2958-2962.

- Reeves RE, Warren LG, Susskind B, Lo HS (1977) An energy-conserving pyruvate-to-acetate pathway in *Entameoba histolytica*. Pyruvate synthase and a new acetate thiokinase. J Biol Chem 252: 726-731.
-
- Reyes-Lopez M, Bermudez-Cruz RM, Avila EE & de la Garza M (2011) Acetaldehyde/alcohol dehydrogenase-2 (EhADH2) and clathrin are involved in internalization of human transferrin by *Entamoeba histolytica*. Microbiology 157: 209-219.

- Rodríguez-Romero A, Hernández-Santoyo A, del Pozo Yauner L, Kornhauser A, Fernández-Velasco DA (2002) Structure and inactivation of triosephosphate Isomerase from *Entamoeba histolytica*. J Mol Biol 322: 669-675.

- Saavedra-Lira E, Ramirez-Silva L, Pérez-Montford R (1998) Expression and characterization of recombinant pyruvate phosphate dikinase from *Entamoeba histolytica*. Biochim Biophys Acta 1382: 47-54.

- Saavedra E, Olivos A, Encalada R & Moreno-Sanchez R (2004) Entamoeba histolytica: kinetic and molecular evidence of a previously unidentified pyruvate kinase. Exp Parasitol 106: 11-21.

- Saavedra E, Encalada R, Pineda E, Jasso-Chávez R, Moreno-Sánchez R (2005) Glycolysis in *Entamoeba histolytica*. Biochemical characterization of recombinant glycolytic enzymes and flux control analysis. FEBS J 272: 1767-1783.

- Saavedra E, Marin-Hernandez A, Encalada R, Olivos A, Mendoza-Hernandez G & Moreno-Sanchez R (2007) Kinetic modeling can describe in vivo glycolysis in *Entamoeba histolytica*. FEBS J 274:, 4922-4940

- Samanta SK, Ghosh SK (2012) The chitin biosynthesis pathway in *Entamoeba* and the role of glucosamine-6-P isomerase by RNA interference. Mol Biochem Parasitol 186: 60-68.

- Sánchez L, Horner D, Moore D, Henze K, Embley T, Müller M (2002) Fructose-1,6-biphosphate aldolases in amitochondriate protists constitute a single protein subfamily with eubacterial relationships. Gene 295: 51-59.

- Sargeaunt PG (1987) Zymodemes of *Entamoeba histolytica.* Parasitol Today 3(5):158.

- Saucedo-Mendiola ML, Salas-Pacheco JM, Nájera H, Rojo-Domínguez A, Yépez-Mulia L, Avitia-Domínguez C, Téllez-Valencia A (2013) Discovery of Entamoeba histolytica hexokinase 1 inhibitors through homology modeling and virtual screening. J Enzyme Inhib Med Chem. doi:10.3109/14756366.2013.779265
-

- Segovia-Gamboa NC, Talamás-Rohana P, Ángel-Martínez A, Cázares-Raga FE, González-Robles A, Hernández-Ramírez VI, Martínez-Palomo A, Chávez-Munguía B (2011) Differentiation of *Entamoeba histolytica*: a possible role for enolase. Exp Parasitol 129: 65-71

- Serrano R, Reeves RE (1974) Glucose transport in *Entamoeba histolytica*. Biochem J 144: 43-48.

- Serrano R, Reeves RE (1975) Physiological significance of glucose transport in *Entamoeba histolytica*. Exp Parasitol 37: 411-416.

- Sirover MA (2011) On the functional diversity of glyceraldehyde-3-phosphate dehydrogenase: biochemical mechanisms and regulatory control. Biochim Biophys Acta 1810: 741-51.

- Snoep JL (2005) The Silicon Cell initiative: working towards a detailed kinetic description at the cellular level. Curr Opin Biotechnol 16: 336-43.

- Susskind BM , Warren LG, Reeves RE (1982) A pathway for the interconversion of hexose and pentose in the parasitic amoeba *Entamoeba histolytica*. Biochem J 204:, 191-196.

- Takeuchi T, Weinbach EC, Diamond LS (1977a) *Entamoeba histolytica*: localization and characterization of phosphoglucomutase, uridine diphosphate glucose pyrophosphorylase, and glycogen synthase. Exp Parasitol 43(1):115-21.

- Takeuchi T, Weinbach EC, Diamond LS (1977b) *Entamoeba histolytica*: localization and characterization of phosphorylase and particulate glycogen. Exp Parasitol 43(1):107-14.

- Taylor EW, Bentley S, Youngs D, Keighley MR (1981) Bowel preparation and the safety of colonoscopic polypectomy. Gastroenterology 81(1):1-4.

- Teusink B, Walsh MC, van Dam K, Westerhoff HV (1998) The danger of metabolic pathways with turbo design.Trends Biochem Sci 23: 162-169.
-
- Tovy A, Siman-Tov R, Gaentzsch R, Helm M, Ankri S (2010) A new nuclear function of the *Entamoeba histolytica* glycolytic enzime enolase: the metabolic regulation of cytosine-5 methyltransferase 2 (Dnmt2) activity. PLOS Pathogens **6:** e1000775.

- Wassmann C, Hellberg A, Tannich E, Bruchhaus I (1999) Metronidazole resistance in the protozoan parasite *Entamoeba histolytica* is associated with increased expression of iron-containing superoxide dismutase and peroxiredoxin and decreased expression of ferredoxin 1 and flavin reductase. J Biol Chem. 274**:** 26051-6.

- Westerhoff HV (2011) Systems biology left and right. Methods Enzymol 500: 3-11.

- Wilson JE (2003) Isozymes of mammalian hexokinase: structure, subcellular localization and metabolic function.J Exp Biol 206: 2049-2057.

- Yong TS, Li E, Clark D, Stanley SL Jr. (1996) Complementation of an *Escherichia coli* adhE mutant by the *Entamoeba histolytica* EhADH2 gene provides a method for the identification of new antiamebic drugs Proc Natl Acad Sci USA 93: 6464-6469.

- Zuo X, Coombs GH (1995) Amino acid consumption by the parasitic, amoeboid protists *Entamoeba histolytica* and *E. invadens.*FEMS Microbiol Lett 130: 253-8.

Index terms

3-phosphoglycerate kinase, 9

3-phosphoglycerate mutase, 9

Acetate kinase, 16

Acetate thiokinase, 15

Acetyl-CoA synthetase, 15

Alcohol dehydrogenases, 14

Aldehyde dehydrogenase, 14

Aldolase, 7

Amino acid synthesis, 18

Bifunctional aldehyde-alcohol dehydrogenase, 13

Bottom-up systems biology, 21

Chitin synthesis, 18

Controlling mechanisms, 3

Drug targets, 25

Elasticity analysis, 25

Elasticity coefficient, 25

Enolase, 10

Ferredoxin:NAD^+ oxidoreductase, 14

Flux control coefficient, 20

Gene-silencing, 26

Glucose transport, 4

Glyceraldehyde-3-phosphate dehydrogenase, 8

Glycogen degradation, 18

Glycogen synthesis, 17

Hexokinase, 4

Hexose phosphate isomerase, 5

Intermediary metabolism, 3

Iron-sulfur clusters, 13

Kinetic modeling, 21, 22

Malate dehydrogenase, 11

Malic enzyme, 11

Metabolic Control Analysis, 3, 20

Pathway control distribution, 21

PEP carboxytransphosphorylase, 11

Phosphoglucomutase, 17

Pyrophosphate-dependent phosphofructokinase, 6

Pyruvate kinase, 10

Pyruvate metabolism, 12

Pyruvate phosphate dikinase, 10

Pyruvate:ferredoxin oxidoreductase, 12

Top-bottom systems biology, 21

Triosephosphate isomerase, 8

Turbo design of glycolysis, 6

Table 1. Kinetic properties of carbohydrate metabolism enzymes from *E. histolytica*

Enzyme	*Vmax* recombinant enzymes*	*Vmax* in cell extracts**	Kinetic parameters***	C^{Jetoh}_{enzyme}§	References
GLUT	ND	27-67	Km_{gluc} : 1600-2500 $Km_{2\text{-}DOG}$: 40,000	ND	(Serrano and Reeves 1974, Serrano and Reeves 1975)
HK	FW: 86-158 RW: NA	95	Km_{gluc} : 25-40 $Km_{ATP:}$: 77-290 $Ki_{AMP\ vs\ ATP}$: 0.6-36 $Ki_{ADP\ versus\ ATP}$: 36-235 Ka_{PPi}: 68-150	0.73	(Saavedra et al. 2005, Saavedra et al. 2007, Reeves et al. 1967, Kroschewski et al. 2000)
HPI	FW: 392-608 RW: 182-620	233	Km_{Glu6P}: 610-750 Km_{Fru6P}:130-480 Ki_{Ery4P}: 5.9	0.08	(Saavedra et al 2005, Saavedra et al. 2007, Marín-Hernández et al. 2011)
PPi-PFK	FW: 112-298 RW: 338-392	213	Km_{Fru6P}: 100-695 Km_{PPi}: 50-380 $Km_{Fru1,6BP}$: 109-124 Km_{Pi}: 1140-2300	0.13	[(Saavedra et al. 2005, Saavedra et al. 2007, Reeves et al. 1974, Reeves et al. 1976, Deng et al. 1998)
ATP-PFK	ND	1.4	Km_{Fru6P}: 3800 Km_{ATP}: 120	ND	(Saavedra et al. 2007, Chi et al. 2001)
ALDO	FW: 15-31 RW: 29-34	160	$Km_{Fru1,6BP}$: 4-28 Km_{Gly3P}:108-210 Km_{DHAP}: 105-265 Ki_{PPi} : 210-420	0.09	(Saavedra et al. 2005, Saavedra et al. 2007, Kalra et al. 1969)
TPI	FW: 199-284 RW: 1096-3364	4366	Km_{DHAP}: 445-1655 Km_{Gly3P}: 320-830	0.003	(Saavedra et al. 2005, Saavedra et al.2007, Landa et al. 1997)
GAPDH	FW: 13-27 RW: 36-40	405	Km_{Gly3P}: 59-86 Km_{NAD+}: 59-83	0.08	(Saavedra et al. 2005, Saavedra et al. 2007)
PGK	FW: 279-628 RW: 62-87	3182	$Km_{1,3\ BPG}$: 125-127 Km_{GDP}: 40-292 Km_{ADP}: 600-3400 Km_{3PG}: 505-570 Km_{GTP}: 61-75 Km_{ATP}: 1840-3000	0.04	(Saavedra et al. 2005, Saavedra et al. 2007, Reeves and South 1974, Encalada et al. 2009)
PGAM	FW: 53-42 RW: 6-13	116	Km_{3PG}: 500-840 Km_{2PG}: 66-106 Ki_{PPi} : 173-660	0.65	(Saavedra et al. 2005, Saavedra et al. 2007)

ENO	FW: 89-103 RW: 26-33	508	Km_{2PG}: 55-60 Km_{PEP}:63-102 Ki_{PPi} : 137-280 Ki_{3PG} : 460-610	0.08	(Saavedra et al. 2005, Saavedra et al. 2007)
PPDK	FW: 8-12 RW: 1.5-2.3	304	Km_{PEP}: 20-30 Km_{AMP}: 2-20 Km_{PPi}: 91-470 Km_{Pyr}:68-305 Km_{ATP}: 284	0.0009	(Saavedra et al. 2005, Saavedra et al. 2007, Reeves 1968, Saavedra-Lira et al. 1998)
PYK	ND	28	Km_{PEP}: 18-25 Km_{ADP}: 210- 1050	ND	(Saavedra et al. 2007, Saavedra et al. 2004)
PFOR	ND	1080-1145	Km_{Pyr}:1500-3500 Km_{CoA}: 6-13 $Ki_{acetyl\text{-}CoA}$: 24-36 $IC_{50\ oxygen}$: 34 $IC_{50\ H2O2}$: 6-35	0.09	(Pineda et al. 2010, Pineda et al. 2013)
ADHE	FwALDH:230 Fw:ADH: 500	ALDH: 75-93 ADH: 469	$Km_{acetyl\text{-}CoA}$: 15-40 $Km_{acetaldehyde}$: 150-230 Km_{NADH}: 150-280 Km_{EtOH}: 85000 Km_{NAD+}: 150, 550	0.33	(Pineda et al. 2010, Pineda et al. 2013, , Espinosa et al. 2001, Bruchhaus and Tanich 1994, Yong et al. 1996)
Ac-CoAS	ND	176-254	$Km_{acetyl\text{-}CoA}$: 120	<0.05	(Pineda et al. 2010, Pineda et al. 2013)
AcK	FW: 800	60	$Km_{acetyl\text{-}P}$: 20-70 Km_{Pi} : 2200-2600	ND	(Reeves and Guthrie 1975, , this group)

*_Vmax_ in the forward (Fw) and reverse (RW) reaction in μmoles/min x mg protein. ** _Vmax_ of the Fw reaction in nmoles/min x mg cell protein where determined at pH 6.0 in cytosol-enriched cell fractions [8] except for GLUT which was determined in whole cells (Serrano and Reeves 1974, Serrano and Reeves 1975). *** values in μM. § Flux control coefficient (C^J_{ai}) over etOH flux reported in (Saavedra et al. 2005, Pineda et al. 2013), . ND, not determined. NA, not applicable. Full name of enzymes are described in legend to Fig. 1

Figure legends

Fig. 1 Glucose metabolism in *Entamoeba histolytica*

The main end-product of glucose metabolism is EtOH indicated with a thick arrow; acetate flux represents only 10% of the EtOH flux (thin arrow). Main branches of the fermentative pathway are marked in different colors. Abbreviation are: AcCoAS, acetyl-CoA synthetase (ADP-forming); AcK, acetate kinase (PPi forming); ADHE, bifunctional aldehyde:alcohol dehydrogenase; ALDO, fructose-1,6 bisphosphate aldolase; ATP-PFK, ATP-dependent phosphofructokinase; ENO, enolase; Fd:NAD^+OR, ferredoxin:NAD^+ oxidoreductase; GAPDH, glyceraldehyde-3-phosphate dehydrogenase; Gln, glutamine; Glu, glutamate; GN6PI, glucosamine-6-phosphate isomerase; GS, glycogen synthase; GP, glycogen phosphorylase;HK, hexokinase; HPI, hexose-6-phosphate isomerase; MDH, malate dehydrogenase; ME, malic enzyme; PEPCT, phosphoenolpyruvate carboxytransphosphorylase; PFOR, pyruvate:ferredoxin oxidoreductase; PGK, 3-phosphoglycerate kinase; PGAM, 3-phosphoglycerate mutase; PGM, phosphoglucomutase; PPDK, pyruvate phosphate dikinase; PPi-PFK, PPi-dependent phosphofructokinase; PYK, pyruvate kinase; UDP-GlucPPiase, UDP-glucose pyrophosphorylase; TK, transketolase; TPI, triosephosphate isomerase; UDP-Gluc, UDP-glucose; Xylu5P, xylulose-5-phosphate. Dashed arrows indicate enzymes present in amebas whose contribution to the pathway fluxes are unknown. Dotted arrow indicates that the gene encoding PEPCT has not been identified.

Fig. 2 MCA and drug targeting

Fig. 2A Flux control coefficient distribution for a two-steps pathway

The plots represent how the pathway flux can change by varying the activity of the pathway enzymes. The C^J_{ai} for each enzyme is equal to the slope of the tangent of the experimental points closer to the reference value of 100%. In this example, enzyme 1 has a C^J_{ai} close to 1 whereas enzyme 2 has negligible control.

Fig. 2B *In silico* titration of amebal glycolytic enzymes and its effect on the pahtway flux. Inhibition of the most controlling pathway enzymes (HK and PGAM) have more effects on the flux than inhibiton of low controlling enzymes (PPi-PFK and PPDK).

Conclusiones generales del artículo de revisión:

En la revisión bibliográfica se analizó el metabolismo de la glucosa en *E. histolytica*, haciendo especial énfasis en la glucólisis del parásito.

De acuerdo con esta revisión, el metabolismo intermediario amibiano es un buen campo de estudio en la búsqueda de nuevos blancos para el diseño de fármacos. En este sentido, para el caso de la glucólisis amibiana se han propuesto a las enzimas dependientes de pirofosfato, PPi-PFK y PPDK, como candidatos terapéuticos, debido a que estas enzimas no se encuentran en las células del hospedero. Para la PPi-PFK se ensayaron compuestos análogos al PPi como inhibidores (Bruchhaus et al, 1996). Desafortunadamente, las concentraciones en las que se afectó el crecimiento amibiano estuvieron entre decenas de micromolar hasta milimolar; con estas concentraciones tan elevadas no se puede descartar que el compuesto tenga otros blancos metabólicos dentro del parásito.

Este tipo de aproximaciones, en las que se busca que al inhibir una sola enzima de una vía metabólica se afecte significativamente el flujo a través de la misma, obedece al concepto de que existe una sola "etapa limitante" en las vías metabólicas. En la actualidad esta forma de visualizar el control del metabolismo ha cambiado gracias al Análisis de Control Metabólico (MCA, por sus siglas en inglés) cuyos fundamentos se han revisado recientemente (Fell, 1997; Moreno-Sánchez *et al,* 2008; Nelson y Cox, 2008).

A través del MCA se puede determinar de manera cuantitativa la contribución al control del flujo de la vía de cada una de las enzimas de una vía metabólica. Haciendo uso de las estrategias de control metabólico se determinó casi en su totalidad la distribución de control de la glucólisis amibiana. Con esta aproximación se determinó que los principales puntos de control son la HK y la PGAM, y que para inhibir en 50% el flujo se necesita inhibir el 24% de la actividad de la HK o 55% a la PGAM, o el 18 % de ambas enzimas a la par. Con todo lo anterior se resalta la importancia de la determinación cuantitativa de la contribución al control del flujo de cada una de las enzimas de una vía metabólica.

No obstante el esfuerzo que se hizo en la construcción del modelo cinético de la glucólisis de *E. histolytica*, aún queda mucho trabajo por hacer para comprender más a fondo la manera como el metabolismo intermediario del parásito es regulado.

1.4. Breve descripción de la piruvato:ferredoxina oxidoreductasa

La PFOR es la enzima encargada de descarboxilar oxidativamente al piruvato y unirle una molécula de coenzima A para generar acetil-CoA. Durante esta reacción, los dos electrones, producto de la oxidación del piruvato, se transfieren a dos moléculas de ferredoxina oxidadas. La PFOR se encuentra en organismos microaerofílicos tales como *Trichomonas vaginalis, Clostridium acidi-urici y E. histolytica*, entre otros (Uyeda *et al*, 1977; Reeves, 1974).

La PFOR contiene tres centros fierro- azufre (Fe-S) del tipo 4-4 (Fig. 1.5) a través de los cuales se transfieren los electrones desde el sitio de unión al piruvato hasta la zona de reconocimiento de la ferredoxina. Estos centros se encuentran entre sí a una distancia menor de 15 Å, lo que permite la transferencia de electrones entre ellos (Charon et al, 1999)].

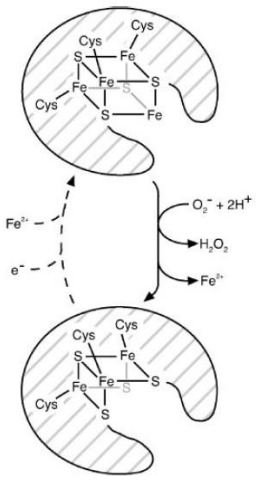

Figura 1.5. Estructura de los centros 4Fe-4S y efecto del oxígeno sobre su estabilidad.
Tomado de Pan e Imlay (2001).

Debido a la naturaleza óxido-reductora de los centros Fe-S, estos son muy sensibles a desestabilizarse por oxígeno. Lo que se ha propuesto es que cuando el gas entra en contacto con el centro Fe-S, extrae un electrón del Fe, haciendo que el centro cambie su estado de oxidación de $[4Fe\text{-}4S]^{2+}$ a $[4Fe\text{-}4S]^{3+}$; este cambio lo

vuelve inestable, haciendo que se libere una molécula de Fe^{2+}, convirtiéndose en $[3Fe\text{-}4S]^{1+}$, lo que provoca que el centro sea inactivo para llevar a cabo reacciones de óxido-reducción (Jang e Imlay 2007). Un efecto oxidativo similar ocurre con las especies reactivas de oxígeno como el superóxido ($O_2^{\bullet -}$) o el agua oxigenada (H_2O_2).

Las enzimas que contienen centros Fe-S son inhibidas fuertemente por oxígeno y EROs. La sensibilidad a la inactivación depende del tipo de centro Fe-S del que se trate, siendo los más sensibles los tipo 4-4 (Brzóska et al 2006) y de qué tan expuesto se encuentre el centro dentro de la estructura de la proteína. En el caso de la PFOR, en casi todos los organismos que la contienen, la enzima es altamente inhibida por EROs, por lo que está presente principalmente en organismos anaerobios y microaerofílicos. De manera interesante, la PFOR de la bacteria *Desulfovibrio africanus* es insensible a la inactivación por O_2 debido a que la enzima posee una secuencia extra en el extremo carboxilo que protege al centro Fe-S más próximo al exterior de la proteína, lo que bloquea el acceso del oxígeno. Cuando se eliminó esta secuencia por mutagénesis dirigida, la enzima se volvió sensible a la inactivación por O_2 (Pieulle *et al,* 1995).

1.4.1 Antecedentes de la PFOR de E. histolytica

En los años 70s, Reeves reportó la existencia en *E. histolytica* es una enzima capaz de generar acetil-CoA a partir de piruvato y CoA, a la cual nombró piruvato sintasa (Reeves *et al*, 1977). Determinó una velocidad máxima en extractos amibianos de 1.1 U/mg de proteína celular, demostró que la enzima no podía utilizar NAD^+ o $NADP^+$ como aceptores de electrones y que la enzima era rápidamente inactivada por aire.

La clonación del gen que codifica para la EhPFOR se reportó en 1996 (Rodríguez et al, 1996). El gen es de 3.4 kilopares de bases y en el análisis de la secuencia de aminoácidos que codifica, se encontró la secuencia para tres centros Fe-S del tipo 4-4. Por inmunodetección se estableció que la enzima se encuentra

asociada a la membrana celular (Rodríguez et al, 1998). Recientemente, la secuencia del genoma de *E. histolytica* (Clark *et al,* 2007) indicó que existen 2 genes que codifican para la PFOR; las diferencias entre las secuencias son menores al 10%. Por otro lado, existen 7 genes para ferredoxinas cuyas secuencias de amino ácidos tienen similitud con las secuencias de ferredoxinas de arqueas y eubacterias.

Recientemente, reportamos que al incubar amibas en condiciones suprafisiológicas de oxígeno (0.62 mM de oxígeno) por 30 min, se acumularon los intermediarios glucolíticos G6P, fructosa-6-fosfato (F6P) y piruvato, y disminuyó la producción de etanol y parcialmente la concentración de ATP. A la par de estos cambios en el flujo de la glucólisis, se observó una disminución del 90% en la actividad de la PFOR (Ramos-Martínez et al, 2009). Resultados muy similares se han reportado al exponer cultivos amibianos a estrés oxidativo generado por H_2O_2 o paraquat por hasta 12 h, en esta condición se acumularon los intermediarios glucolíticos, principalmente las hexosas fosfato y el piruvato, se disminuyó en 50% el contenido de ATP y la producción de etanol; a la par de estos cambios en las concentraciones de metabolitos se observó la disminución del 80% de la actividad de PFOR, seguida por la inhibición de la PGAM y la ADHE (Husain el at, 2012).

Finalmente, en experimentos recientes en colaboración con un grupo de investigación del Hospital General de México, en los que se trató de dilucidar los mecanismos moleculares involucrados en la capacidad de invasión y formación de absceso hepático en diferentes cepas de amibas, se estableció que *E. dispar* y la cepa no virulenta de *E. histolytica* tienen una menor capacidad de desintoxicar las EROs, comparada con la cepa virulenta de *E. histolytica* (Santos y Olivos-García, manuscrito en preparación). En todos los casos, la actividad de PFOR se inhibió drásticamente al exponer las células a estrés oxidativo, pero de manera relevante, solamente en la cepa infectiva la inhibición de esta enzima fue reversible. Estas observaciones indicaron que en amibas, la PFOR era uno de los principales blancos del estrés oxidativo generado durante el reto con oxígeno.

De estos antecedentes experimentales surgió la hipótesis de que la inhibición de la PFOR podría tener un papel relevante en el metabolismo energético cuando las

amibas se encuentren en condiciones aeróbicas durante la invasión a los tejidos del hospedero y al enfrentarse a la respuesta inmune, en donde los macrófagos producen especies reactivas para combatir la enfermedad. La predicción fue que en amibas expuestas a condiciones aeróbicas, la posible inhibición de la PFOR por las EROs generadas podría hacer que la enzima controlara de manera importante el flujo de la vía metabólica. Por lo tanto, esta tesis se enfocó en determinar experimentalmente el coeficiente de control que tiene la PFOR sobre el flujo de la glucólisis del parásito en condiciones aeróbicas. Esto nos permitiría evaluar el posible papel de esta enzima en el control del flujo glucolítico en condiciones que podrían representar estrés oxidante al parásito. La aplicación de estrategias cuantitativas para determinar los mecanismos de control de las vías metabólicas como el MCA nos permitiría dilucidar el papel controlador de la PFOR. A continuación se describen los fundamentos del análisis de control metabólico.

1.5. Introducción al Análisis de Control Metabólico

El MCA permite determinar cuantitativamente el grado de control que cada una de las enzimas de una vía metabólica ejerce sobre el flujo y la concentración de intermediarios. A través del MCA se ha demostrado que el control de una vía metabólica no reside en una sola enzima o transportador (el “rate limiting step” que se menciona en los libros de texto de Bioquímica), sino que el control está distribuido en diferentes grados entre todas las enzimas que la conforman (Fell, 1997; Moreno-Sánchez et al, 2008).

El MCA permite establecer la estructura de control de una vía metabólica, la cual está descrita por el coeficiente de control de flujo (C_{aEi}^{J}), el coeficiente de control de concentración (C_{aEi}^{X}) y por los coeficientes de elasticidad (ε_{X}^{aEi}) de cada una de las enzimas. El C_{ai}^{J} se puede definir como el porcentaje de control que ejerce la actividad (a) de una enzima i (*Ei*) sobre el flujo metabólico *J*. Formalmente se define con la siguiente ecuación:

$$C_{aEi}^{J} = \frac{\delta J}{\delta aEi} \cdot \frac{aEi0}{J0} \qquad \text{(Ecuación 1)}$$

en donde se describe la variación en el flujo de la vía metabólica cuando se realizan cambios infinitesimales en la actividad de la enzima i (δJ δaEi). Para que el coeficiente de control sea un valor adimensional, se multiplica por el factor escalar (aEi_0/J_0) el cual corresponde a la actividad de la enzima y el flujo de la vía en condiciones basales, esto es, sin haber sido manipulados. La suma de los coeficientes de control de flujo de todas las enzimas y transportadores de una vía metabólica debe ser igual a 1 (teorema de la sumatoria) (Fell, 1997; Moreno-Sánchez et al, 2008)

De acuerdo con la ecuación 1, cuando se varía la velocidad de una enzima o transportador y esto induce una variación *proporcional* en el flujo de la vía, dicha enzima tiene un alto coeficiente de control (cercano a 1); al contrario, cuando la variación en la velocidad de una enzima modifica poco el flujo de la vía, la enzima tiene un coeficiente de control bajo (Moreno-Sánchez et al 2008). Esto se ilustra en la Fig 1.6, donde se muestran la respuesta del flujo de la vía metabólica al variar la actividad de la enzima con diferentes valores de C_{aEi}^{J}.

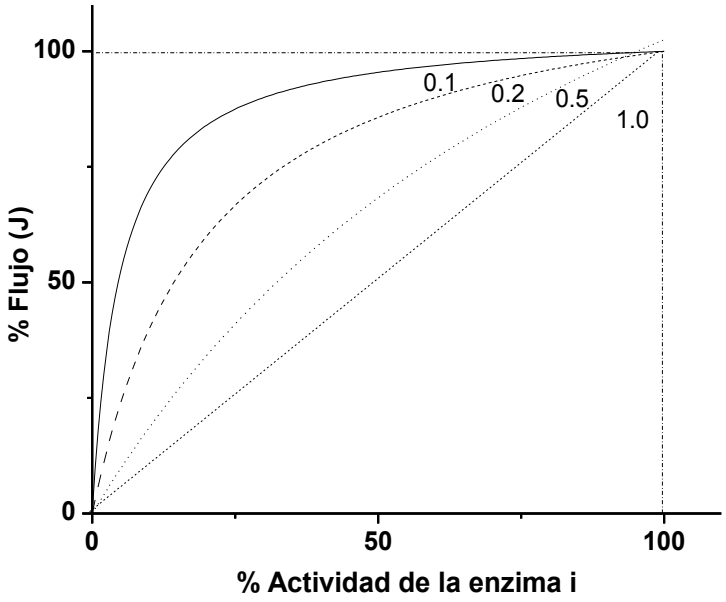

Figura 1.6. Dependencia del flujo con la variación en la actividad de enzimas con diferentes coeficientes de control de flujo. El C^{J}_{aEi} se calcula en el punto de J_o, aEi_o. Modificado de Moreno-Sánchez el at 2008.

1.5.1 Estrategias experimentales para determinar los coeficientes de control de las enzimas de una vía metabólica

Para determinar el C^{J}_{aEi} se requiere hacer variaciones graduales en la actividad de una enzima (sin alterar la actividad del resto de las enzimas de la vía) y medir en paralelo los cambios en el flujo metabólico. Estos datos se normalizan en porcentaje y con ellos se construye la gráfica como la que se presenta en la Fig. 1.6 y se calcula la pendiente de la recta tangente (o la derivada) en el punto de referencia ai_0/J_0; este valor corresponde al C^{J}_{aEi}.

Se han diseñado diferentes estrategias experimentales para determinar los C^{J}_{aEi} de cada una de las enzimas de una vía y por lo tanto conocer la estructura de control de una vía metabólica; una de ellas es la **titulación con inhibidores específicos.** Se fundamenta en la utilización de inhibidores enzimáticos altamente específicos para titular la actividad de la enzima de interés. Si el inhibidor afecta a

una enzima con C_{aEi}^{J} alto, provocará una inhibición inmediata en el flujo de la vía a bajas concentraciones del inhibidor y el patrón de inhibición de la curva de flujo *versus* concentración de inhibidor sería del tipo de decaimiento exponencial (Fig. 1.7). Por otro lado, si la enzima tiene un C_{aEi}^{J} bajo, se necesitará inhibirla en mayor proporción para verse afectado el flujo, en cuyo caso el patrón de inhibición del flujo será de una hipérbola invertida (Fig. 1.7) (Moreno-Sánchez et al, 2008).

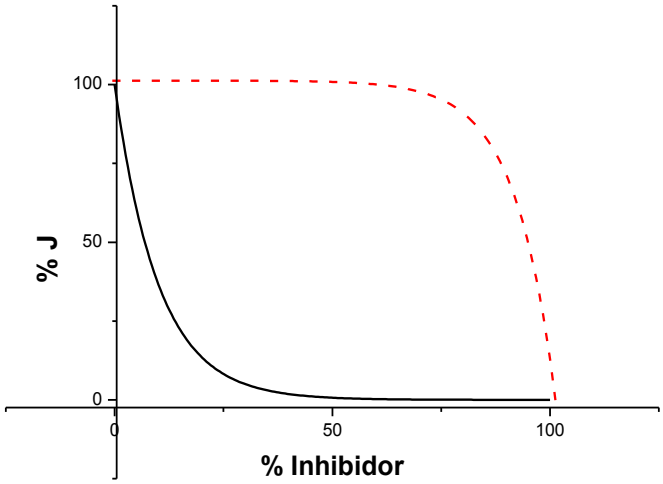

Fig. 1.7. Determinación experimental del C_{aEi}^{J} por titulación con inhibidores específicos. En línea continua se ejemplifica una enzima con alto C_{aEi}^{J} , en la cual a bajas concentraciones de inhibidor se afecta el flujo significativamente, por otro lado en línea punteada se muestra una enzima con bajo C_{aEi}^{J}, la cual se debe inhibir en mayor proporción para observar la disminución en el flujo observándose un plató a bajas concentraciones del inhibidor.

Esta estrategia de titulación de la actividad con inhibidores se empezó a utilizar a finales de los años 70s para estudiar el control de la gluconeogénesis en hepatocitos de rata (Groen et al, 1986). Sin embargo, uno de los inconvenientes más grandes de esta estrategia experimental es la falta de inhibidores específicos para cada una de las enzimas de vías metabólicas como la glucólisis. Sin embargo, esta

estrategia fue muy útil para determinar la estructura de control de la fosforilación oxidativa en células de mamífero debido a que existen inhibidores altamente selectivos para cada componente de la cadena respiratoria y el sistema fosforilante (Moreno-Sánchez R *et al* 2008)-.

Otra estrategia utilizada en el MCA para establecer la estructura de control de una vía metabólica es el **análisis de elasticidades**. Brevemente, el coeficiente de elasticidad (ε_X^{aEi}) se define como un valor numérico adimensional que representa la variación en la actividad (a) de una enzima, transportador o un grupo de estos (Ei) en función de la variación en la concentración de uno de sus ligandos (X) (Moreno-Sánchez, et al 2008). Los coeficientes de elasticidad tienen valores positivos para aquellos metabolitos que aumentan la velocidad de la enzima (sustratos o activadores) y negativos para aquellos metabolitos que la disminuyen (productos de la reacción o inhibidores). Una enzima que se encuentre trabajando cerca de su saturación por sustrato o producto, no será sensible a variaciones en la concentración de su ligando, y por lo tanto su elasticidad será cercana a cero; en contraste una enzima que se encuentre trabajando a concentraciones de ligando alejadas a la saturación, una pequeña variación de X modificará su velocidad y por lo tanto su elasticidad será cercana a 1. Existe una relación inversa entre el ε_X^{aEi} y el C_{aEi}^J. Aquellas enzimas con baja elasticidad tendrán un coeficiente de control de flujo alto en la vía metabólica y viceversa, aquellas enzimas que posean una alta elasticidad no ejercerán un control elevado en la vía.

Para determinar experimentalmente los coeficientes de elasticidad lo que se hace es dividir la vía metabólica en función a un metabolito común (X); en un grupo de experimentos se varía la concentración del sustrato inicial de la vía (S_0) para variar la concentración de X y en paralelo se mide el flujo de la vía y se grafica como se muestra en la Fig 1.8. La pendiente en el punto de interés (Xo, Jo), de los datos normalizados en porcentaje, es el coeficiente de elasticidad del bloque consumidor de X ya que se mide la respuesta de las reacciones que consumen el sustrato X. En otro grupo de experimentos se inhibe alguna de las enzimas posteriores al metabolito X para hacer que se acumule y se mide en paralelo el flujo de la vía. De esta gráfica

se obtiene la elasticidad del bloque productor de X ya que la acumulación de este metabolito hará que disminuya la velocidad de las reacciones que lo sintetizan debido a que es su producto. El análisis de elasticidades se explica con mayor detalle en el capítulo 5 de esta tesis.

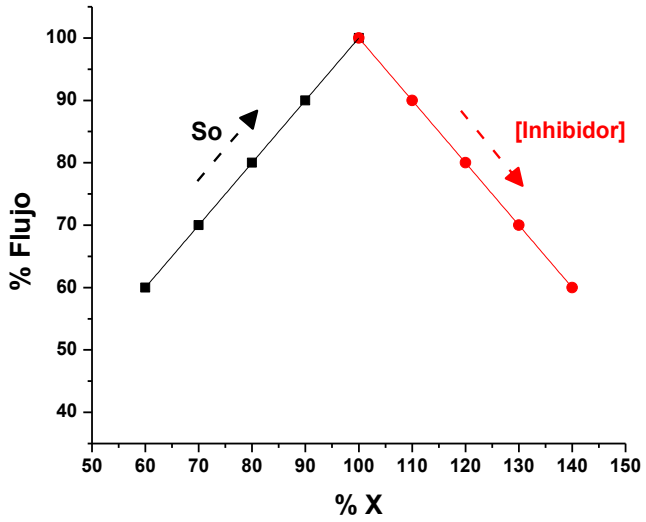

Fig. 1.8. Determinación experimental del análisis de elasticidades.

1.6. Distribución de control de la glucólisis amibiana

Nuestro grupo de trabajo reportó la construcción de un modelo cinético para determinar la estructura de control de la glucólisis amibiana (Saavedra et al, 2007). Para la construcción de este modelo se caracterizaron cinéticamente diez enzimas glucolíticas amibianas, de la HK a la PPDK (Fig. 1.4). La caracterización cinética se realizó para todas las enzimas en las mismas condiciones de pH y temperatura, las cuales fueron cercanas a las fisiológicas, además de que se determinaron los valores de *Vmax* de las enzimas en los parásitos. Con estos datos se construyó un modelo

computacional de la glucólisis amibiana utilizando un programa de simulación de vías metabólicas. El modelo se depuró y se validó cuando pudo predecir las concentraciones de metabolitos y los flujos metabólicos determinados en parásitos.

Desafortunadamente, para la construcción del modelo no se contaba con información de las características cinéticas de las enzimas que transforman el piruvato a etanol, esto es, la PFOR y la alcohol deshidrogenasa bifuncional (ADHE). Las predicciones del modelo fueron que la reacción conjunta PFOR-ADHE tenía un C_{ai}^{J} de 0.001, el cual podría subestimar el control de estas enzimas debido a la falta de parámetros cinéticos con el que se incluyeron en esta primera versión del modelo cinético. Además, para ese modelo no se consideró que la PFOR podría estar inhibida en las condiciones aeróbicas en las que se hicieron las mediciones de flujos y concentraciones de intermediarios. Debido a que el estrés oxidativo que se produce al someter a los parásitos a condiciones aeróbicas inhibe fuertemente a la PFOR, esta enzima podría representar un punto de control importante del flujo glucolítico.

CAPÍTULO 2. PLANTEAMIENTO DEL PROBLEMA, HIPÓTESIS Y OBJETIVOS

2.1 Planteamiento del problema

La glucólisis es la principal vía metabólica para producir ATP en *E. histolytica*. La inhibición de alguna de las enzimas glucolíticas podría ser una estrategia terapéutica alternativa. Por lo tanto, sería altamente conveniente identificar la(s) enzima(s) o reacciones que controlan de manera relevante el flujo de esta vía.

La EhPFOR es un blanco importante del estrés oxidativo en amibas expuestas a concentraciones suprafisiológicas de O_2 (0. 62 mM) donde se observa un 90% de inhibición de la actividad de la enzima. Asimismo, en los trofozoítos sometidos a estas condiciones se observó un decremento en el flujo glucolítico de 20 % y una disminución en el ATP (30 %) (Ramos-Martínez et al, 2009). Esto hizo suponer que la actividad de la PFOR estaba lo suficientemente inhibida para representar un punto de control del flujo glucolítico del parásito.

Por otro lado, dentro de nuestro grupo de trabajo se empezó a evaluar la estructura de control de la glucólisis amibiana a través de modelado cinético de la vía metabólica (Saavedra *et al*, 2007). Sin embargo, debido a la falta de información cinética para la PFOR, su ecuación se incluyó sin detalles cinéticos lo que pudo traer como consecuencia la subestimación de su coeficiente de control del flujo. Asimismo, no se consideró el posible efecto inhibidor sobre la PFOR que tiene la exposición a condiciones aeróbicas del parásito.

Por lo tanto, en esta tesis se analizó el posible papel controlador de la EhPFOR en el metabolismo energético de *E. histolytica* a través de la determinación experimental de su coeficiente de control sobre el flujo glucolítico.

Si la PFOR tiene un papel preponderante en el metabolismo energético del parásito y debido a que la enzima no se encuentra en el hospedero, podría ser un sitio de interés terapéutico para el diseño de fármacos que inhiban su actividad como un posible tratamiento alternativo de la amibiasis.

2.2. Hipótesis

Debido a que la EhPFOR se inhibe fuertemente por oxígeno, esta enzima puede representar un punto de control importante en la glucólisis de amiba cuando el parásito se expone a condiciones aerobias.

2.3. Objetivo general

Determinar el coeficiente de control que tiene la EhPFOR sobre el flujo de la glucólisis en *E. histolytica* en condiciones aeróbicas.

2.4. Objetivos particulares

1. Diseñar un protocolo de medición de la actividad de PFOR en extractos celulares del parásito en condiciones controladas de oxígeno.
2. Caracterizar cinéticamente a la enzima.
3. Determinar los mecanismos de inactivación de la enzima por oxígeno
4. Evaluar la cinética de inactivación de la PFOR en trofozoítos y analizar el impacto de su inhibición en el flujo glucolítico.
5. Determinar el coeficiente de control sobre el flujo glucolítico de la EhPFOR utilizando la estrategia de titulación con inhibidores.
6. Determinar la distribución de control de la vía metabólica a través de análisis de elasticidades usando células completas del parásito.
7. Comparar los coeficientes de control de la PFOR obtenidos por ambas estrategias.

CAPÍTULO 3. CARACTERIZACIÓN CINÉTICA DE LA PFOR, MECANISMO DE INHIBICIÓN POR O_2 *in vitro* Y SU RELEVANCIA *in vivo*

Debido a la poca información sobre las características cinéticas de la EhPFOR, la primera parte de mi proyecto de tesis se enfocó en desarrollar un protocolo de medición de la actividad de PFOR y caracterizar cinéticamente a la enzima en extractos amibianos en condiciones de oxígeno controladas. Una vez que se caracterizó cinéticamente a la enzima, se realizó el estudio de los mecanismos de inactivación por oxígeno y EROs de la enzima en el extracto. Por último, se determinó el efecto que tiene la inhibición de la PFOR sobre el metabolismo energético en amibas completas.

Los resultados obtenidos para este capítulo se publicaron en el artículo

Pyruvate:ferredoxin oxidoreductase and bifunctional aldehyde-alcohol dehydrogenase are essential for energy metabolism under oxidative stress in *Entamoeba histolytica.*

Pineda E, Encalada R, Rodríguez-Zavala JS, Olivos-García A, Moreno-Sánchez R, Saavedra E. **FEBS Journal.** 2010. 277(16):3382-95.

FEBS J factor de impacto 2012= 4.25. Ranking: 2012: 74/290 (Biochemistry & Molecular Biology)

En la figura 3.1 se muestran los tres principales aspectos que se evaluaron en esta parte del estudio y posteriormente se hace un breve resumen de la **ESTRATEGIA EXPERIMENTAL** y los **RESULTADOS PRINCIPALES y su discusión**.

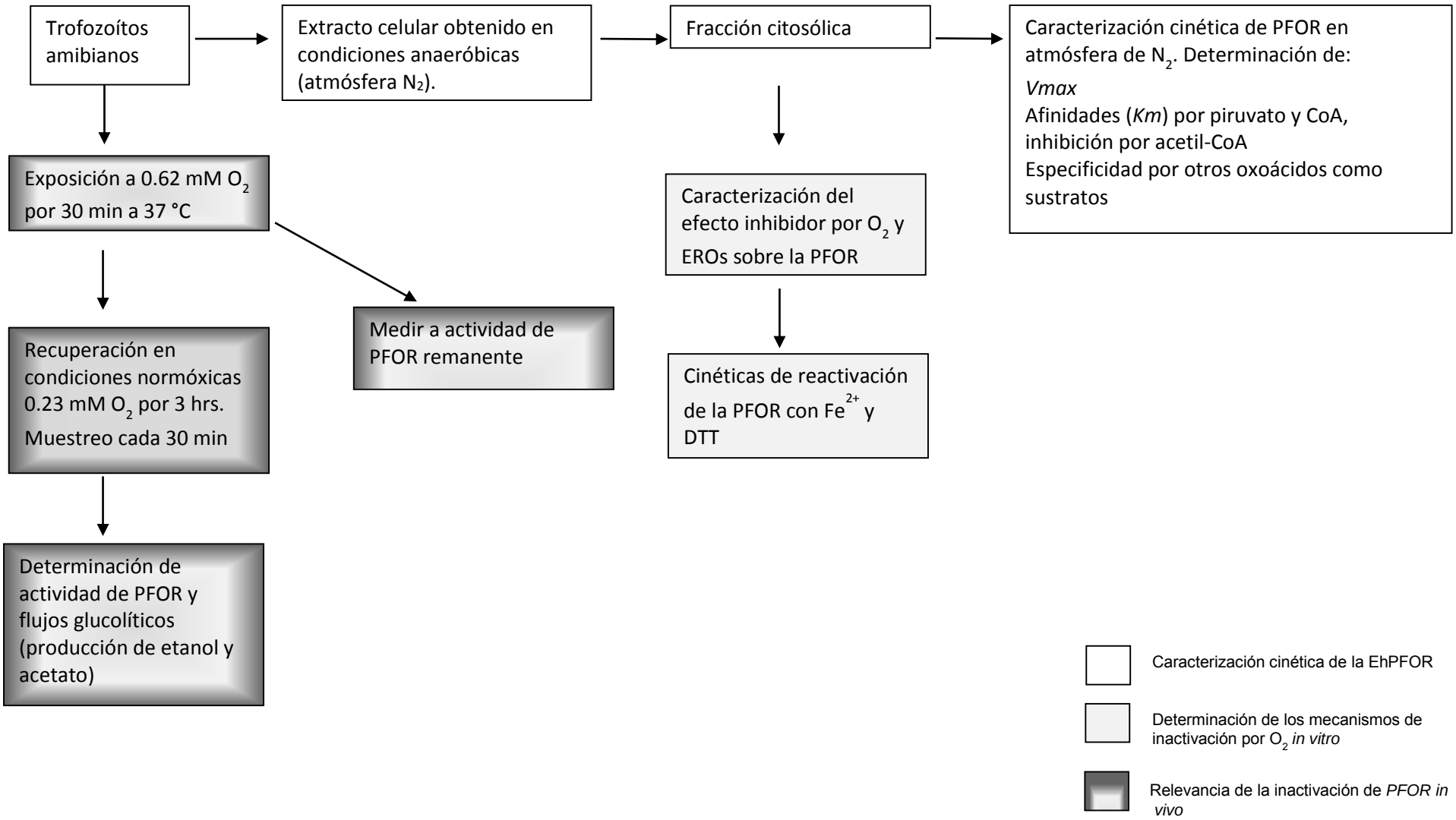

Fig. 3.1. Estrategia experimental

3.1. Caracterización cinética de la EhPFOR en extractos celulares en condiciones controladas de oxígeno

Debido a la poca información que existía en la literatura sobre la PFOR amibiana, el primer objetivo fue caracterizar cinéticamente a esta enzima en extractos amibianos en condiciones de pH y temperatura que estén cercanas a las fisiológicas (pH 6 y 7; 37ºC).

La estrategia experimental fue cosechar y lavar los trofozoítos amibianos con PBS a 4°C, la pastilla celular se resuspendió en un volumen igual de solución de lisis (100 mM KH_2PO_4 previamente gaseado con N_2, 25 mM β-mercaptoetanol, 1 mM PMSF, 5 mM EDTA y 1% Tritón X-100). Las células se rompieron por tres ciclos de congelación en N_2 líquido y descongelación a 37 °C. El lisado se centrifugó a 21,000 g por 10 min, se recuperó la fracción soluble para almacenarla a -20 °C. Todo el procedimiento se realizó en una atmósfera de N_2.

La caracterización cinética de la EhPFOR se realizó en un ensayo que contenía 100 mM Na_2HPO_4 pH 7.4, 0.25 mM azul de nitrotetrazolio (NBT) (o 2 mM de metilviológeno para los ensayos a pH 6.0 y 7.0), 2-6 µg de proteína de la fracción soluble del extracto amibiano y 10 mM de piruvato. La reacción se inició adicionando 0.1 mM CoA. Se monitoreó la reducción del NBT a 560 nm o del metilviológeno a 604 nm en un espectrofotómetro (Shimadzu; Kioto, Japón), en cada trazo se restó la actividad basal (actividad en ausencia de alguno de los sustratos de PFOR). En el ensayo se aseguró que la actividad fuera linealmente dependiente de la cantidad de proteína. Este ensayo también se realizó en una atmósfera de N_2.

Los resultados de la caracterización cinética se muestran en la Tabla 3.1. Atendiendo a sus eficiencias catalíticas (*Vmax/Km)* la EhPFOR es más eficiente a pH 7.0 que a 6.0. La enzima no utiliza $NADP^+$ o NAD^+ como aceptor de electrones, lo que coincide con lo reportado para la PFOR de otros organismos. Además del piruvato, la enzima puede utilizar con mucha menor afinidad a otros α-cetoácidos como sustratos, como el oxaloacetato (OAA) y el α-cetobutirato (α-KB), con valores

de *Km* 4 -8 veces mayores al del piruvato. El α-cetoglutarato (α-KG) no es sustrato de la enzima. Estos resultados sugieren que en *E. histolytica* los oxoácidos derivados de la degradación de aminoácidos no pueden servir como sustratos oxidables para la PFOR para obtener ATP por la reacción de la AcCoAS, como se ha propuesto a partir del análisis del contenido de genes del genoma del parásito (Clark et al 2007).

La acetil-CoA, producto de la reacción, es un inhibidor de tipo competitivo con respecto a la CoA, con valores de *Ki* entre 20 y 40 μM. La concentración de acetil-CoA determinada por nuestro grupo de trabajo es 20-40 veces mayor al valor de *Ki* de la PFOR por este sustrato (0.9 mM de acetil-CoA y 0.4 mM de CoA, Citlali Vázquez Martínez, tesis de Licenciatura), esto sugiere que *in vivo* la enzima puede estar parcialmente inhibida por acetil-CoA.

Tabla 3.1. Caracterización cinética de la EhPFOR en extractos a 37 °C.

	pH 6.0			*pH 7.0*		
	Vmax	*Km*	*Vmax/Km*	*Vmax*	*Km*	*Vmax/Km*
Sustratos						
Piruvato	0.9 ± 0.3 (4)	3.5 (2)	0.26	1.3 ± 0.2 (6)	1.5 (2)	0.87
CoA		0.013 (2)			0.006 (2)	
OAA	0.6	14	0.04	1.0	11.5	0.09
α-KB	0.8 (2)	10 (2)	0.08	0.9 (2)	13 (2)	0.07
α-KG	ND	ND		NA	NA	
Moduladores						
$Ki_{acetyl\text{-}CoA\ vs\ CoA}$		0.036			0.024	
IC_{50} oxígeno			0.034 ± 0.003 (4)*			
IC_{50} H_2O_2			0.006, 0.035**			

*Vm*ax en µmoles/min x mg de proteína, *Km* en mM. Los números en paréntesis indican el número de extractos amibianos independientes ensayados. *IC_{50} a 4 h de exposición, **IC_{50} a 1 h y 30 min, respectivamente. α- KB: α- cetobutirato, α-KG: α- cetoglutarato.

3.2. Mecanismos de inhibición de la PFOR por oxígeno

Se ha descrito que la PFOR de muchos organismos se inhibe fuertemente por O_2 y EROs, por lo que el siguiente objetivo fue estudiar la inhibición de la EhPFOR por oxígeno.

En la figura 3.2 se muestran solamente algunos resultados de los publicados de la cinética de inactivación por oxígeno. Como se puede apreciar en el panel A, la EhPFOR pierde el 92 ± 6 % de su actividad después de 30 min de incubación en PBS saturado con O_2 (0.62 mM de O_2 a 36 °C y 2240 m sobre el nivel del mar). Esta inactivación se revierte al incubar con 1 mM de Fe^{2+} y 5 mM de DTT por 30 min (56 ± 8% de la actividad inicial). La reactivación fue dependiente del tiempo de exposición a O_2 (ver Fig 1B del artículo).

Como ya se describió anteriormente, las PFORs de bacterias y otros parásitos son altamente sensibles a la inactivación por O_2 y EROS debido a que contienen

centros Fe-S. Se ha propuesto que el O_2 y/o EROS interaccionan directamente con estos centros y los oxida (Imlay J, 2006). Una forma de proteger de la inactivación es incubando a la enzima con alguno de sus sustratos y/o productos. Por lo tanto, se incubó al extracto con los sustratos de la PFOR, CoA y piruvato y con su producto acetil-CoA a concentraciones cercanas al valor de *Km* determinado para cada sustrato (1 mM piruvato, 0.05 mM acetil-CoA y CoA). De estos metabolitos, el acetil-CoA fue el más eficiente en proteger de la inactivación por O_2, seguida de la CoA ($K_{inactivación}$ de primer orden: 0.006 min^{-1} y 0.03 min^{-1} respectivamente, contra 0.07min^{-1} del control). Al contrario, el piruvato aceleró la inactivación ($K_{inactivación}$: 0.12 min^{-1}) (Figura 3.2B), lo cual se ha observado para otras descarboxilasas de piruvato que, como la PFOR, contienen tiamina pirofosfato en su estructura (Chabrière *et al*, 1999). El mecanismo propuesto para esta inactivación es que el N4' del anillo de aminopiridina de la tiamina pirofosfato extrae un protón del C2 del anillo de tiazol, lo que provoca la formación de un radical carbanión que inicia el ataque nucleofílico en el carbonilo del piruvato (Tittman K, 2009) Nosotros hipotetizamos que la fprmación del radical libre de la tiamina pirofosfato en presencia de piruvato puede propiciar una mayor exposición de los centros Fe-S al medio, lo que incrementaría su susceptibilidad a O_2 y a EROS..

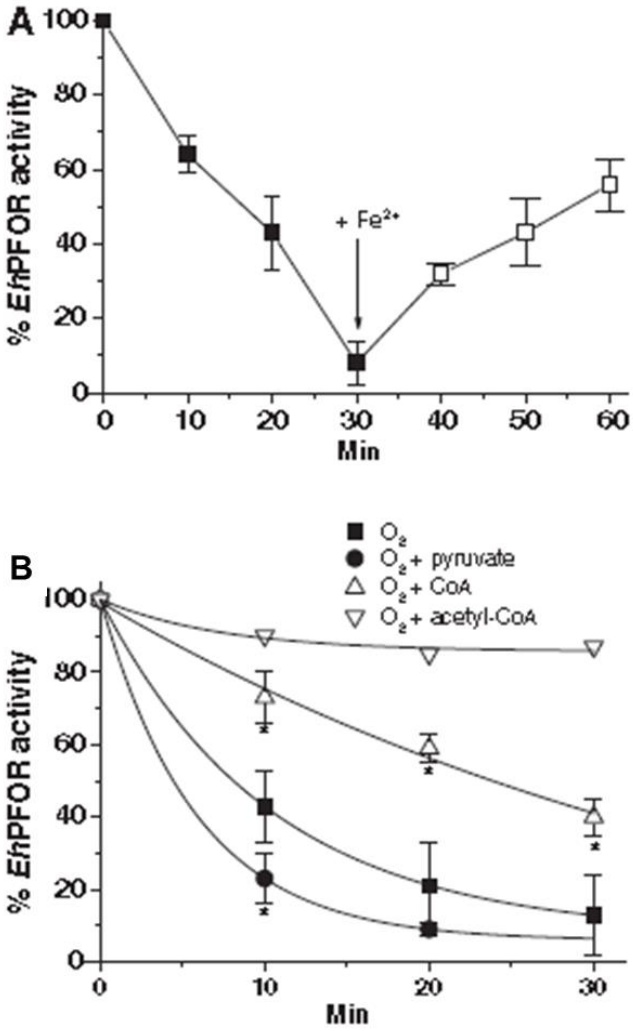

Figura 3.2. Inactivación de la EhPFOR por O_2 y EROs.

A) Cinética de inactivación en condiciones saturantes de O_2 (0.62 mM O_2). En el punto indicado la enzima se incubó en presencia de 1 mM Fe^{2+} y 5 mM DTT.

B) Protección por los sustratos. El extracto se incubó con O_2 en presencia de 1 mM piruvato o 0.05 mM de acetil-CoA o CoA. Actividad control (100%) = 1.03 ± 0.17 µmoles/min x mg de proteína.

Posteriormente se hizo énfasis en determinar qué especie de EROs producida en la incubación con O_2 era responsable de la inhibición de la PFOR, evaluando el efecto protector de las enzimas antioxidantes superóxido dismutasa (SOD) y catalasa (Fig. 3.3). Los resultados indicaron que la SOD protege más del 85% de la actividad hasta 60 min de exposición al O_2; en contraste, la catalasa protegió un ~30%. La

mezcla de ambas enzimas se comportó de manera similar a lo que ocurre al incubar solamente con SOD (Fig. 3.3).

Debido a que la catalasa protegió parcialmente de la inactivación, se evaluó la inactivación de la PFOR por H_2O_2 (Fig. 2 del artículo). De acuerdo con los resultados, la EhPFOR es fuertemente inhibida por H_2O_2 de manera dosis dependiente. El valor de IC_{50} fue de 35 µM y 6 µM a 30 min y 1 h de exposición, respectivamente. Al incubar el extracto con 50 µM del H_2O_2 se observó que la enzima se inhibió en 80% a 50 min de incubación; en esta condición la inactivación era parcialmente reversible, a tiempos mayores de exposición la inactivación fue irreversible. Los sustratos piruvato y CoA y el producto acetil-CoA no protegieron del daño causado por peróxido de hidrógeno. .

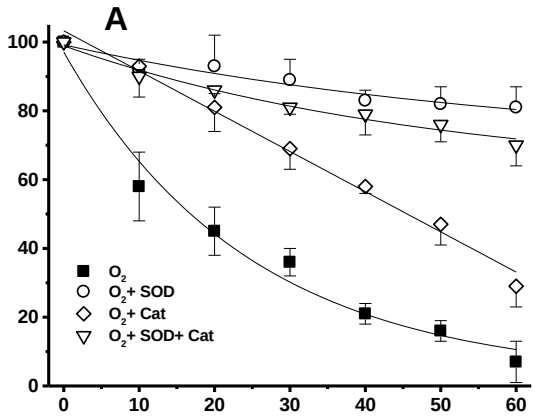

Figura 3.3 Efecto protector de las enzimas antioxidantes SOD y catalasa sobre la inactivación de la PFOR por O_2. Los extractos amibianos se expusieron a condiciones saturantes de oxígeno en presencia o ausencia de 50 U de las enzimas antioxidantes indicadas.

3.3. Evaluación de la cinética de inactivación de la PFOR in vivo y su impacto en el flujo glucolítico

Previos reportes de nuestro grupo (Ramos-Martínez et al, 2009) indicaban que al exponer amibas a un reto suprafisiológico de oxígeno por 30 min se incrementaban los niveles de G6P, F6P y piruvato, a la par de una disminución en la producción de etanol y ATP, lo que sugería una inhibición de la vía a partir de la PFOR. Por lo tanto, se hizo un análisis completo del efecto de la exposición a oxígeno sobre la glucólisis en células vivas e intactas de trofozoítos de *E. histolytica*.

Para estos experimentos se incubaron 1 $x10^6$ amibas por tubo eppendorf en 1 mL de PBS (137 mM NaCl, 2.7 mM KCl, 10 mM Na_2HPO_4, 2 mM KH_2PO_4 pH 7.4) con 5 mM de glucosa y saturado con O_2. Las muestras se incubaron por 30 min a 37 °C, en paralelo se incubaron amibas control en PBS normóxico + glucosa. Después de la incubación se cosecharon las células y se resuspendieron en PBS normóxico suplementado con glucosa, y se regresaron a incubación a 37°C. Durante esta incubación se tomaron alícuotas a diferentes tiempos para determinar la actividad de PFOR, ADHE y AcCoAS, el contenido de especies reactivas al ácido tiobarbitúrico y los flujos hacia etanol y acetato.

De todas las enzimas de la glucólisis evaluadas (de la hexocinasa a la PPDK además de la acetato tiocinasa, Tabla 2 del artículo), solamente la PFOR y la actividad de aldehído deshidrogenasa de la ADHE (ALDH) se encuentran fuertemente inhibidas (Fig. 3.4A) con 90% y 68% de inhibición, respectivamente, después del reto con oxígeno. A la par de la disminución en la actividad de estas enzimas se observó una disminución en la producción de etanol y el incremento en la producción de acetato durante los primeros 90 min después del reto con oxígeno (Fig. 3.4B).

De manera importante, la actividad de PFOR y de ALDH se recuperaron durante la incubación en normoxia (Figura 3.4A), tiempo en el cual se restableció la producción de etanol, con la consecuente disminución en la producción de acetato (Fig. 3.4B). No hubo diferencia significativa entre los flujos recuperados durante la

incubación en normoxia y en los flujos determinados en amibas sin exposición a O_2 (2.8 ± 0.2 nmoles de acetato/min x mg de proteína y 15.3 ± 3 nmoles de etanol/min x mg de proteína contra 1.9 ± 0.5 nmoles de acetato/min x mg de proteína y 14.4 ± 4.1 nmoles de etOH/ min x mg de proteína, respectivamente).

Estos datos indicaron que no solamente la PFOR, sino también la actividad de ADHE, son inhibidas por el estrés oxidante y esto disminuye el flujo glucolítico hacia etanol y favorece el de acetato. Además, los resultados indican que las amibas tienen la capacidad de restaurar las actividades de las enzimas inhibidas y recuperar los flujos glucolíticos a valores cercanos a los de parásitos no expuestos al estrés. Así mismo, este análisis demostró por primera vez, que las amibas expuestas a condiciones de aerobiosis (normoxia, 0.23 mM oxígeno) sintetizan preferentemente etanol (90%) y que solamente el 10% de del flujo glucolítico se desvía a acetato.

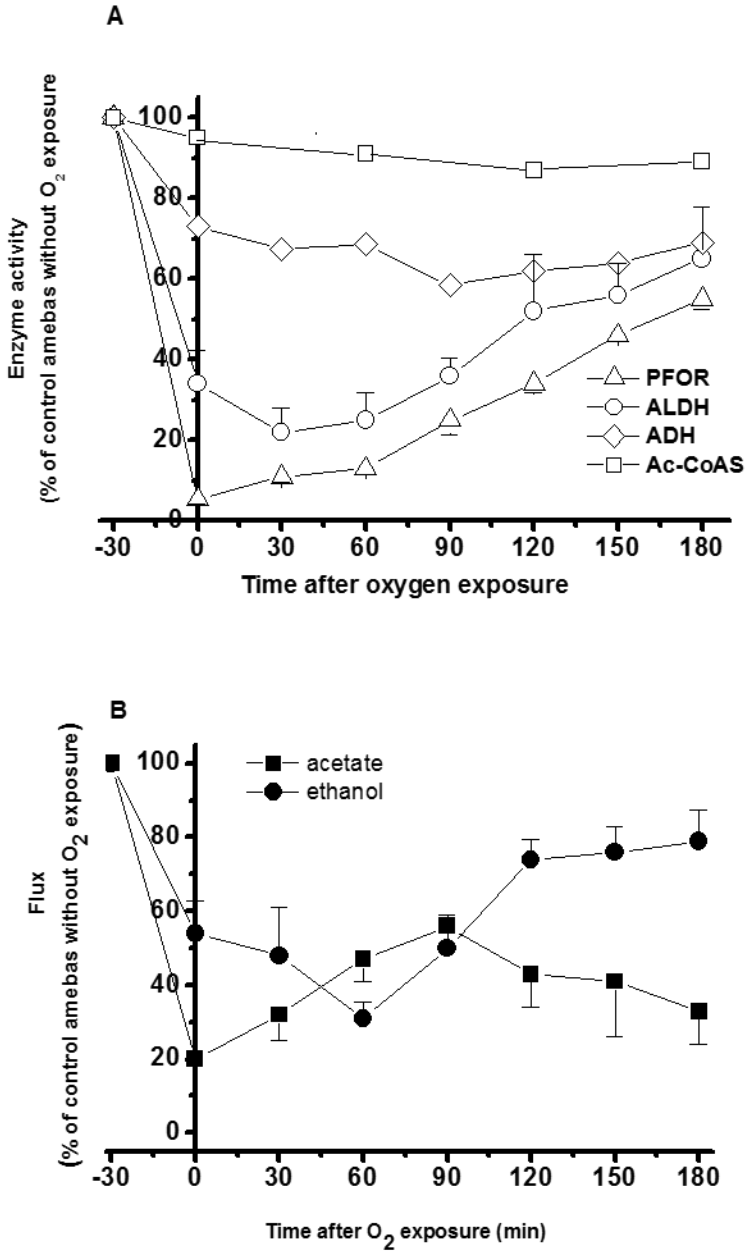

Figura 3.4. Efecto de la inactivación de la EhPFOR in vivo

Trofozoítos de *E. histolytica* se incubaron por 30 min en PBS saturado con oxígeno; posteriormente se cambió el medio por PBS equilibrado con aire y se incubaron por 180 min. Se tomaron alícuotas a diferentes tiempos para medir la actividad remanente de las enzimas y los flujos de la vía.

3.4. Artículo: Pyruvate:ferredoxin oxidoreductase and bifunctional aldehyde-alcohol dehydrogenase are essential for energy metabolism under oxidative stress in Entamoeba histolytica.

the FEBS Journal

Pyruvate:ferredoxin oxidoreductase and bifunctional aldehyde–alcohol dehydrogenase are essential for energy metabolism under oxidative stress in *Entamoeba histolytica*

Erika Pineda[1], Rusely Encalada[1], José S. Rodríguez-Zavala[1], Alfonso Olivos-García[2], Rafael Moreno-Sánchez[1] and Emma Saavedra[1]

1 Departamento de Bioquímica, Instituto Nacional de Cardiología Ignacio Chávez, México D.F., México
2 Departamento de Medicina Experimental, Facultad de Medicina, Universidad Nacional Autónoma de México, México D.F., México

Keywords
Fe–S cluster; glycolysis; oxidative stress; pyruvate:ferredoxin oxidoreductase (PFOR); reactive oxygen species (ROS)

Correspondence
E. Saavedra, Departamento de Bioquímica, Instituto Nacional de Cardiología Ignacio Chávez, Juan Badiano No. 1 Col. Sección XVI, CP 14080 Tlalpan, México D.F., México
Fax: +5255 55730994
Tel: +5255 5573 2911 ext 1298
E-mail: emma_saavedra2002@yahoo.com

(Received 9 February 2010, revised 4 June 2010, accepted 17 June 2010)

doi:10.1111/j.1742-4658.2010.07743.x

The *in vitro Entamoeba histolytica* pyruvate:ferredoxin oxidoreductase (*Eh*PFOR) kinetic properties and the effect of oxidative stress on glycolytic pathway enzymes and fluxes in live trophozoites were evaluated. *Eh*PFOR showed a strong preference for pyruvate as substrate over other oxoacids. The enzyme was irreversibly inactivated by a long period of saturating O_2 exposure (IC_{50} 0.034 mm), whereas short-term exposure (< 30 min) leading to > 90% inhibition allowed for partial restoration by addition of Fe^{2+}. CoA and acetyl-CoA prevented, whereas pyruvate exacerbated, inactivation induced by short-term saturating O_2 exposure. Superoxide dismutase was more effective than catalase in preventing the inactivation, indicating that reactive oxygen species (ROS) were involved. Hydrogen peroxide caused inactivation in an Fe^{2+}-reversible fashion that was not prevented by the coenzymes, suggesting different mechanisms of enzyme inactivation by ROS. Structural analysis on an *Eh*PFOR 3D model suggested that the protection against ROS provided by coenzymes could be attributable to their proximity to the Fe–S clusters. After O_2 exposure, live parasites displayed decreased enzyme activities only for PFOR (90%) and aldehyde dehydrogenase (ALDH; 68%) of the bifunctional aldehyde–alcohol dehydrogenase (*Eh*ADH2), whereas acetyl-CoA synthetase remained unchanged, explaining the increased acetate and lowered ethanol fluxes. Remarkably, PFOR and ALDH activities were restored after return of the parasites to normoxic conditions, which correlated with higher ethanol and lower acetate fluxes. These results identified amebal PFOR and ALDH of *Eh*ADH2 activities as markers of oxidative stress, and outlined their relevance as significant controlling steps of energy metabolism in parasites subjected to oxidative stress.

Abbreviations
AcCoAS, acetyl-coenzyme A synthetase; Cat, catalase; ADH, alcohol dehydrogenase; ADH2, bifunctional aldehyde–alcohol dehydrogenase; ALDH, aldehyde dehydrogenase; *Da*PFOR, pyruvate:ferredoxin oxidoreductase from *Desulfovibrio africanus*; *Eh*ADH2, bifunctional aldehyde– alcohol dehydrogenase from *Entamoeba histolytica*; EhPFOR, pyruvate:ferredoxin oxidoreductase from *Entamoeba histolytica*; OAA, oxaloacetate; PEP, phosphoenolpyruvate; PFOR, pyruvate:ferredoxin oxidoreductase; PYK, pyruvate kinase; ROS, reactive oxygen species; SD, standard deviation; SE, standard error; SOD, superoxide dismutase; TBARS, thiobarbituric acid-reactive substances; TPP, thiamine diphosphate; a-KB, a-ketobutyrate; a-KG, a-ketoglutarate.

Introduction

The energy metabolism of *Entamoeba histolytica*, the causal agent of human amebiasis, is less complex than in higher organisms [1]. The parasite lacks functional mitochondria and has neither tricarboxylic acid cycle nor oxidative phosphorylation enzyme activities; thus, glycolysis is the main pathway to generate ATP for cellular work. Therefore, the glucose catabolism pathway enzymes seem to be suitable targets for therapeutic intervention.

Glycolysis in this parasite differs in several respects from that in the human host. *E. histolytica* contains two pyrophosphate-dependent enzymes, PP_i-dependent phosphofructokinase and pyruvate phosphate dikinase [2–4], which functionally replace the allosterically modulated ATP-dependent phosphofructokinase and pyruvate kinase (PYK) activities. The latter two activities have also been detected in amebal trophozoites [5,6]; however, their low activities most probably do not significantly contribute to glycolytic flux [7]. Amebas contain a guanine nucleotide-dependent phosphoglycerate kinase instead of the adenine nucleotide-dependent phosphoglycerate kinase [8,9], and several of their glycolytic enzymes display allosteric modulation by AMP and PP_i [7,10].

Furthermore, pyruvate, the end-product of carbohydrate catabolism by glycolysis, is oxidatively decarboxylated by pyruvate:ferredoxin oxidoreductase (PFOR) [11], instead of the pyruvate dehydrogenase complex present in human cells. PFOR transfers the electrons produced during pyruvate oxidation to ferredoxin, whereas acetyl-CoA is consecutively reduced to acetaldehyde and ethanol (under microaerophilic conditions), mainly by the activity of a bifunctional NADH-dependent aldehyde–alcohol dehydrogenase (*Eh*ADH2), or to ethanol and acetate (under aerobic conditions) by the latter and acetyl-CoA synthetase (ADP-forming) [1,11–13].

*Eh*ADH2 has been previously studied regarding its kinetic properties and its role in fermenting parasite metabolism [13–16]. In contrast, amebal PFOR has been scarcely studied regarding its kinetic features. Of high clinical relevance is the fact that reduced ferredoxin produced in the PFOR reaction is the main electron donor for the antiamebic agent metronidazole and derivatives, which, once activated, induce the killing of *E. histolytica* and other PFOR-containing parasites [17].

An early report on *E. histolytica* PFOR (*Eh*PFOR) by Reeves [11] showed decreased enzyme activity under aerobic conditions. Recently, we reported that amebas stressed with a supraphysiological concentration of O_2 displayed high reactive oxygen species (ROS) production and strong PFOR inhibition, which was accompanied by exacerbated accumulation of glycolytic intermediates, particularly pyruvate [18]. This observation suggested that *Eh*PFOR inhibition might be of physiological relevance when amebas are exposed to an aerobic environment during invasion of the host tissues [19]. Under such conditions, low *Eh*PFOR activity could limit the glycolytic flux, and the ATP supply might therefore be drastically decreased, leading to parasite death. Therefore, the aims of the present work were: (a) to determine the main kinetic properties of *Eh*PFOR, focusing on O_2 exposure and ROS inhibition, which has not been previously evaluated in this enzyme; and (b) to analyze the effects of oxidative stress on glycolytic and fermentative enzymes and pathway fluxes in live parasites.

Results

Kinetic characterization of *Eh*PFOR in amebal extracts

PFORs in several anaerobic parasites have been found attached to plasma and hydrogenosomal membranes [20,21], whereas *Eh*PFOR has been found associated with plasma membranes and cytosolic structures [22]. Hence, *E. histolytica* trophozoites were disrupted in the absence or presence of several Triton X-100 concentrations (Table S1). In the presence of 1% detergent, > 90% of *Eh*PFOR total activity was consistently recovered in the solubilized fraction. In its absence or at lower detergent concentrations, a variable enzyme partition was observed between the soluble and insoluble fractions, whereas higher detergent concentrations resulted in a decrease in specific activity (Table S1). *Eh*PFOR activity in solubilized samples was relatively unstable when stored under N_2 at)20 ºC, a 50% decrease in activity being seen after 1 day. However, when the enzyme in the extract was stored under the same conditions but in the presence of 1 mm Fe^{2+} and 5 mm dithiothreitol, a 50% decrease in activity was observed only after 1 week (Fig. S1A).

*Eh*PFOR showed significant activity in the broad pH interval from 6 to 8, with the highest peak at pH 7.3 (Fig. S1B). The kinetic parameters V_{max} and K_m were determined in the glycolytic direction at 37 ºC with pH values of 6.0 and 7.0, conditions that resemble the physiological conditions of the parasites in culture (Table 1). No significant variation was observed in the V_{max} values at either pH value, but

Table 1. Kinetic parameters of *Eh*PFOR at 37 ºC. Figures in parentheses indicate numbers of individual amebal extracts assayed. The IC_{50} for oxygen was determined at pH 6.0, 7.0 and 7.4; as the values differed by only 10%, they were pooled together. The IC_{50} values for H_2O_2 are at pH 7.4 at 1 h and 30 min, respectively. ND, not detected; NA, not assayed.

	pH 6.0			pH 7.0		
	V_{max} [mol min^{-1} (mg cellular protein)$^{-1}$]	K_m (mM)	V_{max}/K_m	V_{max} [mol min^{-1} (mg cellular protein)$^{-1}$]	K_m (mM)	V_{max}/K_m
Substrates						
Pyruvate	0.9 ± 0.3 (4)	3.5 (2)	0.26	1.3 ± 0.2 (6)	1.5 (2)	0.87
CoA		0.013 (2)			0.006 (2)	
OAA	0.6	14	0.04	1.0	11.5	0.09
a-KB	0.8 (2)	10 (2)	0.08	0.9 (2)	13 (2)	0.07
a-KG	ND	ND		NA	NA	
Modulators						
$K_{i\ acetyl\text{-}CoA\ versus\ CoA}$ (mM)	0.036			0.024		
IC_{50} O_2 (mM)	0.034 ± 0.003 (4)					
IC_{50} H_2O_2 (mM)	0.006, 0.035					

slightly higher affinities were obtained for the substrates pyruvate and CoA at pH 7.0. *Eh*PFOR activity was also able to use other a-ketoacids, such as oxaloacetate (OAA) and a-ketobutyrate (a-KB), although with 3.5–8-fold lower affinity and one order of magnitude lower catalytic efficiency (V_{max}/K_m) than that for pyruvate; a-ketoglutarate (a-KG) was not a substrate (Table 1).

Acetyl-CoA, the product of the PFOR reaction, was a competitive inhibitor against CoA (Fig. S2), with a K_i value of 0.024–0.036 mm (Table 1). *Eh*PFOR showed no activity when using NAD^+ or $NADP^+$ as electron acceptor, in agreement with the PFOR kinetic properties described for amebas and other anaerobes [11,20,21].

*Eh*PFOR inhibition by O_2

PFOR inactivation under aerobic conditions has been documented for the enzymes from several sources [23,24]. The amebal enzyme lost 90% of its initial activity after incubation for 1–2 h in room air on ice, whereas, under anaerobic conditions (N_2-flushed assay buffer), the enzyme activity remained constant for at least 2 h (data not shown). On the other hand, 92% ± 6% of the activity in the soluble fraction was lost after 30 min of incubation in O_2-saturated (0.63 ± 0.04 mm O_2, at 36 ºC and 2240 m altitude) assay buffer (Fig. 1A). Remarkably, 56% ± 8% of the initial activity was restored by a subsequent incubation with 1 mm Fe^{2+} under anaerobic (N_2 atmosphere) and reducing conditions (Fig. 1A). Other metals, such as Co^{2+}, Cu^{2+}, Mn^{2+} and Fe^{3+}, or anaerobiosis and dithiothreitol alone did not reactivate the inhibited enzyme (data not shown). Furthermore, exposures to O_2 longer than 30 min resulted in a progressive decrease in enzyme reactivation by Fe^{2+} (Fig. 1B), most probably because of irreversible dam- age.

The inhibition observed with O_2-saturated buffer (first-order inactivation constant; k_{inac} = 0.07 min^{-1}) was partially prevented by incubation with CoA (k_{inac} = 0.03 min^{-1}) and completely prevented by incubation with acetyl-CoA (k_{inac} = 0.006 min^{-1}) (Fig. 1C). On the other hand, enzyme inhibition in a high O_2 concentration was enhanced by the presence of pyruvate (k_{inac} = 0.12 min^{-1}) (Fig. 1C). Thiamine diphosphate (TPP) or acetyl-CoA addition did not prevent the inactivation caused by O_2+ pyruvate (data not shown).

The O_2 concentration required for half-maximal inhibition (IC_{50}) of *Eh*PFOR activity was determined. First, solubilized fractions were incubated for 30 min at different O_2 concentrations (see Experimental procedures and Fig. S3A,B for details) and *Eh*PFOR activity was determined. Under these conditions, an O_2 IC_{50} value of 0.15 mm was obtained (Fig. S3B). With longer incubation times (4 h), a lower IC_{50} of 0.034 mm for O_2 was determined (Fig. 1D; Table 1). In order to rule out enzyme inhibition by the dithionite used for O_2 titration, amebal samples were incubated in N_2-saturated buffer in the absence or presence of 2 mm dithionite. After 4 h under these conditions, *Eh*PFOR activity was not significantly affected (Fig. 1D, inset).

*Eh*PFOR inhibition by ROS

To determine whether superoxide (O_2^-) or hydrogen peroxide (H_2O_2) endogenously generated by the amebal

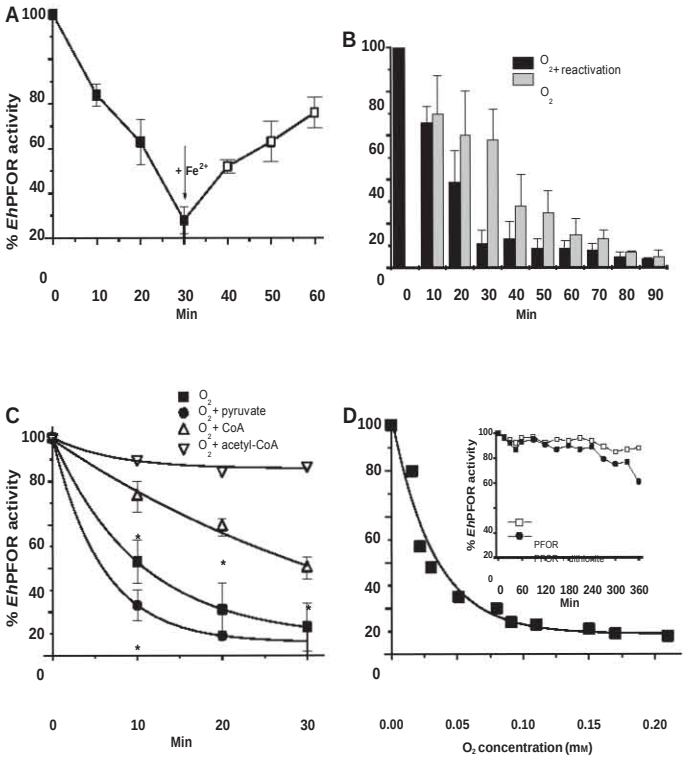

Fig. 1. *Eh*PFOR inactivation by O_2 exposure. (A) Kinetics of enzyme inactivation under O_2-saturating conditions and reactivation. Aliquots of amebal solubilized extracts were incubated in O_2-saturated buffer on ice, and samples were withdrawn at different times to determine PFOR activity at 37 ºC. For reactivation, the sample was incubated in O_2-saturated buffer for 30 min. Then, 1 mM Fe^{2+} and 5 mM dithiothreitol were added where indicated, and the sample was kept under an anaerobic atmosphere. (B) Dependency of enzyme reactivation on the time of O_2 exposure. Aliquots of amebal solubilized extracts were incubated in O_2-saturated buffer for the indicated times. Then, a 30 min reactivation treatment was performed as described in (A), and PFOR activity was determined. (C) Protection by substrates. Amebal solubilized extracts were exposed to O_2 in the absence or presence of 1 mM pyruvate or 50 lM of CoA or acetyl-CoA. Aliquots were withdrawn at different times, and PFOR activity was determined. Two-tailed Student's *t*-test for nonpaired samples, $*P < 0.05$ versus O_2-exposed sample. (D) Determination of the IC_{50} for O_2 after 4 h of incubation. Aliquots of normoxic buffer were added with different amounts of dithionite, and the O_2 concentration was determined by oxymetry. Then, samples of amebal solubilized extract were incubated in such buffers for 4 h on ice, and the remaining enzyme activity was determined. Inset: *Eh*PFOR time stability in N_2-saturated buffer in the absence or presence of 2 mM dithionite. For (A)–(D), 100% activity was 1.03 ± 0.17 UÆmg$^{)1}$ protein ($n = 5$). For each experimental condition, at least three assays were performed with different amebal batches. Data for all figures are mean ± SD.

extract during the O_2 exposure was involved in *Eh*PFOR inactivation (and hence avoiding the arbitrary selection of ROS-testing concentrations), the samples were incubated in the O_2-saturated assay buffer in the absence or in the presence of superoxide dismutase (SOD), catalase (Cat) or a combination of the two. SOD was more efficient than Cat in protecting *Eh*PFOR activity from the oxidative damage (Fig. 2A). A similar protection pattern (with SOD > Cat) was observed when the samples were first incubated for 10 min in the O_2-saturated buffer and the antioxidant enzymes were then added. Under this last condition, the remaining PFOR activity (approximately 60%) was better preserved with SOD present during the incubation (data not shown).

As Cat only partially prevented enzyme inactivation, *Eh*PFOR inactivation by H_2O_2 was examined in detail. The enzyme was strongly inhibited in a dose-dependent manner by H_2O_2 (Fig. 2B), with IC_{50} values of 35 lm after 30 min and 6 lm after 1 h. Furthermore, samples were incubated under anaerobic conditions in the presence of 50 lm H_2O_2; at different times, samples were treated with Cat and then subjected to reactivation treatment. Under these conditions, the enzyme was > 80% inhibited by H_2O_2 after 50 min of exposure but the inhibition was still substantially reversible, whereas longer incubation times (> 70 min) resulted in progressive and irreversible loss of activity (Fig. 2C). In contrast to what occurred in O_2-saturated buffer, CoA and acetyl-CoA did not protect from the damage caused by H_2O_2 (data not shown).

Modeling *Eh*PFOR

A 3D model of *Eh*PFOR was built by using the *Desulfovibrio africanus* PFOR (*Da*PFOR) tertiary structure

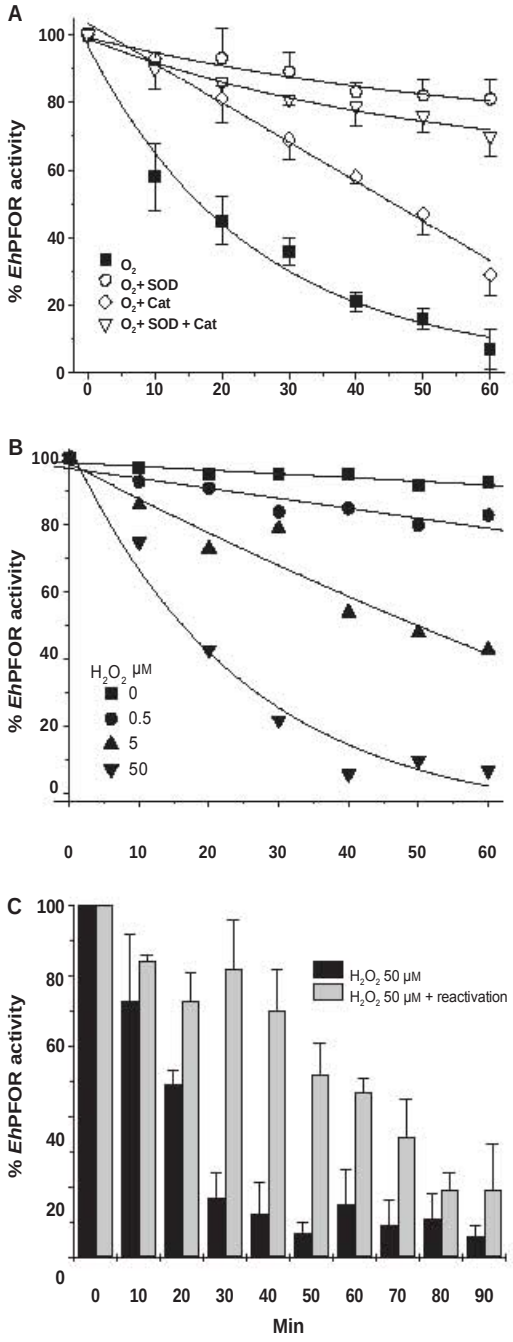

Fig. 2. Effect of ROS on *Eh*PFOR activity. (A) Protection by antioxidant enzymes. The amebal solubilized extract was exposed to O_2-saturating conditions in the absence or presence of 50 units of SOD and/or Cat. (B) Kinetics of enzyme inactivation by H_2O_2. Amebal samples were incubated with the indicated H_2O_2 concentration in N_2-saturated buffer. (C) *Eh*PFOR inactivation by H_2O_2 and reactivation. Amebal solubilized extracts were incubated with 50 µM H_2O_2. At different times, the samples were treated for 20 min with 10 units of Cat and *Eh*PFOR was reactivated for 30 min at 4 ºC with 1 mM Fe^{2+} under reducing and anaerobic conditions. For (A) and (C), data are mean ± SD; 100% activity is as in Fig. 1.

in complex with pyruvate as template [25]. Because of the high percentage of identity between the amino acid sequences (54%), overlapping of the model with the crystal structure was almost complete, with minimal nonmatching regions in the surfaces of the proteins (Fig. 3). The extra C-terminal portion in the *Da*PFOR structure responsible for protection against O_2 [25] was absent in the amebal enzyme. Unfortunately, 3D structures with coenzymes, which could provide an explanation of their protective roles against oxidative stress damage, have not been reported.

In vivo effects on glucose-fermenting enzymes and fluxes under oxidative stress

Recently, we reported that amebas incubated for 30 min in O_2-saturated conditions displayed increased $O_2^{\cdot-}$ and H_2O_2 production, a high level of PFOR inhibition, very substantial accumulation of hexosephosphates and pyruvate, and decreased ethanol and ATP levels [18]. The pattern of metabolite changes suggested an arrest of glycolytic flux, most probably at the level of PFOR. Therefore, the impact of O_2 exposure on the kinetics of oxidative stress damage for both glycolytic enzymes and fluxes was examined, immediately after subjecting the parasites to O_2 exposure and later during a phase of recovery under normoxic conditions (0.18 ± 0.09 mM O_2 at 36 ºC).

Lipid peroxidation measured as levels of thiobarbituric acid-reactive substances (TBARS) was used as an index of oxidative stress damage. The level of TBARS measured immediately after O_2 exposure was increased by 85% ± 11%, but it progressively diminished in the

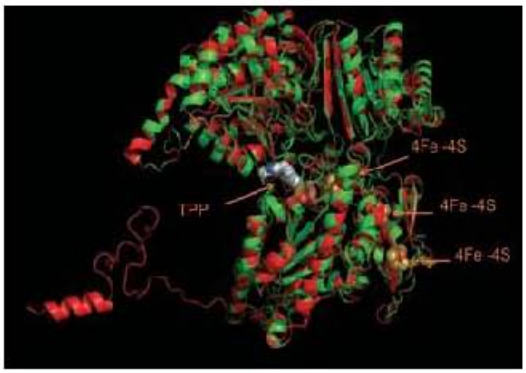

Fig. 3. Predicted 3D structure of *Eh*PFOR. Overlapping of the *Da*PFOR crystal structure (1b0p) in red and the *Eh*PFOR predicted model in green by using SWISS-MODEL. The TPP coenzyme and the three Fe–S clusters are shown as spheres. The C-terminal region in *Da*PFOR responsible for O_2 protection is shown only in red.

subsequent 3 h after return of the parasites to normoxic conditions (Fig. 4A), suggesting slow ROS detoxification by the amebal antioxidant system.

On the other hand, intact amebas exposed to O_2 for 30 min showed a decrease in PFOR activity of > 90% (Table 2), in agreement with the results obtained in cellular extracts. The strongest inhibition was seen for PFOR; however, significant inhibition (68%) was also observed for the aldehyde dehydrogenase (ALDH) activity of *Eh*ADH2, although its alcohol dehydrogenase (ADH) activity remained unaffected (Table 2). The inhibited ALDH activity was not restored by adding Fe^{2+} to the kinetic assay, and the presence of this metal did not increase the ADH activity (data not shown). All other evaluated glycolytic and fermenting enzymes (Table 2) were not significantly inhibited, including acetyl-CoA synthetase (AcCoAS).

Remarkably, after O_2 exposure, live amebas were able to gradually restore PFOR and ALDH activities under normoxic conditions and in the absence of external iron sources or supplements (Fig. 4B). Restoration of enzyme activities from the highest inhibited state (0 min for PFOR and 30 min for ALDH) was more clearly evident 90 min after recovery was initiated. During the full recovery period, ADH activity of *Eh*ADH2 and AcCoAS remained fairly constant (Fig. 4B).

In parallel with the pattern of enzyme inhibition, decreased ethanol production and enhanced acetate production were achieved at 60 and 90 min, respectively, during recovery from the O_2 exposure (Fig. 4C), which correlated well with the inhibition of ALDH activity of *Eh*ADH2 and the constant AcCoAS activity (Fig. 4B). Thereafter, the end-metabolite pattern changed, with higher ethanol production and lower acetate production (Fig. 4C), which was in agreement with

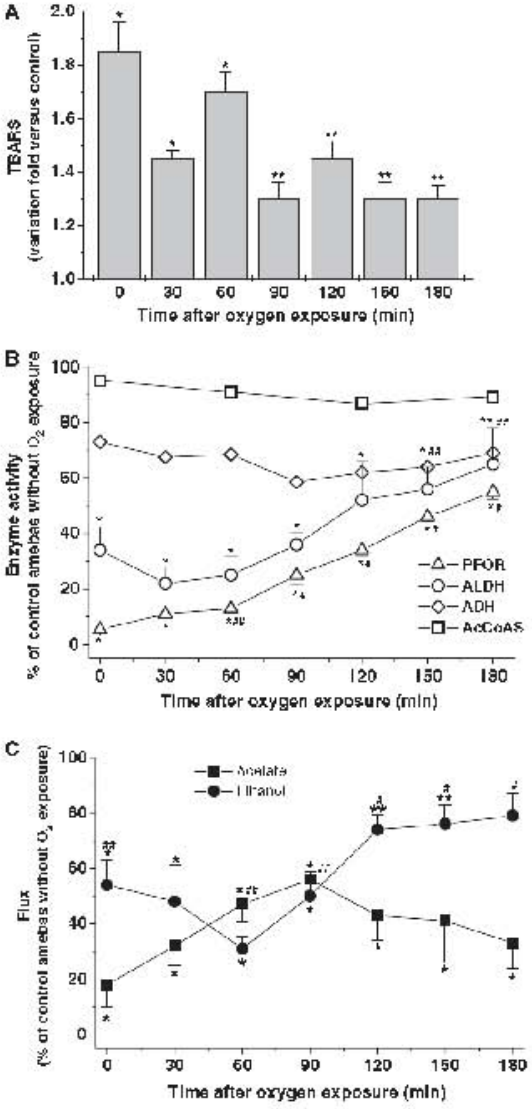

Fig. 4. Amebal lipid peroxidation, enzyme activities and metabolic fluxes after O_2 exposure. Amebas (1×10^6) were incubated for 30 min at 36 °C in 1 mL of O_2-saturated (0.83 ± 0.04 mM O_2) NaCl-P_i supplemented with 10 mM glucose. After this period, the cells were centrifuged and resuspended in normoxic (0.18 – 0.09 mM O_2 at 36 °C and 2240 m altitude) NaCl-P_i glucose and returned to the water bath. At different time intervals, samples were centrifuged, and enzyme activities and lipid peroxidation levels were determined in the cellular pellet, and ethanol and acetate levels in the supernatant. (A) Lipid peroxidation was measured as TBARS. A value of 1 refers to TBARS production by control amebas without O_2 exposure at each time point, a value that was fairly constant at 15 ± 7 pmol per 10^6 cells. The number of independent cell cultures was four. Values shown are mean + SE. Two-tailed Student's *t*-test for compared samples: $^{*}P < 0.005$ and $^{**}P < 0.05$ versus control amebas. (B) For enzyme activities, 100% indicates the enzyme activities before O_2 exposure, which were 1.05 ± 0.11 U·mg^{-1} (*n* = 6), 0.075 – 0.233 U·mg^{-1} (*n* = 3), 0.77 ± 0.28 U·mg^{-1} (*n* = 4) and 0.176 U·mg^{-1} (*n* = 1) for PFOR, ALDH and ADH for *Eh*ADH2, and acetyl-CoA synthetase, respectively (from Table 2). (C) For metabolite concentrations, 100% means the amounts of ethanol and acetate determined in amebas incubated under normoxic conditions for 3 h at 36 °C, which were 2923 ± 1222 nmol ethanol/10^6 cells and 733 ± 127 nmol acetate/10^6 cells (*n* = 4). Values shown in (B) and (C) are mean + SE. Two-tailed Student's *t*-test for compared samples: $^{a}P < 0.005$ and $^{b}P < 0.05$ versus control amebas. Under normoxic conditions for 3 h: $^{a}P < 0.005$ and $^{b}P < 0.05$ versus the value with the highest inhibition state (PFOR and acetate, *t* = 0; ALDH, *t* = 30 min; ethanol, *t* = 60 min).

Table 2. Glycolytic enzyme activities after incubation of amebas under O_2-saturating conditions. Amebas were incubated in normoxic (control) or O_2-saturated NaCl/P_i for 30 min. Enzyme activities were determined in amebal solubilized (PFOR) and cytosolic fractions. HK, hexokinase; HPI, glucose-6-phosphate isomerase; PP_i-PFK, pyrophosphate-dependent phosphofructokinase; ALDO, fructose-1,6-bisphosphate aldolase; TPI, triosephosphate isomerase; GAPDH, glyceraldehyde-3-phosphate dehydrogenase; PGK, 3-phosphoglycerate kinase; PGAM, cofactor-independent 3-phosphoglycerate mutase; ENO, enolase; PPDK, pyruvate phosphate dikinase; ME, malic enzyme. The values in parentheses indicate the numbers of different preparations assayed for both conditions.

Enzyme	Control (mU·mg^{-1} protein)	Activity remaining after O_2 exposure (%)
HK	57	82 (2)
HPI	430	96 (1)
PP_i-PFK	543	80 (2)
ALDO	325	96 (1)
TPI	13 438	91 (1)
GAPDH	179	92 (2)
PGK	1367	93 (1)
PGAM	107	90 (1)
ENO	402	94 (1)
PPDK	466	93 (1)
PFOR	1080 ± 102	10 ± 6 (6)
NADH-ALDH	75 ± 33	32 ± 12 (3)
NADH-ADH	469 ± 286	66 ± 11 (4)
$NADP^+$-ADH	9.8 ± 5.6	93 ± 5 (3)
ME	174	89 (1)
AcCoAS	176	95 (1)

reactivation of the ALDH activity of *Eh*ADH2 (Fig. 4B). A reactivation process, rather than *de novo* synthesis, for the ALDH activity seemed more likely, because the ADH activity present in the same *Eh*ADH2 did not vary (Fig. 4B).

The flux rates during amebal recovery were 2.8 ± 0.2 and 15.3 ± 3 nmol·min^{-1} (10^6 cells)$^{-1}$ for acetate (0–90 min) and ethanol (60–180 min), respectively (Fig. 4C). These flux values were nonsignificantly different from those determined in control amebas incubated in normoxic conditions for 3 h at 36 ºC [1.9 ± 0.5 and 14.4 ± 4.1 nmol·min^{-1} (10^6 cells)$^{-1}$ for acetate and ethanol, respectively]. These results indicated that, after an initial arrest in fermenting flux caused by PFOR and ALDH inhibition, amebas were able to fully restore fluxes to control levels. Interestingly, nonvirulent *E. histolytica* HM1:IMSS amebas were unable *in vivo* to recover PFOR activity after a similar O_2 exposure (data not shown), which was in agreement with differences in antioxidant capabilities between virulent and nonvirulent *E. histolytica* HM1:IMSS strains, as recently reported [18].

Discussion and Conclusions

PFOR has been described for anaerobic bacteria such as *Bacteroides* [26], *D. africanus* [25,27] and several anaerobic human parasites from the genera *Entamoeba* [11], *Trichomonas* [20] and *Giardia* [21]. A typical feature of the parasites is the absence of the pyruvate dehydrogenase complex, which, in aerobic cells, is responsible for pyruvate conversion to acetyl-CoA to feed the tricarboxylic acid cycle, which produces NADH for oxidative phosphorylation. As the parasites lack functional mitochondria as well as tricarboxylic acid cycle and oxidative phosphorylation enzyme activities, PFOR is located at the crossroads of glycolysis and carbohydrate fermentation. In the present work, a functional kinetic characterization was carried out on *Eh*PFOR, which is required for a full description and understanding of amebal glycolysis and fermentation pathways.

*Eh*PFOR kinetic properties

PFOR activity was obtained from *E. histolytica* trophozoites in an active and solubilized form only by using mild extraction with a nonionic detergent under anoxic conditions. This suggested that the enzyme was loosely bound to hydrophobic cellular components, in agreement with PFOR detection in plasma membrane and cytoplasmic structures in amebal trophozoites [22].

The *Eh*PFOR activity in solubilized fractions showed highly similar K_m values to others previously reported for amebas ($K_{m\ CoA}$ 0.002 mm [11]), *Tritrichomonas foetus* ($K_{m\ pyruvate}$ 3.2 mm; $K_{m\ CoA}$ 0.0025 mm [23]), *D. africanus* ($K_{m\ pyruvate}$ 2.5 mm; $K_{m\ CoA}$ 0.005 mm [27]), and *Hydrogenobacter thermophilus* ($K_{m\ pyruvate}$ 3.45 mm; $K_{m\ CoA}$ 0.0054 mm [28]); however, these K_m values contrasted with those reported for the *Trichomonas vaginalis* purified enzyme ($K_{m\ pyruvate}$ 0.14 mm [20]).

Although PFOR activity in *E. histolytica* used other oxoacids as substrates (Table 1), and other oxoacid reductase activities have been detected in this parasite by zymogram analysis [29], as well as in *Giardia duodenalis* [21] and *T. vaginalis* [30], the amebal activity was rather specific for pyruvate: the catalytic efficiencies (V_{max}/K_m) seen with OAA and a-KB were one order of magnitude lower and there was lack of activity with a-KG. These results contrasted with those for *T. vaginalis* purified PFOR, which can use a-KB and a-KG with high affinity (K_m^{app} values of 0.1 and 0.5 mm, respectively), although with lower catalytic efficiency (V_m^{app}/K_m^{app} values of 0.63 and 0.01, respectively, relative to 1 for pyruvate) [20]. Our results suggested that,

in *E. histolytica*, oxoacids (other than pyruvate) derived from amino acid degradation cannot be oxidiz- able substrates for ATP supply (through the AcCoAS ADP-forming reaction), as previously suggested by amebal genome analysis [31].

The mixed-type inhibition of acetyl-CoA and CoA reported for the *T. vaginalis* [20] and *Halobacterium halobium* [32] PFORs contrasted with the competitive-type inhibition found for *Eh*PFOR. This discrepancy might be a consequence of the high inhibitor concentrations used in the first two studies (0.05–0.4 mM) [20,32]. Although no levels of CoA and acetyl-CoA have been reported for amebas, competitive inhibition might occur under physiological conditions, owing to the close K_m values for substrate and product.

*Eh*PFOR inhibition under oxidant conditions

As previously reported [11], the amebal PFOR in solubilized parasite extracts is highly susceptible to inactivation under aerobic conditions. Our results indicated that, under saturating O_2 conditions, the enzyme was fully inactivated after a short incubation (30 min). At this time, *Eh*PFOR inactivation could be reversed to a great extent by incubation with Fe^{2+}, whereas longer incubation under O_2 exposure resulted in a lower reactivation rate.

The almost complete protection with exogenous SOD against the acute O_2 exposure indicated that O_2^- was the main ROS involved in enzyme inactivation (Fig. 2A). Although H_2O_2 also potently inhibited the activity (Fig. 2B) in a reversible fashion (Fig. 2C), Cat was not as efficient as SOD in preventing the damage, probably because O_2^- was still being formed (Fig. 2A). Moreover, H_2O_2 damage could not be prevented by the addition of substrates or products, which indicated a different mechanism of inhibition to that observed with O_2.

These results were in agreement with previous reports indicating that microaerophilic organisms con- taining PFORs and other Fe–S enzymes, when incu- bated under aerobic or pro-oxidant conditions, lose the activity of such enzymes, producing an arrest in important metabolic pathways [26,33]. The damage occurs when ROS oxidize an iron atom of the [4Fe–4S]$^{2+}$ cluster, which transforms into an unstable [4Fe–4S]$^{3+}$ form that rapidly decays into a new stable form, [3Fe–4S]$^{1+}$, with the concomitant release of Fe^{2+} [26,34]. By increasing the exposure to the oxidant agent, the latter cluster form continues its disintegra- tion in an irreversible way, releasing up to three Fe^{2+} ions per Fe–S center [33]. The integrity of the Fe–S cluster is thus essential for catalysis in these enzymes. Addition of Fe^{2+} allows for the recovery of cluster integrity, and hence functional activity of the enzymes. Regarding the reversible inactivation by H_2O_2 of *Eh*PFOR, it might be possible that the concentration and incubation length were not sufficient to induce the formation of the most oxidized state of the Fe–S cluster, allowing its reactivation by Fe^{2+} addition.

The enzymes responsible for O_2^- generation in amebal extracts have not been clearly identified in *D. histolytica*. On the other hand, a set of antioxidant enzymes (including SOD but not Cat) have been identified in the parasite [35,36]. Interestingly, *in vitro*, higher PFOR reactivation was observed in virulent than in nonvirulent amebal solubilized fractions [18], strongly supporting the proposal of differential antioxidant capabilities between the different types of ameba [19,36–38].

*Eh*PFOR O_2 inhibition was partially or fully prevented by micromolar concentrations of the substrate CoA and the product acetyl-CoA (Fig. 1C). The K_m values determined for these metabolites (Table 1) are well within the physiological levels described for human liver cells (0.050–0.20 and 0.015–0.30 mM, respectively) [39]. To our knowledge, protection against ROS inactivation by coenzymes has not been previously described for other PFORs. *Da*PFOR, which is naturally resistant to inactivation under aero- bic conditions, contains an extra domain at the C-ter- minal region that spans the vicinal subunit of the dimer and that overlays the Fe–S cluster region; specif- ically, Met1203b protects the proximal Fe–S cluster [25]. As the amebal enzyme lacks this peptide segment, as shown in the 3D model of *Eh*PFOR, other protec- tive mechanisms are very probably involved. An explanation for the protective effect of the coenzymes against oxidative stress in *Eh*PFOR is that they bind close to the Fe–S clusters, blocking the access of ROS. In this regard, a preliminary docking analysis with coenzymes in the 3D model of *Eh*PFOR suggested that the CoA-binding site was, indeed, close to the proximal Fe–S cluster (data not shown). However, the CoA-reactive SH was orientated away from the thia- min, and hence it appeared that the docked complex is not productive, indicating that further structural analy- sis is necessary.

The stronger *Eh*PFOR inhibition by O_2 and pyru- vate incubation was in agreement with previous observations in other PFORs [40–42]. It has been proposed that in the PFOR reaction mechanism, the N4¢ of the aminopyridine ring from TPP extracts a proton from C2 of the thiazole ring, promoting the formation of a carbanion radical that performs the nucleophilic attack on the carbonyl group of pyruvate [43]. We

hypothesized that the formation of the TPP free radical induced by pyruvate binding may promote greater exposure of the Fe–S clusters to the medium, and thus increased susceptibility to ROS in the absence of the proper cosubstrate.

In vivo inactivation and reactivation of fermenting enzymes and their effect on metabolic fluxes

Although the experimental design of acute stress using saturating O_2 concentrations allowed for PFOR enzyme kinetic analysis after short incubations, and hence without loss of activity caused by protein instability, such O_2 concentrations are not found under parasite physiological conditions. Thus, an effort was made to determine a physiological IC_{50} value for O_2 after lengthy incubation times (4 h). Under these conditions, an IC_{50} for O_2 of 34 μm was obtained, which is close to the O_2 concentration values found in hamster liver (22.6 μm) [44] as well as in human liver (38.3 μm) and gastric mucosa (65.8 μm) tissues [45]. Hence, in aerobic tissues, *Eh*PFOR activity might indeed be partially impaired.

It was previously demonstrated that amebas incubated under O_2-saturating conditions display accumulation of glycolytic intermediaries and decreased ATP and ethanol levels [18]. Hence, the activities of all glycolytic and fermentative enzymes were determined here, and the results showed a potent inhibitory effect of O_2 exposure on PFOR and the ALDH activity of *Eh*ADH2 (Table 2).

PFOR activity in live parasites was almost completely abolished (> 90%) after 30 min of exposure to saturating O_2 conditions (Fig. 4B). Remarkably, the parasites were able to gradually restore the PFOR activity in the absence of external iron sources or reducing agents under normoxic conditions (air-saturated buffer) (Fig. 4B), which suggested that either enzyme reactivation or *de novo* synthesis of PFOR or both events occurred. There is little information about the biogenesis of Fe–S clusters in amebas. It has been reported that *E. histolytica* possesses a nitrogen fixation system (NIF) for Fe–S cluster assembly [46], with a mitosomal localization [47]. However, the mechanisms involved in Fe–S cluster repair have not been elucidated. In *Escherichia coli*, it has been suggested that the mechanisms of assembly and repair of Fe–S centers in proteins are different because of the differences in rates observed for each phenomenon, the latter occurring within minutes of enzyme inactivation [34]. A repair mechanism can be suggested for *Eh*PFOR within the first minutes after inactivation; at longer incubation times, *de novo* synthesis cannot be ruled out.

An additional significant inhibitory effect (68%) of O_2 exposure was obtained for the ALDH component of *Eh*ADH2 (which continued being inactivated until 30 min after recovery under normoxic conditions), whereas its ADH activity remained relatively unchanged (Fig. 4B). This inhibition pattern can be directly ascribed to the bifunctional enzyme; the other ALDH reported in amebas prefers NADPH and cannot use acetyl-CoA as substrate [48], whereas ADH1 uses NADPH as cofactor [49]. Moreover, our results are in agreement with the structural properties described for *Eh*ADH2, indicating the presence of two catalytically independent domains, the N-terminal domain, displaying ALDH activity, and the C-terminal domain, containing an iron-binding domain, which is involved in ADH activity. The integrity of both domains and that of the iron-binding domain are required for ALDH activity [16]. Moreover, the enzyme is essential for amebal growth [16,50]. The effect of oxidative stress has been also studied in the *E. coli* bifunctional ALDH–ADH (named as ADHE); H_2O_2 and O_2^- inhibit the enzyme with K_i values of 5 and 120 μm, respectively, through a process involving irreversible oxidation of the Fe^{2+} present in the ADH domain [51]. Whether this is the case for the amebal enzyme remains to be elucidated, because Fe^{2+} did not reverse the inhibitory effect on the ALDH activity and had no activating effect on the ADH activity, suggesting other inactivating mechanisms.

In a similar fashion to what occurred with PFOR, the ALDH activity of *Eh*ADH2 started recovering 60 min after return of the parasites to normoxic conditions. For this case, enzyme reactivation instead of *de novo* synthesis is proposed, because the ADH activity remained constant during the ALDH recovery phase.

In parallel with PFOR reactivation, an increase in acetate flux developed in the first 90 min, most probably because of acetyl-CoA accumulation resulting from ALDH inhibition and unchanged activity of AcCoAS. As the $K_{m\ acetyl\text{-}CoA}$ of AcCoAS (0.1 mm; Fig. S4) is one order of magnitude higher than that of ALDH (0.015 mm) [15], flux through the latter to ethanol is favored over flux through the former to acetate, in amebas not subjected to O_2 exposure. On the other hand, the strong ALDH inhibition induced by O_2 exposure very likely brings about an increased level of acetyl-CoA, which activates AcCoAS and hence acetate production.

One should be aware that although ATP can be produced through this acetate-producing branch, a

sustained acetate flux is difficult to attain, because alternative routes of NADH oxidation need to be turned on (phosphoenolpyruvate (PEP) carboxytransphosphorylase, malic enzyme and malate dehydrogenase [1]) in competition with the predominant acetyl-CoA reduction to ethanol by *Eh*ADH2.

Net ethanol synthesis was absent in the first 60 min after O_2 exposure, because of the strong inhibition of the ALDH activity of *Eh*ADH2. Furthermore, ALDH reactivation was observed, with the concomitant ethanol flux restoration and NADH oxidation necessary for recycling of the NAD^+ pool for glycolysis.

The changing metabolite patterns during aerobic and anaerobic glucose catabolism described here are in agreement with early reports on monoxenically cultured *E. histolytica* [12]; however, the mechanisms underlying these transitions are now partly elucidated. The results indicated that, even under the normoxic conditions used in the present study to recover the parasites (which are still above the O_2 physiological concentrations found in parasite cultures or intestinal lumen), the route for ethanol synthesis predominated over that for acetate production [14.4 ± 4.1 versus 1.9 ± 0.5 nmolÆmin$^{)1}$ (10^6 cells)$^{)1}$, respectively]. Thus, ethanol production is the main pathway of glucose catabolism and energy production in the parasite, with minor and transient contributions of the acetyl-CoA–acetate pathway.

Our results also indicated that PFOR and the ALDH activity of *Eh*ADH2 were the main targets of ROS generated under prolonged and ⁄ or acute aerobic conditions. Owing to the higher PFOR sensitivity, this enzyme is proposed as a specific and sensitive marker of oxidative stress in *E. histolytica*. Both *Eh*PFOR and *Eh*ADH2 appear to be the main flux-controlling steps of glycolysis under oxidative stress conditions.

The above results support our previous hypothesis that prolonged aerobic exposure and ROS generation, induced by the inflammatory process prevailing in liver tissues when amebas are arriving at the site of infection and before an ischemic process is developed (6 h) [52], have detrimental effects on the viability and energy metabolism of the parasite [19]. This event seems to be one of several factors derived from both host and parasite that can determine the outcome of the infection.

Experimental procedures

Reagents and chemicals

Acetyl-CoA, ATP, Cat from bovine liver, CoA, phenylmethanesulfonyl fluoride, PYK⁄lactate dehydrogenase from rabbit muscle, SOD, EDTA, TPP, Mes, 1,1,3,3-tetraethoxypropane butylhydroxytoluene, pyrazole and pyruvate were from Sigma (St Louis, MO, USA); methyl viologen, b-mercaptoethanol and PEP were from ICN Biomedicals (Aurora, OH, USA); Nitro Blue tetrazolium was from Amersham (Parklands, Rydelmare, Australia); Triton X-100 was from Bio-Rad (Hercules, CA, USA); sodium dithionite, acetic acid and n-butanol were from JT Baker (Phillipsburg, NJ, USA); ferrous ammonium sulfate was from Qui´mica Meyer (Mexico City, Mexico); Tris and 1,4-dithiothreitol were from Research Organics (Cleveland, Ohio, USA); H_2O_2 from Laboratorios American (Mexico City, Mexico); and acetate kinase from *Methanosarci- na thermophila* was kindly provided by R. Jasso-Cha´ vez (Instituto Nacional de Cardiologi´a de Me´xico).

Amebal extracts

E. histolytica trophozoites of the HM1:IMSS strain were recovered from hamster amebic liver abscesses and grown on TYI-S-33 medium at 36 ºC, as previously described [53]. The parasites were harvested, and the cellular pellet was resuspended in an equal volume of lysis buffer consisting of 100 mm KH_2PO_4 (pH 7.5) previously purged with N_2, 25 mm b-mercaptoethanol, 1 mm phenylmethanesulfonyl fluoride, 5 mm EDTA and 1% Triton X-100. The procedures were conducted under an N_2 atmosphere. The cells were disrupted by three cycles of freezing in liquid N_2 and thawing at 37 ºC. The cellular lysate was centrifuged at 21 000 g; the soluble fraction was separated, aliquoted in 0.2 mL tubes and stored under an N_2 atmosphere at)20 ºC. For other glycolytic enzyme activities, cytosolic fractions from control and O_2-exposed amebas were obtained as previously described [7].

Enzyme kinetics

*Eh*PFOR activity was determined under an N_2 atmosphere in the amebic Triton-extracted fraction in an assay containing 100 mm Na_2HPO_4 (pH 7.4) buffer (previously purged with N_2), 0.25 mm Nitro Blue tetrazolium (or 2 mm methyl viologen for the kinetic characterization at pH 6.0 and 7.0), 2–6 lg of protein of the amebic fraction, and 10 mm pyruvate, and the reaction was started by addition of 0.1 mm CoA. Nitro Blue tetrazolium and methyl viologen reduction was monitored at 560 and 604 nm, respectively, in a spectrophotometer (Shimadzu, Kyoto, Japan). The absorbance baseline in the absence of one of the substrates was always subtracted. Care was taken to ensure that the activity was linearly dependent on the sample protein content. For determination of the K_m values, pyruvate was varied from 1.1 to 40 mm (with 0.05 mm CoA), CoA from 0.001 to 1.2 mm (with 1 mm pyruvate), and OAA, a-KB and a-KG from 0.01 to 100 mm (with 0.05 mm CoA). The substrates were routinely calibrated. For the kinetic characterization

at different pH values, the incubation buffer was a mixture of 50 mm imidazole and 10 mm each of acetate, Mes and Tris, adjusted to the indicated pH value. For determination of glycolytic enzyme activities, the protocols described previously were followed [7]. The kinetic assay for the ADH activity of *Eh*ADH2 was performed in 100 mm pyrophosphate/phosphoric acid buffer (pH 8.8) purged with N_2, 10 mm freshly prepared cysteine, 2 mm NAD^+, and freshly prepared cytosolic extract (0.05–0.15 mg of protein), and the reaction was started by addition 170 mm absolute ethanol. For its ALDH activity, the assay contained 100 mm Mops/KOH buffer (pH 7.5), 0.3 mm NADH, 10 mm pyrazole (to inhibit the ADH activity), and 0.1–0.2 mg of protein of freshly prepared extract; the reaction was started by addition of 0.2 mm acetyl-CoA. Basal activity with NADH and the extract was always subtracted. Complete inhibition of the ADH activity with pyrazole was determined separately in the ADH assay. Acetyl-CoA synthetase activity was determined by following the release of CoA-SH from acetyl-CoA with 5,5¢-dithiobis(2-nitrobenzoic acid). The assay contained 50 mm Tris/HCl (pH 7.5), 0.2 mm acetyl-CoA, 40 mm potassium phosphate, 10 mm $MgCl_2$, 0.05–0.1 mg of freshly prepared extract and 0.15 mm 5,5¢-dithiobis(2-nitrobenzoic acid). The reaction was started by the addition of 2 mm ADP.

In vitro PFOR inhibition assays

The enzymatic assay buffer (100 mm Na_2HPO_4, pH 7.4) was saturated with medicinal O_2 by constant bubbling for 30 min at room temperature. Final O_2 concentrations of 0.63 ± 0.04 mm (at 36 ºC, 2240 m altitude) were reached as determined in a Clark-type O_2 electrode. Amebal soluble fraction samples (3–5 mg of protein) were diluted 10 times in the O_2-saturated buffer, and the remaining PFOR activity was determined at different times. To determine *Eh*PFOR reactivation, soluble samples were diluted in the O_2-saturated buffer for 30 min on ice, 1 mm ferrous ammonium sulfate (Fe^{2+}) and 5 mm dithiothreitol were added, the samples were kept on ice under an N_2 atmosphere, and PFOR activity was determined at the indicated times. Fe^{3+}, Co^{2+}, Cu^{2+} and Mn^{2+} (1 mm) were also tested instead of Fe^{2}.

To determine the *Eh*PFOR IC_{50} value for O_2, O_2-saturated (0.63 ± 0.04 mm O_2) or normoxic (0.18 ± 0.09 mm O_2) enzymatic assay buffer was treated with different amounts of dithionite (maximal concentration of 2.0 mm) to generate different concentrations of dissolved O_2, as determined with an O_2 electrode. The O_2 concentrations of the solutions kept in sealed Eppendorf tubes were stable for at least 4 h on ice. Amebic samples (4–6 mg of protein in 150 µL) were diluted in 1.35 mL of each buffer and incubated for 4 h on ice, and the remaining *Eh*PFOR activity was determined. A control experiment was prepared with a sample diluted in N_2-purged buffer, and incubated for 4 h on ice in the absence or presence of 2 mm dithionite.

For *Eh*PFOR protection assays, soluble samples were incubated in O_2-saturated buffer in the absence or presence of either 1 mm pyruvate, 0.05 mm CoA, 0.05 mm acetyl-CoA, 50 U of SOD, or 50 U of Cat or SOD+ Cat, and the remaining activity was determined at different times. *Eh*PFOR was also inhibited by incubation with 50 µm H_2O_2 (previously calibrated) on ice under an N_2 atmosphere; at different times, an aliquot was withdrawn and incubated for a further 20 min with 10 U of Cat to eliminate excess H_2O_2, and this was followed by incubation with Fe^{2+} under an N_2 atmosphere and reducing conditions, as described above, to explore reactivation.

In vivo enzyme inactivation and glycolytic fluxes

One million trophozoites per Eppendorf tube were aliquoted, resuspended in 1.1 mL of NaCl/P_i (137 mm NaCl, 2.7 mm KCl, 10 mm Na_2HPO_4, 2 mm KH_2PO_4; pH 7.4) supplemented with 5 mm glucose and previously saturated with O_2, and incubated in a water bath at 36 ºC. Control samples were processed in parallel, with amebas suspended in the same buffer under normoxic conditions. After 30 min, the cells were quickly harvested at 4 ºC, resuspended in 1.1 mL of normoxic NaCl/P_i + glucose, and returned to the water bath. Eight to 10 tubes were withdrawn for each time point, and centrifuged at 2000 g for 5 min. The cellular pellets from the same incubation time point were pooled and disrupted for determination of *Eh*PFOR, *Eh*ADH2 and AcCoAS activities as described above, whereas the supernatant was extracted with perchloric acid, as described previously [7], for ethanol and acetate determination. Ethanol was determined in hexane-extracted supernatant neutralized samples in a gas chromatograph GC 2010 (Shimadzu), equipped with an SP-2330 fused silica capillary column (80% polybiscyanopropyl/20% cyanopropylphenyl siloxane, 60 m · 0.25 mm · 0.2 µm) (Supelco, St Louis MO, USA). In this procedure, 1/50 of the added ethanol is determined; then, the final value is normalized. Acetate was determined in 50 mm Hepes/1 mm EGTA (pH 8.0) buffer, 7 mm $MgCl_2$, 6 mm ATP, 2 mm PEP, 0.15 mm NADH and 0.45 U of PYK/lactate dehydrogenase. The assay was started by the addition of 1–1.5 U of acetate kinase.

Lipid peroxidation assay

Lipid peroxidation levels (equivalents of malondialdehyde) were measured as described previously [18], in amebas exposed and unexposed to the O_2 and during recovery under normoxic conditions.

Data analysis

Data are reported as means ± standard deviations (SDs), except in Fig. 4B,C, where means ± standard errors (SEs) are shown. A two-tailed Student's *t*-test for nonpaired

samples was also applied where indicated. The number of independent preparations assayed is indicated in parentheses.

Modeling the *Eh*PFOR tertiary structure

A 3D model for the *Eh*PFOR amino acid sequence (GenBank accession number: EH_051060) was obtained with swiss-model software (available at http://swissmodel.expasy.org/) [54,55], and by using the crystal structure reported for *Da*PFOR (accession number: 1b0p) [25] as template. The amino acid sequence identity between the enzymes is 54.4%. Analysis of the resulting structures and generation of figures were performed with pymol (http://www.pymol.org).

Acknowledgements

This study received financial support from CONACyT-Mexico grants 83084 to E. Saavedra and 59175. E. Pineda is supported by CONACyT fellowship No. 210311. We thank M. El-Hafidi for his help with ethanol determination by GC, and M. Nequiz for his help with amebal culture.

References

1 Reeves RE (1984) Metabolism of *Entamoeba histolytica*. *Adv Parasitol* 23, 105–142.

2 Reeves RE, Serrano R & South DJ (1976) 6-Phosphofructokinase (pyrophosphate). Properties of the enzyme from Entamoeba histolytica and its reaction mechanism. *J Biol Chem* 251, 2958–2962.

3 Saavedra-Lira E, Ramírez-Silva L & Pérez-Montfort R (1998) Expression and characterization of recombinant pyruvate phosphate dikinase from *Entamoeba histolyti- ca*. *Biochim Biophys Acta* 1382, 47–54.

4 Saavedra E, Encalada R, Pineda E, Jasso-Chávez R & Moreno-Sánchez R (2005) Glycolysis in *Entamoeba histolytica*. Biochemical characterization or recombinant glycolytic enzymes and flux control analysis. *FEBS J* 272, 1767–1783.

5 Chi AS, Deng Z, Albach RA & Kemp RG (2001) The two phosphofructokinase gene products of *Entamoeba histolytica*. *J Biol Chem* 276, 19974–19981.

6 Saavedra E, Olivos A, Encalada R & Moreno-Sánchez R (2004) *Entamoeba histolytica*: kinetic and molecular evidence of a previously unidentified pyruvate kinase. *Exp Parasitol* 106, 11–21.

7 Saavedra E, Marín-Hernández A, Encalada R, Olivos A, Mendoza-Hernández G & Moreno-Sánchez R (2007) Kinetic modeling can describe *in vivo* glycolysis in *Entamoeba histolytica*. *FEBS J* 274, 4922–4940.

8 Reeves RE & South DJ (1974) Phosphoglycerate kinase (GTP). An enzyme from Entamoeba histolytica selective for guanine nucleotides. *Biochem Biophys Res Commun* 58, 1053–1057.

9 Encalada R, Rojo-Domínguez A, Rodríguez-Zavala JS, Pardo JP, Quezada H, Moreno-Sánchez R & Saavedra E (2009) Molecular basis of the unusual catalytic preference for GDP/GTP in *Entamoeba histolytica* 3-phosphoglycerate kinase. *FEBS J* 276, 2037–2047.

10 Moreno-Sánchez R, Encalada R, Marín-Hernández A & Saavedra E (2008) Experimental validation of metabolic pathway modeling. An illustration with glycolytic segments from Entamoeba histolytica. *FEBS J* 275, 3454–3469.

11 Reeves RE, Warren LG, Susskind B & Lo HS (1977) An energy conserving pyruvate-to-acetate pathway in *Entamoeba histolytica*. *J Biol Chem* 257, 726–731.

12 Montalvo FE, Reeves RE & Warren LG (1971) Aerobic and anaerobic metabolism in *Entamoeba histolytica*. *Exp Parasitol* 30, 249–256.

13 Lo HS & Reeves RE (1978) Pyruvate-to-ethanol pathway in *Entamoeba histolytica*. *Biochem J* 171, 225–230.

14 Yang W, Li E, Kairong T & Stanley SL (1994) *Entamoeba histolytica* has an alcohol dehydrogenase homologous to the multifunctional *adhE* gene product of *Escherichia coli*. *Mol Biochem Parasitol* 64, 253–260.

15 Bruchhaus I & Tannich E (1994) Purification and molecular characterization of the NAD+-dependent acetaldehyde/alcohol dehydrogenase from *Entamoeba histolytica*. *Biochem J* 303, 743–748.

16 Espinosa A, Yan L, Zhang Z, Foster L, Clark D, Li E & Stanley SL (2001) The bifunctional *Entamoeba histolytica* alcohol dehydrogenase 2 (EhADH2) protein is necessary for amebic growth and survival and requires an intact C-terminal domain for both alcohol dehydrogenase and acetaldehyde dehydrogenase activity. *J Biol Chem* 276, 20136–20143.

17 Upcroft P & Upcroft JA (2001) Drug targets and mechanisms of resistance in the anaerobic protozoa. *Clin Microbiol Rev* 14, 150–164.

18 Ramos-Martínez E, Olivos-García A, Saavedra E, Nequiz M, Sánchez EC, Tello E, El-Hafidi M, Saralegui A, Pineda E, Delgado J *et al.* (2009) *Entamoeba histolytica*: oxygen resistence and virulence. *Int J Parasitol* 39, 693–702.

19 Olivos-Garcia A, Saavedra E, Ramos-Martínez E, Nequiz M & Pérez-Tamayo R (2009) Molecular nature of virulence in *Entamoeba histolytica*. *Infect Genet Evol* 9, 1033–1037.

20 Williams K, Lowe PN & Leadlay PF (1987) Purification and characterization of pyruvate:ferredoxin oxidoreductase from the anaerobic protozoon *Trichomonas vaginalis*. *Biochem J* 246, 529–536.

21 Townson SM, Upcroft JA & Upcroft P (1996) Characterisation and purification of pyruvate:ferredoxin

oxidoreductase from *Giardia duodenalis*. *Mol Biochem Parasitol* 79, 183–193.

1 Rodriguez MA, Garcí a-Pé rez RM, Mendoza L, Sá nchez T, Guillen N & Orozco E (1998) The pyruvate:ferre- doxin oxidoreductase enzyme is located in the plasma membrane and in a cytoplasmic structure in *Entamoeba*.
Microb Pathog 25, 1–10.

2 Lindmark DG & Mü ller M (1973) Hydrogenosome, a cytoplasmic organelle of the anaerobic flagellate *Tritrichomonas foetus*, and its role in pyruvate metabolism. *J Biol Chem* 248, 7724–7728.

3 Imlay JA (2006) Iron–sulphur clusters and the problem with oxygen. *Mol Microbiol* 59, 1073–1082.

4 Chabriè re E, Charon MH, Volbeda A, Pieulle L, Hatchikian EC & Fontecilla-Camps JC (1999) Crystal structures of the key anaerobic enzyme pyruvate:ferredoxin oxidoreductase, free and in complex with pyruvate. *Nat Struct Biol* 6, 182–190.

5 Pan N & Imlay JA (2001) How does oxygen inhibit central metabolism in the obligate anaerobe *Bacteroides thetaiotaomicron*? *Mol Microbiol* 39, 1562–1571.

6 Pieulle L, Guigliarelli B, Asso M, Dole F, Bernadac A & Hatchikian EC (1995) Isolation and characterization of the pyruvate:ferrdoxin oxidoreductase from the sulfate-reducing bacterium *Desulfovibrio africanus*. *Biochim Biophys Acta* 1250, 49–59.

7 Yoon KS, Ishii M, Kodama T & Igarashi Y (1997) Purification and characterization of pyruvate:ferredoxin oxidoreductase from *Hydrogenobacter thermophilus* TK-6. *Arch Microbiol* 167, 275–279.

8 Samarawickrema NA, Brown DM, Upcroft JA, Thammapalerd N & Upcroft P (1997) Involvement of superoxide dismutase and pyruvate:ferredoxin oxidoreductase in mechanisms of metronidazole resistance in *Entamoeba histolytica*. *J Antimicrob Chemother* 46, 833–840.

9 Brown DM, Upcroft JA, Dodd HN, Chen N & Upcroft P (1999) Alternative 2-keto acid oxidoreductase activities in *Trichomonas vaginalis*. *Mol Biochem Parasitol* 98, 203–214.

10 Clark CG, Alsmark UC, Tazreiter M, Saito-Nakano Y, Ali V, Marion S, Weber C, Mukherjee C, Bruchhaus I, Tannich E *et al.* (2007) Structure and content of the *Entamoeba histolytica* genome. *Adv Parasitol* 65, 51–190.

11 Kerscher L & Oesterhelt D (1981) The catalytic mechanism of 2-oxoacid:ferredoxin oxidoreductase from *Halobacterium halobium.* One-electron transfer at two distinct steps of the catalytic cycle. *Eur J Biochem* 116, 595–600.

12 Jang S & Imlay JA (2007) Micromolar intracellular hydrogen peroxide disrupts metabolism by damaging iron–sulfur enzymes. *J Biol Chem* 282, 929–937.

13 Djaman O, Outten W & Imlay JA (2004) Repair of oxidized iron–sulfur clusters in *Escherichia coli*. *J Biol Chem* 279, 44590–44599.

14 Akbar MA, Chatterjee NS, Sen P, Debnath A, Pal A, Bera T & Das P (2004) Genes induced by a high-oxygen environment in *Entamoeba histolytica*. *Mol Biochem Parasitol* 133, 187–196.

15 Vicente JB, Ehrenkaufer GM, Saraiva LM, Teixeira M & Singh U (2009) *Entamoeba histolytica* modulates a complex repertoire of novel genes in response to oxidative and nitrosative stresses: implications for amebic pathogenesis. *Cell Microbiol* 11, 51–69.

16 Gilchrist CA & Petri WA (2009) Using differential gene expression to study *Entamoeba histolytica* pathogenesis. *Trends Parasitol* 25, 124–131.

17 Biller L, Schmidt H, Krause E, Gelhaus C, Matthiesen J, Handal G, Lotter H, Janssen O, Tannich E & Bruchhaus I (2009) Comparison of two genetically related *Entamoeba histolytica* cell lines derived from the same isolate with different pathogenic properties. *Proteomics* 9, 4107–4120.

18 Kim KW, Yamane H, Zondlo J, Busby J & Wang M (2007) Expression, purification and characterization of human acetyl-CoA carboxylase 2. *Protein Expr Purif* 53, 16–23.

19 Williams KP, Leadlay PF & Lowe PN (1990) Inhibition of pyruvate:ferredoxin oxidoreductase from *Trichomonas vaginalis* by pyruvate and its analogues. Comparison with the pyruvate decarboxylase component of the pyruvate dehydrogenase complex. *Biochem J* 268, 69–75.

20 Ragsdale SW (2003) Pyruvate ferredoxin oxidoreductase and its radical intermediate. *Chem Rev* 103, 2333–2346.

21 Cavazza C, Contreras-Martel C, Pieulle L, Chabriè re E, Hatchikian EC & Fontecilla-Camps JC (2006) Flexibil- ity of thiamine diphosphate revealed by kinetic crystal- lographic studies of reaction of pyruvate–ferredoxin oxidoreductase with pyruvate. *Structure* 14, 217–224.

22 Tittmann K (2009) Reaction mechanisms of thiamin diphosphate enzymes: redox reactions. *FEBS J* 276, 2454–2468.

23 Jiang J, Nakashima T, Liu KJ, Goda F, Shima T & Swartz HM (1996) Measurement of PO_2 in liver using EPR oximetry. *J Appl Physiol* 80, 552–558.

24 Vaupel P, Kallinowski F & Okunieff P (1989) Blood flow, oxygen and nutrient supply, and metabolic microenvironment of human tumors: a review. *Cancer Res* 49, 6449–6465.

25 Ali V, Shigeta Y, Tokumoto U, Takahashi Y & Nozaki T (2004) An intestinal parasitic protist *Entamoeba histolytica*, possesses a non redundant nitrogen fixation-like system for iron–sulfur cluster assembly under anaerobic conditions. *J Biol Chem* 279, 16863–16874.

26 Maralikova B, Ali V, Nakada-Tsukui K, Nozaki T, van der Giezen M, Henze K & Tovar J (2009) Bacterial-type oxygen detoxification and iron–sulfur cluster assembly in amoebal relict mitochondria. *Cell Microbiol* 12, 331–342.

1 Zhang WW, Shen PS, Descoteaux S & Samuelson J (1994) Cloning and expression of the gene for an NADP(+)-dependent aldehyde dehydrogenase of *Entamoeba histolytica*. *Mol Biochem Parasitol* 63, 157–161.
2 Kumar A, Shen PS, Descoteaux S, Pohl J, Bailey G & Samuelson J (1992) Cloning and expression of an NADP(+)-dependent alcohol dehydrogenase gene of *Entamoeba histolytica*. *Proc Natl Acad Sci USA* 89, 10188–10192.
3 Espinosa A, Perdrizet G, Paz-Y-Miñ o CG, Lanfranchi R & Phay M (2009) Effects of iron depletion on *Entamoeba histolytica* alcohol dehydrogenase 2 (EhADH) and trophozoite growth: implications for antiamoebic therapy. *J Antimicrob Chemother* 63, 675–678.
4 Echave P, Tamarit J, Cabiscol E & Ros J (2003) Novel antioxidant role of alcohol dehydrogenase E from *Escherichia coli*. *J Biol Chem* 278, 30193–30198.
5 Pé rez-Tamayo R, Montfort I, Tello E & Olivos A (1992) Ischemia in experimental acute amebic liver abscess in hamsters. *Int J Parasitol* 22, 125–129.
6 Olivos-Garcí a A, Gonzá lez-Canto A, Ló pez-Vancell R, Garcí a de Leó n MC, Tello E, Nequiz-Avendañ o M, Montfort I & Pé rez-Tamayo R (2003) Amebic cysteine proteinase 2 (EhCP2) plays either a minor or no role in tissue damage in acute experimental amebic liver abscess in hamsters. *Parasitol Res* 90, 212–220.
7 Peitsch MC (1995) Protein modeling by E-mail. *Biotechnology* 13, 658–660.
8 Arnold K, Bordoli L, Kopp J & Schwede T (2006) The SWISS-MODEL Workspace: a web-based environment for protein structure homology modelling. *Bioinformatics*, 22, 195–201.

Supporting information

The following supplementary material is available:
Fig. S1. (A) *Eh*PFOR storage stability. (B) *Eh*PFOR pH dependency.
Fig. S2. *Eh*PFOR inhibition by acetyl-CoA.
Fig. S3. (A) Oxygen titration of buffer assay. (B) *Eh*PFOR IC_{50} for oxygen short exposure.
Fig. S4. K_m for acetyl-CoA of AcCoAS.
Table S1. *Eh*PFOR recovery by detergent extraction.

This supplementary material can be found in the online version of this article.

Please note: As a service to our authors and readers, this journal provides supporting information supplied by the authors. Such materials are peer-reviewed and may be re-organized for online delivery, but are not copy-edited or typeset. Technical support issues arising from supporting information (other than missing files) should be addressed to the authors.

3.5. Datos que no se mostraron en el artículo

3.5.1 Reactivación de la EhPFOR

Durante la estandarización del protocolo de reactivación de la EhPFOR después de la exposición con O_2, se ensayaron diferentes estrategias para obtener la mayor reactivación. Para otras enzimas que contienen centros Fe-S (fumarasa, aconitasa, 6-fosfogluconato deshidratasa) y que se han expuesto a condiciones de estrés oxidante se reportó que se puede restablecer la estructura de estos centros incubando con 1 mM Fe^{2+} y 5 mM DTT (Imlay, 2006). A la par de este ensayo de reactivación se incubó el extracto celular en una atmosfera de N_2, de manera individual o en combinación con Fe^{2+} y DTT. La mejor reactivación se obtuvo en la combinación de Fe^{2+}, DTT y N_2 (70% de la actividad inicial), seguida por el Fe^{2+} solo y el Fe^{2+} en condiciones anaerobias (Fig.3.5). El ambiente anaerobio o reductor por sí solos no fueron capaces de restablecer la actividad de la enzima, lo que coincide con los reportes previos que indican que la inactivación de la enzima se debe a la desestabilización del centro 4Fe-4S haciendo que se libere un átomo de Fe^{2+}, lo que produce un centro Fe-S no reactivo (Pan e Imlay 2001; Djaman et al 2004).

Además del Fe^{2+}, se ensayaron otros metales con estado de oxidación +2 y radio iónico ~1.26 Å similares al del Fe a una concentración de 1 mM (Fig. 3.5B). De los metales evaluados solamente el Fe^{2+} fue capaz de reactivar a la EhPFOR. De manera interesante, el Fe^{3+} tampoco tuvo efecto sobre la actividad de la enzima, lo cual resalta la necesidad del Fe^{2+} en la recuperación de la estructura del centro Fe-S. El mecanismo propuesto para la reactivación es que el Fe^{2+} libre se incorpora al centro haciendo que este recupere su estructura tipo 4Fe-4S (Pan e Imlay 2010).

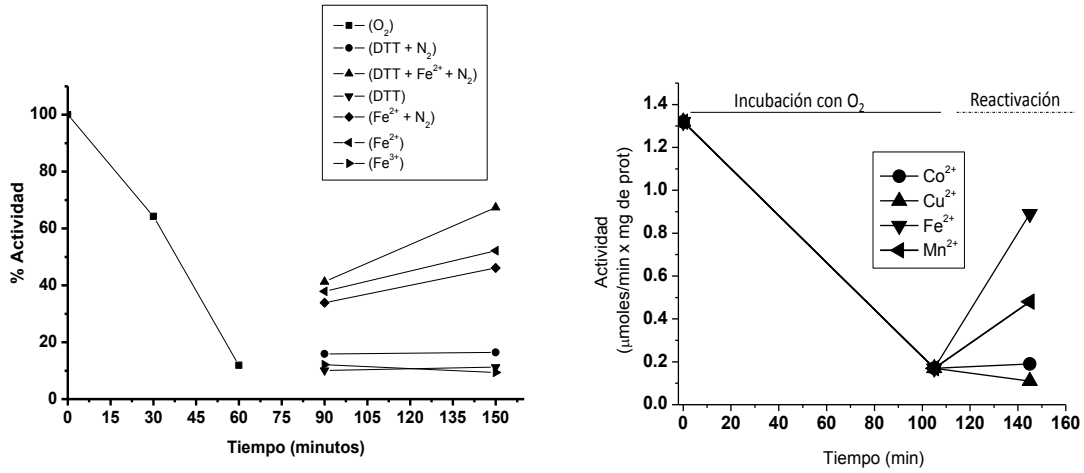

Figura 3.5. Reactivación de la PFOR

A) El extracto se incubó en PBS saturado con O_2 por 30 min, después de ese tiempo se tomaron alícuotas para incubar con DTT, Fe^{2+}, Fe^{3+}, N_2 o la mezcla de estos por 30 min. B) Reactivación con 1 mM de diferentes metales.

3.5.2 Efecto de las EROs sobre la actividad de la EhPFOR

Debido a que la catalasa protegió a la PFOR de la inactivación durante la exposición a O_2, se concluyó que el H_2O_2 también era una de las especies involucradas en la inactivación de la enzima. Por lo tanto, se intentó inhibir a la NADPH:flavina oxidoreductasa, que es una de las enzimas que genera H_2O_2 a partir del O_2 (Bruchaus et al, 1998), utilizando el cloruro de difenil iodonio (DPI), que es un inhibidor de enzimas que contiene flavinas (*Ki* 1-10 µM) (O' Donnell et al, 1993). El extracto amibiano se incubó en condiciones suprafisiológicas de oxígeno en presencia o ausencia de 10 µM de DPI y se monitoreó la actividad a diferentes tiempos. El DPI no solo no protegió a la enzima de la inactivación por oxígeno, sino que por sí mismo es un inhibidor muy potente (Fig. 3.6). Estos resultados concordaron con lo observado para la PFOR de *Trichomonas vaginalis,* en donde al incubar las células con 10 µM del inhibidor por 2 h se observó que la actividad de la PFOR se inhibía drásticamente (Leitsch et al 2010). El mecanismo de la inactivación por DPI aún no se ha dilucidado. Aunque este resultado no fue útil para el objetivo que se estaba persiguiendo, permitió establecer que el DPI es un inhibidor fuerte y

específico de la PFOR amibiana, lo cual nos sirvió para determinar su coeficiente de control a través de la titulación con inhibidores, lo cual se describe en el capítulo 4.

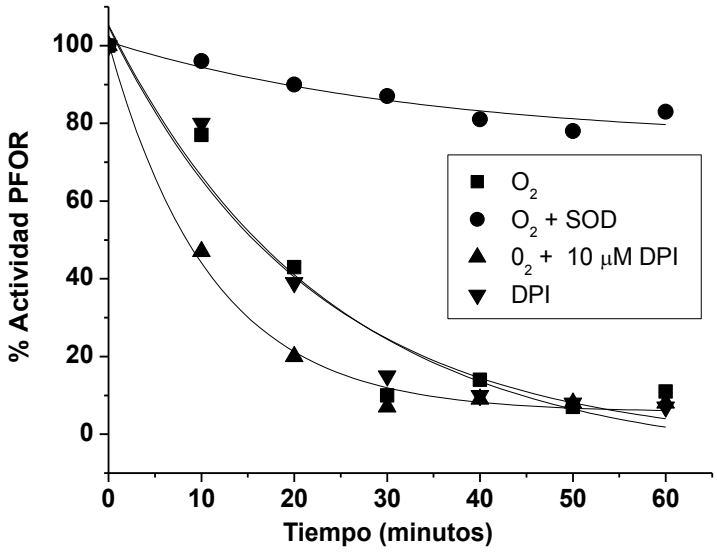

Fig. 3.6 Inhibición de la PFOR por DPI

El extracto se incubó en presencia de O_2, en ausencia o presencia de 1U de SOD o 10 μM del DPI. El trazo de triángulos invertidos fue incubación con 10 μM de DPI sin el reto con oxígeno que demuestra que el compuesto por sí mismo inhibe a la PFOR.

3.5.3 Caracterización cinética de la ADHE recombinante

De acuerdo con nuestros resultados, en amibas expuestas a condiciones suprafisiológicas de O_2 se observa una inhibición drástica de la PFOR pero también de la actividad de aldehído deshidrogenasa de la ADHE y la inhibición de estas enzimas promovió una disminución en la producción de etanol y ATP (Ramos-Martínez et al, 2009). Estos resultados indicaron que la ADHE podría ejercer un control importante sobre la glucólisis amibiana en condiciones de estrés oxidante, por esta razón se estudiaron las características cinéticas de esta enzima.

Se clonó el gen que codifica para la ADHE siguiendo metodologías estandarizadas en el laboratorio (Saavedra et al, 2005). El gen consta de 2.6 Kpb y tuvo 45-30 % de similitud con las secuencias de otras ADHs bacterianas. La proteína se sobre-expresó acoplada a una etiqueta de histidinas en bacterias de *E. coli* y se purificó por cromatografía de afinidad a cobalto siguiendo metodologías estandarizadas (Saavedra et al 2005). La proteína se obtuvo con una pureza mayor al 90% (Fig. 3.7).

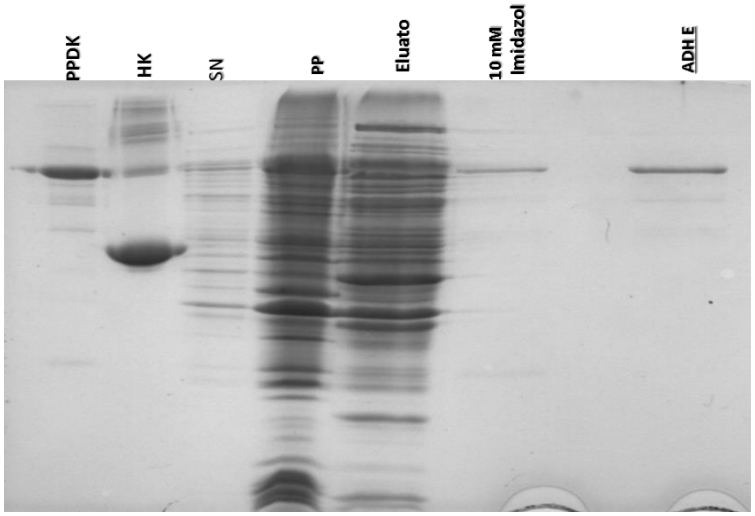

Fig. 3.7. Marcha de purificación de la ADHE
Marcadores de peso molecular PPDK (100 KDa) y HK (54 KDa); SN, fracción soluble del extracto bacteriano; PP, fracción insoluble del extracto bacteriano; eluato, lo que no se pegó a la resina acoplada a Cobalto; 10 mM, lavado con 10 mM de imidazol; ADHE, enzima purificada (99 KDa).

La caracterización cinética se realizó a pHs óptimo y fisiológico utilizando metodologías reportadas previamente (Bruchhaus el al 1994; Saavedra et al, 2005). La enzima mostró cinéticas hiperbólicas para todos los sustratos que se ajustan a la ecuación de Michaelis-Menten (Fig. 3.8). En la Tabla 3.2, se resumen las *Kms* y la velocidad máxima (*Vmax*) obtenidas para la enzima.

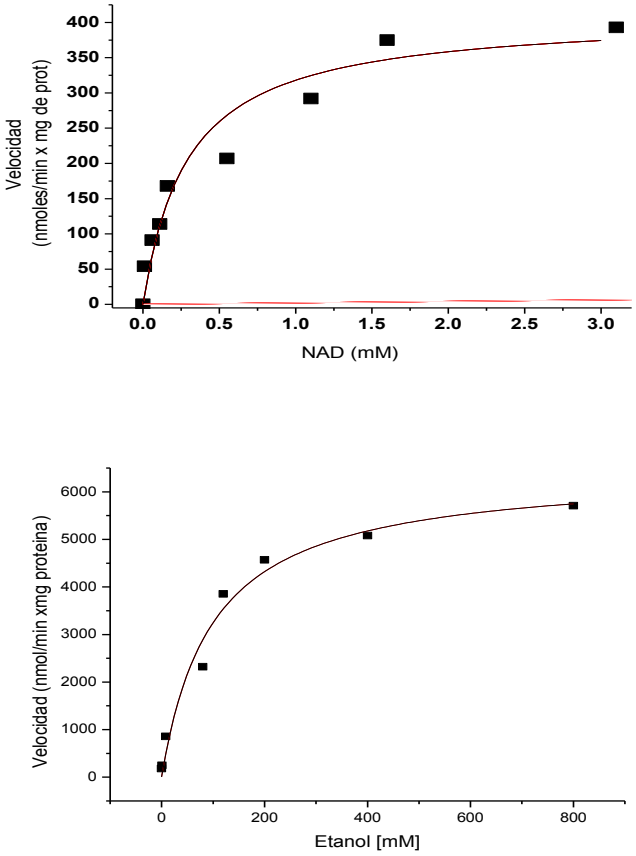

Fig. 3.4. Cinéticas de saturación por los sustratos NAD y etanol en el sentido reverso de la reacción. Las mediciones se hicieron a pH 6.0 y 37 ° C.

Tabla 3.2. Parámetros cinéticos de la EhADHE recombinante

Reacción Fw	**pH 6.0**	**pH 7.0**
Vmax	3527 ± 2980	4843 ± 3200
$Km_{acetil\text{-}CoA}$	33.4 (2)	54 (2)
Km_{NADH}	23 (2)	31 (2)
Reacción Rw		
Vmax	727 ± 430	984 ± 523
Km_{etanol}	106 (1)	94 (2)
Km_{NAD+}	2.1 (1)	1.4 (1)

Vmax en mU/mg prot. *Km* en mM. La temperatura fue de 37 º C

3.6. Discusión General de los resultados de sección parte del estudio

Los antecedentes directos de este trabajo (Ramos-Martínez et al 2009) resaltaban la importancia de la PFOR amibiana en parásitos sometidos a condiciones suprafisiológicas de oxígeno. La alta susceptibilidad de la enzima a ser inhibida por EROs sugería que la enzima podía ser limitante cuando los parásitos se sometían a condiciones aeróbicas y dicha inhibición podría tener efectos negativos sobre el metabolismo energético del parásito. Debido a la escasa información de la PFOR de *E. histolytica*, la primera parte de esta tesis se enfocó en caracterizar cinéticamente a la enzima y estudiar sus mecanismos de inactivación por O_2.

Los valores de *Km* por los sustratos acetil-CoA y piruvato de la PFOR obtenidos a través de la caracterización cinética están cerca de las concentraciones fisiológicas de estos metabolitos en los trofozoítos de *E. histolytica* (1 mM piruvato, 0.05 mM CoA), lo que podría sugerir que la enzima no está limitada por sustratos. Por otro lado, la EhPFOR es más afín por piruvato que por el resto de los oxoácidos

ensayados, lo que descarta la hipótesis propuesta por otros grupos de trabajo que propone que los oxoácidos provenientes de la degradación de aminoácidos tales como α-cetoglutarato o α-cetobutirato pueden entrar a la glucólisis a nivel de la PFOR y ser una fuente de ATP al convertirse en acetato por la AcCoAS (Clark et al. 2007). Asimismo, de todas las enzimas glucolíticas evaluadas, la PFOR es una de las que tiene mayor actividad. Por lo tanto, desde el punto de vista cinético, la PFOR podría no ser limitante para el flujo glucolítico.

A pesar de esta aparente alta eficiencia catalítica de la PFOR, su alta susceptibilidad de inhibición por EROs seguía siendo una posible causa de limitación cuando los parásitos se sometieran a estrés oxidante. La EhPFOR es fuertemente inhibida por exposición a oxígeno; sin embargo, la inactivación es reversible al adicionar Fe^{2+} en condiciones reductoras. Esto concuerda con lo observado en otras enzimas con centros Fe-S (Pan e Imlay, 2001), aunque la reactivación depende del tiempo de exposición a los oxidantes y obviamente en las células dependería de la existencia de mecanismos antioxidantes eficientes para evitar el daño estructural irreversible. Los metabolitos acetil-CoA y CoA pueden proteger de la inactivación; en contraste, el piruvato aceleró el proceso de inactivación, pero esto solamente en una condición de alto estrés oxidante.

En los nuevos experimentos reportados en esta tesis, al exponer los trofozoítos al reto de oxígeno se observó el arresto en el flujo glucolítico y una fuerte inhibición de la PFOR, lo que concordó con nuestro hallazgo anterior (Ramos-Martínez et al 2009). Sin embargo, los resultados también resaltaron el efecto del oxígeno sobre la actividad de aldehído deshidrogenasa de la ADHE, la cual no había sido incluida en los análisis anteriores. Por lo tanto, ahora se puede concluir que el efecto adverso en los flujos glucolíticos que se observaron se deben atribuir a la inhibición que ejerce el estrés oxidante en las actividades de PFOR y ADHE.

Por otro lado, a la par de la inhibición de la PFOR y la ADHE se observó la disminución en la producción de etanol y acetato, pero al re-incubar a las amibas en normoxia, la actividad de dichas enzimas se recuperó sin necesidad de adicionar Fe^{2+} a las células. Esto sugiere que los trofozoítos tiene la maquinaria necesaria

para restablecer la función de las proteínas. Al respecto, se ha reportado que las amibas contienen únicamente el sistema NIF (Nitrogen Fixation-like) para síntesis de centros fierro azufre, el cual es más parecido a lo que se encuentra en bacterias, y también se estableció que la síntesis de los centros Fe-S se lleva a cabo preferentemente en el citosol, y en mucho menor medida en el mitosoma (Ali et al, 2004, Ali y Nozaki 2012).

Es importante puntualizar que en los primeros 60 min de incubación en normoxia después de someter a los parásitos al O_2, aun cuando la PFOR inicia su recuperación, el flujo hacia etanol no se ve favorecido sino hasta que la ALDH-ADHE se recupera después del minuto 60, en el cual además de incrementarse la producción de etanol disminuye el flujo hacia acetato (Fig. 3.4). Estos resultados sugirieron que tal vez la PFOR no ejercía un control importante en la producción de etanol, no así la ADHE, cuya reactivación propició la recuperación en el flujo hacia acetato.

La ADHE es una enzima bifuncional que posee actividad de aldehído y alcohol deshidrogenasa en dominios catalíticamente independientes (Bruchhaus y Tannich, 1994). En el dominio de ADH se encuentra un sitio de unión a Fe^{2+}, el cual puede ser blanco del estrés oxidativo. Se ha reportado que para que la enzima tenga actividad de ALDH es necesaria la integridad de los dos dominios y del sitio de unión al metal. De hecho´, al separar ambos dominios solo se mantiene activo el dominio de ADH y mutaciones en este dominio afectan también la actividad de ALDH (Espinosa *et al* 2001). De manera adicional, la ADHE se ha identificado como una proteína que une a la holotransferrina para internalizar hierro del medio extracelular (Reyes-López et al, 2011). Por lo tanto, la ADHE está involucrada en el metabolismo del hierro esencial para el crecimiento del parásito, y es susceptible al estrés oxidante.

3.7 Conclusión

De acuerdo con estos resultados, la PFOR es de las enzimas glucolíticas con mayor actividad, junto con la TPI y la PGK, y aún cuando se inhibe drásticamente por O_2, la actividad remanente es todavía suficiente para mantener el flujo glucolítico. Esto sugería que la PFOR podría no tener un alto C_{ai}^{J} sobre el flujo glucolítico en el parásito. La disminución en la producción de etanol en amibas expuestas a O_2 se debe a que a la par de la PFOR se inhibe la actividad de ALDH de la ADHE, lo que afecta el flujo de la vía. Estos resultados sugieren que la ADHE podría tener un alto coeficiente de control en la vía. Estas hipótesis fueron analizadas determinando los coeficientes de control de flujo de estas dos enzimas.

De manera importante, la PFOR y la ADHE son los principales blancos glucolíticos del oxígeno y las EROS, por lo que pueden funcionar como marcadores de estrés oxidativo.

CAPÍTULO 4. DETERMINACIÓN DEL COEFICIENTE DE CONTROL DE LA PFOR Y LA ADHE SOBRE EL FLUJO GLUCOLÍTICO EN CONDICIONES AERÓBICAS

Una de las estrategias para determinar los mecanismos que controlan el metabolismo de la glucosa en *E. histolytica* es aplicar los fundamentos del MCA para determinar los coeficientes de control del flujo (C_{ai}^{J}) para cada una de las enzimas involucradas en dicho metabolismo. Al respecto, nuestro grupo de investigación reportó el primer modelo cinético (computacional) de la glucólisis amibiana que incluye las ecuaciones de velocidad desde la HK y PPDK (Saavedra et al 2007). Debido a la escasa información cinética de la PFOR y la ADHE, estas no se incluyeron en dicho modelo y por lo tanto el bajo C_{ai}^{J} que se reportó (1%) podría haberse subestimado. Sin embargo, debido a la relevancia de la actividad de la PFOR y ADHE como posibles limitantes del metabolismo energético en condiciones de estrés oxidante demostrada anteriormente, surgió la necesidad de realizar un análisis cuantitativo para determinar el grado de control que tienen estas enzimas sobre el flujo glucolítico en condiciones aeróbicas. Por lo tanto, además de determinar el C_{ai}^{J} de la PFOR, que se propuso como el objetivo inicial de esta tesis, ahora se incluyó la determinación del control de la ADHE, ambos en condiciones aeróbicas.

Los resultados obtenidos se publicaron en el artículo:

The bifunctional aldehyde-alcohol dehydrogenase controls ethanol and acetate production in *Entamoeba histolytica* under aerobic conditions.

Pineda E, Encalada R, Olivos-García A, Néquiz M, Moreno-Sánchez R, Saavedra E. FEBS Lett. 2013. **587**(2):178-84. Factor de impacto 2012 =3.58

A continuación se resumen la estrategia experimental y los resultados principales del trabajo.

4.1 Estrategia experimental general

Trofozoítos amibianos se cosecharon y lavaron con solución PBS (137 mM NaCl, 2.7 mM KCl, 10 mM Na_2HPO_4, 2 mM KH_2PO_4 pH 7.4). Se resuspendieron a una concentración de 1x 10^6 parásitos/ mL en PBS equilibrado con aire (0.16 mM de O_2 a 37 °C y 2240 m sobre el nivel del mar) suplementado con 10 mM de glucosa. Se tomaron alícuotas de 1 mL de la mezcla, se colocaron en tubos Eppendorf y se incubaron a 37°C en presencia de 0.1 µM de DPI por 0, 10, 20, 40 y 60 min para titular la actividad de PFOR o con 0.05 µM de disulfiram por 0, 10, 20 y 30 min para inhibir la actividad de ADHE. Se tomaron 6 tubos para cada tiempo, se centrifugaron para eliminar el buffer con el inhibidor y el precipitado celular de dos muestras se mezcló y se trató para obtener el extracto citosólico (utilizando la metodología descrita en el capítulo anterior) para determinar la actividad de PFOR o ADHE.

El resto de las muestras se utilizaron para determinar los flujos de la siguiente manera. A dos muestras se les adicionó 1 mL de PBS normóxico suplementado con glucosa y se realizó la extracción con ácido perclórico para determinar la concentración de etanol y acetato en el tiempo cero. Las muestras restantes se resuspendieron en la misma solución amortiguadora de pH se incubaron a 37 °C por 30 min; al final de esta incubación se recuperó el sobrenadante, se extrajo con ácido perclórico y se determinaron los metabolitos etanol y acetato de acuerdo a la metodología descrita (Saavedra et al, 2007). Las muestras control no incluyeron los inhibidores y se trataron de igual manera. Para la determinación de los metabolitos glucolíticos se utilizaron 20 x10^6 amibas control o tratadas con los inhibidores.

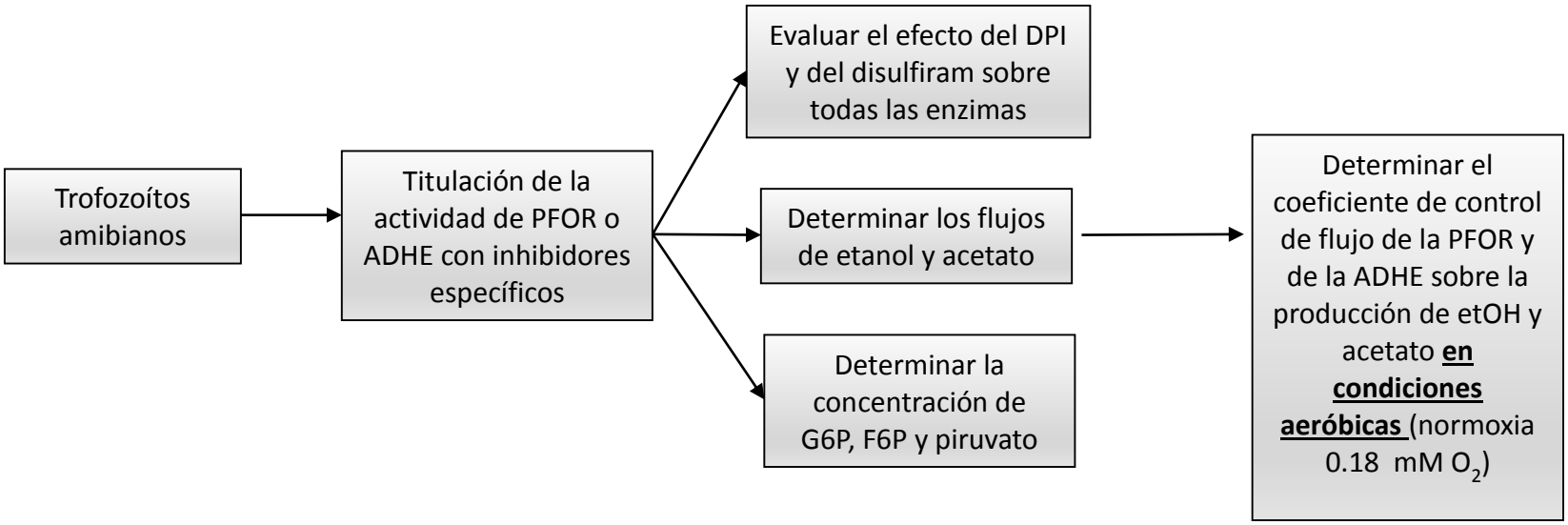

Fig 4.1 Estrategia general del estudio.

4.2. Resultados

4.2.1 Estrategia de inhibición de la actividad enzimática

Para determinar el coeficiente de control de flujo de una enzima es necesario variar su actividad en la célula y en paralelo medir el flujo de la vía metabólica. De la gráfica de flujo *versus* actividad enzimática se calcula el C_{ai}^{J} (Fig. 1.6) (Fell, 1997; Moreno-Sánchez et al, 2008).

Una estrategia experimental para variar la actividad de una enzima es a través de la utilización de inhibidores específicos, con la condición de que estos inhiban únicamente a la enzima de la cual se está determinando el coeficiente de control o alternativamente, que no inhiban a otras enzimas de la vía que se está analizando en las condiciones experimentales en las que se está haciendo el análisis y además que no afecten la viabilidad de la célula. Por lo tanto, la primera tarea para cumplir el objetivo era encontrar compuestos que inhibieran preferentemente a la PFOR o a la ADHE y encontrar las condiciones en las que no se afectaran al resto de las enzimas glucolíticas amibianas.

Como se describió anteriormente en el capítulo 3, el DPI es un inhibidor potente de la PFOR. En la figura 4.2A se muestra la cinética de inhibición de la PFOR en amibas expuestas a diferentes concentraciones de DPI; el compuesto inhibe a concentraciones submicromolares, con una IC_{50} es de 0.62 µM a 60 min de incubación. Además se determinó que el DPI es un inhibidor irreversible de la PFOR amibiana (Fig.1B del artículo); esto es importante para la determinación del coeficiente de control de la enzima pues es necesario que la actividad inhibida se mantenga constante durante la medición de los flujos metabólicos. Se seleccionó la estrategia de incubar con 0.1 µM de DPI por 60 min debido a que en esta condición no se afectan el resto de las enzimas glucolíticas, además de que la viabilidad celular se mantiene en 90% a lo largo del experimento.

En el caso de la ADHE se ensayaron diferentes inhibidores de deshidrogenasas (gosipol, pirazol, disulfiram) a diferentes concentraciones y tiempos

de exposición; sin embargo, todos estos inhibidores afectaron en mayor o menor medida a la GAPDH, que es otra deshidrogenasa presente en la vía glucolítica. El menor efecto sobre la GAPDH se observó al utilizar disulfiram. Se decidió trabajar a una concentración de 0.05 µM DSF, la cual equivale a la IC_{50} para la ADHE; aunque no se alcanzaba una total inhibición de esta enzima, esta concentración inhibía en solamente un 17% a la GAPDH (Fig. 4B y Tabla 1 del artículo). Es importante mencionar que la viabilidad de los trofozoítos se mantuvo por arriba del 85% en estas condiciones.

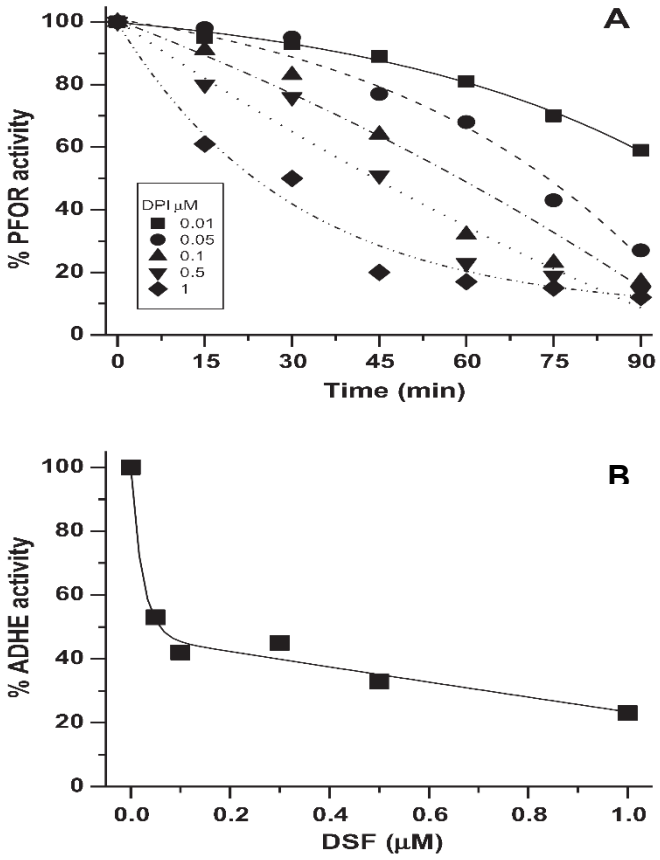

Figura 4.2. Efecto del DPI y el disulfiram sobre la PFOR y ADHE, respectivamente.

A) Cinética de inactivación de la PFOR de extractos amibianos con diferentes concentraciones de DPI.
B) Cinética de inactivación de la ADHE en presencia de disulfiram (DSF) por 30 min.

4.2.2 Determinación de los coeficientes de control del flujo glucolítico

Una vez establecidas las condiciones para lograr la inhibición parcialmente específica de las enzimas de interés y establecer que en estas condiciones los inhibidores no afectaran la viabilidad de los parásitos, el siguiente paso fue determinar el C_{ai}^{J} para cada una de estas enzimas sobre la producción de etanol y acetato. Para estos experimentos se incubaron amibas con 0.1 µM DPI o 0.05 µM DSF por diferentes tiempos en PBS equilibrado con el aire (que corresponde a 0.18 mM O_2 disuelto) y se midió la actividad de PFOR o ADHE, respectivamente. A cada grado de inhibición se determinaron el etanol y acetato producidos para calcular los flujos de síntesis de estos metabolitos. Con estos datos se construyeron las gráficas de actividad enzimática contra el flujo de la vía (Fig. 4.3). Los C_{ai}^{J} corresponden a la pendiente del ajuste en cada una de las gráficas. Los coeficientes de control obtenidos se muestran en la Tabla 4.1.

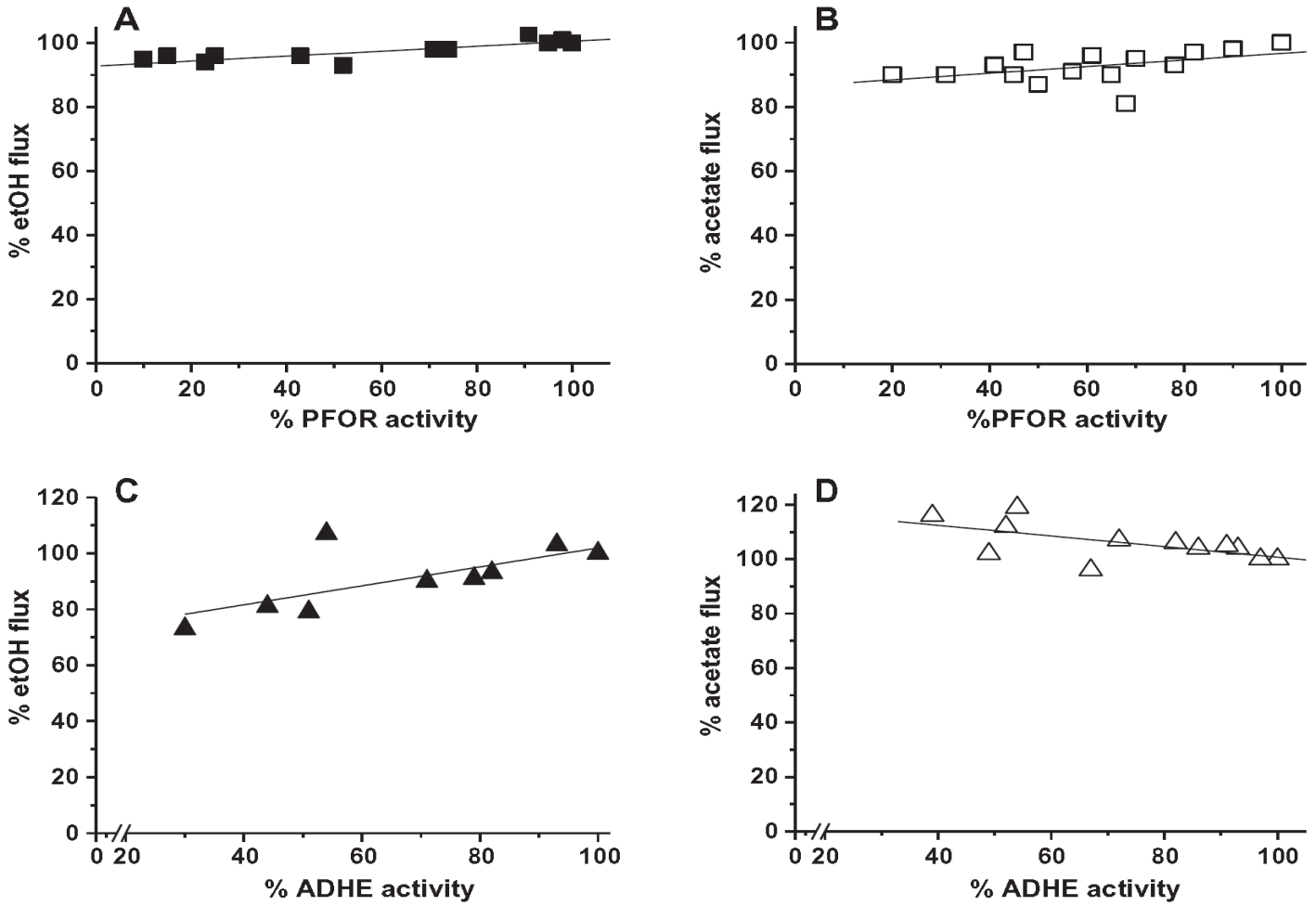

Figura 4.3. Determinación de los coeficientes de control de la PFOR y la ADHE sobre el flujo glucolítico.

Trofozoítos amibianos se incubaron en presencia de DPI 0.1 μM (A y B) o disulfiram 0.05 μM (C y D) por diferentes tiempos. A cada punto se determinó la actividad de PFOR o ADHE y los flujos hacia etanol y acetato.

Tabla 4.1. Coeficientes de control de la PFOR y la ADHE hacia la síntesis de etanol y acetato en condiciones aeróbicas.

Enzyme	C^{Jetoh}_{ai}	$C^{Jacetate}_{ai}$
PFOR	0.072 ± 0.015	0.09 ± 0.03
ADHE	0.33 ± 0.13	- 0.19 ± 0.08

Promedio ± DS de la regresión lineal de las gráficas de la Fig. 4.3

Los resultados indicaron que la PFOR controla menos del 10% la producción de etanol y acetato, en contraste la ADHE ejerce el 33% del control hacia la producción de etanol y el - 19% el flujo hacia acetato; este coeficiente de control tiene signo negativo porque la ADHE compite con la acetato tiocinasa por la acetil-CoA que se genera en la glucólisis, representando así una fuga hacia la producción de etanol.

Finalmente se analizó el efecto de la inhibición de cada una de estas enzimas sobre algunos de los intermediarios de la glucólisis amibiana (Fig. 4.4). La inhibición de la PFOR conduce a la acumulación de 2.5 veces la concentración de G6P, 50% de incremento en F6P y 2 veces incremento en el piruvato; de manera relevante, esta inhibición no afectó los niveles de ATP. Por otro lado, la inhibición de la ADHE condujo a una mayor acumulación de los intermediarios (4.5 veces G6P, 60% F6P y 3 veces piruvato) y de manera relevante, la inhibición de la ADHE sí provocó la disminución en la poza de ATP a cerca del 50%.

Estos resultados indicaron que contrario a la hipótesis planteada para la tesis, en condiciones aeróbicas de normoxia, la ADHE controla más que la PFOR el flujo glucolítico.

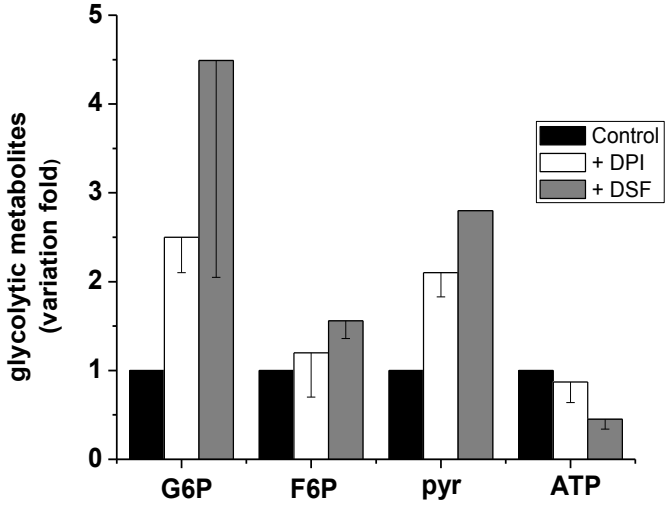

Figura 4.4: Concentración de metabolitos en amibas incubadas con DPI o disulfiram.
Las amibas se incubaron con 0.1 µM de DPI por 60 min o 0.05 µM de disulfiram por 30 min a 36 °C. Las concentraciones control fueron G6P 2.81 ± 0.75 mM, F6P 1.04 ± 0.18 mM, piruvato 0.87 ± 0.4 y ATP 2.74 ± 0.88 mM.

4.3. Discusión

Los resultados iniciales de este trabajo doctoral indicaron que dentro de las enzimas glucolíticas, la PFOR y la ADHE son los principales blancos del estrés oxidativo generado al exponer amibas a condiciones aerobias. Este efecto podría ser relevante de manera fisiológica cuando las amibas están invadiendo tejidos y se exponen a concentraciones de oxígeno mayores a las que se encuentran en el colon (38.3 µM en hígado y 65 µM en mucosa gástrica versus 15 µM en el colon) (Jiang *et a*l, 1996; Vaupel P *et al,* 1989;). El efecto estresante del oxígeno va a depender del tiempo de exposición. Al respecto, se ha reportado que en las etapas iniciales del modelo del absceso hepático amibiano en hámster transcurren al menos 6 h a partir

de que las amibas se inyectan por la vena porta del roedor para que se forme el foco isquémico (Olivos-García *et al*, 2003). En este lapso se sabe que la supervivencia de los trofozoítos se ve drásticamente comprometida y uno de los factores que podrían estar involucrados en la eliminación de los parásitos es el estrés oxidante al que están expuestos. .

Estos hallazgos resaltaron la importancia del efecto del estrés oxidativo sobre la supervivencia y probablemente sobre el metabolismo energético amibiano. Debido a lo anterior es que se consideró relevante determinar el grado de control de la PFOR y la ADHE sobre el flujo glucolítico, ya que en condiciones aeróbicas estas enzimas podrían ser limitantes debido a su potencial de ser inhibidas por EROs.

Los resultados del MCA indicaron que la ADHE ejerce un control significativo hacia la producción de etanol (y en menor medida en la producción de acetato) mientras que la PFOR tiene menor control del flujo glucolítico. Estos resultados concuerdan con los hallazgos descritos en el capítulo 3, en donde al someter amibas a condiciones suprafisiológicas de oxígeno se inhibe preferentemente la PFOR (90%) y en menor proporción la ADHE (68%). Sin embargo, aún cuando las células gradualmente recuperaron la actividad de la PFOR no se observó el restablecimiento inmediato del flujo hacia etanol, y es hasta que la ADHE inicia su reactivación cuando la velocidad de producción de etanol empieza a restablecerse.

Todo lo anterior se explica cuando se consideran las velocidades máximas de ambas enzimas en los extractos amibianos. La PFOR, junto con la triosafosfato isomerasa (TPI) y la 3-fosfoglicerato cinasa (PGK), es de las enzimas glucolíticas con mayor actividad (1000 nmoles/min*mg de proteína celular). A pesar de que se inhibe en un 90% en células expuestas a concentraciones suprafisiológicas de O_2, la actividad de PFOR remanente es superior al flujo glucolítico de etanol determinado en condiciones aeróbicas (26-17nmoles/ min*mg proteína celular). En contraste, la actividad de la ADHE en extractos se encuentra alrededor de 80 nmoles/min*mg de proteína, por lo que la inhibición de la enzima a un 50% quedaría en valores cercanos a los del flujo glucolítico.

Aunado a lo anterior, al inhibir a la ADHE se observó un incremento mayor en las pozas de hexosas fosfato y piruvato y la disminución en la concentración de ATP mientras que para la PFOR, aunque las hexosas y triosasfosfato aumentaron, los niveles de ATP no cambiaron de manera estadísticamente significativa. Todos estos resultados apoyan la conclusión de que en condiciones de estrés oxidante la ADHE controla más que la PFOR.

Recientemente se estableció que la capacidad antioxidante amibiana puede estar relacionada con la virulencia del parásito (Santos y Olivos-García, manuscrito en preparación). En cepas de *E. histolytica* no virulenta y *E. dispar* la capacidad de contender contra las EROs generadas durante la exposición a O_2 es menor que en la cepa virulenta de *E. histolytica*. En las cepas no virulentas la actividad de PFOR se inhibió de manera irreversible, no así en la cepa invasiva de *E. histolytica,* en donde aún cuando la inactivación de la enzima se llevó a cabo, el daño no fue tan severo como para hacer irreversible el proceso. Estos resultados sugieren que la PFOR puede funcionar como indicador de estrés oxidativo.

Debido a que la ADHE no se encuentra en el hospedero, se puede proponer a esta enzima como un sitio adecuado de intervención terapéutica basado en su participación relevante en el control de la glucólisis amibiana. Al respecto, se ha estudiado el efecto de compuestos derivados de cicloalcanos que inhiben *in vitro* a la ADHE a concentraciones menores a 50 µM y que inhiben el crecimiento del parásito. (Espinosa *et al* 2004). Desafortunadamente no se ha determinado si la inhibición es específica para ADHE, por lo que no se puede descartar que en el efecto sobre la viabilidad contribuyan otros procesos.

4.5. Conclusión:

De acuerdo con nuestros resultados, la PFOR es de las enzimas glucolíticas con mayor actividad, junto con la TPI y la PGK, y aún cuando se inhibe drásticamente por O_2, la actividad remanente es todavía suficiente para mantener el flujo glucolítico,

por lo que esta enzima puede no poseer un alto C_{ai}^{J} sobre el flujo glucolítico en el parásito. La disminución en la producción de etanol en amibas expuestas a O_2 se debe a que a la par de la PFOR se inhibe la actividad de aldehído deshidrogenasa de la ADHE, lo que afecta el flujo de la vía, por lo tanto se puede suponer que esta enzima posee un alto coeficiente de control en la vía.

La PFOR y la ADHE son los principales blancos glucolíticos del oxígeno y las EROS, por lo que pueden funcionar como marcadores de estrés oxidativo.

4.6. Artículo: The bifunctional aldehyde-alcohol dehydrogenase controls etanol and acetate production in Entamoeba histolytica under aerobic conditions

FEBS Letters 587 (2013) 178–184

FEBS Letters

journal homepage: www.FEBSLetters.org

The bifunctional aldehyde–alcohol dehydrogenase controls ethanol and acetate production in *Entamoeba histolytica* under aerobic conditions

Erika Pineda [a], Rusely Encalada [a], Alfonso Olivos-García [b], Mario Néquiz [b], Rafael Moreno-Sánchez [a], Emma Saavedra [a,*]

[a] Departamento de Bioquímica, Instituto Nacional de Cardiología Ignacio Chávez, México D.F. 14080, Mexico
[b] Departamento de Medicina Experimental, Facultad de Medicina, Universidad Nacional Autónoma de México, México D.F. 04510, Mexico

ARTICLE INFO

Article history:
Received 22 August 2012
Revised 15 November 2012
Accepted 19 November 2012
Available online 28 November 2012

Edited by Judit Ovádi

Keywords:
Protozoan parasite
Energy metabolism
Oxidative stress
Glycolysis
Flux control
Ethanol production
Acetate production

ABSTRACT

By applying metabolic control analysis and inhibitor titration we determined the degree of control (flux control coefficient) of pyruvate:ferredoxin oxidoreductase (PFOR) and bifunctional aldehyde-alcohol dehydrogenase (ADHE) over the fluxes of fermentative glycolysis of *Entamoeba histolytica* subjected to aerobic conditions. The flux-control coefficients towards ethanol and acetate formation determined for PFOR titrated with diphenyleneiodonium were 0.07 and 0.09, whereas for ADHE titrated with disulfiram were 0.33 and 0.19, respectively. ADHE inhibition induced significant accumulation of glycolytic intermediates and lower ATP content. These results indicate that ADHE exerts significant flux-control on the carbon end-product formation of amoebas subjected to aerobic conditions.

1. Introduction

Entamoeba histolytica is the human intestinal parasite that causes amebiasis. This organism as a trophozoite lives under microaerophilic environments of <5% atmospheric O_2 (i.e., <30 μM dissolved) in *in vitro* cultures [1]; these O_2 concentration values are similar to those usually found in the human colon [2]. Hence, the parasite is adapted to a fermentative glycolysis as the main pathway to produce ATP for cellular work. Remarkably, its glycolytic pathway deviates in several aspects from that in the human host [3]. It contains the pyrophosphate-dependent enzymes PPi-phosphofructokinase and pyruvate phosphate dikinase as well as a GDP-dependent 3-phosphoglycerate kinase (GDP-PGK) [4–6], which replace the functions in mammalian cells of the ATP-phosphofructokinase, pyruvate kinase and ADP-dependent PGK, respectively. Furthermore, amebas lack lactate dehydrogenase and the pyruvate dehydrogenase complex, nor do they have pyruvate decarboxylase as yeasts. Instead, pyruvate (Pyr) is oxidatively decarboxylated to acetyl-CoA and CO_2 by pyruvate:ferredoxin oxidoreductase (PFOR, E.C. 1.2.7.1) [3,7] where the reductive equivalents are transferred to ferredoxin. Acetyl-CoA can be converted to ethanol (etOH) by the action of a bifunctional aldehyde–alcohol dehydrogenase (ADHE, E.C. 1.2.1.10 1.1.1.1) [3,7], which consumes two NADH molecules per etOH produced, regenerating the NAD^+ moiety necessary for continuous glycolytic flux. Alternatively, acetyl-CoA can also be transformed to acetate by the ADP-forming acetyl-CoA synthetase (AcCoAS, E.C. 6.2.1.13) [3,8] in a reaction that produces one mol of ATP per mol of formed acetate [3].

Early reports [8,9] established that under anaerobic conditions (N_2 atmosphere) the major end-products of glycolysis in monoxenic amebas were 67% etOH and 33% acetate (etOH production rate of 5.7 nmoles/min×mg protein, and acetate production rate of 2.1 nmoles/min×mg protein). In contrast, under aerobic conditions (buffer equilibrated with air at 37 °C), these rates were inverted and acetate production was favored (acetate 3.5 nmoles/min×mg protein; etOH 1.7 nmoles/min×mg protein; recalculated from [8] assuming that 1×10^6 amebas equals 1 mg of protein as described before [10]). Later, the same group demonstrated that axenic ame-

Abbreviations: acetyl-CoA, acetyl-coenzyme A; acetyl-CoA synthetase (ADP forming), AcCoAS; CoA, coenzyme A; DPI, diphenyleneiodonium chloride; ADHE, bifunctional aldehyde-alcohol dehydrogenase; PFOR, pyruvate:ferredoxin oxidoreductase; ROS, reactive oxygen species; disulfiram, tetraethylthiuram disulfide

* Corresponding author. Address: Departamento de Bioquímica, Instituto Nacional de Cardiología Ignacio Chávez, Juan Badiano No. 1 Col. Sección XVI, Tlalpan, México D.F. 14080, Mexico.
E-mail address: emma_saavedra2002@yahoo.com (E. Saavedra).

0014-5793/$36.00
http://dx.doi.org/10.1016/j.febslet.2012.11.020

bas produce acetate only under aerobic conditions [9]. Recently, we reported that after exposure to a supraphysiological O_2 concentration (0.63 mM for 30 min) amebas showed decreased etOH (~30% remaining) and increased (40%) acetate contents during a recovery period of 60–90 min compared to control amebas without stress. These changes were consequence of PFOR and ADHE inhibition induced by the reactive oxygen species (ROS) generated under such conditions [11,12]. Although these studies allowed us to determine the effects on energy metabolism of a strong and acute oxidative-stress condition, such high O_2 concentration used is not found in living tissues or in *in vitro* experimentation. Therefore, it was considered necessary to explore the effect of an oxidant condition such as that found in *in vitro* experiments (~0.18 mM O_2 concentration) to determine how the energy metabolism is affected and to identify which pathway component controls the acetate and etOH formation under this aerobic condition.

By applying the fundamentals of metabolic control analysis (MCA) it can be quantitatively determined the degree of control that an individual enzyme exerts on a pathway flux, namely the flux control coefficient ($C^J_{a_i}$). The $C^J_{a_i}$ values represent the impact on the pathway flux (J) of slightly changing the activity (a) of only one of its enzymes (i) in the cell; thus, a $C^J_{a_i}$ value of 1 means that the enzyme totally controls the pathway flux and it represents the one and only rate-limiting step of the pathway (for a review on MCA and its applications see [13]). However, MCA studies have demonstrated that the control of a pathway flux is shared in different degrees amongst all the pathway enzymes [13].

To determine physiological meaningful $C^J_{a_i}$ values under a particular metabolic state, the enzyme activity in the cell has to be titrated and in parallel the steady-state pathway flux has to be determined. From plots of pathway flux versus enzyme activity, the $C^J_{a_i}$ can be calculated from the derivative at the point of interest (wild type enzyme activity level). One of the MCA strategies to determine the $C^J_{a_i}$ is to titrate with specific inhibitors the enzyme activity in the cell [13]. Although this strategy has been successfully used in several cell types to determine the $C^J_{a_i}$ of each respiratory complex over oxidative phosphoryation (ATP synthesis) [13], this strategy has not been used for glycolysis because of the lack of inhibitors that specifically target one glycolytic enzyme without affecting the rest of the pathway enzymes and transporters. Recently, it was determined that diphenyleneiodonium (DPI), an inhibitor of electron-transport chain flavo-enzymes inhibits *Trichomonas vaginalis* PFOR [14], whereas tetraehylthiuram disulfide (disulfiram; DSF) is a potent inhibitor of aldehyde and alcohol dehydrogenases [15]. Therefore, DPI and DSF can be used as specific inhibitors to determine the flux control coefficients of these glycolytic enzymes.

In the present study we report the determination of the control coefficients of PFOR and ADHE on the fluxes of etOH and acetate formation in amebas subjected to moderate aerobic conditions. The aerobic condition was selected because when the parasites are invading the colon adjacent tissues or in *in vitro* experiments where air-equilibrated solutions are used, they become exposed to an environment with a higher O_2 concentration than that found in the microaerophilic milieu from which they migrate. Since PFOR and ADHE are the enzymes with higher susceptibility to damage caused by oxygen stress, they can compromise the energy metabolism of the parasite.

2. Materials and methods

2.1. Reagents and chemicals

Disulfiram and DPI chloride were from SIGMA (St. Louis MO, USA). All other reagents for enzyme activity and metabolite determination were of analytical grade.

2.2. Amebas

Virulent *E. histolytica* trophozoites of the HM1:IMSS strain were isolated from experimentally induced amebic liver abscesses in hamsters and cultured in TYI-S-33 medium as previously described [16]. This procedure was routinely repeated every four weeks to ensure a stable virulent phenotype. Before use, the parasites were harvested at 450×*g* and washed twice with phosphate buffer saline (PBS; 137 mM NaCl, 2.7 mM KCl, 10 mM Na_2HPO_4, 2 mM KH_2PO_4) at pH 7.4.

2.3. In vivo enzyme titration assays

Amebas were suspended at a density of 1×10^6 per ml in aerobic (air-equilibrated) PBS supplemented with 10 mM glucose (PBS-G buffer; 0.18 ± 0.09 mM O_2 concentration at 36 °C and 2240 m altitude; $n = 3$). Samples of 1 ml were poured into eppendorf tubes and incubated at 36 °C in the presence of either 0.1 μM DPI for 0, 10, 20, 40 and 60 min to titrate PFOR activity, or 0.05 μM DSF for 0, 10, 20 and 30 min to titrate ADHE activity. At least six tubes were removed at the indicated times, one pair of samples were pooled together whereas the others were kept individual and all the tubes were centrifuged to remove the inhibitors. The cellular pellet from the pooled samples was processed to obtain cytosolic extracts for enzyme activity determinations as described below. The other tubes were processed for pathway flux determination as follows. The cells in two tubes were re-suspended in 1 ml of PBS-G and immediately extracted with perchloric acid for further acetate and etOH determination ($t = 0$). The cells from another pair of tubes were re-suspended in a similar fashion and incubated for 30 min at 37 °C; thereafter, the samples were centrifuged and the supernatant recovered for metabolite determination. Similar series of tubes were processed in the absence of the inhibitor and used as control of enzyme activities and fluxes. At the end of each incubation protocol, the cell viability was determined by Trypan blue exclusion.

2.4. Enzyme activity determinations in amebal cytosolic fractions

To determine the glycolytic and AcCoAS enzyme activities of amebas subjected to aerobic conditions, the cells were harvested and re-suspended in an equal volume of lysis buffer (25 mM Tris–HCl, pH 7.6, 1 mM EDTA pH 8.0, 5 mM dithiothreitol and 1 mM phenylmethylsulfonyl fluoride) and the activity determined under aerobic conditions as previously described [10,12]. For determination of PFOR and ADHE activities, the lysis buffer (which was supplemented with detergent for PFOR determination), lysis procedure and enzyme activity measurements were conducted under reductive conditions and a N_2 atmosphere as described before [12]. ADHE activity was determined as described elsewhere [12] using saturating concentrations of acetyl-CoA and NADH as substrates but in the absence of pyrazol. Since the activity was determined under initial velocity conditions (in the absence of products) mainly the aldehyde dehydrogenase activity was evaluated.

2.5. Determination of metabolites

Metabolites (glucose-6-phosphate, G6P; fructose-6-phosphate, F6P; Pyr and ATP) were determined using 20×10^6 trophozoites of control amebas or exposed to the inhibitors. Samples were treated and metabolites quantified as described before [10]. For the estimation of the metabolite intracellular molar concentrations, it was assumed that amebal trophozoites have an intracellular water volume of 20 μl per 10^7 cells [10].

2.6. Ethanol and acetate measurement

Samples from the different conditions were extracted with perchloric acid and neutralized as described before [10]. Acetate was determined as described elsewhere [12]. Ethanol was determined in filtered acid extracts using a gas chromatograph GC 2010 (Shimadzu; Kyoto, Japan), equipped with an HP-PLOT/U fused silica capillary column (divinylbenzene/ethylene glycol dimethacrylate, 30 m × 0.32 mm × 10 μm) (Agilent, St Louis MO, USA).

3. Results

3.1. Determining the specificity of DPI and DSF inhibition on PFOR and ADHE activities in trophozoites

To determine the flux control coefficient using the specific inhibitor titration approach (reviewed in [13]), it is first necessary to determine that the inhibitor affected only one pathway enzyme during the experiment.

DPI is a potent (K_i values of 1–10 μM) irreversible-type inhibitor of flavin-dependent oxido-reductases. *T. vaginalis* exposed for 2 h to 10 μM DPI showed no detectable levels of PFOR activity [14]. In a similar fashion, *E. histolytica* trophozoites exposed to submicromolar DPI concentrations showed a time-dependent PFOR inactivation (Fig. 1A). The cell viability at the highest DPI concentration was 84% and 76% after incubations of 60 and 90 min, respectively. The experimental condition of 1 h incubation with 0.1 μM DPI was selected because PFOR activity can be reliably titrated without compromising parasite viability (remaining PFOR activity of 25% ± 20 with 90% cell viability). Using this inhibitor concentration it was also necessary to determine that at each incubation time, there was neither increased inhibition nor reactivation of the enzyme for a further period of at least 30 min, time required for pathway fluxes determination. Indeed, DPI caused an irreversible and steady time-dependent PFOR inactivation (Fig. 1B). Moreover, under this condition DPI only inhibited PFOR activity, showing negligible effects on the rest of the glycolytic, ADHE and AcCoAS enzymes (Table 1).

The ADHE activity in amebas was titrated with several inhibitors of NAD^+-dependent dehydrogenases such as gossypol and pyrazol. Amebas incubated for 30 min with gossypol displayed an IC_{50} of 5 μM for ADHE (Fig. S1A in Supplementary material), but this concentration also inhibited GAPDH (58% remaining activity, Table S1) and it diminished trophozoites viability by 66% at the end of the incubation. Pyrazol inhibited ADHE within the cells with an IC_{50} of 0.2 mM (Fig. S1B) but it also had effect on GAPDH, showing 13% and 7% remaining ADHE and GAPDH activities after treatment with 0.5 mM of the inhibitor for 30 min (Table S2; cell viability was 76% at the end of the incubation). Finally, DSF potently inhibited ADHE activity with an IC_{50} of 0.05 μM and, although the inhibition was not complete at this concentration (Fig. 1C), the activity could be reliable titrated (Fig. 1D) and the degree of inhibition was constant after the 30 min period of flux measurement (data not shown). Therefore, 0.05 μM DSF mainly affected ADHE activity (Table 1) and did not compromise cell

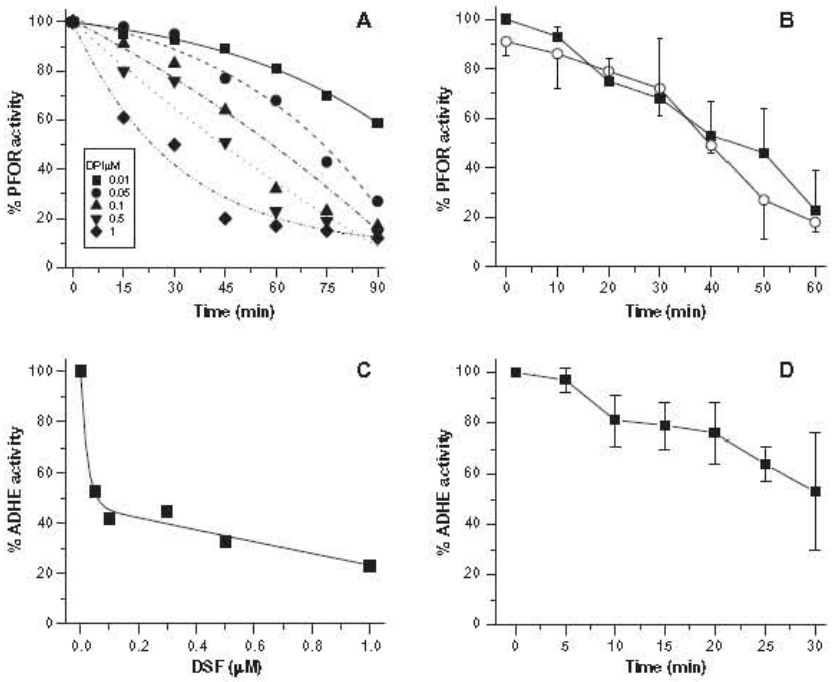

Fig. 1. Effect of DPI and DSF on PFOR and ADHE activities within the cells. (A) Time-course of PFOR activity inhibition in amebas exposed to the indicated DPI concentrations. Control activity: 0.98 U/mg protein. (B) Irreversible nature of the PFOR inhibition by DPI. Two groups of amebas were exposed to 0.1 μM DPI. After different times, one group was processed for immediate PFOR determination (squares) whereas the other was harvested, washed and re-incubated in fresh aerobic PBS–G for further 30 min and PFOR activity was determined at the end of the incubation (circles). Control activity was 1.12 ± 0.11 U/mg of protein; n = 3. (C) Inhibition of the ADHE activity by DSF in amebas incubated for 30 min with the indicated inhibitor concentrations. Control activity was 0.091 U/mg of protein. (D) Time-course of ADHE inhibition by 0.05 μM disulfiram. ADHE control activity: 0.073 ± 0.019 U/mg of protein. The plot shows the results of three different experiments (mean ± S.D.).

Table 2
Flux control coefficients of PFOR and ADHE towards the synthesis of ethanol and acetate in amebas exposed to aerobic conditions. The values shown represent the mean ± S.D. of the linear regression displayed in Fig. 3.

Enzyme	C_{ai}^{Jetoh}	$C_{ai}^{Jacetate}$
PFOR	0.072 ± 0.015	0.09 ± 0.03
ADHE	0.33 ± 0.13	−0.19 ± 0.08

Fig. 1B and D). When PFOR or ADHE in amebal trophozoites were inhibited with DPI and DSF, respectively, there was accumulation of G6P, F6P and Pyr, in parallel to a decrease in the ATP content (Fig. 3); however, most of the changes were statistically significant only when ADHE was inhibited. This pattern of metabolite changes correlated with the higher C_{ai}^{J} of ADHE over the aerobic fermentative glycolytic flux in *E. histolytica*.

The results described above were schematized in Fig. 4, in which the metabolic changes induced by PFOR and ADH inhibition in amebas subjected to aerobic conditions are represented. Compared to the control condition (Fig. 4A), PFOR inhibition (Fig. 4B) promoted (i) ~10% (Fig. 2A and B) decrease in etOH an acetate fluxes (represented by the thickness of the arrow); (ii) 2.5-fold, 50% and 2-fold accumulation of G6P, F6P and Pyr, respectively; and (iii) not significant decrease in ATP content (Fig. 3). In contrast, ADHE inhibition (Fig. 4C) induced (i) significant 30% decreased flux to etOH and 15% increased flux to acetate (Fig. 2C and D); (ii) hexose-phosphates and Pyr hyper-accumulation; and (iii) 50% decrease in ATP content (Fig. 3).

4. Discussion

When amebas leave the lumen of the human intestine and invade the tissues they find higher oxygen concentrations (38.3 and 65 μM in human liver and gastric mucosa tissues, respectively) [17]. Furthermore, in the hamster's amebic hepatic abscess model, after amebas are injected into the portal vein, it takes at least 6 h to develop ischemic and hypoxic foci, time at which the trophozoites initiate proliferation [18]. Moreover, it has been determined that virulent amebas have a more robust antioxidant defense compared to non-virulent amebas [11] and recently, we reported that in amebas subjected to a supra-physiological O_2 concentration (0.63 mM), PFOR and ADHE were drastically inhibited [12]. We hypothesized

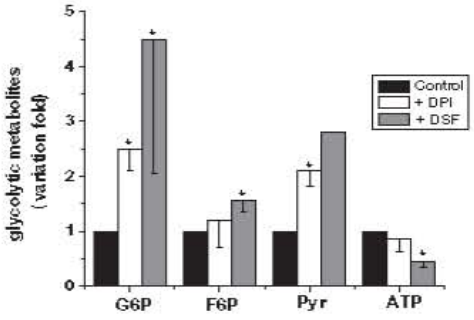

Fig. 3. Metabolite concentrations in amebas incubated with DPI and DSF under aerobic conditions. One million amebas per ml were incubated in aerobic PBS–G in the absence or presence of 0.1 μM DPI for 60 min (PFOR) and 0.05 μM DSF for 30 min (ADHE) at 36 °C. Control metabolite concentrations (mM) were 2.81 ± 0.75 (n – 3) for G6P; 1.04 ± 0.18 (n – 3) for F6P, Pyr 0.87 ± 0.4 (n – 3) and 2.74 ± 0.88 (n – 3) for ATP. The plots show the results of three biological replicas (with the exception of Pyr in DSF treated amebas, where results with only one cell preparation is shown). One-tailed Student's *t*-test for non-paired samples. *$P < 0.03$ versus control.

that during these periods under oxidizing conditions, the energy metabolism of amebas might be impaired, which in the long term affects the parasite's survival abilities. However, such high O_2 concentrations are not normally found *in vivo* or used in *in vitro* experiments. Therefore, it was relevant to determine under aerobic conditions (0.18 mM dissolved O_2 concentration) the control that the oxygen-inhibited PFOR and ADHE have on the glucose fermentation fluxes of the amebas.

Using the MCA quantitative approach we determined that PFOR, despite being susceptible to inhibition by ROS [12] did not exert significant control (less than 10%) over the glycolytic flux in amebas subjected to aerobic conditions. In turn, ADHE exerted significant control on both the etOH and acetate fluxes under aerobic conditions (30% and 19% in average; Table 2). The rest of the control (60%) must lie in the reactions that produce Pyr but not in that of AcCoAS. Preliminary results using the elasticity analysis approach to determine the control distribution of a metabolic pathway [13] suggest that the group of enzymes that consume Pyr (which comprises PFOR, ADHE and AcCoAS), has a C_{ai}^{Jetoh} value near to the sum of the C_{ai}^{Jetoh} for ADHE and PFOR obtained here (cf. Table 2) (Erika Pineda & Emma Saavedra, unpublished results). This suggests that the flux-control exerted by AcCoAS is negligible.

Our present results indicated that ADHE determines the fate of Pyr in the energy metabolism of the parasite subjected to aerobic conditions. The reason of the low PFOR control is that it is the second fastest pathway enzyme after TPI within the cell (Table 1). Therefore, PFOR has overcapacity over the glucose fermentative metabolism even under aerobic conditions in which partial inhibition of the enzyme can occur. On the other hand, ADHE displayed a higher flux-control most probable because of its low activity in the cell; its flux-control coefficient value is comparable to those of HK and PGAM that are the enzymes that also control the glycolytic flux, as determined by kinetic modeling of the entire pathway [10].

In *E. histolytica*, ADHE is the only enzyme able to transform acetyl-CoA to etOH at expenses of NADH oxidation, thus being the predominant enzyme involved in the regeneration of NAD^+ for a continuous glycolysis. In the amebal genome there are five open reading frames (ORFs) encoding for ADHE which however share 98–100% sequence identity [19], which suggests that only one enzyme isoform encoded by 5 duplicated genes is present in amebas. On the other hand, there are many other ORFs for alcohol dehydrogenases and one for an aldehyde dehydrogenase in amebas [19], and some of them have been kinetically characterized showing the use of free aldehyde/etOH and NADP(H) as substrates [20–22]. Since the ADHE enzymatic assay employed here used acetyl-CoA and NADH as substrates, the effect of DSF inhibition was determined only over this enzyme; however, effect of DSF on other aldehyde or alcohol dehydrogenases cannot be ruled out but their contribution to fermentative glycolysis is expected to be negligible because they are unable to use AcCoA as substrate.

The *E. histolytica* ADHE has an iron-binding domain that is essential for activity [23] and which may be involved in the enzyme strong inactivation under oxidizing conditions [12]. Its high sensitivity to ROS and its high control over the glucose metabolism under aerobic conditions may compromise the cellular ATP production as demonstrated by a marked decrease in ATP content when it was specifically inhibited by DSF. ADHE may also be inhibited by O_2 under closer physiologically conditions after prolonged exposure to aerobiosis. In addition to its emerging relevance for the control of the energy metabolism of *E. histolytica* under aerobic conditions, recently it has been demonstrated that ADHE is also involved in iron uptake [24]. These features make this enzyme a suitable and novel therapeutic target for drug intervention.

The present results also indicated that despite the 15% increased flux towards acetate under aerobic conditions, the extra ATP synthesized by the AcCoAS in the acetate branch does not suf-

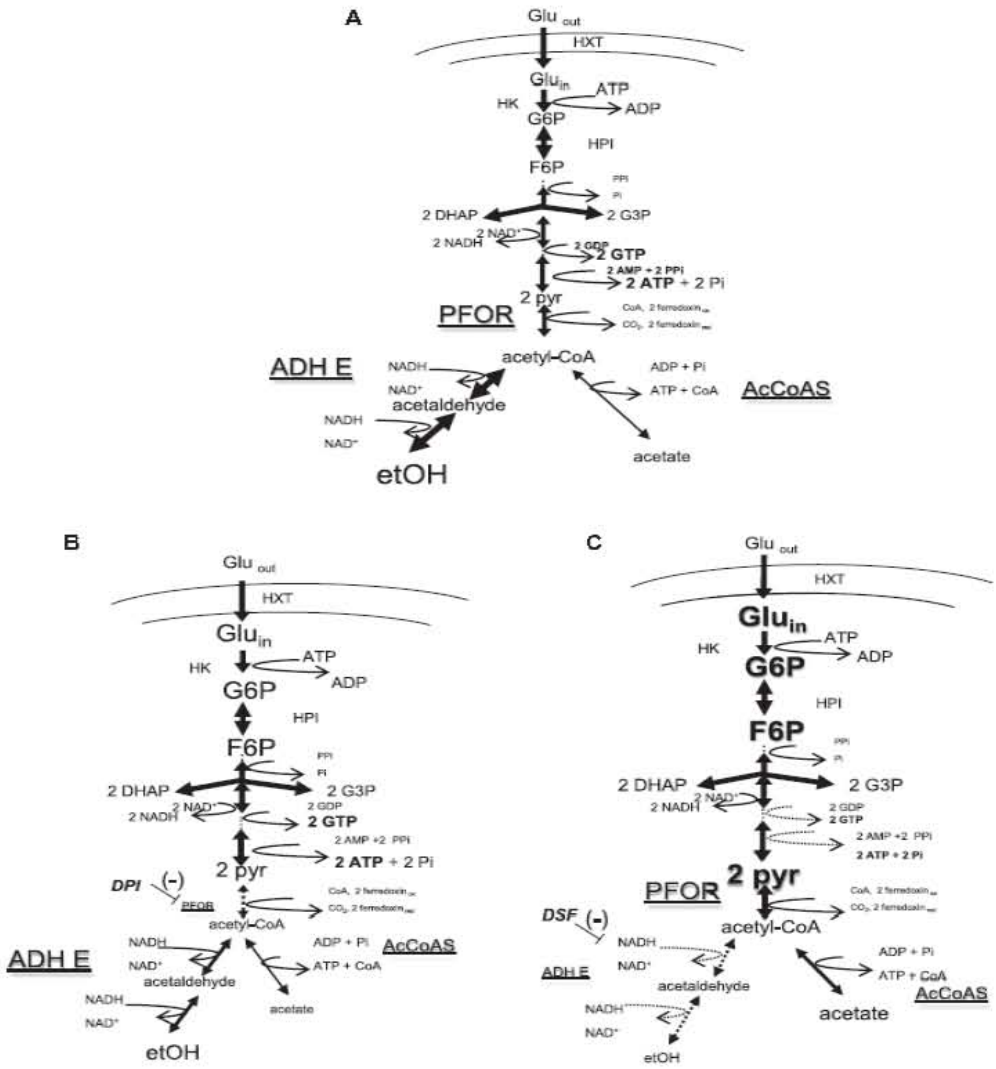

Fig. 4. Schematic representation of the glycolytic pathway in amebas incubated under aerobic conditions. Amebas incubated in the absence of inhibitors (A), with 0.1 μM DPI for 1 h (B) or with 0.05 μM DSF for 30 min (C). The thickness of the arrows represents the relative flux rates through the enzymatic reactions. The size of the metabolite abbreviation represents its relative concentration. HXT, glucose transporter; HK, hexokinase; HPI, hexosephosphate isomerase; Glu_{out}, external glucose; Glu_{in} internal glucose; G3P, glyceraldehyde-3-phosphate; DHAP, dihydroxyacetone phosphate; PPi, pyrophosphate; Pi, inorganic phosphate. Glu_{in} was assumed to accumulate in B and C.

fice to maintain the basal ATP levels. Therefore, the contribution of the acetate branch to ATP synthesis seems low under aerobic conditions. Instead, acetate formation may mainly function for draining acetyl-CoA accumulation, which may slow down the glycolytic flux, since most of the pathway reactions are physiologically reversible with the exception of those of HK and the glucose transporter. Hence, AcCoAS may serve to replenish the CoA necessary for a continuous glycolysis.

Interestingly, unbalanced accumulation of hexose-phosphates and Pyr was observed in amebas treated with either DSF or DPI (Fig. 3). This result contrasted with the balanced changes in glycolytic metabolites seen in amebas subjected to 0.63 mM O_2 [11]. The change in the metabolite profile induced by the DSF and DPI may favor increased fluxes through glycolytic branches, e.g. the non-oxidative pentose phosphate pathway and glucosamine-6-phosphate synthesis at the F6P level; and/or increased glycogen degradation at the G6P level. In turn, an increase in erythrose-4-phosphate brought about by an enhanced flux through the PPP may metabolically affect hexose-phosphate isomerase (HPI) activity since this metabolite is a potent competitive inhibitor of the enzyme (K_i – 5.9 μM) [25]. Indeed, increases in intermediaries of several glycolytic branches have been documented in amebas subjected to oxidative stress caused by hydrogen peroxide and methyl viologen [26]. Hence, an environmental stress causing inhibition of the latter reactions of glycolysis may function as a signal for carbon-skeletons mobilization to other important glycolytic branches.

Acknowledgments

This work was partially supported by CONACyT-Mexico Grant No. 83084 to E.S. and UNAM-DGAPA-PAPIIT IN204310 to A.O.-G. E.P. was supported by CONACyT Ph.D. fellowship No. 210311. E.P. acknowledges partial financial support provided by the Programa de Doctorado en Ciencias Biomédicas, UNAM.

Appendix A. Supplementary data

Supplementary data associated with this article can be found, in the online version, at http://dx.doi.org/10.1016/j.febslet.2012.11.020.

References

[1] Band, R.N. and Cirrito, H. (1979) Growth response of axenic *Entamoeba histolytica* to hydrogen, carbon dioxide, and oxygen. J. Protozool. 26, 282–286.
[2] Ladas, S.D., Karamanolis, G. and Ben-Soussan, E. (2007) Colonic gas explosion during therapeutic colonoscopy with electrocautery. World J. Gastroenterol. 13, 5295–5298.
[3] Reeves, R.E. (1984) Metabolism of *Entamoeba histolytica*. Adv. Parasitol. 23, 105–142.
[4] Saavedra, E., Encalada, R., Pineda, E., Jasso-Chávez, R. and Moreno-Sánchez, R. (2005) Glycolysis in *Entamoeba histolytica*. Biochemical characterization of recombinant glycolytic enzymes and flux control analysis. FEBS J. 272, 1767–1783.
[5] Saavedra-Lira, E., Ramírez-Silva, L. and Pérez-Montfort, R. (1998) Expression and characterization of recombinant pyruvate phosphate dikinase from *Entamoeba histolytica*. Biochim. Biophys. Acta 1382, 47–54.
[6] Encalada, R., Rojo-Domínguez, A., Rodríguez-Zavala, J.S., Pardo, J.P., Quezada, H., Moreno-Sánchez, R. and Saavedra, E. (2009) Molecular basis of the unusual catalytic preference for GDP/GTP in *Entamoeba histolytica* 3-phosphoglycerate kinase. FEBS J. 276, 2037–2047.
[7] Lo, H.S. and Reeves, R.E. (1978) Pyruvate-to-ethanol pathway in *Entamoeba histolytica*. Biochem. J. 171, 225–230.
[8] Montalvo, F.E., Reeves, R.E. and Warren, L.G. (1971) Aerobic and anaerobic metabolism in *Entamoeba histolytica*. Exp. Parasitol. 30, 249–256.
[9] Reeves, R.E., Warren, L.G., Susskind, B. and Lo, H.-S. (1977) An energy-conserving pyruvate-to-acetate pathway in *Entamoeba histolytica*. J. Biol. Chem. 252, 726–731.
[10] Saavedra, E., Marín-Hernández, A., Encalada, R., Olivos, A., Mendoza-Hernández, G. and Moreno-Sánchez, R. (2007) Kinetic modeling can describe *in vivo* glycolysis in *Entamoeba histolytica*. FEBS J. 274, 4922–4940.
[11] Ramos-Martínez, E., Olivos-García, A., Saavedra, E., Nequiz, M., Sánchez, E.C., Tello, E., El-Hafidi, M., Saralegui, A., Pineda, E., Delgado, J., Montfort, I. and Pérez-Tamayo, R. (2009) *Entamoeba histolytica*: oxygen resistance and virulence. Int. J. Parasitol. 39, 693–702.
[12] Pineda, E., Encalada, R., Rodríguez-Zavala, J.S., Olivos-García, A., Moreno-Sánchez, R. and Saavedra, E. (2010) Pyruvate:ferredoxin oxidoreductase and bifunctional aldehyde-alcohol dehydrogenase are essential for energy metabolism under oxidative stress in *Entamoeba histolytica*. FEBS J. 277, 3382–3395.
[13] Moreno-Sánchez, R., Saavedra, E., Rodríguez-Enríquez, S. and Olín-Sandoval, V. (2008) Metabolic control analysis: a tool for designing strategies to manipulate metabolic pathways. J. Biomed. Biotechnol. 597913.
[14] Leitsch, D., Kolarich, D. and Duchêne, M. (2010) The flavin inhibitor diphenyleneiodonium renders *Trichomonas vaginalis* resistant to metronidazole, inhibits thioredoxin reductase and flavin reductase, and shuts off hydrogenosomal enzymatic pathways. Mol. Biochem. Parasitol. 171, 17–24.
[15] Carper, W.R., Dorey, R.C. and Beber, J.H. (1987) Inhibitory effect of disulfiram (antabuse) on alcohol dehydrogenase activity. Clin. Chem. 33, 1906–1908.
[16] Olivos-García, A., González-Canto, A., López-Vancell, R., García de León, M.del C., Tello, E., Nequiz-Avendaño, M., Montfort, I. and Pérez-Tamayo, R. (2003) Amebic cysteine proteinase 2 (EhCP2) plays either a minor or no role in tissue damage in acute experimental amebic liver abscess in hamsters. Parasitol. Res. 90 (3), 212–220.
[17] Vaupel, P., Kallinowski, F. and Okunieff, P. (1989) Blood flow, oxygen and nutrient supply, and metabolic microenvironment of human tumors: a review. Cancer Res. 49, 6449–6465.
[18] Olivos-García, A., Nequiz-Avedaño, M., Tello, E., Martínez, R.D., González-Canto, A., López-Vancell, R., García de León, M.C., Montfort, I. and Pérez-Tamayo, R. (2006) Inflammation, complement, ischemia and amoebic survival in acute experimental amoebic liver abscesses in hamsters. Exp. Mol. Pathol. 77, 66–71.
[19] Clark, C.G., Alsmark, U.C., Tazreiter, M., Saito-Nakano, Y., Ali, V., Marion, S., Weber, C., Mukherjee, C., Bruchhaus, I., Tannich, E., Leippe, M., Sicheritz-Ponten, T., Foster, P.G., Samuelson, J., Noël, C.J., Hirt, R.P., Embley, T.M., Gilchrist, C.A., Mann, B.J., Singh, U., Ackers, J.P., Bhattacharya, S., Bhattacharya, A., Lohia, A., Guillén, N., Duchêne, M., Nozaki, T. and Hall, N. (2007) Structure and content of the *Entamoeba histolytica* genome. Adv. Parasitol. 65, 51–190.
[20] Kumar, A., Shen, P.S., Descoteaux, S., Pohl, J., Bailey, G. and Samuelson, J. (1992) Cloning and expression of an NADP(+)-dependent alcohol dehydrogenase gene of *Entamoeba histolytica*. Proc. Natl. Acad. Sci. USA 89, 10188–10192.
[21] Rodríguez, M.A., Báez-Camargo, M., Delgadillo, D.M. and Orozco, E. (1996) Cloning and expression of an *Entamoeba histolytica* NADP$^+$-dependent alcohol dehydrogenase gene. Biochim. Biophys. Acta 1306, 23–26.
[22] Zhang, W.W., Shen, P.S., Descoteaux, S. and Samuelson, J. (1996) Cloning and expression of the gene for an NADP(+)-dependent aldehyde dehydrogenase of *Entamoeba histolytica*. Mol. Biochem. Parasitol. 63, 157–161.
[23] Espinosa, A., Yan, L., Zhang, Z., Foster, L., Clark, D., Li, E. and Stanley Jr., L. (2001) The bifunctional *Entamoeba histolytica* alcohol dehydrogenase 2 (EhADH2) protein is necessary for amebic growth and survival and requires an intact C-terminal domain for both alcohol dahydrogenase and acetaldehyde dehydrogenase activity. J. Biol. Chem. 276, 20136–20143.
[24] Reyes-López, M., Bermúdez-Cruz, R.M., Avila, E.E. and de la Garza, M. (2011) Acetaldehyde/alcohol dehydrogenase-2 (EhADH2) and clathrin are involved in internalization of human transferrin by *Entamoeba histolytica*. Microbiology 157, 209–219.
[25] Marín-Hernández, A., Gallardo-Pérez, J.C., Rodríguez-Enríquez, S., Encalada, R., Moreno-Sánchez, R. and Saavedra, E. (2011) Modeling cancer glycolysis. Biochim. Biophys. Acta 1807 (6), 755–767.
[26] Husain, A., Sato, D., Jeelani, G., Soga, T. and Nozaki, T. (2012) Dramatic increase in glycerol biosynthesis upon oxidative stress in the anaerobic protozoan parasite *Entamoeba histolytica*. PLoS Negl. Trop. Dis. 6 (9), e1831.

CAPÍTULO 5. DETERMINACIÓN DE LA DISTRIBUCIÓN DE CONTROL DE LA GLUCÓLISIS EN CÉLULAS INTACTAS DE *E. histolytica* A TRAVÉS DEL ANÁLISIS DE ELASTICIDADES

En el capítulo anterior se describió la identificación de inhibidores de la PFOR y ADHE que en condiciones muy controladas pueden considerarse relativamente específicos para estas enzimas. Esto abrió la posibilidad de determinar la distribución de control de toda la vía metabólica a través del análisis de elasticidades y no solamente de las enzimas de la parte final de la vía, como la PFOR y ADHE. Estos resultados servirían para validar los coeficientes de control determinados para la PFOR y la ADHE por titulación con inhibidores. Además, la distribución de control obtenida de esta manera se puede comparar con la obtenida previamente por modelado cinético (Saavedra et al 2007) para establecer la validez de las predicciones del modelo que se construyó.

Los resultados de este trabajo se incluyeron en el artículo siguiente (en preparación, ver ANEXO)

In vivo* determination of the reaction steps that control the glucose catabolism in *Entamoeba histolytica

Erika Pineda E, Encalada R, Vázquez C, Néquiz M, Olivos-García A, Moreno-Sánchez R and Saavedra E.

A continuación se amplía la información sobre los fundamentos del análisis de elasticidades para una mejor comprensión de esta sección.

5.1. Introducción al análisis de elasticidades

El análisis de elasticidades es otra estrategia experimental utilizada en el MCA para determinar la estructura de control de una vía metabólica. El coeficiente de elasticidad se define como un valor numérico adimensional que representa la variación en la velocidad de una enzima, transportador o un grupo de estos (aEi) en función de una variación infinitesimal en la concentración de un ligando X (ya sea sustrato, producto o modulador alostérico) (Moreno-Sánchez, et al 2008) y se define con la siguiente ecuación:

$$\varepsilon_X^{aEi} = \frac{\delta aEi}{\delta X} \cdot \frac{Xo}{aEio} \qquad \text{(Ecuación 2)}$$

los coeficientes de elasticidad tienen valores positivos para metabolitos que aumentan la velocidad de la enzima o transportador (sustratos o activadores) y valores negativos para aquellos metabolitos que disminuyen la velocidad (productos de la reacción o inhibidores).

A diferencia de una cinética enzimática típica en la que se varía el ligando a las concentraciones deseadas, en el caso de las elasticidades, las variaciones de los ligandos se establecen por las reacciones completas de toda la vía metabólica en la célula. Por lo tanto los coeficientes de elasticidad pueden considerarse como la capacidad de las enzimas de una vía metabólica de responder y ajustarse a los cambios en los flujos metabólicos que se establecen en la célula. De esta manera, cuando una enzima se encuentra trabajando cerca de su *Vmax*, ya sea porque está saturada con sus sustratos o alcance el máximo de su capacidad catalítica debido a que hay poca enzima en la célula comparada con el resto de las de la vía, dicha enzima será poco sensible a variaciones en su sustrato o producto y su coeficiente de elasticidad se acercará a 0. Al contrario, cuando una enzima se encuentra trabajando a concentraciones de sustrato o producto por debajo del valor de su *Km* o

cuando haya un exceso de enzima con respecto a las demás enzimas de la vía, con una pequeña variación en el ligando la velocidad de la enzima (o transportador) se modificará y por lo tanto el coeficiente de elasticidad se acercará a valores de 1 o mayores. Existe una relación inversa entre el coeficiente de elasticidad $\varepsilon^{aEi}{}_X$ y el coeficiente de control de flujo $C^J{}_{aEi}$; cuando una enzima posee una baja elasticidad (~0) no es capaz de modificar su velocidad al variar la concentración de sus metabolitos ligandos y en este caso su $C^J{}_{aEi}$ se acercará a un valor de 1, por lo que será un punto de control. En contraste, aquellas enzimas con un coeficiente de elasticidad alto (≥1) pueden fácilmente responder a variaciones en la concentración de sus ligandos y por lo tanto su $C^J{}_{aEi}$ se acercará a un valor de 0. Esta relación inversa entre estos coeficientes se establece en el Teorema de la conectividad.

Para determinar la distribución de control de una vía metabólica por análisis de elasticidades (Moreno-Sánchez et al, 2008) la vía se divide en dos bloques en torno a un metabolito (X), el cual es común para dos segmentos, uno el productor de X (aEi1) y otro el consumidor de X (aEi2)

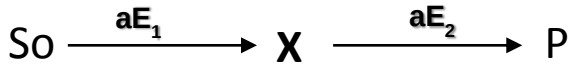

donde So es el sustrato inicial de la vía, X es un intermediario y P es el metabolito final de la vía con el cual se monitorea experimentalmente el flujo. Para el ejemplo anterior, el teorema de la conectividad se expresaría como:

$$C^J_{aE1}\varepsilon^{aE1}_X + C^J_{aE2}\varepsilon^{aE2}_X = 0 \qquad \text{(Ecuación 3)}$$

por lo tanto, de los coeficientes de elasticidad de cada enzima, transportador o grupo de enzimas o reacciones se pueden calcular sus $C^J{}_{aEi}$ resolviendo el sistema de ecuaciones para dos incógnitas.

Para determinar experimentalmente las elasticidades de los bloques productor y consumidor de cada intermediario (X) de la glucólisis amibiana (Fig. 1. 8) se tiene que hacer variar la concentración de X en la célula y determinar en paralelo el flujo

metabólico de la vía como un reflejo de la velocidad parcial de los bloques. Esto es porque en una vía metabólica sin ramificaciones y con estequiometría invariable, en el estado estacionario los flujos (velocidades) a través de cada reacción son iguales. Para hacer que la concentración del intermediario X aumente gradualmente, se varía el sustrato inicial So de la vía y se mide la concentración del intermediario X y el flujo metabólico. Estos datos se normalizan considerando los parámetros de la condición control como 100% y se construye la gráfica de % metabolito vs % flujo (Fig. 1.8) y se calcula la pendiente en el punto de interés del 100%, cuyo valor correspondería a la elasticidad del bloque consumidor de X ($\varepsilon^{aE2}{}_X$). Por otro lado, para determinar la $\varepsilon^{aE1}{}_X$ del bloque productor de X se utiliza un inhibidor que afecte a la enzima o a alguna de las enzimas del bloque consumidor (con la condición de que el inhibidor no afecte a las enzimas del bloque productor) con el objetivo de que aumente la concentración de X con la consecuente disminución en el flujo de la vía, y del gráfico se obtiene el coeficiente de elasticidad del bloque productor.

De los $\varepsilon^{aEi}{}_X$ determinados de esta manera se calculan los C_{aEi}^{j} a partir del Teorema de la conectividad descrito anteriormente, el cual produce las ecuaciones 4 y 5 si se considera también el Teorema de la sumatoria, que establece que la suma de los C_{aEi}^{J} de todas las reacciones de una vía metabólica deben sumar 1:

$$C_{aE1}^{J} = \frac{\varepsilon_X^{aE2}}{\varepsilon_X^{aE2} - \varepsilon_X^{aE1}} \qquad C_{aE2}^{J} = -\frac{\varepsilon_X^{aE1}}{\varepsilon_X^{aE2} - \varepsilon_X^{aE1}} \qquad \text{(Ecuaciones 4 y 5)}$$

Si se titulan de esta manera varios intermediarios de una vía metabólica, se puede determinar los C_{aEi}^{J} de reacciones individuales y por lo tanto establecer la estructura de control de toda la vía metabólica. Sin embargo, una limitación de esta aproximación es que los intermediarios de interés deben encontrarse en concentraciones que puedan ser detectadas experimentalmente y que los cambios en sus pozas sean diferentes estadísticamente.

5.2. Diseño experimental

Para el análisis de elasticidades en la glucólisis de *E. histolytica* se titularon de la manera descrita anteriormente la concentración de G6P, F6P y piruvato (Fig. 1.4) debido a que son de los metabolitos más abundantes de la vía (Saavedra et al, 2007) y un esquema de la estrategia experimental se muestra en la Fig. 5.1. La elasticidad del bloque consumidor de estos metabolitos se determinó incrementado la concentración del metabolito X por variación en la concentración de glucosa a la que se incuban los parásitos, tomando como concentración control 10 mM glucosa. Por otro lado, para determinar la elasticidad del bloque productor de estos metabolitos se utilizaron el DPI y O_2 como inhibidores específicos de la PFOR y la ADHE en la parte baja de la vía tal como se describió en el capítulo 4 y los cuales inducen acumulación de los metabolitos X.

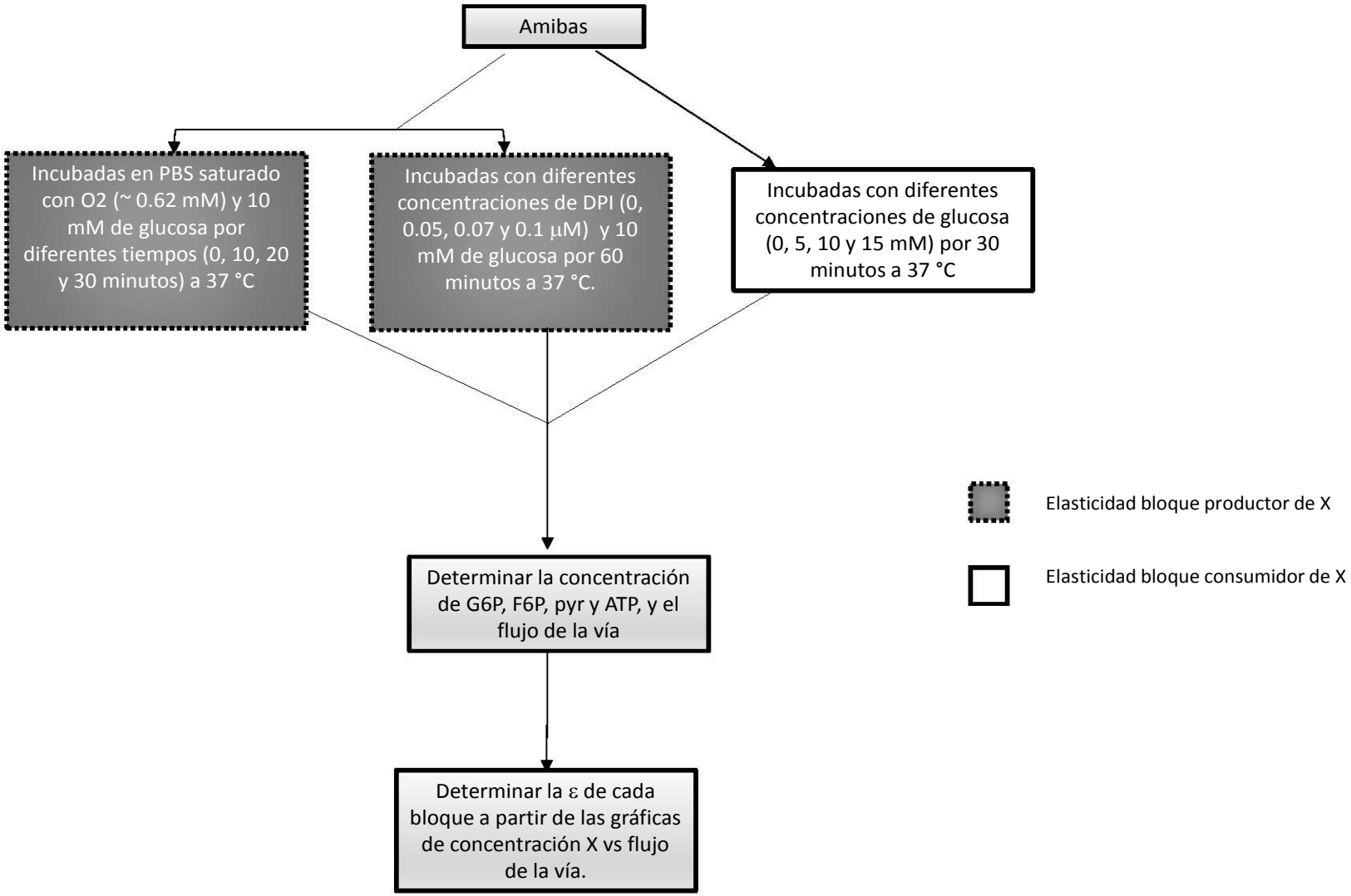

Fig. 5.1 Determinación experimental de los coeficientes de elasticidad

5.3. Resultados

5.3.1 Requisitos para la aplicación del análisis de elasticidades

Para aplicar el análisis de elasticidades de la manera apropiada es necesario cumplir los siguientes requisitos.

1) Titular la concentración del intermediario a evaluar sin afectar a los intermediarios comunes que compartan los bloques productor y consumidor. En la figura 5.2 se muestra la titulación de G6P, F6P y pyr en amibas incubadas con diferentes concentraciones de glucosa. Podemos observar que la poza de estos metabolitos varía tomando como punto de referencia 10 mM de glucosa. Por otro lado, la concentración de ATP, que es un intermediario común en los bloques productor y consumidor, se mantuvo constante en las condiciones del experimento. Resultados similares se obtuvieron al exponer las amibas a O_2 o DPI (Fig. 2 del manuscrito anexo).

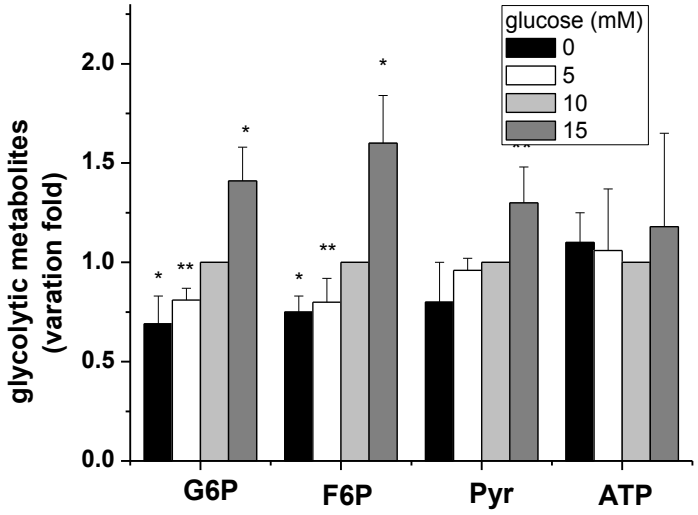

Fig. 5.2 Titulación de intermediarios glucolíticos en *E. histolytica*.

Las amibas se incubaron por 30 min en diferentes concentraciones de glucosa y se cuantificaron los metabolitos en extractos ácidos. * p<0.05, **p<0.05 vs 10 mM de glucosa. El 100 % de cada metabolito fue 3.4 ± 1.2 mM G6P, 1.3 ± 0.2 mM F6P, 0.84 ± 0.12 mM piruvato.

2) Mantener constante la *Vmax* de las enzimas del bloque que no se está titulando. Cuando se titule la actividad de una enzima del bloque consumidor con algún inhibidor, las *Vmax* (esto es, el contenido de enzima activa en la célula) de las enzimas del bloque productor no deben afectarse.

Cuando se utilizó el DPI y el O_2 como inhibidores ya se mostró en el capítulo 4 que estos compuestos, en el protocolo experimental que quedó definido y que es el mismo que se utilizó para realizar el análisis de elasticidades, solamente afectan las *Vmax* de PFOR y ADHE (Tabla 1 del artículo del capítulo 4). Como control, también se determinó la *Vmax* de las enzimas glucolíticas en amibas incubadas con diferentes concentraciones de glucosa. Como se puede observar en la Tabla 5.1, la actividad de las enzimas glucolíticas se mantiene constante en todas las concentraciones de glucosa y tiempos ensayados.

Tabla 5.1. *Vmax* de las enzimas glucolíticas en amibas incubadas en diferentes concentraciones de glucosa. Se muestran los valores al tiempo cero y 30 min de incubación.

Enzima	glucosa 0 mM		glucosa 15 mM	
	(t=0 min)	(t=30 min)	(t=0 min)	(t=30 min)
HK	87	92	89	103
HPI	198	230	206	227
PPi-PFK	203	197	210	195
ALDO	142	150	133	164
TPI	3986	4024	3950	3986
GAPDH	302	277	332	324
PGK	2080	2197	2066	2098
PGAM	110	106	91	105
ENO	479	502	519	516
PPDK	274	303	290	279
PFOR	906	980	950	988
ADHE	84	90	85	84
AcCoAS	145			133

Vmax en nmoles/min x mg de proteína

5.3.2 Determinación de los coeficientes de elasticidad

Una vez que se determinó que la estrategia experimental cumplía con los requisitos anteriores se procedió a realizar el análisis de elasticidades.

En la Fig. 5.3 se muestran las gráficas de concentración de metabolito vs flujo de la vía que se obtuvieron cuando se inhibió con O_2. Las pendientes positivas representan la ε^{aEi}_{X} del bloque consumidor mientras que las negativas representan la ε^{aEi}_{X} del bloque productor. Es importante resaltar que los puntos experimentales estuvieron muy cerca del punto de interés, por lo que el valor de elasticidad se obtuvo de la pendiente de la línea recta obtenida del ajuste utilizando todos los puntos. Se puede observar que para los tres metabolitos titulados, el bloque productor siempre presentó la menor elasticidad, lo cual se verificó al calcular los valores de elasticidad, los cuales se muestran en la Tabla 5.2. Un análisis experimental similar se realizó utilizando DPI como inhibidor del bloque consumidor de los metabolitos.

Figura 5.3. Determinación experimental de los coeficientes de elasticidad.

Trofozoítos amibianos se incubaron en diferentes concentraciones de glucosa (símbolos negros) o durante diferentes tiempos en PBS saturado con O_2 (símbolos blancos) y en paralelo se determinó la concentración de metabolitos y el flujo hacia etanol. La línea continua representa el mejor ajuste de 3 experimentos independientes (representados con diferentes símbolos). En C la línea continua representa la suma de los flujos de etanol y acetato y la línea discontinua muestra únicamente el flujo de etanol.

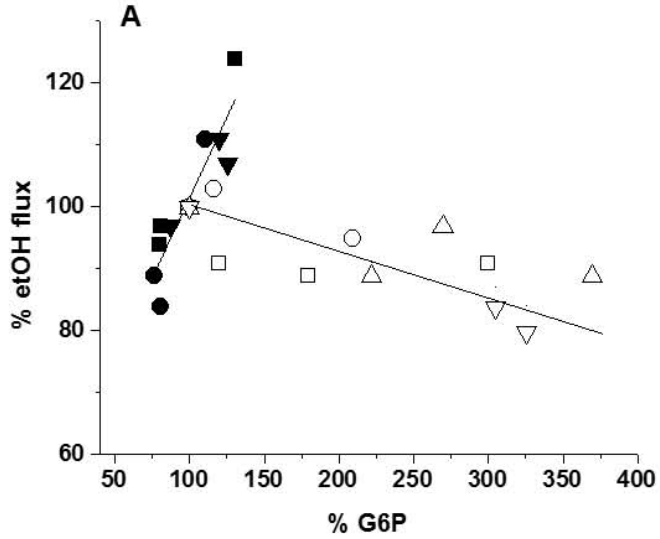
A
120
100
80
60
% etOH flux
50
100
150
200
250
300
350
400
% G6P

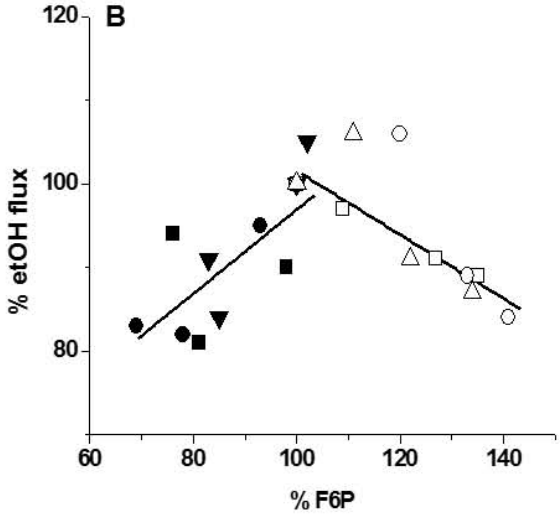
B
120
100
80
% etOH flux
60
80
100
120
140
% F6P

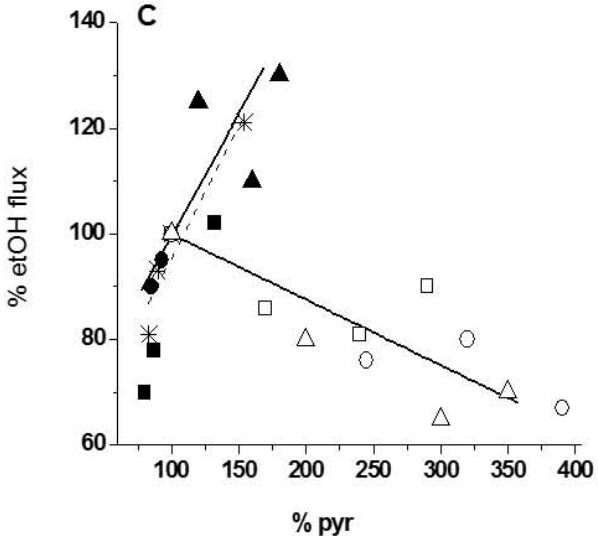
C
140
120
100
80
60
% etOH flux
100
150
200
250
300
350
400
% pyr

5.3.3 Determinación de los C^J_{aEi}

Una vez determinados los coeficientes de elasticidad de los bloques productor y consumidor para cada metabolito, se calcularon sus C^J_{aEi} aplicando las ecuaciones 4 y 5 de este capítulo. Los valores obtenidos de los C^J_{aEi} se muestran en la Tabla 5.2

Finalmente, debido a que el piruvato es un metabolito cercano al punto donde se bifurca la glucólisis amibiana hacia la producción de etanol y acetato, se deben de calcular los C^J_{aEi} de estas ramas aplicando el Teorema de la Ramificación postulado para vías ramificadas (Kacser 1983), el cual establece que el flujo total de la vía es igual a la suma del flujo a través de sus ramificaciones; esta relación se ejemplifica en el siguiente esquema adaptado del de Kacser

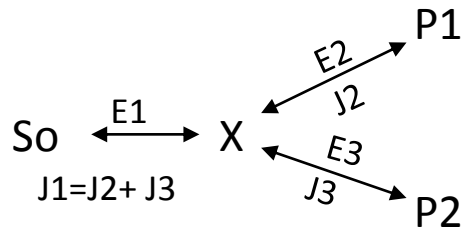

donde So= sustrato inicial, X es el intermediario, P1 y P2 son los dos productos finales de la vía y J2 y J3 son los flujos metabólicos respectivos que dan lugar a P1 y P2.

A partir del teorema de la ramificación y de los teoremas de la sumatoria y de la conectividad que se describieron anteriormente, se obtienen las siguientes ecuaciones para determinar los C^J_{aEi} utilizando las elasticidades de los bloques:

$$C_{Pyr\ prod}^{JEtOH} = \frac{-\varepsilon_{Pyr}^{PFOR\ -ADHE}}{\varepsilon_{Pyr}^{Pyr\ prod} - \alpha\varepsilon_{Pyr}^{PFOR\ -AcCoAS} - (1-\alpha)\varepsilon_{Pyr}^{PFOR\ -ADHE}}$$

$$C_{PFOR-ADHE}^{JEtOH} = \frac{\varepsilon_{Pyr}^{Pyr\ prod} - \alpha\varepsilon_{Pyr}^{PFOR\ -AcCoAS}}{\varepsilon_{Pyr}^{Pyr\ prod} - \alpha\varepsilon_{Pyr}^{PFOR\ -AcCoAS} - (1-\alpha)\varepsilon_{Pyr}^{PFOR\ -ADHE}}$$

$$C_{PFOR-AcCoAS}^{JEtOH} = \frac{\alpha\varepsilon_{pyr}^{PFOR\ -ADHE}}{\varepsilon_{Pyr}^{Pyr\ prod} - \alpha\varepsilon_{Pyr}^{PFOR\ -AcCoAS} - (1-\alpha)\varepsilon_{Pyr}^{PFOR\ -ADHE}}$$

(Ecuaciones 6-8)

en donde *pyr prod* es el bloque productor de piruvato (o sea la vía desde el transporte de glucosa hasta la PPDK y las ramificaciones como la síntesis de glucógeno) y *PFOR-ADHE* y *PFOR-AcCoAS* son los bloques que participan en la producción de etanol y acetato, respectivamente. El valor de α corresponde al porcentaje del flujo total que se va hacia la producción de acetato y se le asignó un valor de 0.1, debido a que solamente el 10% del flujo de glucosa se va hacia la síntesis de acetato mientras que el 90% restante se transforma en etanol (Pineda et al. 2010).

Tabla 5.2 Coeficientes de elasticidad y de control para los bloques productores y consumidores de los metabolitos evaluados.

Se muestran los valores determinados utilizando oxígeno como inhibidor y entre paréntesis los resultados obtenidos cuando se utilizó el DPI. Valores promedio ± DE. PFOR-ADHE y PFOR-AcCoAS corresponden a los bloques de enzimas involucrados en la síntesis de etanol y acetato respectivamente.

Metabolito	$\varepsilon^{prod}{}_X$	$\varepsilon^{cons}{}_X$	$C^{Jetoh}{}_{prod}$	$C^{Jetoh}{}_{cons}$
G6P	-0.16 ± 0.0.05 (-0.24 ± 0.07)	0.60 ± 0.09 (0.61 ± 0.34)	0.79 ± 0.08 (0.72 ± 0.12)	0.21 ± 0.04 (0.28 ± 0.09)
F6P	-0.39 ± 0.24 (-0.39 ± 0.17)	0.51 ± 0.28 (0.56 ± 0.26)	0.57 ± 0.21 (0.59 ± 0.16)	0.43 ± 0.15 (0.41 ± 0.17)
Pyr	-0.12 ± 0.04 (-0.12 ± 0.03)	$\varepsilon^{PFOR\text{-}ADHE}{}_X$ 0.42 ± 0.13 (0.8 ± 0.36) $\varepsilon^{PFOR\text{-}AcCoAS}{}_X$ 0.52	0.77 ± 0.13 (0.87 ±0.17)	$C^{JetOH}{}_{PFOR\text{-}ADHE}$ 0.31 ± 0.15 (0.13 ± 0.0) $C^{JetOH}{}_{PFOR\text{-}AcCoAS}$ -0.08

Por último, a partir de los C^J_{aEi} obtenidos para cada uno de los bloques de la vía metabólica (Tabla 5.2) se puede determinar el C^J_{aEi} de segmentos más pequeños de la vía. De esta manera, al restar el C^J_{aEi} del bloque productor de F6P menos el C^J_{ai} del bloque productor de G6P se puede establecer el C^J_{aEi} del bloque conformado por la HPI y la degradación de glucógeno (Fig. 1.4). Para determinar el C^J_{aEi} del bloque que comprende desde la PPi-PFK hasta la PPDK, al C^J_{aEi} del bloque productor de pyr se le restó el C^J_{aEi} del bloque productor de F6P. Por último, debido a que el DPI inhibe específicamente a la PFOR pero no a la ADHE, se pudo discernir los C^J_{aEi} individuales de estas enzimas haciendo la resta correspondiente. Con esta estrategia se pudo determinar la estructura de control de la glucólisis amibiana la cual se resume en la Tabla 5.3.

Tabla 5.3 Distribución de control de la glucólisis amibiana

Los coeficientes de control de flujo de cada bloque de enzimas se recalcularon de los C_{ai}^{J} determinados para los bloques productores y consumidores de cada metabolito indicados en la Tabla 5.2.

	$C^{JetOH}{}_{aEi}$	
Enzima o grupo de enzimas (aEi)	**O_2**	**DPI**
HXT, HK, degradación de glucógeno	0.79 ± 0.08	0.72 ± 0.12
HPI, síntesis de glucógeno	-0.22 ± 0.13	-0.13 ± 0.02
fugas de triosas fosfato	0.20 ± 0.11	0.28 ± 0.13
PFOR-ADHE	0.31 ± 0.15	0.13 ± 0.04
PFOR-AcCoAS	-0.08	ND
PFOR	0.13	
ADHE	0.18	
AcCoAS	-0.08	

5.4. Discusión del análisis de elasticidades de la glucólisis en E. histolytica

En este capítulo se determinó en células intactas la estructura de control de la glucólisis de *E. histolytica* en condiciones aeróbicas a través del análisis de elasticidades.

De acuerdo con los resultados obtenidos, el bloque conformado por el transportador de glucosa, la HK y la degradación de glucógeno es el que presenta el mayor control de flujo en la vía metabólica. Estos resultados coinciden parcialmente con los obtenidos por modelado cinético reportado previamente por nuestro grupo de trabajo (Saavedra et al. 2007), en los cuales la HK tuvo el mayor porcentaje de control debido a que tenía una de las menores *Vmax* de las enzimas de la glucólisis y parcialmente por su fuerte inhibición por AMP en concentraciones fisiológicas del metabolito (*Ki* 36 µM, concentración de AMP en extractos amibianos: 1.6 mM, Saavedra et al 2007). En esa versión del modelo no se incluyó explícitamente al transportador de glucosa; sin embargo, resultados preliminares del grupo indican que este tiene una menor *Vmax* que la HK. Asimismo, la degradación de glucógeno es muy activa en amibas incubadas en estas condiciones, por lo que muy probablemente este alto coeficiente de control debe de estar repartido entre las tres reacciones. Los resultados encontrados a partir del análisis de elasticidades nos ayudarán a validar la distribución de control en una versión actualizada del modelo que incluya la caracterización cinética de la PFOR y ADHE reportadas en esta tesis.

Por otro lado, el bloque constituido por las enzimas a partir de la PPi-PFK hasta la PPDK controla cerca del 25%. Este coeficiente de control puede ser principalmente de la PGAM, ya que esta enzima junto con la HK, el transportador de glucosa y la ADHE son las enzimas de la glucólisis que tienen los menores valores de *Vmax* (Tabla 5.1).

Finalmente, la ADHE posee un coeficiente de control de flujo de ~20%, el cual coincide parcialmente con el valor determinado por titulación con disulfiram reportado en el capítulo 4. Aunque los valores no son exactamente los mismos cuando se utilizan

diferentes estrategias experimentales del MCA, todos los análisis coinciden que los principales sitios de control del flujo de la vía recaen en las mismas enzimas.

Con los resultados descritos en este capítulo se puede establecer que los principales puntos de control de la glucólisis de *E. histolytica* son el transportador de glucosa/HK/degradación de glucógeno, la ADHE, seguidos por la PGAM. Estas enzimas y el transportador pueden ser sitios potenciales de intervención terapéutica debido a que su secuencia no es similar a la secuencia de las enzimas glucolíticas en humanos. Se ha reportado que la secuencia del transportador de glucosa amibiano es más parecido a los transportadores encontrados en bacterias (Clark et al 2007) y algo similar ocurre con la ADHE, cuyo gen posee una alta similitud con la ADHE de *E. coli.* De acuerdo con lo anterior se puede proponer una terapia multisitio que afecte al transporte de glucosa junto con la ADHE para inhibir la glucólisis amibiana y comprometer el metabolismo energético del parásito. Hasta este momento no se han estudiado inhibidores de estas enzimas como tratamiento para la amibiasis.

Capítulo 6. DISCUSIÓN y CONCLUSIONES GENERALES Y PERSPECTIVAS

6.1. Discusión general de la tesis

Los antecedentes experimentales directos de esta tesis sugerían que la PFOR podía ser un punto de control importante en la glucólisis amibiana en condiciones de estrés oxidante debido a su fuerte inhibición por oxígeno.

En la primera parte de mi proyecto de doctorado caractericé cinéticamente a la PFOR, determiné sus mecanismos de inactivación por O_2 y EROs y la relevancia de esta inhibición para el flujo glucolítico en los trofozoítos. Los resultados indicaron que la EhPFOR es de las enzimas más abundantes en el parásito y que su actividad no se encuentra limitada por deficiencia en sus sustratos y su capacidad de catálisis. De las enzimas glucolíticas, la EhPFOR es el principal sitio de inhibición del O_2 y sus EROs; la exposición a estas especies oxidantes promueve la inhibición en 90% de la enzima. Sin embargo, debido a la abundancia de la enzima en el parásito, la actividad remanente después del reto suprafisiológico con oxígeno es comparable a las actividades de HK y PGAM (y el transporte de glucosa), que son las reacciones más lentas en la vía. Por lo tanto, la inhibición de la PFOR no podría ser más limitante que aquella de las enzimas más lentas de la vía.

Por otro lado, en los experimentos de recuperación del reto suprafisiológico de oxígeno en condiciones de normoxia, se observó que la actividad de la PFOR se recuperó a niveles similares de los parásitos control pero la producción de etanol no se restableció con la misma cinética, lo que sugirió que podría existir otra reacción limitante para restablecer el flujo glucolítico en su totalidad. De manera relevante, durante el reto con oxígeno, además de la PFOR, se inhibió la actividad de aldehído deshidrogenasa de la ADHE. Aunque el porcentaje de inhibición de la ADHE por O_2 es menor al porcentaje de inhibición de la PFOR (50% y 90%, respectivamente), la *Vmax* remanente de la ADHE es apenas mayor al flujo de etanol de 23 nmol/min*mg proteína, lo que sugería que la ADHE era más limitante que la PFOR en condiciones de estrés. Aunado a lo anterior, la recuperación *in vivo* de la actividad de ADHE sí propicia el

restablecimiento de la producción de etanol a niveles similares a los de las amibas no tratadas.

De acuerdo con estas observaciones y contrariamente a la hipótesis inicial de esta tesis, la PFOR posee un coeficiente de control bajo sobre el flujo glucolítico en condiciones de normoxia. Sin embargo, la ADHE parece ser la principal responsable del arresto en la producción de etanol bajo condiciones de estrés oxidante en *E. histolytica*. Hasta el momento, estos resultados se describieron de manera cualitativa en el artículo publicado del 2010 (Pineda et al, 2010), por lo que se aplicaron los fundamentos del MCA para determinar cuantitativamente el grado de control del flujo glucolítico de estas enzimas en condiciones de estrés oxidante.

Los coeficientes de control de la PFOR y la ADHE determinados por titulación con inhibidores en la segunda parte de este trabajo validaron las predicciones cualitativas del control. De acuerdo con los resultados, la PFOR controla alrededor del 10% el flujo glucolítico en el parasito, mientras que la ADHE posee ~ 30% del control sobre la vía en condiciones aerobias. Estos resultados resaltaron la importancia de la ADHE cuando la amiba se expone a concentraciones mayores a las que se encuentra sometida en la luz del intestino o en cultivo. Durante la invasión a tejidos o como respuesta del sistema inmune del hospedero que genera EROs para contender la infección, la inhibición de la ADHE puede limitar el flujo de la vía y comprometer la producción de ATP y la viabilidad del parásito. Esto correlaciona con que cuando se inhibe específicamente y de manera parcial a la ADHE con disulfiram en condiciones de normoxia disminuye el ATP, mientras que cuando se inhibió a la PFOR con DPI, el nivel de ATP se mantuvo relativamente constante.

Finalmente, debido a que durante la determinación de los C_{aEi}^{J} de la PFOR y la ADHE se encontraron inhibidores relativamente específicos para cada una de estas enzimas, en nuestras condiciones experimentales, fue posible realizar el análisis de elasticidades para determinar la estructura de control de toda la vía glucolítica amibiana. Con esta estrategia del MCA se determinó que los principales puntos de control de la vía son el bloque de reacciones inicial constituido por el HXT, la HK y la

degradación de glucógeno, seguido por la ADHE en la última reacción de la vía y posiblemente la PGAM en las reacciones de transformación de las triosas fosfato debido a su poca actividad en el trofozoíto. Con estos resultados se validaron los coeficientes de control determinados para la PFOR y la ADHE a través de la titulación con inhibidores y concuerdan de manera gruesa con los resultados de una versión inicial del modelo cinético de la glucólisis de *E. histolytica* reportado por nuestro grupo de trabajo.

Con base en estos resultados, la propuesta de esta tesis es que la ADHE, junto con el transportados de glucosa, HK, degradación de glucógeno y PGAM pueden ser sitios potenciales de intervención terapéutica debido a su alto C_{aEi}^{J} y a que su secuencia no es similar a la secuencia de las enzimas en el hospedero, esto puramente basado en los mecanismos de control de la vía metabólica. Asimismo, descarta a las enzimas dependientes de pirofosfato PPi-PFK y PPDK, como blancos terapéuticos, como se había propuesto anteriormente (Saavedra-Lira et al, 1998), ya que debido al poco control que tienen sobre el flujo glucolítico requeriría el desarrollo de inhibidores altamente potentes y específicos y no competitivos para afectar el metabolismo de la glucosa inhibiendo a estas enzimas.

Asimismo, estos análisis de la distribución del control del flujo glucolítico en *E. histolytica* indican que las enzimas/reacciones que controlan las últimas reacciones de la glucólisis son diferentes en células de mamífero. En el caso de los pares PYK/PPDK, piruvato deshidrogenasa/PFOR y lactato deshidrogenasa/ADHE, en los dos primeros pares las enzimas/complejos en mamíferos están altamente reguladas alostéricamente y pueden tener control relevante en las transiciones homeostáticas. Por otro lado, para el último par, la enzima de amiba controla mientras que la lactato deshidrogenasa carece de control aún en células con alta actividad glucolítica como las células tumorales (Marín-Hernández et al, 2011).

6.2. Conclusiones generales

- La PFOR se inhibe drásticamente por oxígeno y EROs; esta inhibición es reversible en condiciones *in vitro* y de manera relevante, también *in vivo* en células intactas. Los metabolitos acetil-CoA y CoA a concentraciones fisiológicas protegen a la enzima de la inhibición.

- Aun cuando la PFOR es inhibida fuertemente por oxígeno, esto no limita el flujo de etanol debido a que la enzima es de las más abundantes en el parásito.

- La PFOR y la ADHE son las principales enzimas glucolíticas de *Entamoeba histolytica* que son blancos del O_2 y las EROs; esto hace que las enzimas puedan utilizarse como marcadores de estrés oxidativo generado *in vivo.*

- La ADHE tiene un elevado C_{aEi}^{J} en condiciones aerobias, por lo que su inhibición por oxígeno puede comprometer la producción de ATP y la viabilidad del parásito.

- Los principales puntos de control de la glucólisis amibiana son el grupo de enzimas del transporte de glucosa/HK/degradación de glucógeno, seguidos por la ADH y la PGAM, estas enzimas son las que poseen un mayor potencial terapéutico debido a su alto C_{aEi}^{J} y a que su secuencia es diferente a la de las enzimas de la glucólisis en el hospedero.

6.3. Perspectivas

- Dilucidar el mecanismo químico de la desestabilización de los centros Fe-S por O_2 y EROs de la EhPFOR, enfocándose en determinar la existencia del intermediario [3Fe-4S], esto en la enzima recombinante.
- Determinar el efecto de la inhibición de las enzimas glucolíticas con C_{aEi}^{J} más altos sobre el crecimiento de los trofozoítos amibianos. En este sentido, aún no se han reportado inhibidores específicos del HXT, HK, degradación de glucógeno y PGAM,

pero para la ADHE se puede evaluar el DSF, cuyo efecto sobre la enzima se evaluó en esta tesis.

- Determinar si la distribución de control de esta vía se mantiene en otro estado estacionario, como podría ser el estrés nutricional o el provocado por las especies reactivas de nitrógeno que son subproductos del metronidazol.
- Evaluar el papel de la PFOR, la AcCoAS y la ADHE en el cambio de los flujos hacia etanol y acetato (switch metabólico) en condiciones anaerobias, haciendo especial énfasis en determinar los mecanismos regulatorios que hacen posible este cambio en el metabolismo.

7. BIBLIOGRAFÍA

- Ali V, Shigeta Y, Tokumoto U, Takahashi Y, Nozaki T. (2004). An intestinal parasitic protist, *Entamoeba histolytica*, possesses a non-redundant nitrogen fixation-like system for iron-sulfur cluster assembly under anaerobic conditions. J Biol Chem.279(16):16863-74.
- Ali V, Nozaki T.(2012). Iron-sulphur clusters, their biosynthesis, and biological functions in protozoan parasites. Adv Parasitol. 83:1-92.
- Bruchhaus I, Tannich E (1994) Purification and molecular characterization of the NAD+-dependent acetaldehyde/alcohol dehydrogenase from *Entamoeba histolytica. Biochem J* 303, 743-48
- Bruchhaus I, Richter S, Tannich E (1998). Recombinant expression and biochemical characterization of an NADPH:flavin oxidoreductase from *Entamoeba histolytica*. *Biochem J*. 330 (Pt 3):1217-21.
- Caballero-Salcedo A, Viveros-Rogel M, Salvatierra B, Tapia-Conyer R, Sepúlveda-Amor J, Gutiérrez G, Ortiz-Ortiz L (1994). Seroepidemiology of amebiasis in México. *Am J Trop Med Hyg.* 50(4):412-9.
- Chabrière E, Charon MH, Volbeda A, Pieulle L, Hatchikian EC & Fontecilla-Camps JC (1999) Crystal structures of the key anaerobic enzyme pyruvate:ferredoxin oxidoreductase, free and in complex with pyruvate. *Nat Struct Biol* **6**, 182-90.
- Charon MH, Volbeda A, Chabriere E, Pieulle L, Fontecilla-Camps JC (1999) Structure and electron transfer mechanism of piruvate:ferredoxina oxidoredectase. *Curr Opin Struct Biol*. 9(6):663-9.
- Clark CG, Alsmark UC, Tazreiter M, Saito-Nakano Y, Ali V, Marion S, Weber C, Mukherjee C, Bruchhaus I, Tannich E, Leippe M, Sicheritz-Ponten T, Foster PG, Samuelson J, Noël CJ, Hirt RP, Embley JP, Gilchrist CA, Mann BJ, Singh U, Ackers JP, Bhattacharya S, Bhattacharya A, Lohia A, Guillen N, Duchêne M, Nozaki T & Hall N (2007) Structure and content of the *Entamoeba histolytica* genome. *Adv Parasitol* 65, 51-190Deng Z, Huang M, Singh K, Albach RA, Latshaw SP, Chang KP and Kemp RG (1998) Cloning and expression of the gene for the active PPi-dependent phosphofructokinase of *Entamoeba histolytica*. *Biochem J* 329, 659-664.
- Djaman O, Outten W & Imlay JA (2004) Repair of oxidized iron-sulfur clusters in *Escherichia coli. J Biol Chem* 279, 44590-99.
- Espinosa A, Clark D, Stanley SL Jr (2004). *Entamoeba histolytica* alcohol dehydrogenase 2 (EhADH2) as a target for anti-amoebic agents. *J Antimicrob Chemother*. 54(1):56-9.
- Espinosa A, Yan L, Zhang Z, Foster L, Clark D, Li E & Stanley SL (2001) The bifunctional *Entamoeba histolytica* alcohol dehydrogenase 2 (EhADH2) protein is necessary for amebic growth and survival and requires an intact C-terminal domain for both alcohol dehydrogenase and acetaldehyde dehydrogenase activity. *J Biol Chem* 276, 20136-43.
- Fell D (1997) Understanding the control of metabolism. Portland Press, London.
- Imlay JA (2006) Iron-sulphur clusters and the problem with oxygen. *Mol Microbiol* 59, 1073-1082.

- Jang S, Imlay JA (2007) Micromolar intracellular hydrogen peroxide disrupts metabolism by damaging iron-sulfur enzymes. *J Biol Chem* 282, 929-937
- Jiang J, Nakashima T, Liu KJ, Goda F, Shima T & Swartz HM (1996) Measurement of PO_2 in liver using EPR oximetry. *J Appl Physiol* 80, 552-58.
- Leitsch D, Kolarich D, Duchêne M (2010). The flavin inhibitor diphenyleneiodonium renders *Trichomonas vaginalis* resistant to metronidazole, inhibits thioredoxin reductase and flavin reductase, and shuts off hydrogenosomal enzymatic pathways. Mol Biochem Parasitol. 171(1):17-24.
- Mackey-Lawrence NM, Petri WA Jr (2011). Amoebic dysentery. *Clin Evid* (Online). 13;2011. doi:pii: 0918
- McAuliffe GN, Anderson TP, Stevens M, Adams J, Coleman R, Mahagamasekera P, Young S, Henderson T, Hofmann M, Jennings LC, Murdoch DR (2013). Systematic application of multiplex PCR enhances the detection of bacteria, parasites, and viruses in stool samples. *J Infect*. 67(2):122-9.
- Moreno Sánchez R, Saavedra E, Rodríguez-Enríquez S, Olín-Sandoval V (2008). Metabolic control analysis: a tool for designing strategies to manipulate metabolic pathways. *J. Biomed Biotechnol*. :597913 doi: 1155/2008/597913.
- Nelson DL y Cox MM (2008) Principles of Metabolic Regulation. In Lehninger. Principles of biochemistry, 5a edición, W.H. Freeman and company, New York, 569-82.
- O'Donnell BV, Tew DG, Jones OT, England PJ (1993). Studies on the inhibitory mechanism of iodonium compounds with special reference to neutrophil NADPH oxidase. *Biochem J.* 290 (Pt 1):41-9.
- Olivos-García A, González-Canto A, López-Vancell R, García de León MC, Tello E, Nequiz-Avendaño M, Montfort I & Pérez-Tamayo R (2003) Amebic cysteine proteinase 2 (EhCP2) plays either a minor or no role in tissue damage in acute experimental amebic liver abscess in hamsters. *Parasitol Res* 90, 212-220.
- Pan N & Imlay JA (2001) How does oxygen inhibit central metabolism in the obligate anaerobe *Bacteroides thetaiotaomicron*? *Mol Microbiol* 39, 1562-71.
- Pieulle L, Guigliarelli B, Asso M, Dole F, Bernadac A & Hatchikian EC (1995) Isolation and characterization of the pyruvate:ferrdoxin oxidoreductase from the sulfate-reducing bacterium *Desulfovibrio africanus*. *Biochim Biophys Acta* 1250, 49-59.
- Ramos-Martínez E, Olivos-García A, Saavedra E, Nequiz M, Sánchez EC, Tello E, El-Hafidi M, Saralegui A, Pineda E, Delgado J, Montfort I & Pérez-Tamayo R (2009) *Entamoeba histolytica*: oxygen resistence and virulence. *Int J Parasitol* 39, 693-02.
- Reeves R E (1984) Metabolism of *Entamoeba histolytica*. *Adv. Parasitol*. 23, 105-42
- Reeves RE, (1968) A new enzyme with the glycolytic function of pyruvate kinase. *J Biol Chem* 243, 3202-04.
- Reeves Re, Montalvo F, Sillero A (1967) Glucokinase from *Entamoeba histolytica* and related organisms. *Biochemistry* 6, 1752-1760
- Reeves RE, Serrano R and South DJ (1976) 6-phosphofructokinase (pyrophosphate). Properties of the enzyme from *Entamoeba histolytica* and its reaction mechanism. *J Biol Chem* 251, 2958-62

- Reeves RE, Warren LG, Susskind B, Lo HS (1977). An energy conserving pyruvate to acetate pathway in *Entamoeba histolytica*. *J Biol Che*m **257** (2) 756-58
- Reyes-López M, Bermúdez-Cruz RM, Avila EE, de la Garza M.(2011) Acetaldehyde/alcohol dehydrogenase-2 (EhADH2) and clathrin are involved in internalization of human transferrin by *Entamoeba histolytica*. *Microbiology.* 157(Pt 1):209-19
- Saavedra E, Encalada R, Pineda E, Jasso-Chávez R, Moreno-Sánchez R (2005) Glycolysis in *Entamoeba histolytica*. Bichemical characterization or recombinant glycolytic enzymes and flux control analysis. *FEBS J* 272, 1767-83
- Saavedra E, Marín-Hernández A, Encalada R, Olivos A, Mendoza-Hernández G, Moreno-Sánchez R (2007). Kinetic modeling can describe in vivo glycolysis in *Entamoeba histolytica FEBS J.* 274(18):4922-40.
- Saavedra-Lira E, Ramírez-Silva L and Pérez-Montfort R (1998) Expresion and characterization of recombinant pyruvate phosphate dikinase from *Entamoeba histolytica*. *Biochim Biophys* Acta 1382, 47-54.
- Tittmann K (2009) Reaction mechanisms of thiamin diphosphate enzymes: redox reactions. *FEBS J* 276, 2454-68.
- Uyeda K, Rabinowitz JC (1977). Pyruvate-ferredoxin oxidoreductase. IV. Studies on the reaction mechanism. *J Biol Chem*. 246(10):3120-5.
- Vaupel P, Kallinowski F & Okunieff P (1989) Blood flow, oxygen and nutrient supply, and metabolic microenvironment of human tumors: a review. *Cancer Res* 49, 6449-65.
- Walsh JA (1986) Amebiasis in the world. *Arch Invest Med (Mex).* 17 Suppl 1:385-9.
- WHO/PAHO/UNESCO (1997) A consultation with experts on amoebiasis *Epidemiol Bull* 18, 13-14.
- Ximénez C, Morán P, Rojas L, Valadez A, Gómez A, Ramiro M, Cerritos R, González E, Hernández E, Oswaldo P (2011). Novelties on amoebiasis: a neglected tropical disease. *J Glob Infect Dis*. 3(2):166-74.
- Zermeño V, Ximénez C, Morán P, Valadez A, Valenzuela O, Rascón E, Diaz D, Cerritos R (2013). Worldwide genealogy of *Entamoeba histolytica*: an overview to understand haplotype distribution and infection outcome. *Infect Genet Evol.* 17:243-52.

-

8. ANEXO

In vivo identification of the steps that control energy metabolism and survival of Entamoeba histolytica

Erika Pineda[1], Rusely Encalada[1], Citlali Vázquez[1], Mario Néquiz[2], Alfonso Olivos-García[2], Rafael Moreno-Sánchez[1] and Emma Saavedra[1, #]

[1] Departamento de Bioquímica, Instituto Nacional de Cardiología Ignacio Chávez. México D.F., 14080, México.

[2] Departamento de Medicina Experimental, Facultad de Medicina, Universidad Nacional Autónoma de México. México D.F., 04510, México.

[#]Corresponding author
Emma Saavedra, Ph.D.
Departamento de Bioquímica. Instituto Nacional de Cardiología Ignacio Chávez.
Juan Badiano No. 1 Col. Sección XVI, Tlalpan, México D.F., 14080, México
Tel. (5255) 5573-2911 ext. 1298.
e-mail: emma_saavedra2002@yahoo.com

Running title: Control of *Entamoeba* glycolysis and cell survival

Keywords

Glycolysis; ameba; ATP supply, Metabolic Control Analysis; elasticity analysis; flux control coefficient.

ABBREVIATIONS:

Acetyl-CoA, acetyl-coenzyme A; AcCoAS, acetyl-CoA synthetase (ADP forming); ADHE, bifunctional aldehyde-alcohol dehydrogenase; ALDO, fructose-1,6-bisphosphate aldolase; DPI, diphenyleneiodonium chloride; disulfiram, tetraethylthiuram disulfide; 2-DOG, 2-deoxyglucose; ENO, enolase; Fru6P, fructose-6-phosphate; GAPDH, glyceraldehyde-3-phosphate dehydrogenase; Glc6P, glucose-6-phosphate; HXT, glucose transport; HK, hexokinase; HPI, hexosephosphate isomerase; PFOR, pyruvate:ferredoxin oxidoreductase; PGAM, 3- phosphoglycerate mutase; PGK, 3-phosphoglycerate kinase; PPDK, pyruvate phosphate dikinase; PPi-PFK, pyrophosphate-dependent phosphofructokinase; PPP, non-oxidative pentose phosphate pathway; Pyr, pyruvate; TPI, triosephosphate isomerase.

ABSTRACT

The steps that control the *Entamoeba histolytica* glycolytic flux were here identified by elasticity analysis, an experimental approach of Metabolic Control Analysis. The concentrations of glycolytic metabolites were gradually varied in live trophozoites by (i) feeding with different glucose concentrations and (ii) inhibiting the final pathway steps; in parallel, the changes in the pathway flux were determined. From the metabolite concentration-flux relationship, the elasticity coefficients of individual or groups of pathway reactions were determined and used to calculate their respective degrees of control on the glycolytic flux (flux control coefficients). The results indicated that the pathway flux was mainly controlled (72-79%) by the glucose transport/ hexokinase/glycogen degradation group of reactions, and by the bifunctional aldehyde-alcohol dehydrogenase (ADHE; 18%). Further, inhibition of the first pathway reactions with 2-deoxyglucose (2DOG) decreased the glycolytic flux and ATP content by 75% and 50%, respectively. Cell viability was also decreased by 2DOG (25%) and more potently by 2DOG *plus* the ADHE inhibitor disulfiram (50%). Amino acid degradation was unable to replace glycolysis for ATP supply, which indicated that glucose was the main nutrient for amebal ATP synthesis and survival. These results indicated that glycolysis in the parasite is mainly controlled by the initial pathway reactions and that their inhibition can decrease the parasite energy load and survival.

INTRODUCTION

Entamoeba histolytica, the causal agent of human amebiasis, lacks functional mitochondria and does not have Krebs cycle nor oxidative phosphorylation enzymes, which strongly suggests that glycolysis is the main pathway for ATP synthesis in the parasite [1]; however, quantitative studies indicating the percentage of ATP provided by glycolysis have not been reported. On the other hand, several comprehensive studies have shown that the amebal glycolytic enzymes diverge importantly from those of the host: (i) *E. histolytica* has the pyrophosphate-dependent enzymes phosphofructokinase (PPi-PFK) and pyruvate phosphate dikinase (PPDK), which are not allosterically modulated [1-5], catalyze reversible reactions under physiological conditions, and replace the tightly regulated and flux controlling ATP-dependent phosphofructokinase 1 and pyruvate kinase, respectively, present in the host. (ii) Amebal hexokinases (HK) are not inhibited by glucose-6-phosphate (Glc6P) like human HK, but they are by AMP and ADP [1, 2, 6]. (iii) Amebas contain a heavy metal-dependent fructose1,6 bisphosphate aldolase (ALDO), a 2,3 bisphosphoglycerate-independent 3-phosphoglycerate mutase (PGAM) and a 3-phosphoglycerate kinase (PGK) that prefers GDP over ADP for the first reaction of substrate level phosphorylation [1, 2, 7, 8]. (iv) Pyruvate (Pyr) is converted to acetyl-CoA (acetyl-CoA) by pyruvate:ferredoxin oxidoreductase (PFOR), instead of the allosteric pyruvate dehydrogenase complex [9, 10]. Under aerobic conditions, 90% of the acetyl-CoA formed is converted to ethanol (EtOH) by a bifunctional aldehyde-alcohol dehydrogenase (ADHE), whereas the remaining is transformed to acetate by acetyl-CoA synthetase ADP-forming (AcCoAS), which generates one mole of ATP per mole of acetyl-CoA consumed [10, 11]. It has been proposed that this last reaction may supply additional ATP to the cell [12], although this hypothesis has not been yet experimentally assessed.

The peculiarities of the amebal pathway enzymes may lead to different mechanisms of control and regulation of the amebal glucose catabolism compared to those of the host. However, the pathway controlling steps cannot be identified by comparison of the individual enzyme kinetic properties; instead, studies of the complete

pathway function in the cell have to be carried out to establish how the pathway is controlled and whether glycolysis is indeed the main cellular ATP supplier.

The steps that mainly control the glycolytic flux in *E. histolytica* can be identified using the fundamentals of Metabolic Control Analysis (MCA), which is an experimental biochemical approach of Systems Biology focused on determining the control and regulation of metabolic pathways/biological processes [13-15]. The MCA fundamentals help to determine the degree of control that the activity of an enzyme/ transporter/ biological process (*ai*) exerts on a pathway flux (*J*) which is called flux control coefficient (C^J_{ai}) [13, 14]. MCA studies of central metabolic pathways have demonstrated that the control of their fluxes is distributed among all the pathway enzymes, usually with two or three steps displaying the highest control, thus the concept of a unique rate-limiting step turn to be inadequate [13-15].

Several experimental MCA approaches can be used to determine the C^J_{ai} (reviewed in [14]). Elasticity analysis or "top-down" approach has the advantage that the control of flux can be determined in organelles, cells, tissues or even organs, without previous extensive kinetic knowledge of the individual pathway enzyme components [16, 17]. It requires determination of the elasticity coefficient ($\boldsymbol{\varepsilon}^{ai}_X$). This value represents the robustness of a pathway step *ai* (which can be an enzyme, a series of pathway steps group together or even entire metabolic pathways) to change its rate in response to changes in the concentration of a ligand (X), which can be a substrate or activator (positive $\boldsymbol{\varepsilon}^{ai}_X$) or a product or inhibitor (negative $\boldsymbol{\varepsilon}^{ai}_X$). There is an inverse relationship between the $\boldsymbol{\varepsilon}^{ai}_X$ and the C^J_{ai}. A pathway step with low elasticity cannot proportionally adapt its rate to changes in the concentrations of the pathway metabolites and represents a constraint, thus it has high control on the pathway flux; in contrast, pathway reactions with high elasticities can easily adjust their rates to metabolite changes and therefore have low flux control coefficients. From the $\boldsymbol{\varepsilon}^{ai}_X$ coefficients, the C^J_{ai} can be calculated by applying the summation and connectivity theorems of MCA [16, 17].

In the present work we used elasticity analysis to establish how glycolysis is controlled in live trophozoites of *E. histolytica* which allowed to identifying the main controlling pathway steps. Moreover, the effect of inhibition of these controlling steps on energy metabolism parameters and cell viability was evaluated.

RESULTS

Elasticity analysis experimental design

To determine the ε^{ai}_{X} values by elasticity analysis [16], the pathway steps were clustered in two groups linked by a common pathway intermediary (X); one group represented the producer branch of metabolite X (hereafter designated as *prod*) and the other group was the consumer branch of the same metabolite (hereafter designated as *cons*) (Scheme 1). A requisite was that metabolite X had to be abundant in the cell so that changes in its concentration could accurately be determined. For the present study Glc6P, Fru6P and Pyr were selected since they met these requirements. Further, the concentration of each intermediary X was varied in the cells (i) by feeding the pathway with different glucose concentrations and (ii) by inhibiting the final pathway steps with O_2 or diphenyleneiodonium (DPI), and the changes in the steady-state pathway fluxes to both EtOH and acetate productions were in parallel determined at each variation (Scheme 1). It is worth recalling that in a metabolic pathway under steady-state, the rates of each individual pathway reaction are equal to the pathway flux of the end metabolite, after adjusting for the stoichiometry of the reactions [13, 14, 16, 17]. Repeating the analysis for several metabolites along the pathway allows determination of the ε^{ai}_{X} of different groups of pathway steps (Scheme 1).

Pathway steady-state assumption for elasticity analysis

To determine the ε^{ai}_{X} , it was first necessary to verify that several requisites were attained for correct application of elasticity analysis [14, 16].

1) Unchanged enzyme activities. When the activity(ies) of the enzyme(s) belonging to the consumer group are manipulated by using the inhibitors O_2 or DPI; the *Vmax* (*i.e.*, the content of active enzyme) of the reactions of the producer group should not change. It was previously demonstrated that under the protocols of O_2 and DPI inhibition (see material and methods section for details), among the amebal glycolytic enzymes only PFOR and ADHE were affected [10, 18]. Furthermore, no changes in the *Vmax* of the pathway enzymes were observed in amebas incubated with different glucose concentrations (Table 1).

2) Titratable changes in metabolite contents. Amebas incubated with different glucose concentrations indeed showed reliable and reproducible changes in the intracellular contents of Glc6P, Fru6P and Pyr above and below the reference concentration of 10 mM glucose (Fig. 1A). On the other hand, treatment of amebas with O_2 and DPI induced reliable and reproducible increases in Glc6P, Fru6P and Pyr contents in comparison to control cells (Figs. 1B and 1C).

3) Shared metabolites. Metabolites that connect both groups of reactions should not vary during the titration experiments. ATP is the most relevant linking metabolite, as is consumed by HK and produced by PGK (as GTP) and PPDK (Scheme 1). However, ATP did not significantly vary under any experimental protocol used in the present study (Figs. 1A, 1B, 1C).

4) Constant flux rates and metabolite concentrations. The rates of EtOH and acetate syntheses and the concentrations of Glc6P, Fru6P and Pyr were constant over a time period of at least 30 min for trophozoites incubated with 5, 10 or 15 mM glucose (data not shown).

These results indicated that the experimental design used in the present study was suitable for determination of the elasticity coefficients.

Determination of the elasticity coefficients

Although EtOH is the predominant end-product of amebal glucose metabolism under aerobic conditions [10, 18], it was nevertheless initially assessed whether significant variation in the ε^{ai}_{X} values of the Pyr producer group might develop when, besides the EtOH flux, the acetate flux was also added up; however, no significant changes were attained (Fig. 2C, dotted line). Therefore, for the remaining titrations shown in Fig. 2, only the EtOH flux was plotted.

The ε^{ai}_{X} values of the producer groups for each metabolite were determined from the negative slopes of the linear fitting of the data shown in Fig. 2, which were obtained by titrating with O_2 (Figs. 2A-2C) and DPI (Figs. 2D-2F). The ε^{ai}_{X} values have negative signs because metabolite X was accumulated in response to the inhibitor and, as a product of the producer group of reactions, it inhibits the rate in the forward direction (Scheme 1). On the other hand, the ε^{ai}_{X} of the consumer group was determined from the positive slopes, which resulted of titration with different glucose concentrations; these experiments yielded positive values because metabolite X represents the substrate of the consumer group and favors its forward rate (Scheme 1).

The ε^{ai}_{X} values determined by two different titration protocols were similar for both producer and consumer branches (Table 2), except for that of the Pyr consumer branch PFOR-ADHE because O_2 inhibits PFOR and ADHE whereas DPI only inhibits PFOR.

Determination of the flux control coefficients

The C^{J}_{ai} values for each group of reactions were calculated from the ε^{ai}_{X} values by solving the equations 1-5 described in the Material and Methods section (Table 2). For the three evaluated metabolites, the highest C^{J}_{ai} was always exerted by the producer group of reactions, *i.e.* the enzymes/processes in the initial glycolytic steps. Thus, the Glc6P producer branch (HXT, HK, and glycogen degradation) (Scheme 1) exerted the main control of the amebal glucose fermentation flux.

From the difference in C^J_{ai} of the Glc6P and Fru6P producer branches (Table 2), it was calculated that glycogen synthesis *plus* HPI, the steps in the middle of these metabolites (Scheme 1), exerted relevant negative control (Table 3) because the first represents a leak from the Glc6P to ethanol flux. The same reasoning was used for estimating the PPi-PFK to PPDK flux control (Table 3), by considering the C^J_{ai} difference between the Fru6P and Pyr producer branches (Table 2).

Finally, titration with the inhibitors also allowed for determining the individual C^J_{ai} of PFOR, ADHE and AcCoAS (Table 3). The C^J_{ai} of 0.31 of the Pyr consumer branch obtained from the O_2 experiments corresponded to PFOR *plus* ADHE because both enzymes are strongly inhibited by oxidative stress, with no effect on AcCoAS [10]. In turn, the Pyr consumer C^J_{ai} of 0.13 obtained from the DPI plots can be attributed to PFOR because, under the experimental conditions used, this inhibitor does not affect ADHE or AcCoAS [18]. Therefore, it can be assumed that the difference of 0.18 between these last two values corresponded to the C^J_{ai} of ADHE. In turn, by applying the branch theorem [16, 17] a C^J_{ai} of -0.08 for AcCoAS on the flux to EtOH was revealed (Table 3; Scheme 1).

Inhibition of the main controlling steps affects not only glycolysis, but also ATP levels and cell viability

The most controlling steps of amebal glycolysis were located in the first steps, HXT, HK and glycogen metabolism. 2-desoxiglucose (2DOG) is a competitive inhibitor against glucose of the HXT activity; the inhibitor is also phosphorylated by HK and in this state it also blocks the flux at the level of HK, HPI and the glycogen metabolism [19]. In the presence of 10 mM external glucose, 30 mM 2DOG was able to decrease by 70 % the amebal glycolytic flux to EtOH (from 44.3 to 15.3 nmol EtOH/min*mg protein) (Fig. 3A). In the absence of added glucose, EtOH production from glycogen degradation was also 60% blocked by 30 mM 2DOG (Fig. 3A). These results indicated that EtOH production derived from both external glucose (~60%) and glycogen degradation (~40%). It was previously demonstrated that disulfiram (DSF) was a potent inhibitor of

555 the flux-controlling ADHE but also of GAPDH (47% and 17% inhibition, respectively, at
556 0.05 μM) [18]. Although this lack of specificity prevented its use for elasticity analysis,
557 DSF could synergize with 2DOG to abate the pathway flux (Fig. 3A). In contrast,
558 inhibition with DPI, which under the present experimental conditions specifically inhibits
559 PFOR by 90% [18], did not significantly affect the glycolytic flux or cell viability.
560 The changes in the glycolytic flux in response to 30 mM 2DOG were mainly
561 caused by pathway inhibition but not by cell death since cell viability was maintained
562 above 75% during the course of the experimental incubation (Fig. 3B); higher 2DOG
563 concentrations (40 mM) decreased cell viability by more than 50% (data not shown).
564 Remarkably, after 2 h incubation with the inhibitor, 30 mM 2DOG decreased the ATP
565 content by 50% (Fig. 3C) whereas DSF alone decreased the ATP content only by 20%
566 (Fig. 3C), which was in agreement with the lower C^{J}_{ADHE} determined (Table 3).
567 Furthermore, simultaneous inhibition of the two controlling enzyme groups with 2DOG
568 and DSF severely decreased cell viability and ATP concentration. In contrast, inhibition
569 of PFOR with DPI neither significantly affected cell viability or ATP nor synergized with
570 2DOG or 2DOG+DSF (Fig. 3C); thus, these results further supported the PFOR role as
571 a low-controlling step of amebal glycolysis. Perhaps most importantly, the results also
572 indicated that to significantly affect cell viability, the amebal ATP pool has to be
573 decreased by more than 50%.
574
575
576 *Contribution of amino acid degradation to ATP supply*
577 The experiments above indicated that carbon skeletons derived from external
578 glucose or glycogen degradation accounted for most of the ethanol flux and ATP
579 synthesis. However, hypotheses have been proposed that amino acid degradation can
580 be an additional ATP supply source [12]. Therefore, trophozoites were incubated in the
581 absence of glucose and in the presence of Biosate, the amino acid source of TYI-S-33
582 medium, and the glycolytic flux, cell viability and ATP were assessed (Fig 4). Amebas
583 without glucose and in the absence or presence of biosate did not show differences in
584 cell viability (Fig 4A), ethanol flux and ATP content (Fig 4B and 4C). The presence of

biosate did not prevent the abatement of these cellular parameters when glycogen degradation was inhibited by 2DOG. Therefore, amino acids contained in biosate seemed not to be a source for energy supply in amebas.

DISCUSSION

Control of amebal glycolytic flux

The results of the present paper show for the first time the experimental determination of the distribution of control of *E. histolytica* glycolysis using live parasites and applying the elasticity analysis approach of the MCA Theory. An advantage of using this strategy was that the pathway control distribution was determined (i) without a detailed knowledge of the full data set of kinetic parameters of the pathway enzymes required for kinetic modeling; (ii) not having the complete set of purified enzymes as *in vitro* pathway reconstitution or a battery of specific inhibitors for each pathway step as for enzyme titration with inhibitors [14]; or without having the complete metabolome of the parasite. It was only required to have knowledge of the pathway structure and stoichiometry to establish the reactions linked by a common metabolite and to modulate the rates of reaction groups by feeding or inhibiting the pathway.

The results indicated that glycolysis in this parasite was mainly controlled by HXT, HK and glycogen degradation. We previously applied kinetic modeling [20] and pathway reconstitution with the recombinant enzymes [21] of *Entamoeba* glycolysis to identify glycolytic controlling steps and the underlying controlling mechanisms. These last two approaches made the assumption that the *in vitro* enzyme behavior was similar to that *in vivo*; however, the main shortcomings were that neither the HXT nor the final pathway steps (PFOR, ADHE and AcCoAS) were explicitly included in pathway modeling and in the second strategy only short pathway segments could be reconstituted (HK-ALDO and PGAM-PPDK).

Although elasticity analysis did not permit us to determine the individual contribution of the HXT and HK to the control of the glycolytic flux, the results indicated that within them large control resides. Serrano and Reeves early suggested that

glucose transport was the rate-limiting step of glucose catabolism, although no evidences were provided validating their hypothesis [22]. Efforts in our laboratory to determine the C^J_{ai} of HXT in live trophozoites by titration with cytochalasin B and measuring the pathway flux have been impaired by the exceedingly high contribution of glycogen degradation to the flux when the HXT is inhibited (Encalada R & Saavedra E, unpublished results). For instance, in the absence of external glucose, a condition that partially may mimic HXT inhibition, glycogen degradation accounts for 40% EtOH formation (Fig. 3A). However, a high control of HXT can be expected since previous MCA studies have demonstrated that glucose transport has significant control (50% in average) on the glycolytic flux in human erythrocytes [23], yeast [24], tumor cells [25] and *Trypanosoma brucei* [26].

The abundant glycogen content in amebas (2.9 M glucose equivalents), derived from culturing the parasite under high glucose [20] may account for the relevant flux-control exerted by the glycogen degradation. In this regard, glycogen degradation can sustain glycolytic flux for a period of up to 2 h before observing a decrease in cell viability (R. Encalada and E Saavedra, unpublished results; and Fig. 4A). On the other hand, HK has low activity in the cell (Table 1) and this deficiency contributes to the high flux-control exhibited by HXT+HK segment. Although kinetic modeling identified HK as the main controlling step of amebal glycolysis [20], the omission of the HXT reaction could have led to overestimation of the HK C^J_{ai}. Nevertheless, the *in vivo* and *in silico* approaches agreed in identifying the first pathway reactions as relevant controlling steps of amebal glycolysis.

The rest of the glycolytic reactions from PPi-PFK to PPDK controlled the flux by approximately 20%, suggesting that these enzymes can cope well with the variation in flux that establishes the first reactions of glycolysis. PGAM may account for most of the control obtained within this enzyme group because it is the third lower glycolytic activity within the cell (Table 1; [10, 18]) and it shows the second highest C^J_{ai} determined by kinetic modeling and pathway reconstitution [20, 21]. In contrast, PPI-PFK and PPDK exhibit low flux-control.

644 PFOR, ADHE and AcCoAS accounted for ~30% of the flux-control on glycolysis.
645 The C^J_{PFOR} determined here by elasticity analysis was in agreement with the C^J_{ai} = 0.07
646 previously determined by inhibitor titration with DPI [18]. In that study it was also
647 determined by titration with DSF that ADHE exhibited a C^J_{ai}= 0.33, which is higher to the
648 value determined here of 0.18. Although the values did not perfectly match, they
649 indicated that ADHE was the main controlling enzyme within the final pathway segment.
650 This is in agreement with the fact that ADHE is the second enzyme with the lowest
651 activity in the cell (Table 1; [10, 18])
652
653 *Inhibition of the main control steps*
654 It was here demonstrated that under specific inhibition conditions of individual
655 enzymes, by only blocking two of the most controlling reactions of amebal glycolysis, the
656 ATP content and cell viability were affected (Fig. 3). Pathway impairment by inhibiting
657 only one controlling step, or inhibiting low controlling steps such as PFOR (Fig. 3) or the
658 PPi-dependent enzymes, would require comparatively higher concentrations of specific
659 drugs leading to unspecific inhibition of other different targets. Thus, to achieve
660 successful blockade of amebal glycolysis, and perhaps of other pathways and cellular
661 processes, accompanied by low or negligible side-effects, at least two of the most
662 controlling steps should be intervened.
663 Our results also indicated that 2-oxoacids from amino acid catabolism cannot be
664 a source for ATP production/supply in amebas, as it was suggested from the genome
665 analysis [12]. This observation is also supported by our previous demonstration that
666 amebal PFOR possesses higher affinity for pyruvate than for other 2-oxoacids such as
667 α-ketobutyrate or α-ketoglutarate [10], which derive from amino acid catabolism, and
668 that acetate production amounts only up to 10% of the etOH production [10, 18].
669 Therefore, ATP produced by AcCoAS may not significantly contribute to the ATP pool in
670 the cell.
671
672 CONCLUSION
673

The main control steps in amebal glycolysis are HXT, HK and glycogen degradation, followed by ADHE. Inhibition of these steps promotes energy metabolism failure and compromises cell viability. As amebal HXT and ADHE differ from those present in the mammalian glycolytic pathway, these proteins emerge as novel targets for therapeutic intervention due to their strong influence in modulating the main energy supply pathway.

EXPERIMENTAL PROCEDURE

Amebas

Amebal trophozoites from HM1:IMSS strain were monthly isolated from amebic liver abscesses induced in hamsters to ensure a stable virulence phenotype and metabolic behavior, briefly animals were anesthetized with pentobarbitale and injected intraperitoneally with of 1 x106 trophozoites. Animals were sacrificed by pentobarbital overdose 7 days after infection to recover the parasites and growing them axenically in TYI medium as previously described [27], harvested at 450 x g, washed twice with cold PBS buffer (137 mM NaCl, 2.7 mM KCl, 10 mM Na_2HPO_4, 2 mM KH_2PO_4 at pH 7.4) and immediately used. All animal experiments were conducted according to the directions of the General Health Law of Mexico following the guidelines of Mexican Official Norm Guide for use and care of laboratory animals (NOM-062-ZOO-1999). Efforts were made to minimize the number of animals used and their suffering.

Determination of the elasticity coefficients

The experimental design was briefly outlined at the beginning of the Results section. The ε^{ai}_{X} of the producer branch of each metabolite X (ε^{prod}_{X}) was determined by increasing the concentration of metabolite X in the living trophozoites through inhibition of PFOR and ADHE with DPI (Sigma; St. Louis, MO, USA) and O_2, as described before [18] (Scheme 1). To attain reproducibility in the variations of metabolites and fluxes, amebas were always incubated in 1 ml aliquots at a density of

$1x10^6$ amebas in tightly closed 1.5 mL microfuge tubes. The use of higher cell densities or batch incubations in larger volumes, were detrimental for cell integrity and led to large variations in metabolites and fluxes. Therefore, for the experiments with O_2, amebas were distributed in 40 tubes ($1x10^6$ cells/mL) and centrifuged at 1750 x g for 5 min. Each cell pellet was re-suspended in 1 ml of PBS previously saturated with O_2 at room temperature (approximately 0.63 mM dissolved O_2 as previously reported [10]) and supplemented with glucose to a final concentration of 10 mM. All the samples were incubated at 37ºC and ten samples were withdrawn at 0, 10, 20 and 30 min. After removal, the samples were incubated on ice for 5 min before centrifugation for 5 min at 1750 x g. The supernatant of two samples were saved and extracted with perchloric acid for EtOH and acetate determination. The cell pellets of each time-point were pooled, resuspended in 0.5 ml of PBS and extracted for Glc6P, Fru6P, Pyr and ATP determinations as described below.

For the experiments with DPI, amebas distributed in 44 tubes ($1x10^6$ cells/mL) were centrifuged and re-suspended in 1 ml PBS equilibrated with atmospheric air (0.18 mM dissolved O_2 concentration [10]) and supplemented with 10 mM glucose. Eleven samples *per* DPI concentration were supplemented with 0, 0.05, 0.07 and 0.1 µM DPI. One sample of each concentration was immediately extracted for metabolite determination (t=0), the rest were incubated at 37ºC for 1 h. Thereafter, the samples were processed for metabolite determination as described above for the O_2 experiments. High cell viability has to be strictly maintained on all the incubations to ensure a correct application of elasticity analysis. Following the experimental procedure above described, cell viability was 87± 5 % at the end of the incubation with the highest DPI concentration or the longest incubation with O_2 (see Figs. 3B and 3C).

To determine the $\boldsymbol{\varepsilon}^{ai}_X$ of the consumer group of metabolite X ($\boldsymbol{\varepsilon}^{cons}_X$), different concentrations of the metabolite were attained by incubating amebas with increasing glucose concentrations (Scheme 1). Amebas distributed in 44 tubes ($1x10^6$ cells/mL) were centrifuged and re-suspended in 1 mL PBS equilibrated with atmospheric air and supplemented with 0, 5, 10 or 15 mM glucose. One sample of each concentration was

immediately extracted for metabolite determination (t=0) and the rest were incubated for 30 min at 37ºC. Then, the samples were processed for metabolite determination as described above. Cell viability with 15 mM glucose was 90% after 30 min incubation; higher glucose concentrations were not used because cell viability diminished to 67% (data not shown).

Determination of metabolites, fluxes and enzyme activities

At the end of the incubations in the different protocols, the samples were extracted with perchloric acid, centrifuged and the supernatant neutralized and used to determine Glc6P, Fru6P, Pyr and ATP using standard enzymatic assays [20]. Acetate was determined using acetate kinase [10] whereas EtOH was determined by gas chromatography [18]. In the different experimental settings, the EtOH and acetate fluxes were calculated from the difference in their contents at the end of the incubation *minus* that at t=0. For all the experiments, the control condition (100%) referred to the metabolite concentrations and the pathway fluxes of amebas incubated in 10 mM glucose in the absence of inhibitors.

Determination of enzyme activities of the glycolytic enzymes was made at pH 6.0 as described before [2, 10, 20].

Determination of the elasticity and flux control coefficients

Data of percentage of concentration of metabolite X *versus* percentage of pathway flux were plotted. The $\boldsymbol{\varepsilon}^{ai}_{X}$ values were calculated from the slope of the linear fitting of all the experimental data obtained from at least three independent amebal cultures. For Glc6P and Fru6P the $\boldsymbol{\varepsilon}^{ai}_{X}$ values were used to calculate the C^{J}_{ai} by solving the system of equations derived from the summation (equation 1) and connectivity theorems (equation 2) of MCA [16, 17].

$$C_{prod}^{Jetoh} + C_{cons}^{Jetoh} = 1 \qquad \text{(Eq. 1)}$$

$$C_{prod}^{Jetoh}\,\varepsilon_X^{prod} + C_{cons}^{Jetoh}\,\varepsilon_X^{cons} = 0 \qquad \text{(Eq. 2)}$$

Since Pyr is the immediate glycolytic precursor for EtOH and acetate synthesis, it was necessary to consider the $\varepsilon^{ai}{}_{X}$ of two consumer branches (scheme 1). In this case, the equations used were those proposed by Kacser [16] for a two-branched pathway:

$$C_{Pyr\ prod}^{JEtOH} = \frac{-\varepsilon_{Pyr}^{PFOR-ADHE}}{\varepsilon_{Pyr}^{Pyr\ prod} - \alpha\varepsilon_{Pyr}^{PFOR-AcCoAS} - (1-\alpha)\varepsilon_{Pyr}^{PFOR-ADHE}} \qquad \text{(equation 3)}$$

$$C_{PFOR-ADHE}^{JEtOH} = \frac{\varepsilon_{Pyr}^{Pyr\ prod} - \alpha\varepsilon_{Pyr}^{PFOR-AcCoAS}}{\varepsilon_{Pyr}^{Pyr\ prod} - \alpha\varepsilon_{Pyr}^{PFOR-AcCoAS} - (1-\alpha)\varepsilon_{Pyr}^{PFOR-ADHE}} \qquad \text{(equation 4)}$$

$$C_{PFOR-AcCoAS}^{JEtOH} = \frac{\alpha\varepsilon_{pyr}^{PFOR-ADHE}}{\varepsilon_{Pyr}^{Pyr\ prod} - \alpha\varepsilon_{Pyr}^{PFOR-AcCoAS} - (1-\alpha)\varepsilon_{Pyr}^{PFOR-ADHE}} \qquad \text{(equation 5)}$$

In these equations, α had a value of 0.1, which represented the fraction of the glycolytic flux that diverts towards acetate synthesis, and meant that 90% of the glucose flux is used for EtOH synthesis, as previously demonstrated [10, 18].

Inhibition of the main controlling steps and its effect on energy variables

Amebas were distributed, centrifuged and each re-suspended in PBS as described above, and divided in seven groups of seven samples each. Five groups were supplemented with 10 mM glucose, one serving as control, whereas the others were supplemented with either 30 mM 2DOG (ICN Biomedicals; Aurora, OH, USA), 0.1μM DPI, 0.05 μM DSF (Sigma; St. Louis, MO, USA), or the combination of these three inhibitors. In the remaining two groups, glucose was not added and one of them was mixed with 30 mM 2DOG; from the difference between these two groups, the role of glycogen metabolism on EtOH and acetate fluxes was determined. One sample of each group was immediately incubated on ice for 5 min, centrifuged and the supernantant was saved for EtOH determination (t=0). The remaining samples from the seven groups were incubated at 37ºC and a sample of each group was withdrawn every 20 min and processed for EtOH determination. At the end of the incubation with inhibitors, cell

viability was determined by Trypan blue exclusion as well as the ATP content as described before [20].

Contribution to ATP supply of amino acid degradation

Amebas were re-suspended in PBS without glucose and incubated for 2 h at 36°C in the absence or presence of 3% biosate (BD Bioxon; Estado de México, México) as amino acid source, and in the absence or presence of 30 mM 2DOG. Samples were withdrawn at different times to determine viability and EtOH production as described above. Cellular ATP was determined at the end of incubation

Acknowledgments

This work was supported by CONACyT-México grants Nos. 83084, 178638, 80534, and 123636; DGAPA IN218713 and ICyTDF PICS08-5. EP acknowledges the financial support provided by Programa de Doctorado en Ciencias Biomédicas, UNAM and CONACyT PhD fellowship No. 210311.

Author Contribution Statement

E.P., R.E. and C.V. performed experiments, M.N. and A.O.-G. contributed with biological material; E.P., R. M.-S. and E.S. planned experiments, analyzed data and wrote the paper.

REFERENCES

[1] Reeves R.E (1984) Metabolism of *Entamoeba histolytica*. *Adv Parasitol* **23**, 105-142.

[2] Saavedra E, Encalada R, Pineda E, Jasso-Chávez R and Moreno-Sánchez R (2005) Glycolysis in *Entamoeba histolytica*. Biochemical characterization of recombinant glycolytic enzymes and flux control analysis. *FEBS J* **272**, 1767-1783.

[3] Reeves RE, Serrano R and South DJ (1976) 6-phosphofructokinase (pyrophosphate). Properties of the enzyme from *Entamoeba histolytica* and its reaction mechanism. *J Biol.Chem* **251**, 2958-2962.

[4] Reeves RE (1968) A new enzyme with the glycolytic function of pyruvate kinase. *J Biol Chem* **243**, 3202-3204.

[5] Saavedra-Lira E, Ramírez-Silva L and Pérez-Montfort R (1998) Expression and characterization of recombinant pyruvate phosphate dikinase from *Entamoeba histolytica*. *Biochim Biophys* Acta **1382**, 47-54.

[6] Kroschewski H, Ortner S, Steipe B, Scheiner O, Weidermann G and Duchêne M (2000) Differences in substrate specificity and kinetic properties of the recombinant hexokinase HXK 1 and HXK 2 from *Entamoeba histolytica*. *Mol Biochem Parasitol* **105**, 71-80.

[7] Reeves RE and South D (1974) Phosphoglycerate kinase (GTP) An enzyme from *Entamoeba histolytica* selective for guanine nucleotides. *Biochem Biophys Res Commun* **58**, 1053-1057

[8] Encalada R, Rojo-Dominguez A, Rodriguez-Zavala JS, Pardo JP, Quezada H, Moreno-Sanchez R and Saavedra E (2009) Molecular basis of the unusual catalytic preference for GDP/GTP in *Entamoeba histolytica* 3-phosphoglycerate kinase. *FEBS J* **276**, 2037-204.

[9] Lo HS and Reeves R (1978) Pyruvate-to-ethanol pathway in *Entamoeba histolytica. Biochem J* **171**, 225-230.

[10] Pineda E, Encalada R, Rodriguez-Zavala JS, Olivos-Garcia A, Moreno-Sánchez R and Saavedra E (2010) Pyruvate:ferredoxin oxidoreductase and bifunctional aldehyde-alcohol dehydrogenase are essential for energy metabolism under oxidative stress in *Entamoeba histolytica*. *FEBS J* **277**, 3382-3395.

[11] Reeves RE, Warren LG, Susskind B and Lo HS (1977) An energy conserving pyruvate to acetate pathway in *Entamoeba histolytica*. *J Biol Chem* **257** (2) 726-731.

[12] Clark CG, Alsmark UC, Tazreiter M, Saito-Nakano Y, Ali V, Marion S, Weber C, Mukherjee C, Bruchhaus I, Tannich E, Leippe M, Sicheritz-Ponten T, Foster PG, Samuelson J, Noël CJ, Hirt RP, Embley TM, Gilchrist CA, Mann BJ, Singh U, Ackers JP, Bhattacharya S, Bhattacharya A, Lohia A, Guillén N, Duchêne M, Nozaki T and Hall N. (2007) Structure and content of the *Entamoeba histolytica* genome. *Adv Parasitol* **65**, 51-190.

[13] Fell D. (1997) *Understanding the Control of Metabolism.* Portland Press, London

[14] Moreno-Sánchez R, Saavedra E, Rodríguez-Enríquez S and Olin-Sandoval V (2008) Metabolic Control Analysis: A tool for designing strategies to manipulate metabolic pathways. *J Biomed Biotechnol* 2008:597913.

[15] Westerhoff HV and Palsson BO (2004) The evolution of molecular biology into systems biology. *Nat Biotechnol* **22**(10), 1249-52.

[16] Kacser H (1983) The control of enzyme systems *in vivo*: elasticity analysis of the steady state. *Biochem Soc Trans* **11,** 35-40.

[17] Fell DA and Sauro HM (1985) Metabolic control and its analysis. Additional relationships between elasticities and control coefficients. *Eur J Biochem* **148**, 555-561.

[18] Pineda E, Encalada R, Olivos-García A, Nequiz M, Moreno-Sánchez R and Saavedra E (2013) The bifunctional aldehyde-alcohol dehydrogenase controls the ethanol and acetate production in *Entamoeba histolytica* under aerobic conditions. *FEBS Lett* **587**, 178-184

[19] Ralser M, Wamelink MM, Struys EA, Joppich C, Krobitsch S, Jakobs C and Lehrach H. (2008) A catabolic block does not sufficiently explain how 2-deoxy-D-glucose inhibits cell growth. *Proc Natl Acad Sci U S A*. **105**(46):17807-11.

[20] Saavedra E, Marin-Hernández A, Encalada R, Olivos A, Mendoza-Hernández G and Moreno-Sánchez R (2007) Kinetic modeling can describe *in vivo* glycolysis in *Entamoeba histolytica*. *FEBS J* **274**, 4922-4940.

[21] Moreno-Sánchez R, Encalada R, Marín-Hernández A and Saavedra E (2008) Experimental validation of metabolic pathway modeling. An illustration with glycolytic segments from *Entamoeba histolytica*. *FEBS J* **275**, 3454-3469.

[22] Serrano R and Reeves RE (1975) Physiological significance of glucose transport in *Entamoeba histolytica*. *Exp Parasitol* **37**, 411-416.

[23] Rapoport T, Heinrich R, Jacobasch G and Rapoport S. (1974) A linear steady-state treatment of enzymatic chains. A mathematical model of glycolysis of human erythrocytes. *Eur J Biochem* **42**, 107‑120.

[24] Rossell S, van der Weijden CC, Kruckeberg A, Bakker BM and Westerhoff HV (2002) Loss of fermentative capacity in baker's yeast can partly be explained by reduced glucose uptake capacity. *Mol Biol Rep* **29**, 255-7.

[25] Marín-Hernández A, Gallardo-Pérez JC, Rodríguez-Enríquez S, Encalada R, Moreno-Sánchez R and Saavedra E (2011) Modeling cancer glycolysis. *Biochim Biophys Acta* **1807**(6), 755-67.

[26] Haanstra JR, Kerkhoven EJ, van Tuijl A, Blits M, Wurst M, van Nuland R, Albert MA, Michels PA, Bouwman J, Clayton C, Westerhoff HV and Bakker BM (2011) A domino effect in drug action: from metabolic assault towards parasite differentiation. *Mol Microbiol* **79**, 94-108.

[27] Olivos-García A, González-Canto A, López-Vancell R, García de León M del C, Tello E, Nequiz-Avendaño M, Montfort I and Pérez-Tamayo R (2003). Amebic cysteine proteinase 2 (EhCP2) plays either a minor or no role in tissue damage in acute experimental amebic liver abscess in hamsters. *Parasitol Res* **90** (3), 212-220.

Scheme 1: Elasticity analysis of glucose metabolism in *E. histolytica*

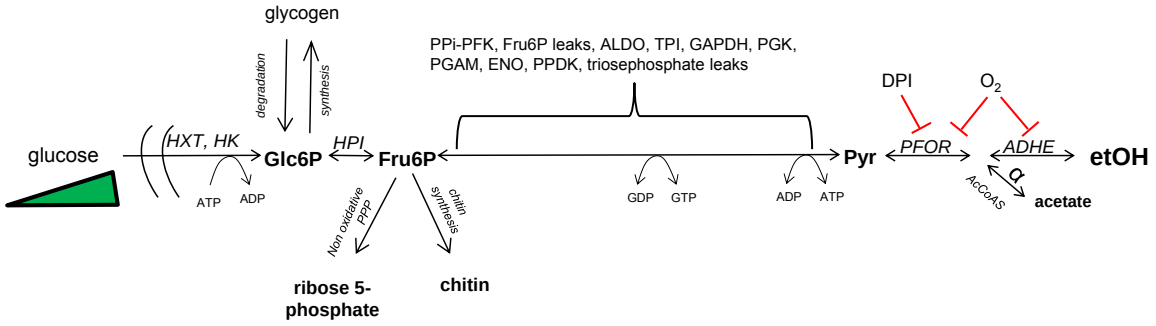

Glc6P, Fru6P and Pyr were gradually varied in trophozoites by (i) supplying different glucose concentrations and (ii) by inhibiting with O_2 or DPI; the EtOH and acetate fluxes were in parallel determined. α represents the proportion of the carbon flux that goes to acetate (10%). From the [metabolite] *versus* pathway flux relationship, the ε^{ai}_{X} for the producer and consumer branches of each metabolite were determined and used to determine their C^{J}_{ai}. Fru6P leaks refer to the use of this metabolite by the non-oxidative pentose phosphate pathway (and perhaps chitin synthesis). Triosephosphate leaks mainly comprise the reactions for amino acid (from 3PG and Pyr) and lipid syntheses.

Table 1 Activities of the pathway enzymes in amebas incubated in PBS with different glucose concentrations and time intervals.

Activity in nmoles/min*mg protein. ND, not determined

	glucose 0 mM		glucose 15 mM	
Enzyme	t=0 min	t=30 min	t=0 min	t=30 min
HK	87	92	89	103
HPI	198	230	206	227
PPi-PFK	203	197	210	195
ALDO	142	150	133	164
TPI	3986	4024	3950	3986
GAPDH	302	277	332	324
PGK	2080	2197	2062	2098
PGAM	110	106	91	105
ENO	479	502	519	516
PPDK	274	303	290	279
PFOR	906	980	950	988
ADHE	84	90	85	84
AcCoAS	145	ND	ND	133

Table 2. Elasticities and flux control coefficients towards EtOH formation of amebal glycolytic reactions

The ε^{ai}_{X} values shown are the mean ± standard deviation of the linear fitting of the whole set of experimental points (positive or negative slopes; Fig. 2), which were derived from different cellular preparations (indicated in the legend to Fig. 2). The C^{JEtOH}_{ai} were calculated from the ε^{ai}_{X} as described in Material and Methods using equations 1-5. Values without parentheses represent the ε^{ai}_{X} determined from the titration with O_2 and within parentheses those determined with DPI titration.

Metabolite	ε^{prod}_{X}	ε^{cons}_{X}	C^{JEtOH}_{prod}	C^{JEtOH}_{cons}
Glc6P	-0.16 ± 0.0.05 (-0.24 ± 0.07)	0.60 ± 0.09 (0.61 ± 0.34)	0.79 ± 0.08 (0.72 ± 0.12)	0.21 ± 0.04 (0.28 ± 0.09)
Fru6P	-0.39 ± 0.24 (-0.39 ± 0.17)	0.51 ± 0.28 (0.56 ± 0.26)	0.57 ± 0.21 (0.59 ± 0.16)	0.43 ± 0.15 (0.41 ± 0.17)
Pyr	-0.12 ± 0.04 (-0.12 ± 0.03)	$\varepsilon^{PFOR\text{-}ADHE}_{Pyr}$ 0.42 ± 0.13 (0.8 ± 0.36) $\varepsilon^{PFOR\text{-}AcCoAS}_{Pyr}$ 0.52	0.77 ± 0.13 (0.87 ±0.17)	$C^{JEtOH}_{PFOR\text{-}ADHE}$ 0.31 ± 0.15 (0.13 ± 0.04) $C^{JEtOH}_{PFOR\text{-}AcCoAS}$ -0.08

926 **Table 3. Flux control distribution of *E. histolytica* glucose metabolism**
927 **towards EtOH formation**

Enzyme or enzyme group (ai)	C^{JEtOH}_{ai} O_2	DPI
HXT, HK, glycogen degradation	0.79 ± 0.08	0.72 ± 0.12
Glycogen synthesis	-0.22 ± 0.13	-0.13 ± 0.02
PPi-PFK, Fru6P leaks, ALDO, TPI, GAPDH, PGK, PGAM, ENO, PPDK, triosephosphate leaks	0.20 ± 0.11	0.28 ± 0.13
PFOR-ADHE	0.31 ± 0.15	0.13 ± 0.04
PFOR-AcCoAS	-0.08	ND
PFOR	0.13 ± 0.04	
ADHE	0.18 ± 0.09	
AcCoAS	-0.08	

928 ND, not determined

929

930

FIGURE LEGENDS

Figure 1: Titration of glycolytic metabolites in amebal trophozoites

Amebas were incubated either with (A) the indicated glucose concentrations for 30 min; (B) PBS saturated with O_2 for the indicated times; or (C) variable DPI concentrations for 60 min. At the end of the incubations, the samples were processed for metabolite determination. Control metabolite concentrations (mM) were: Glc6P 3.4 ± 1.2; Fru6P 1.3 ± 0.2; Pyr 0.84 ± 0.12 and ATP 3.8 ± 0.9. To calculate the intracellular concentration of metabolites it was assumed that amebal trophozoites have an intracellular water volume of 20 µL per 10^7 cells [20]. Two tailed Student's t-test for non-paired samples *versus* 10 mM glucose (A) and in the absence of inhibitors (B, C). * $p < 0.01$; ** $p < 0.05$ vs 10 mM glucose.

Figure 2: Experimental determination in *E. histolytica* of the elasticity coefficients of glycolytic reactions that produce and consume the indicated metabolites.

Amebal trophozoites were incubated in PBS with different concentrations of glucose (positive slopes), and O_2 (A-C) or DPI (D-F) (negative slopes). The pathway flux and metabolite concentrations were in parallel determined. The solid straight lines represent the best-fitting of all the data obtained from three individual amebal cultures indicated with different symbols (except in Fig. 3F in which n=2). In (C) the acetate and ethanol fluxes were added up for the Pyr supply group whereas EtOH (closed symbols) and acetate (asterisks; n=1) fluxes were separated for the Pyr-consuming groups. 100% EtOH flux corresponds to 31 ± 8 nmoles/min* mg protein

Figure. 3: Effect of inhibition of the controlling steps on amebal glycolytic flux, cell viability and ATP content.

A) Amebas were incubated with 10 mM glucose or with no glucose added (- glc) in the absence or presence of 30 mM 2DOG. 0.05 µM DSF, 0.1 µM DPI or the indicated

combination of these inhibitors; the EtOH content was determined at the indicated times. The values shown represent the mean ± SD of three independent cell preparations.

B) Time course of viability in amebas incubated with 2DOG, DPI and/or DSF.

C) Amebas were incubated for 2 h with 10 mM glucose in the absence or presence of the indicated inhibitors. At the end of incubation period, the cell viability was determined by Trypan blue exclusion (data from Fig. 3B) and ATP content by spectrophotometric assays as described above. 100% ATP content corresponds to 2.9 ± 0.6 mM.

Figure 4: Effect of amino acid supply on cell viability, etOH flux and ATP production.

Amebas were incubated without glucose and in the absence or presence of 3% biosate or 30 mM 2DOG. Cell viability (A; n=2) and pathway flux (B; n=1) were determined as in Fig. 3. In C) the ATP concentration was determined at the end of the 2 h incubation and in control amebas was 3.2 mM (n = 2).

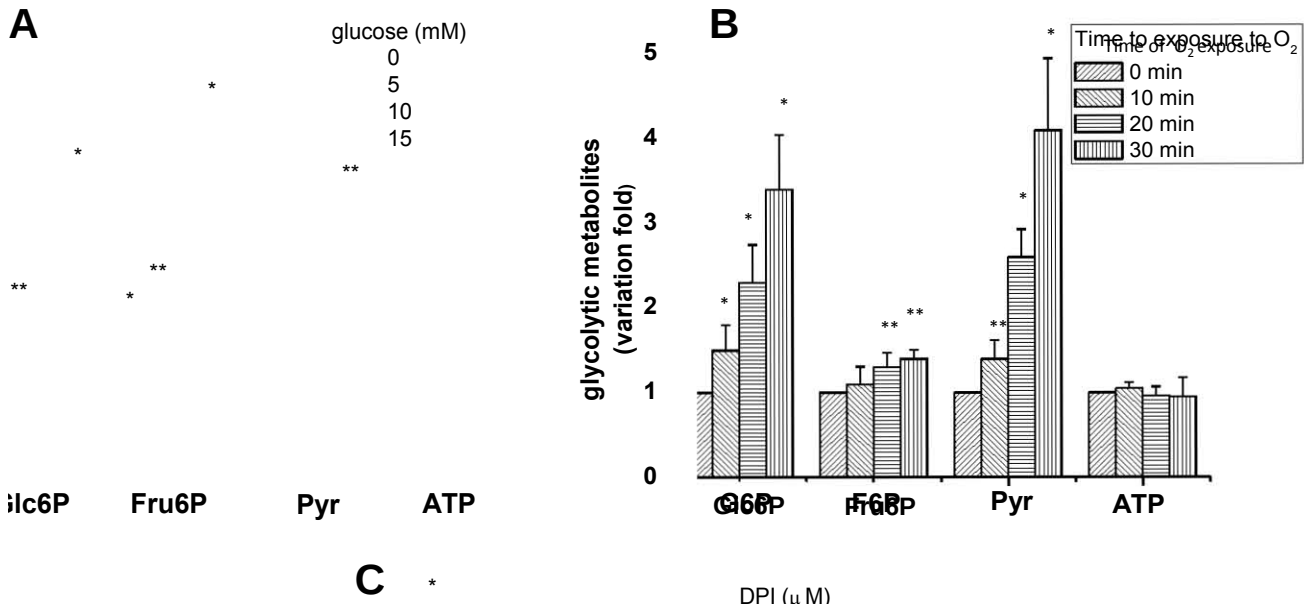

973
974

Figure 1

400

200

Figure 2

Figure 3

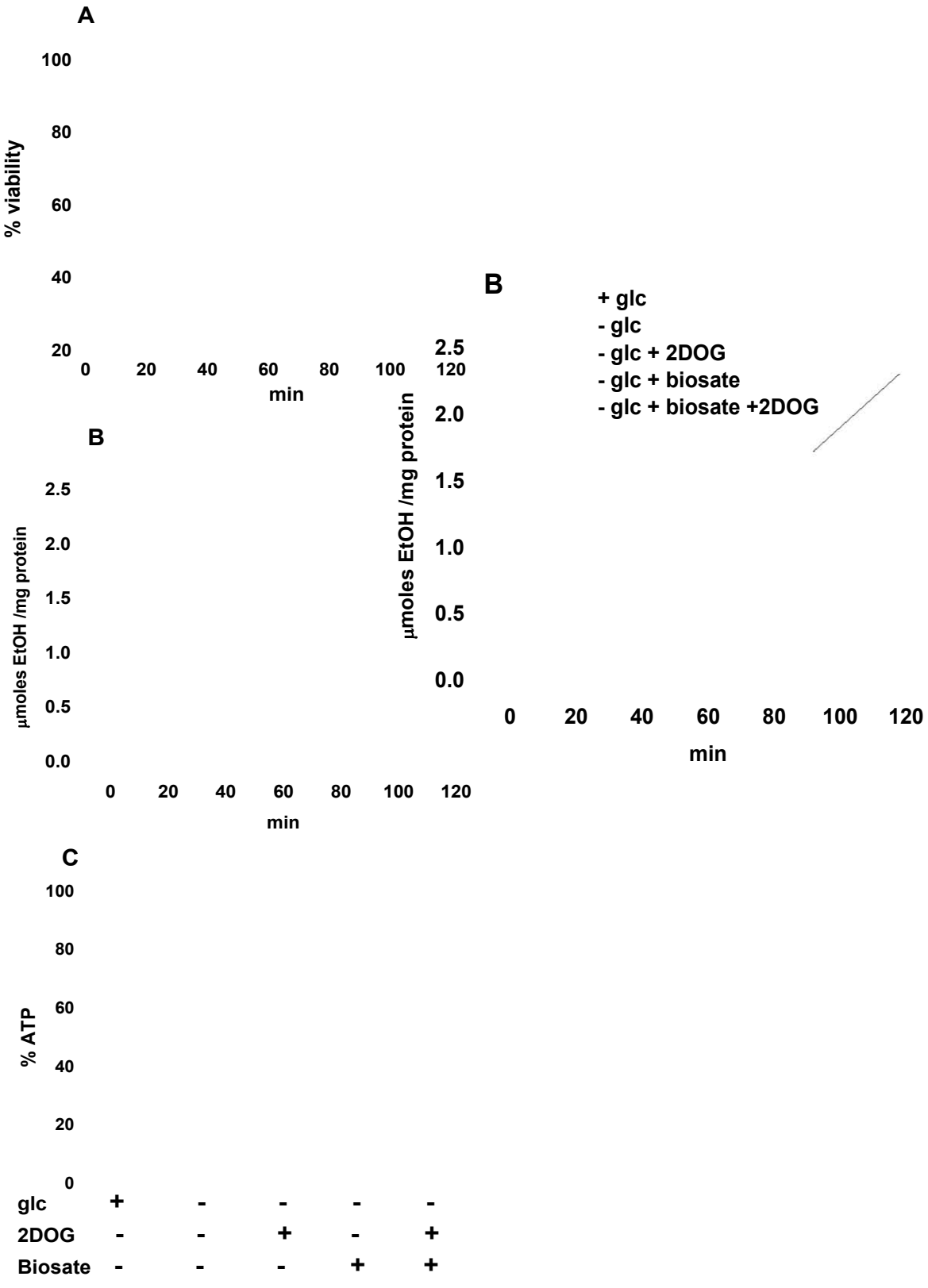
A
% viability
100
80
60
40
20
0
20
40
60
80
100
120
min
B
µmoles EtOH /mg protein
2.5
2.0
1.5
1.0
0.5
0.0
0
20
40
60
80
100
120
min
B
+ glc
- glc
- glc + 2DOG
- glc + biosate
- glc + biosate +2DOG
µmoles EtOH /mg protein
2.5
2.0
1.5
1.0
0.5
0.0
0
20
40
60
80
100
120
min
C
% ATP
100
80
60
40
20
0
glc + - - - -
2DOG - - + - +
Biosate - - - + +

Figure 4